International Journal on Advances in Life Sciences

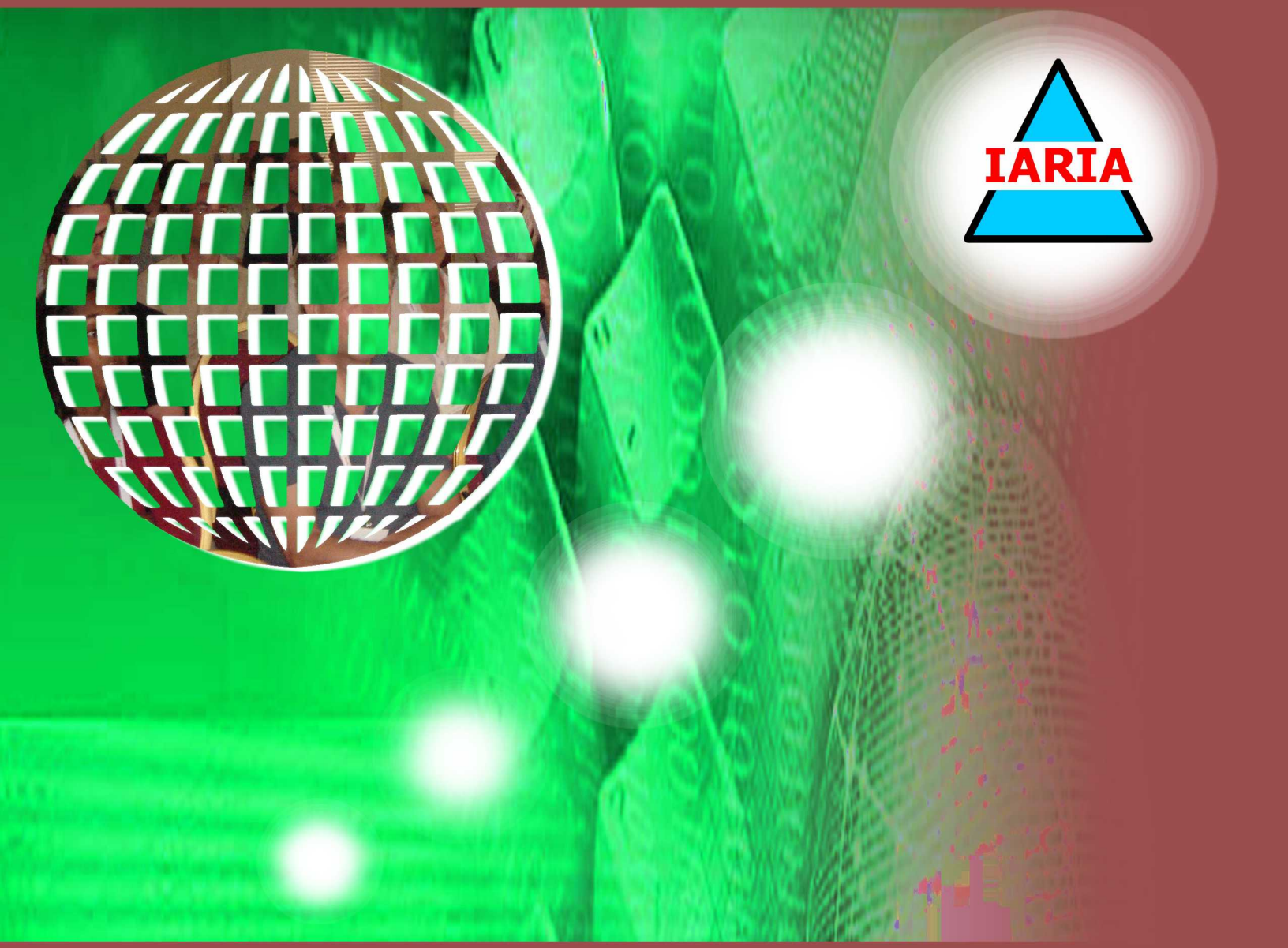

2014 vol. 6 nr. 1&2

The *International Journal on Advances in Life Sciences* is published by IARIA.
ISSN: 1942-2660
journals site: http://www.iariajournals.org
contact: petre@iaria.org

Sponsored by IARIA
www.iaria.org

International Journal on Advances in Life Sciences
Volume 6, Number 1 & 2, 2014

International Journal on Advances in Life Sciences
Volume 6, Numbers 1 & 2, 2014

CONTENTS

Constantine Stephanidis, Institute of Computer Science, Foundation of Research and Technology – Hellas (FORTH), Department of Computer Science, University of Crete, Greece

pages: 74 - 86

Bioimpedance Parameters as Indicators of the Physiological States of Plants in situ A novel usage of the Electrical Impedance Spectroscopy technique

Elisabeth Borges, Physics Department of the University of Coimbra Instrumentation Center, Portugal
Mariana Sequeira, Physics Department of the University of Coimbra Instrumentation Center, Portugal
André Cortez, Physics Department of the University of Coimbra Instrumentation Center, Portugal
Helena Pereira, Physics Department of the University of Coimbra Instrumentation Center, Portugal
Tânia Pereira, Physics Department of the University of Coimbra Instrumentation Center, Portugal
Vânia Almeida, Physics Department of the University of Coimbra Instrumentation Center, Portugal
João Cardoso, Physics Department of the University of Coimbra Instrumentation Center, Portugal
Carlos Correia, Physics Department of the University of Coimbra Instrumentation Center, Portugal
Teresa Vasconcelos, Escola Superior Agrária de Coimbra of the Instituto Politécnico de Coimbra - Centro de Estudos de Recursos Naturais Ambiente e Sociedade, Portugal
Isabel Duarte, Escola Superior Agrária de Coimbra of the Instituto Politécnico de Coimbra - Centro de Estudos de Recursos Naturais Ambiente e Sociedade, Portugal
Neusa Nazaré, Escola Superior Agrária de Coimbra of the Instituto Politécnico de Coimbra - Centro de Estudos de Recursos Naturais Ambiente e Sociedade, Portugal

Vis-a-Vis: Offline-Capable Management of Virtual Trust Structures Based on Real-Life Interactions

Marco Maier, Chadly Marouane, and Claudia Linnhoff-Popien
Mobile and Distributed Systems Group
Ludwig-Maximilians-Universität München, Germany
{marco.maier, chadly.marouane, linnhoff}@ifi.lmu.de

***Abstract*—Online services, particularly those aimed at a specific user base such as a company's employees, face the problem of identity management. Especially when the service constitutes some kind of social network, i.e., the validity of the users' identities matters, secure and reliable means for identity verification and authentication are required. In this paper, predicated on our previous work, we propose an identity management concept based on a) verification through physical presence and b) authentication through ownership. Our approach being a hybrid solution between a centralized authority and decentralized trust management is settled on a sweet spot between security and convenience for the users. In this extended version, we present the newly proposed Tree of Trust structure in more detail, and provide a thourough explanation how the system can be used in a technically more distributed manner, even supporting offline operation.**

Keywords-identity management systems; authentication; social network services; mobile computing

I. INTRODUCTION

In this paper, we present an extended version of our previously introduced concept called "Vis-a-Vis Verification" [1]. The new additions mainly comprise a more detailed explanation of our trust relationship structure and a completely novel explanation of the offline capabilities and mechanisms of our system.

Nowadays, with about 2.8 billion people using the Internet worldwide [2] and over 1.1 billion people participating in the world's largest online social network Facebook [3], online service providers have a clear need for identity management, i.e., *administration*, *verification*, *authentication* and *authorization* of virtual identities and their real-world counterparts.

Especially when a service's users are linked to their real-world identity (i.e., the service constitutes some kind of online social network) and more so, when the service furthermore requires a high level of security, a key part of identity management is to verify that a virtual account really belongs to the real-world person it is supposed to be linked to, and to provide a secure and intuitive means of authentication. Typically in such services, a user Alice would decide for or against granting certain permissions to a virtual user Bob based on whether she wants to grant those permissions to the real-world Bob. Thus, she has to be sure that the user account really belongs to the real-world Bob (verification), and that nobody else can make requests on behalf of that account (authentication).

There are several ways of verifying a user's real-world identity, which to date either are easy to implement and use but quite easy to attack, or are reasonably secure but introduce a huge overhead in the general process of account creation. In the same way, currently used authentication procedures differ in potential for security breaches on the one, and intuitivity on the other hand.

With the now near ubiquitous usage of smartphones, we see huge potential to improve upon the currently used ways of identity verification and authentication in online services. In this work, we present an approach that is based on two key ideas

- New user accounts are verified to belong to a certain real-world identity by requiring an interaction of an existing user with the new user in the real world.
- The users employ their personal smartphone as the credential for authentication, i.e., the security token is stored on the users' smartphone.

Our approach constitutes a hybrid system. There is a central authority, which is the root of the system's trust relations and is controlled by the organisation employing the system. In order to avoid the typical overhead of sophisticated identity verification, verification tasks are distributed among the system's existing users. Consequently, our system provides a high degree of trustworthiness of the user accounts while keeping the introduced overhead at a reasonable level. To the best of our knowledge, to date, no other approach has settled on that sweet spot between security and ease-of-use.

While the basic design of our system depends on synchronous communication with the central authority, we furthermore developed a more sophisticated approach which enables offline verification of new users.

The rest of the paper is structured as follows. In Section II, we give an overview of various concepts for identity verification and authentication, together with their individual strengths and weaknesses. In Section III, we discuss related work which is or could be used similar to our approach. In Section IV, we present our system for identity verification and authentication. After that, we go into more detail about

management operations within our newly proposed trust relationship structure (Section V). In Section VI, we explain the extended version of our verification procedure which enables offline usage. After that, we describe a real implementation of our concept, which has been deployed for production usage (Section VII). In Section VIII, we describe some scenarios how our approach could be used, and in Section IX, we conclude with an outlook at future work.

II. Identity Management

Identity management of online services comprises several sub-topics like authorization and management of user accounts. The focus of this work specifically lies on *identity verification* and *authentication*. We define identity verification as the process to check the real-world identity of a person and to connect this identity to a virtual account. Authentication then requires some kind of credential to prove that a request is made by that virtual account (i.e., on behalf of the real person).

A. Identity Verification

There are several mechanisms to verify an online identity, i.e., to link a virtual account to a real-world person. These mechanisms can be categorized into three groups, namely *verification through another online identity provider*, *verification through a second communication channel* and *verification through physical presence*.

1) Verification through another online identity provider: The idea of this mechanism is to rely on a third party to verify a new user account. The typical and most widely used example is to require an existing email address when a new account shall be created. To confirm the email address, the online service sends a message to the registrant containing a confirmation link. By clicking the link, the new user can ensure that he is the real owner of the email address. In this case, one relies upon the third party to have checked the identity of the potential user. Thus, it depends on the third party whether the real-world identity is verified, and even if so, typically the real-world identity is not handed over to other parties, leaving the online service with the email address only.

An email address of course is only a very weak personal detail for a real identity. Another approach is to rely on real identity providers. For example, online services like Facebook.com, plus.google.com, or LinkedIn.com manage user profiles, which are verified to some degree. These services can be used either through proprietary interfaces (e.g., *Facebook Login* [4]), or by employing standardised mechanisms like OpenID [5].

Verification through a third party often is the most convenient method of identity verification, both for the end user and the online service provider. The main drawback is the dependence on the trustworthiness of the third party.

2) Verification through a second communication channel: Another approach is the integration of a second communication channel into the verification procedure, typically using an endpoint which requires or inherently is linked to a more sophisticated identity verification like a mobile phone number or a postal address.

When using a mobile phone number, the online service e.g., can send a randomly generated unique token as a text message to the phone. The user then has to enter that token into a form at the online service, which ensures the provider that the user really is the owner of that specific phone number.

A similar procedure can be performed by sending the token in a letter to the user's postal address. Though this alternative takes several days to complete, the online service can obtain a verification of the user's name and residency.

Again, one relies on a third party to verify the identity of a new user. However, e.g., mobile phone providers are required by law to verify the identity of their customers in most countries, leading to a higher trustworthiness of those third parties compared to the previous approach (II-A1).

3) Verification through physical presence: The most sophisticated variant of identity verification is verification through physical presence, i.e., the user whose identity has to be checked is in direct proximity of authorized personnel of the online service provider or a trusted third party which acts on behalf of the provider.

Depending on whether the verifying person already knows the to-be-verified user or not, the new user might have to provide official identity documents like passports or ID cards to prove its identity.

Physical verification by the online service provider itself can be regarded as the most secure option. However, it is often unfeasible to establish a dedicated verification entity at the provider and to manually check the identity of maybe thousands of users. Therefore, services like *Postident* [6] by German logistics company *Deutsche Post* exist, which provide personal identity verification for third parties. In this case, a new user could verify its online account in one of the many stores of the logistics company.

Summing up the alternatives, verification through another online identity provider can be regarded as the most convenient but also most insecure variant. Verification through a second channel like the mobile phone network or old-school snail mail is more reliable due to law-enforced requirements or the sheer characteristics of the channel (e.g., name and postal address is correct when the letter arrives). However, it is also less convenient and more costly for the participants. Finally, verification through physical proximity provides the most secure procedure at the cost of increased effort for both the online service provider and the end user.

B. Authentication

Within the scope of online services, authentication can be defined as the act of confirming the origin of a request, i.e., from which user or account the request was sent. One can distinguish between three categories (*factors*) of authentication, namely authentication by *something you know* (*knowledge*), by *something you are* (*inherence*), and by *something you have* (*ownership*).

1) Something you know: This authentication factor involves some kind of secret only the respective user knows. Typical examples are passwords or pass phrases, personal identification numbers (PIN), or challenge response procedures (i.e., asking a

question only the user can answer). This way of authentication usually can be implemented without much overhead at the provider, but is prone to security breaches resulting from users employing secret credentials too easy to guess or infer from other knowledge. Furthermore, this method can be attacked through phishing [7].

2) Something you are: This means of authentication is based on the behavioral and/or biological characteristics of an individual. Typical methods are to recognize fingerprint, face, voice or retinal pattern. Using inherent characteristics of a human being is convenient for the user because she does not have to remember a secret, but often is complex to implement, error prone and furthermore, the user might be unwilling to share such personal details with a provider.

3) Something you have: In this case, authentication is based on the possession of a key, smart card, security token and the like. In the scope of online services, using this method has the advantage that longer and much more complex security tokens can be used, compared to an ordinary password a user has to know by heart. Implementation usually is straight-forward at the provider, and this method furthermore is very intuitive for the users since it resembles the real-world usage of ordinary keys. However, users might be unwilling to carry additional hardware such as smart cards with them.

Comparing the three methods, authentication based on ownership is the best compromise between security on the one hand, and intuitivity for the users on the other hand. However, using a dedicated hardware component might not be feasible. The latter can be prevented when using a user's smartphone to store the token [8].

C. Problem statement

Today, most online services rely on a verification procedure based on third party identity providers, typically only requiring a valid email address, and employ username-password-credentials for authentication (i.e., something you know). As we have explained, verification through physical presence and authentication via something you have would be a very promising combination regarding security and intuitivity and would therefore be a superior solution to those mechanisms currently most widely used. However, existing ideas result in increased inconvenience for the end-user and more complexity at the provider.

In this work, we present a solution that uses that exact combination of identity verification by physical presence and authentication by something you have, which at the same time keeps the typical overhead at a feasible and usable level.

III. Related work

As seen in the previous section, there is a multitude of ways and combinations online services can perform identity verification and authentication. In this section, we focus on systems that resemble our approach with regard to the employed concepts.

Public Key Infrastructures (PKI) are the most widely used method conceptually comparable to our approach. Digital certificates are issued and verified by a Certificate Authority (CA), which can then be used to authenticate oneself. Dependent on the CA and the type of certificate, obtaining this credential requires the verification of one's real-world identity [9]. PKIs are used in conjunction with Secure Socket Layer (SSL) to ensure secure communication, which in general results in increased complexity leading to vulnerabilities, e.g., with regard to validation of SSL certificates within non-browser environments [10]. However, the main disadvantage is that PKIs in its current form are mostly aimed at organisations and corporations, and distribution of certificates to individual users often is not possible to employ with only a reasonable overhead. Since PKIs allow for hierarchical relationships between the CAs among themselves (i.e., one CA may vouch for another), the resulting structure can be regarded as a tree, which is similar to our approach.

An alternative to the rather centralized trust model of a PKI, which relies exclusively on CAs, is the Web of Trust concept. The latter is a decentralized approach to certificate signing, requiring the users to ensure their respective identities among themselves, often based on personal encounters [11]. PGP and GnuPG are well known implementations of this concept, which allow people to exchange messages securely with mutual authentication [12].

A core concept of the Vis-a-Vis system is the so-called *tree of trust* (see Section IV-D). There are similarly named concepts in other areas which should not be confused with our approach. Presti [13] defines a "tree structure of trust" within the scope of Trusted Computing. In this case, the tree's nodes represent the components of the whole Trusted Computing platform, i.e., from the hardware modules up to the applications. Verbauwhede and Schaumont [14] take a similar approach by partitioning different abstraction levels of electronic embedded systems (e.g., the software level or the circuit level) into secure and non-secure parts. They call the resulting structure a "tree of trust", too. Although both approaches regard trees as a suitable structure for representing trust relationships, they are aimed at different scopes than our system.

IV. Vis-a-Vis

In the following, we describe the Vis-a-Vis concept for identity verification and authentication.

A. Authentication

In order to authenticate the users in the Vis-a-Vis system, a notion of the "something you have" principle is used. The idea is based on the omnipresence of mobile devices such as smartphones or tablets, and the assumption that such devices (or specific accounts on them in case of multi user systems) belong to one and only one user. The device is like a key in the physical world. Authenticating the device therefore suffices to authenticate the respective user.

Technically, authentication is performed by issuing a secret, unique token to each device in the system, which then is included in all requests of the device to the backend (i.e., the provider). To prevent leaking the token, communication between mobile devices and the backend has to be encrypted (e.g., by using SSL). To authenticate the backend itself, traditional means such as SSL certificates can be used.

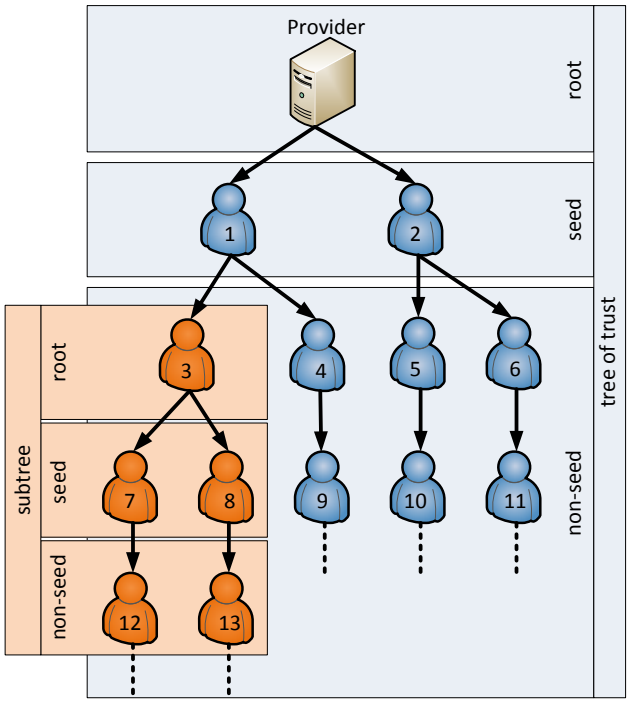

Figure 1. Participants forming a tree of trust, consisting of three levels root, seed and non-seed. Each subtree also is a tree of trust in itself.

B. Participants

Vis-a-Vis is a *hybrid system* with some core components being central elements and most of the other participants self-organizing in a decentralized manner. As such, it is not intended as a single web-wide system but to be deployed individually at organizations. A schematic overview is depicted in Figure 1.

The *Vis-a-Vis provider* is the central entity representing the respective organization. It is fully trusted by default since it manages the whole system. At the moment, there is no interaction beyond provider boundaries and thus, there is no need for further, mutual verification of different Vis-a-Vis providers among themselves.

Providers are responsible to activate *seed users*. These users are verified directly by the provider, by any means regarded secure enough for the given scenario, e.g., by authorized personell such as system administrators verifying a user's identity in person (on-location) or by sending activation information via snail mail. Seed users are fully trusted by the provider.

In order to distribute the verification overhead among the participating entities, seed users can further activate *non-seed users*. The identity of non-seed users is verified by seed users through physical proximity, i.e., seed users may decide to hand over the activation token (from mobile device to mobile device) based on existing knowledge (seed user already knows the new user) or based on official documents (seed user checks, e.g., ID card or passport).

Non-seed users are also allowed to activate new users - in the same manner as seed users - resulting in further non-seed users. As a consequence, non-seed users differ in their distance from the root node (*distance from root*, see Section IV-E), a measure which can be used to quantify the trustworthiness of a user.

C. Protocol

Adding new users to the system is performed in several steps (see Figure 2). First, an online identity (i.e., an account) has to be created for the new user at the provider (step 1). This step can be triggered by the user itself, by the provider (which is reasonable when the future users are known upfront, such as within a company) or by an existing user. It is important to note that in this step, only the account is created (i.e., prepared). It is neither yet activated nor linked to the user's device, i.e., it is not usable, yet.

In order to activate the account, the user needs a one-time key which is generated by the provider. This one-time key can only be given to the new user by the provider itself or by an existing user - the latter case being the more interesting. The new user asks an existing user to verify her identity (steps 2 and 3). The existing user wanting to activate the new user requests the new user's one-time key from the provider (steps 4 and 5) and then forwards it to the new user (step 6). The forwarding has to be done in a way requiring physical proximity (i.e., "vis-a-vis"), e.g., transfer via Near Field Communication (NFC) or optical codes like QR codes.

After receiving the one-time key, the new user sends the key directly to the provider (step 7). The provider now checks whether it is the correct key for the respective user and, when confirmed, sends an authentication token back to the new user (step 8). The user includes this token in all subsequent requests to the backend to confirm their authenticity (step 9).

D. Tree of trust

Performing the above protocol using the described participants results in a tree-like structure. Since this structure describes the evolved trust relations between the users, we can formally define a *tree of trust*

$$T = (V, E) \tag{1}$$

with nodes V and edges E as a rooted tree with *root node* $r \in V$ (the Vis-a-Vis provider), an arbitrary number of *seed nodes* (seed users)

$$S = \{s : s \in V \wedge (r, s) \in E\} \tag{2}$$

and an arbitrary number of *non-seed nodes* (non-seed users) $\bar{S} = V \setminus S$. Each *rooted subtree*

$$T' = (V', E') \tag{3}$$

with $E' \subseteq E$ and $V' = \{v' : v' \in V \wedge (\exists v'' \in V' : (v'', v') \in E' \vee (v', v'') \in E')\}$ is also a tree of trust, i.e., each node can be regarded as the root of its own tree of trust containing users which have been activated by itself or its descendants.

Trees of trust are an analogy to the idea of the web-of-trust. The difference is that trees of trust represent a hierarchy of users allowing for a more intuitive assignment of capabilities with regard to some metric (see Section IV-E) whereas in a meshed graph the structure of trust relationships is harder to grasp.

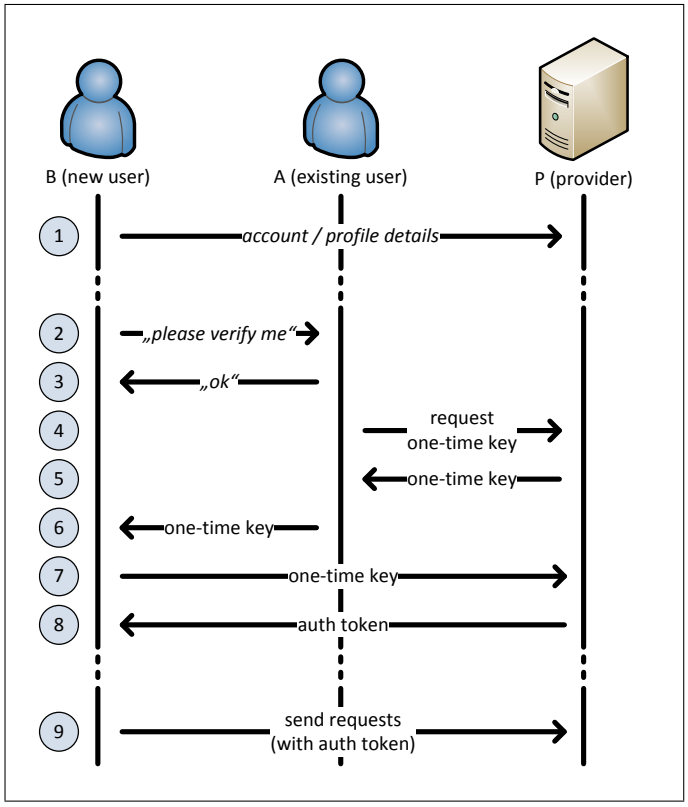

Figure 2. The Vis-a-Vis protocol.

E. Distance from root D_r

There is a single path $P(x, y)$ between each two nodes x and y in the tree, defined as

$$P(x, y) = (v_1, \ldots, v_n) \tag{4}$$

with $v_i \in V, v_1 = x, v_n = y, (v_i, v_{i+1}) \in E$. Based on that we define a measure *distance from root* D_r as

$$D_r(v) = |P(r, v)| \tag{5}$$

A user's distance from its tree's root is a measure for the user's trustworthiness. This measure can be considered when assigning rights or capabilities, e.g., one might limit the length of an *activation chain*, i.e., the path from the tree's root to the user, to a constant C, i.e., $\forall v \in V : D_r(v) < C$.

F. Weighted Tree of Trust

Often it might be desirable to establish a more flexible scheme to assign a trust value to the nodes, considering not only the length of the path from them to the root node but also impact factors like the trustworthiness of the used activation channel.

Furthermore, in some scenarios it is useful to not regard the users as the tree's nodes but their individual devices. Users often possess several mobile devices and it is advisable to issue individual authentication tokens to each device. In case a token is compromised, one can revoke the token without affecting the user's other devices.

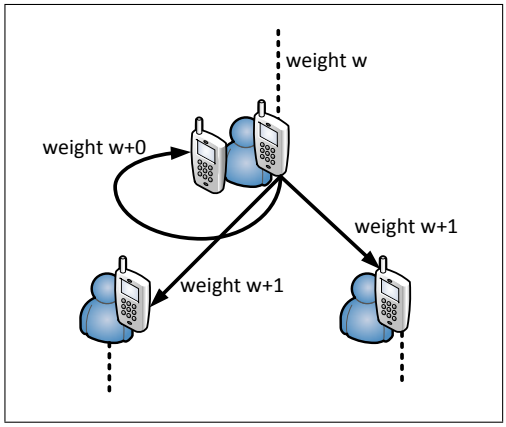

Figure 3. Part of a weighted tree of trust, showing activation of new users (with decreasing trustworthiness) as well as self-activation with edge weight 0 (i.e., no loss of trustworthiness).

Activating a new device by oneself would reduce the trust value of the new device when using the distance from root measure. This can be the desired behaviour, but more often the same person should have the same capabilities on each of its devices.

This problem is solved by introducing weights on the tree's edges (see Figure 3), i.e., each edge (x, y) is assigned a weight w_{xy} correlating to the trustworthiness of the edge itself. Thus, one can define a new trust measure $Trust$ as

$$Trust(v) = \sum \{w_{v_i v_{i+1}} : (v_i, v_{i+1}) \in P(r, v)\} \tag{6}$$

When setting the weight of all edges to 1, $Trust(v) = D_r(v)$.

Using the $Trust$ measure one can allow activation of one's own devices without loss of (calculated) trustworthiness by setting the edge weight to 0. On the other hand, one can also assign edge weights > 1 to mark "more insecure" activations.

V. Tree of Trust Operations

In order to build and maintain the Tree of Trust structure, several operations are required for handling certain events such as a new user joining the system. These basic operations are *adding*, *removing*, *promoting* and *demoting* nodes. For most of these operations there is no definitive way how they should be done, they rather depend on the given scenario. In the following, possible behaviors are described, which span most of the intended use cases.

A. Adding

When a new user gets activated, i.e., an existing user or the provider has verified her identity by performing the Vis-a-Vis protocol, a node corresponding to the user (or rather the user's device) is added to the tree of trust. In case of an unweighted tree, simply adding the node is sufficient. In case of a weighted tree, one has to determine the weight to be assigned to the newly introduced edge in the tree. The weight, e.g., might be dependent on the trustworthiness of the employed channel for performing the verification procedure or the participating users (e.g., when a user activates another device of herself, the weight typically is 0).

B. Removing

The tree of trust itself is not meant to be a structure to manage a system's users themselves but rather their trustworthiness. Thus, it is not required per se to remove inactive users from the tree because the trustworthiness of a user often is not affected by the other users' status. However, oftentimes it might make sense to keep the tree of trust nodes in sync with the system's current state of active and inactive/removed users. Furthermore, in case a device (or its access token) gets stolen, it is required to remove the corresponding node from the tree of trust.

When a node is removed from the tree, it has to be taken care of its child nodes. There are two cases: i) the node has been removed because it has been compromised, i.e., its child nodes' trustworthiness might be affected, and ii) the removed node was in a secure state, i.e., its child nodes' trustworthiness is not affected.

In case i), the child nodes have to be removed recursiveley as well because they might have been activated by an unauthorized user. In order to prevent removal (i.e., deactivation) of a lot of nodes which might have been activated before the node was compromised, it is recommended to store a timestamp of the node's activation, so that only child nodes get removed which have been activated after a given date (e.g., the last time the node is known to have been in an uncompromised state). The other nodes then can be treated like in case ii).

In case ii), child nodes should be kept in the tree and should retain their assigned trustworthiness. This can be accomplished in two ways. One approach is to keep a placeholder of removed nodes in the tree. Such nodes are called *ghost nodes*. They cannot perform any further actions, but are left in the tree to preserve the value of trust calculations for its child nodes. The other way is to reassign child nodes to another parent node. This theoretically can be any node, but usually should be the parent node n_P of the removed node n_R itself. In order to preserve the trust value of a given child node n_C, the newly introduced edge (n_P, n_C) has to be assigned the sum of the weights of the edges (n_P, n_R) and (n_R, n_C), i.e.,

$$w_{n_P,n_C} = w_{n_P,n_R} + w_{n_R,n_C} \tag{7}$$

The first approach has the advantage to retain the activation chains that really happened and it can be applied to unweighted trees as well. The second approach on the other hand does not need to keep track of ghost nodes, but is only applicable to weighted trees.

C. Promoting

It can happen that a user (i.e., her device) gets activated a second time, maybe by a user at a higher level in the tree of trust (leading to a promotion of the user, i.e., an increased trustworthiness). This facilitates self-organization of the userbase, since users might first be verified by the "next best" user (fast activation) and then at a later point in time be reactivated by another user to gain a higher trust value. Analogly, also the weight of an edge could be decreased, which can be reduced to a user being reactivated by the same parent in a more trustworthy manner. The question again is how child nodes should be treated in such events.

The simplest way is to transitively accept increased trust values for all of the node's children as well, i.e., the reactivated node gets reassigned to the new parent node leading to the whole subtree being moved within the tree. Most of the time, this is a reasonable approach.

However, it might also be the case that the child nodes' trustworthiness should not be affected by a promotion of their parent. In this case, the reassignment of a node can be reduced to removing and then adding it again (see Sections V-A and V-B). In case one opts for the ghost node approach, it might be reasonable to keep a reference from the ghost node to the actual node's new location in the tree. When using the second approach, the new parent of the child nodes of course should be the existing parent at its new location in the tree, however, with the weight of the connecting edge adjusted so that the child nodes preserve their previous trust value.

D. Demoting

As a counterpart to promoting, nodes might also get demoted, i.e., reassigned to a parent farther down the tree of trust or the edge weight might be increased. In general, one can treat this event in the same ways as a promotion of a node.

However, demoting a node might affect existing activation chains. i.e., it could be that some activations would have been prohibited by given rules or constraints (e.g., farthest distance from root for new activations) if the demotion had happended earlier. In case the demotion is intentional because of, e.g., the previous trust value being higher than what is reasonable for a given node, it might be required to deactivate and remove certain child nodes.

Depeding on the specific rules and settings in a given system, whenever the trust value of a non-leaf node changes (i.e., in case of promotion or demotion), the corresponding subtree might have to be examined recursively to maybe alter values or status of edges or nodes.

VI. Offline usage

So far, the Vis-a-Vis protocol for account verification and activation (see Section IV-C) depends on a synchronous procedure, i.e., both the existing user and the user to be activated have to be connected to the system, i.e., the Vis-a-Vis provider. We found this to be a rather fierce requirement, especially in one of our intended deployment scenarios (see Section VIII-B).

In this section, we will introduce an extension to the Vis-a-Vis protocol, which allows for offline verification of new users, without synchronously communicating with the Vis-a-Vis provider. The extended protocol even enables transitive activations without requiring communication with the provider until a given account wants to use the service for the first time.

In its basic version, the Vis-a-Vis protocol requires that the account (i.e., profile information) for the new user is created at the provider upfront. This can happen in one go with but can

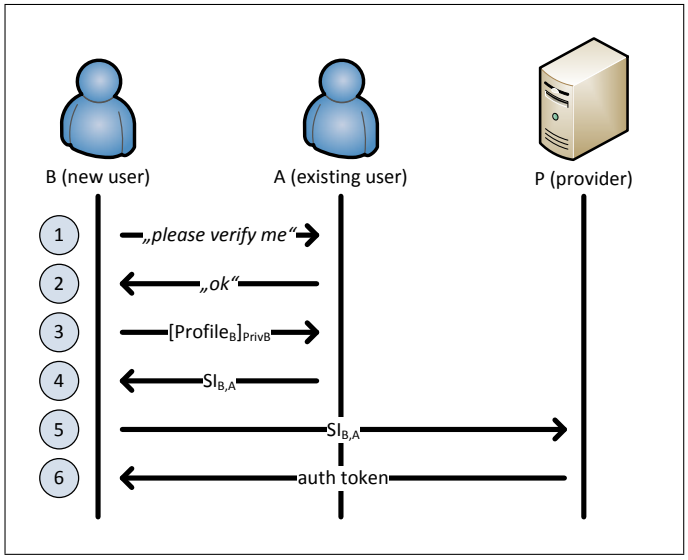

Figure 4. The extended Vis-a-Vis protocol, allowing offline usage.

also be decoupled from the verification itself. In order to activate a given account, the new user then has to be handed over a one-time key from the provider via an existing (authorized) user. This second step requires synchronous communication with the provider and thus has to be replaced by an offline capable mechanism. This mechanism is based on public-key cryptography and is explained in the following.

A. Preliminaries

In the extended activation process, the participating entities again are the provider P, an existing user A and a new user B. P owns a key pair consisting of the private key Priv_P and the corresponding public key Pub_P. The latter has to be known to all participating entities.

Just as before, P stores user profiles containing *Personally Identifying Information (PII)*, such as forename, surname and date of birth. In this extended variant, each user profile furthermore contains the user's public key, i.e., the profile of user A is defined as the tuple:

$$\mathrm{Profile}_A = (\mathrm{Forename}_A, \mathrm{Surname}_A, \mathrm{DateOfBirth}_A, \mathrm{Pub}_A) \quad (8)$$

Of course, A itself has to be in possession of the corresponding private key Priv_A. Essentially, every user in the system owns her own key pair, which then is used to authenticate messages with the help of digital signatures. In the following, the notation $[\mathrm{Data}]_{\mathrm{Priv}_X}$ means that the data packet Data is signed with the private key Priv_X, i.e., its authenticity can be verified with the corresponding public key Pub_X. $[\mathrm{Data}]_{\mathrm{Priv}_X}$ consists of Data itself plus the computed signature $\mathrm{Sig}_{\mathrm{Priv}_X}(\mathrm{Data})$.

B. Offline Verification

The basic idea of the extended protocol is to digitally sign the profile information $\mathrm{Profile}_B$ of a new user B with a private key of which the provider already knows the corresponding public key. The provider then can check that the profile information were verified by an existing user in his system. The extended protocol is depicted in Figure 4.

The process starts with B generating his own key pair consisting of Pub_B and Priv_B and then creating the data packet $[\mathrm{Profile}_B]_{\mathrm{Priv}_B}$. When meeting a suitable existing user A (steps 1 and 2), B transfers this data packet to user A (step 3). The transfer can happen through any communication channel but typically one would employ the same means of data exchange as used for real vis-a-vis transmissions, such as optical codes or NFC.

User A first has to check the validity of the signature of the received packet to make sure that B really is in possession of the corresponding private key of the public key Pub_B, which is included in $\mathrm{Profile}_B$. In case the signature is valid, A signs $\mathrm{Profile}_B$ with his own private key, i.e., A creates the *signed identity*

$$\mathrm{SI}_{B,A} = [\mathrm{Profile}_B]_{\mathrm{Priv}_A} \quad (9)$$

$\mathrm{SI}_{B,A}$ then has to be handed over to user B (step 4). This step now is required to be performed vis-a-vis just like the transmission of the one-time key in the basic protocol (see Section IV-C). It is A's responsibility to transfer the signed identity to the real B only and no one else. So far, the whole process can be performed offline without any interaction with the Vis-a-Vis provider.

Whenever B now is able to establish a connection to the Vis-a-Vis provider, she can authenticate and register herself with the help of the signed identity. To do so, she sends $\mathrm{SI}_{B,A}$ to the provider (step 5). The latter can validate the signature with the help of the users' public keys stored in its database. In case the signature is valid, the provider adds $\mathrm{Profile}_B$ to its database and provides B with a new access token she can use to authenticate herself when accessing any services of the system (step 6).

C. Pending Chain

Regarding the above process, a question may arise: What if B verifies another new user C before B itself has sent its signed identity to the provider, i.e., the provider does not know that B is a valid user? In this case, new accounts such as C arrive in a *pending state*. As C might also verify further users, it is possible for longer *pending chains* to come into existence. Being *pending* means that the provider has received the signed identity of a new user and has provided the user with a (maybe temporary) access token, but has not yet granted any permissions to the new user because there are users in the pending chain, which have not yet presented a valid signed identity to the provider. Whenever the provider receives a new valid signed identity, it has to check all pending users if their pending state can be resolved now.

D. Distributed Permissions

The pending chain essentially is another component in the verification and activation procedure which somehow blocks the process, preventing new users from accessing the system

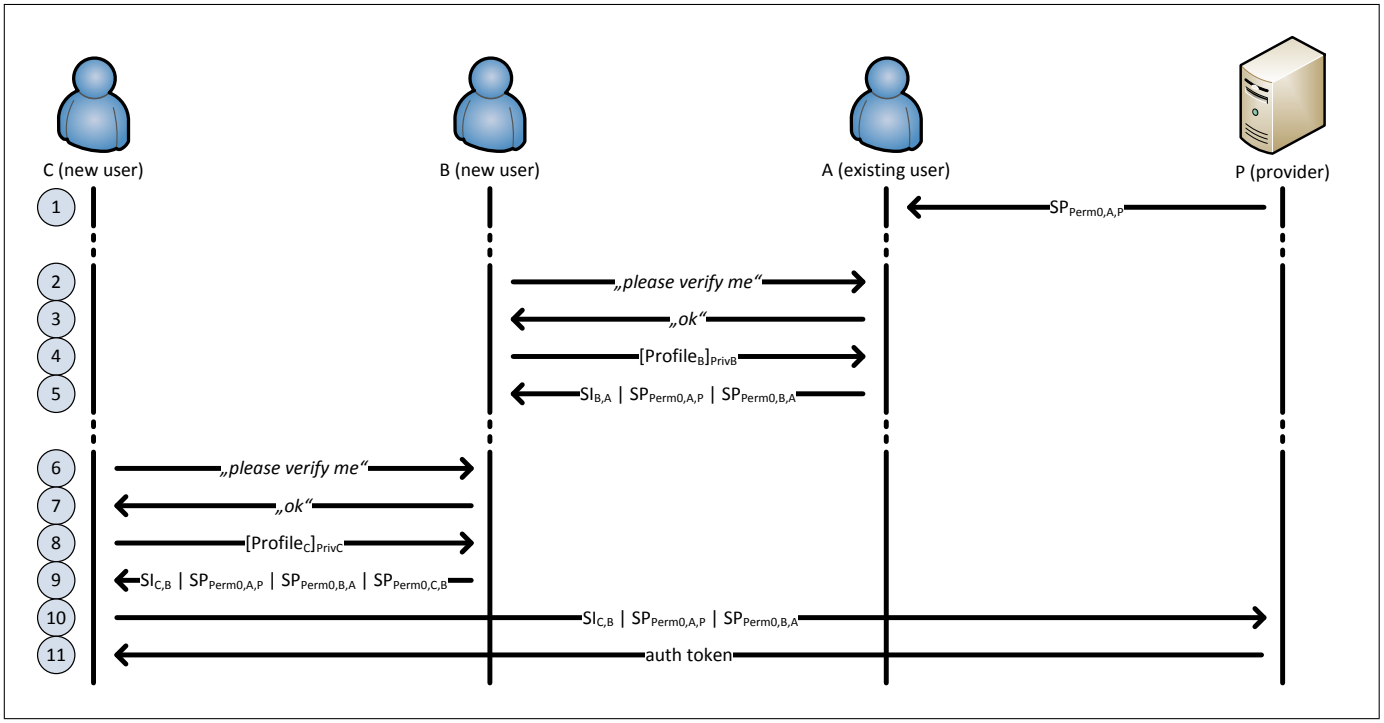

Figure 5. The extended Vis-a-Vis protocol, which is offline-capable and includes distributed permissions management.

before every previous user in the pending chain has been activated. Furthermore, new users cannot make sure that the user who verifies them really is a legit user of the system. In order to solve both these problems, we introduce the concept of *distributed permissions*.

We define a set of permissions

$$\mathrm{Perms} = \{\mathrm{Perm}_0, ..., \mathrm{Perm}_n\} \tag{10}$$

and for each permission Perm_i, we define a set of *prerequisites* $\mathrm{Prereqs}_{\mathrm{Perm}_i} \subseteq \mathrm{Perms}$.

In the most basic case, there is only one permission Perm_0 with the meaning "the user may verify further users". The prerequisite for Perm_0 to be valid is that the issuing entity also has the permission to verify further users, i.e., $\mathrm{Prereqs}_{\mathrm{Perm}_0} = \{\mathrm{Perm}_0\}$. We define a *signed permission* as

$$\mathrm{SP}_{\mathrm{Perm}_i,X,Y} = [(\mathrm{Perm}_i, \mathrm{Pub}_X)]_{\mathrm{Priv}_Y} \tag{11}$$

meaning user Y is issuing permission Perm_0 to user X (represented by her public key Pub_X).

The complete verification procedure with included distributed permissions management is depicted in Figure 5. Let A again be an existing user in the system who should be able to verify new users. A therefore is issued a *signed permission* $\mathrm{SP}_{\mathrm{Perm}_0,A,P}$ by the provider (step 1). When A wants to verify a new user B, she basically follows the procedure as described in Section VI-B but not only hands over the signed identity $\mathrm{SI}_{B,A}$ but also the signed permission $\mathrm{SP}_{\mathrm{Perm}_0,A,P}$ to B. In case B herself should be allowed to verify futher users, A also generates another signed permission $\mathrm{SP}_{\mathrm{Perm}_0,B,A}$ and provides it to B (steps 2 to 5).

As explained in the beginning, every user in the system knows the providers public key Pub_P. B therefore now can validate whether A is a legit user who is allowed to verify further users by checking the signature of the signed permission $\mathrm{SP}_{\mathrm{Perm}_0,A,P}$ with the help of Pub_P and by checking the signature of $\mathrm{SI}_{B,A}$ with the help of Pub_A, which is included in the signed permission. The latter is necessary to make sure that A really is in possession of the private key Priv_A, which corresponds to the public key Pub_A to which the permission Perm_0 was issued.

B now can verify another user C by following the same procedure as above (steps 6 to 9). However, B has to provide several information packets to C, which are needed to represent the current verification state:

1) $\mathrm{SI}_{C,B}$
2) $\mathrm{SP}_{\mathrm{Perm}_0,A,P}$
3) $\mathrm{SP}_{\mathrm{Perm}_0,B,A}$
4) $\mathrm{SP}_{\mathrm{Perm}_0,C,B}$ (optional)

Based on these information, both C itself as well as the Vis-a-Vis provider are able to validate the correctness of C's verification, even without B being activated yet. To do so, one has to recursively check the provided information. First, the signature of the signed identity $\mathrm{SI}_{C,B}$ is checked with the help of public key Pub_B, which is included in the signed permission $\mathrm{SP}_{\mathrm{Perm}_0,B,A}$. Then, it has to be made sure that Pub_B belongs to an entity which is allowed to verify new users, i.e., which has been issued the permission Perm_0. Therefore, the signature of the signed permission $\mathrm{SP}_{\mathrm{Perm}_0,B,A}$ has to be checked with the help of the public key Pub_A,

which is included in the signed permission $\mathrm{SP}_{\mathrm{Perm}_0,A,P}$. Since A is another user and not the provider itself, it now has to be checked whether A has the preconditional permissions to issue Perm_0. In this case, this means that A must also have been issued permission Perm_0. The latter can be validated by checking the signature of the signed permission $\mathrm{SP}_{\mathrm{Perm}_0,A,P}$ with the help of the pre-shared public key Pub_P of the provider.

By including the complete history of issued permissions in a given verification chain (which can be of arbitrary length), the validity of a user verification can be checked independently of the state of previously verified users. Thus, upon receiving and validating such a verification chain (step 10), the provider may hand out an access token to any verified user, no matter if all the other users in the verification chain have been activated yet (step 11). Futhermore, each user who gets verified by another user can also check by herself whether the verification was valid or not, thus preventing misuse of the offline verification feature.

The usage of signed permissions also enables more complex permission sets. One use case would be to limit the length of verification chains, e.g., that only chains of maximum length 2 are allowed. In this case, one could define the following permissions:

- Perm_0: "the user may verify further users"
- Perm_1: "the user may issue Perm_0"
- Perm_2: "the user may issue Perm_1"
- $\mathrm{Prereqs}_{\mathrm{Perm}_0} = \{\mathrm{Perm}_1\}$
- $\mathrm{Prereqs}_{\mathrm{Perm}_1} = \{\mathrm{Perm}_2\}$

An existing user A then might be issued Perm_0 and Perm_1 by the provider. A now can verify another user B because he has permission Perm_0. He furthermore can issue Perm_0 to the new user B because he has permission Perm_1. Consequently, B can verify another user C. However, B cannot issue Perm_0 to another user because B does not have permission Perm_1. Perm_1 can only be issued by someone having permission Perm_2, which in this case is limited to the provider itself, thus preventing longer verification chains.

VII. Implementation

We have implemented and deployed the proposed concept in a real production environment at an educational institution. In this section, we will briefly describe the technical implementation of the various components.

The technical part of the Vis-a-Vis provider has been realised as a backend service, which is programmatically accessed through a REST interface. It furthermore provides a web interface, which is intended for account creation. We employ a weighted tree of trust (see Section IV-F), i.e., regarding the users' devices as the tree's nodes and allowing for self-activation of more than one device. Devices are running a custom application, which stores the authentication token and furthermore is used to access protected content provided by the institution.

When a new user wants to create an account, she does so using a dedicated account creation web interface of the Vis-a-Vis provider. Thereby, the user has to provide some personal credentials like name and date of birth, as well as her affiliation to certain groups or departments of the institution. When submitting the registration request, a QR code containing a unique account ID is shown. The user has to scan the code with her smartphone running our custom application, which results in an association of the user's device to the newly created account. It has to be noted that at that point in time, only the association is created, the account itself is not activated, i.e., the user cannot access any protected content, yet.

After that, the user has two choices. She either proceeds to print out a document containing her account credentials including the associated account ID. She then has to sign the document and to provide it to authorized personnel at the institution. The latter now check the provided credentials, verify the identity of the new user and then can activate the associated account. The user now can access the protected content and has become a seed user, as she was verified by the Vis-a-Vis provider itself. The seemingly cumbersome usage of printed documents is introduced because at the given institution, it is legally required that the to-be-created seed users sign a consent form. Thus, the Vis-a-Vis system is integrated into the existing workflow.

The alternative way of activating an account is via an existing user. The system is configured to allow existing users to activate new users which belong to the same group. In our mobile application, existing users can browse through and select users which they can activate. They can request the needed one-time key from the provider, which then is encoded in a QR code. The new user can scan this code, resulting in the described protocol being carried out (see Section IV-C). Consequently, the new user has become a non-seed user.

VIII. Applications

The Vis-a-Vis concept is predestined to be used at any organisation with a hierarchical structure such as companies, educational institutions, clubs or small project teams. In the following, we describe two use cases, in which our system perfectly fits the inherent structure of the scenario.

A. Use in Companies

A company usually is organised in a hierarchical way, composed of departments and teams, where permissions often should be assigned in accordance to that structure. This perfectly fits the basic building blocks of the Vis-a-Vis system, where senior employees might activate other employees. The hybrid approach of the Vis-a-Vis system ensures that some kind of central authority is present and thus, that seed users can be trusted. Each principal of the respective hierarchy level acts as the responsible seed user of his subordinates. As an example, the CEO of a company would act as a main seed user and unlock its subordinate head of department. In the following, department heads can activate their subordinate team leaders, and so on.

The resulting tree of trust can be used to assign permissions and capabilities, not only based on the user's role but also on her distance to the last directly verified user (which can be measured by the distance from root metric).

B. Use in schools

Another interesting use case is constituted by educational institutions, e.g., schools. This in fact is the scenario in which we have already deployed the system. Within a school, several roles exist, such as teachers, students and parents. These roles are subject to a predetermined hierarchy with different permissions. Furthermore, it is of highest relevance that user identities are verified, i.e., parents and teachers can be sure that they are corresponding with each other.

In this case, initially only the director of a school might have access to the system. As a director representing the highest authority within the school, he has the ability to unlock teachers as seed users. These in turn have the privilege to unlock students who belong to their assigned classes. Students can then activate their parents and give them the permission to access the school network, too.

A key benefit in this use case is the decreasing administrative costs because of the convenient but secure delegation of activation responsibilities.

In case a written agreement from the parents is required by law, the Vis-a-Vis concept is also employable, with parents being authorized directly by the school management (and therefore becoming seed users). Parents then are able to activate further family members by themselves.

In some of our real deployment environments in Germany we found that the school building (sometimes intentionally) is constructed to attenuate or even completely shield mobile network signals, in order to prevent mobile phone usage during lessons and tests. Wifi networks typically are reserved for faculty members. Consequently, our basic (synchronous) protocol was not usable in these environments. We therefore developed the extended protocol as described in Section VI, which allows to verify student accounts within the school building even while being offline. The students later can complete the registration procedure after school, when they are back to having internet access.

IX. Conclusion and future work

In this paper, we presented a novel approach to combine the concept of identity verification through physical presence with the authentication factor ownership, i.e., authentication by something you have. We defined a structure called tree of trust, on which a distance from root metric can be calculated. The latter is a measure for a node's trustworthiness, i.e., it can be used as a parameter for permission assignment. By extending the concept to weighted trees of trust, one can also allow for self-activation of further devices as well as activation by more insecure means, resulting in a lower trustworthiness value. We described several ways for adding, removing, promoting and demoting nodes in the tree, which shows its applicability to various use cases. The system perfectly fits scenarios which inherently exhibit some kind of hierarchy and require a central authority, but in which identity verification tasks should be distributed among the system's users.

In order to allow distributed verification even without internet connection (i.e., without being able to communicate with the central authority), we presented an extended protocol including distributed permissions management, which allows for offline usage of main parts of the Vis-a-Vis system. The distributed permissions system is flexible enough to even allow complex permissions such as to limit the verification chain to a certain maximum length.

In future work, it will be interesting to investigate the integration of proximity proofs, i.e., to check whether the transmission of the one-time key really has taken place vis-a-vis, i.e., in direct physical proximity. This would further increase the system's security and the reliability on the trustworthiness of activated accounts. It is of even higher interest in the case of our extended protocol. The necessary information to represent longer verification chains (including public keys, etc.) can become too large to be encoded in optical codes and NFC is still not supported by lots of devices. Thus, it might be required to offload data transfer to communication channels such as Bluetooth, which has a too long range to be called a vis-a-vis channel. Integrating proximity proofs would greatly improve the system's trustworthiness in this case.

We are furthermore investigating how the offline-capable and distributed trust and permissions features could be extended to allow for peer-to-peer operation in order to completely omit a central authority.

References

[1] M. Maier, C. Marouane, C. Linnhoff-Popien, B. Rott, and S. A. Verclas, "Vis-a-vis verification: Social network identity management through real world interactions," in SOTICS 2013, The Third International Conference on Social Eco-Informatics, 2013, pp. 39–44.

[2] International Telecommunications Union, "Key ict data for the world," http://www.itu.int/en/ITU-D/Statistics/Pages/stat/default.aspx, 2013, last accessed date: 2014-05-31.

[3] "Facebook key facts," http://newsroom.fb.com/Key-Facts, 2013, last accessed date: 2014-05-31.

[4] "Facebook login," https://developers.facebook.com/docs/facebook-login/, 2013, last accessed date: 2014-05-31.

[5] "Openid," http://openid.net/, last accessed date: 2014-05-31.

[6] "Postident," http://www.deutschepost.de/de/p/postident.html, last accessed date: 2014-05-31.

[7] N. Chou, R. Ledesma, Y. Teraguchi, D. Boneh, and J. C. Mitchell, "Client-side defense against web-based identity theft," in Proceedings of the 11th Annual Network and Distributed System Security Symposium, 2004.

[8] T. V. N. Rao and K. Vedavathi, "Authentication using mobile phone as a security token," International Journal of Computer Science & Engineering Technology, vol. 1, no. 9, pp. 569–574, October 2011.

[9] G. Coulouris, J. Dollimore, and T. Kindberg, Distributed Systems: Concepts and Design (4th Edition) (International Computer Science). Boston, MA, USA: Addison-Wesley Longman Publishing Co., Inc., 2005.

[10] M. Georgiev et al., "The most dangerous code in the world: validating ssl certificates in non-browser software," in Proceedings of the 2012 ACM conference on Computer and communications security, 2012, pp. 38–49.

[11] J. Golbeck, B. Parsia, and J. Hendler, "Trust networks on the semantic web," in Cooperative Information Agents VII, ser. Lecture Notes in Computer Science, M. Klusch, A. Omicini, S. Ossowski, and H. Laamanen, Eds. Springer Berlin Heidelberg, 2003, vol. 2782, pp. 238–249.

[12] P. R. Zimmermann, The official PGP user's guide. Cambridge, MA, USA: MIT Press, 1995.

[13] S. L. Presti, "A tree of trust rooted in extended trusted computing," in Proceedings of the Second Conference on Advances in Computer Security and Forensics Programme, 2007, pp. 13–20.

[14] I. Verbauwhede and P. Schaumont, "Design methods for security and trust," in Design, Automation & Test in Europe Conference & Exhibition, 2007, pp. 1–6.

In-Memory Computing Enabling Real-time Genome Data Analysis

Matthieu-P. Schapranow* Franziska Häger* Cindy Fähnrich* Emanuel Ziegler† Hasso Plattner*

*Hasso Plattner Institute
Enterprise Platform and Integration Concepts
August–Bebel–Str. 88
14482 Potsdam, Germany
{schapranow|franziska.haeger|cindy.faehnrich|plattner}@hpi.uni-potsdam.de

†SAP AG
Dietmar-Hopp-Allee 16
69190 Walldorf, Germany
emanuel.ziegler@sap.com

***Abstract*—Latest medical diagnostics, such as genome sequencing, generate increasing amounts of "big medical data". Healthcare providers and medical experts are facing challenges outside of their original field of expertise, such as data processing, data analysis, or data interpretation. Specific software tools optimized for the use by the target audience as well as systematic processes for data processing and analysis in clinical and research environments are still missing. Our work focuses on the integration of data acquired from latest next-generation sequencing technology, its systematical processing, and instant analysis for researchers and clinicians in the course of precision medicine. We focus on the medical field of oncology to optimize the time spent on acquiring, combining, and analyzing relevant data to make well-informed treatment decisions based on latest international knowledge. We share our research results on building a distributed in-memory computing platform for genome data processing, which enables instantaneous analysis of genome data for the first time. For that, we present our technical foundation and building blocks of in-memory technology as well as business processes to integrate genome data analysis in the clinical routine.**

***Keywords*-Genome Data Analysis, Process Integration, In-Memory Database Technology, Precision Medicine, Next-Generation Sequencing, Alignment, Variant Calling.**

I. Introduction

We present our findings in providing specific software tools for clinicians and researchers in the course of precision medicine for integration of high-throughput genome data as source of diagnostic insights [1]. Precision medicine aims at treating patients specifically based on individual dispositions, e.g., genetic or environmental factors [2]. For that, researchers and physicians require a holistic view on all relevant patient specifics when making treatment decisions. Thus, the detailed acquisition of medical data is the foundation for personalized therapy decisions. The more fine-grained the available data is, the more specific the gained insights will be, but the complexity of data processing will rise as well. It requires tool support to identify the relevant portion of data out of the increasing amount of acquired diagnostic data [3].

Figure 1. Data processing steps involved in the analysis of genome data. Sequencing the samples results in chunks of DNA available in digital form. During alignment their position within the whole genome is mapped. Variant calling results in a list of differences of a fixed reference. The analysis obtains new insights based on the list of detected variants.

Figure 1 depicts the genome data workflow in the course of precision medicine. After a sample has been acquired, it is sequenced, which results in short chunks of Deoxyribonucleic Acid (DNA) in digital form. The DNA chunks need to be aligned to reconstruct the whole genome and variants compared to a reference, e.g., normal vs. pathologic tissue, are detected during variant calling. The analysis of genome data builds on the list of detected variants, e.g., to identify driver mutations for a medical finding [4].

Nowadays, Next-Generation Sequencing (NGS) devices are able to generate diagnostic data with an in-

creasing level of detail. In contrast to the first draft of the human genome, which involved thousands of institutes for more than one decade, modern NGS devices process a whole human genome within hours [5]. Nowadays, a sample of human tissue can be processed with more than 30x coverage in approx. 27 hours [6]. However, the increased level of detail results in additional data processing challenges. The following list summarizes selected data processing challenges, which are discussed in more detail in the remainder of our contribution.

- The sheer amount of generated DNA data is a challenge even for modern computer systems, e.g., per sequenced sample of a human tissue approx. 300-500 GB of raw data is generated digitalizing the human DNA with approx. 30x coverage.
- Raw DNA data needs to be processed prior to its analysis, which takes hours to days, i.e., alignment of DNA chunks to reconstruct a complete genome and identify variants compared to a known reference in the variant calling phase as depicted in Figure 1. Reducing the time for data processing would result in earlier start of data analysis.
- The availability of hundreds or thousands of individual cores in a modern computer cluster requires on the one hand the partitioning of the available data so that on the other hand specific algorithms can process this data in parallel.
- The analysis of genome data still involves big data, e.g., hundreds or millions of individual genetic variants. However, only a minority of these variants is connected to a certain disease, the majority of variants are not responsible for any malign changes. Thus, the analysis of genome data is an iterative and not a batch-oriented process. It consists of creating new hypotheses and their verification and requires software tools that support this kind of interactive analysis and exploration of genome data.

Figure 2 provides a comparison of costs for sequencing and main memory modules on a logarithmic scale. Both graphs follow a steadily declining trend, which facilitates the increasing use of NGS for whole genome sequencing and In-Memory Database (IMDB) technology for data analysis. Latest NGS devices enable the processing of whole genome data within hours at reduced costs [9]. The time consumed for sequencing is meanwhile a comparable small portion of the time consumed by the complete workflow. As a result, data processing and its analysis consume a significantly higher portion of the time and accelerating them would affect the overall workflow duration.

Our contribution focuses on how to optimize the time-consuming data processing and analysis aspects of the workflow by combining latest software and hardware

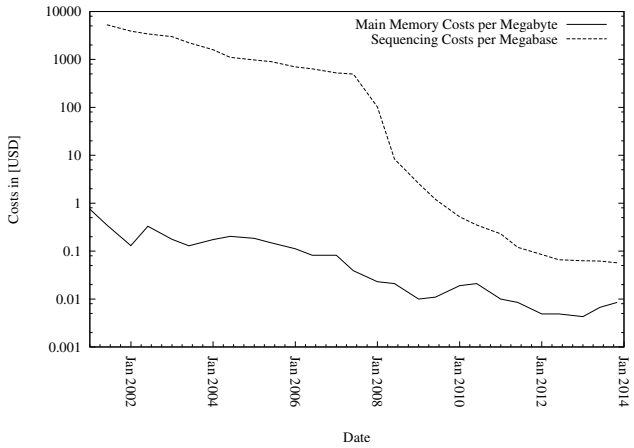

Figure 2. Costs for next-generation sequencing and main memory 2001-2014 adapted from [7], [8].

trends to create an integrated software system, which supports life science experts in their daily work.

The rest of this contribution is structured as follows: In Section II our work is set in the context of related work. We give a deeper understanding of in-memory computing in Section III and share concrete design decisions of our software architecture in Section IV. In Section V we outline our experiment setup and acquired results. An evaluation and discussion of our obtained results is given in Section VI while our work concludes in Section VII.

II. Related Work

The amount of related work in the field of genome data processing has increased in the last years. However, work focusing on the implementation of end-to-end processes and the improvement of scientific work is still rare. Thus, our work focuses on the integration of these aspects.

Pabinger et al. evaluated workflow systems and analysis pipeline tools [10]. They observed that existing tools either miss flexibility or the end-user needs specific know-how to install and operate them properly. We address this by introducing a combined system for modeling and execution of individual pipeline configurations without the need to adapt command line scripts as presented in Section IV-D.

Additionally, Pabinger et al. analyzed a variety of variant analysis tools and evaluated their functionality. For web-based tools they see a drawback in the required data preparation before the desired analysis can start, because "[...] files need to be packed, sorted and indexed before they can be used" [10]. We address time-consuming data transformations and preparations by replacing them by native database operations within our incorporated IMDB as outlined in Section IV.

Wandelt et al. observed in their evaluation a trend towards more and more cloud-based NGS data management solutions [11, Section 4.3]. We also believe that cloud-based software systems for processing and analysis of NGS data have advantages over local installations. For example, the setup, configuration, and operation of such systems requires trained personnel with specific bioinformatics background, which can be reduced by using cloud-based services. Cloud-based approaches also reduce costs for permanent local hardware resources, maintenance, and operation [12].

Wandelt et al. also identified the efficient mapping of workflow tasks in distributed computing environments and the adjustment of a given workflow to a dynamic environment as open issues. Our contribution addresses the modeling of workflows with a dedicated modeling notation as outlined in Section IV-D and their execution and resource allocation with a dedicated framework for scheduling as discussed in Section IV-G.

A first approach to distribute genome data analysis on a cluster of machines is Crossbow [13]. They use Hadoop for parallelization and built a pipeline that uses Bowtie for alignment and SOAPsnp for SNP detection [14], [15]. Their analysis pipeline took less than three hours on Amazon's Elastic Compute Cloud (EC2) with 320-cores distributed across 40 nodes for a 38x coverage genome. However, their approach was designed for a specific pipeline setup and requires extra work for adaptations, e.g., by adding additional variant calling algorithms. We enable users of our platform to adapt their pipelines individually using a graphical modeling notation as described in Section IV-D.

Our work contributes by providing a system architecture that combines processing and analyzing of genome data within a single system as outlined in Section IV. As part of our system architecture, we created a worker framework developed with the Python programming language, which enables integration of computing resources across platform and Operating System (OS) borders. Furthermore, our task scheduler controls the execution of a given workflow, e.g., prioritized processing of individual pipeline steps, as described in Section IV-G. It enables parallel data processing of multiple tasks as described in Section IV-E, e.g., to handle simultaneous user requests or tasks from multiple departments at the same point in time.

Galaxy, GenePattern, or Mobyle are selected related projects in the field of Reproducible Research Systems (RRS), which focus on enabling researchers to acquire, process, and document scientific data in a systematic, transparent, and reproducible way [16], [17], [18].

We address these fields with our platform as well as, e.g., among others by the following aspects:

- Graphical modeling and exchange of analysis workflows using a standardized modeling notation as described in Section IV-D,
- Enabling reproducible research results by sharing data and workflows with other users as described in Section IV-F, and
- Integration of latest international research databases using our annotation framework as described in Section IV-I.

III. Building Blocks of In-memory Computing

We refer to IMDB technology as a toolbox of IT artifacts to enable processing of enterprise data in real-time in the main memory of server systems [19]. Figure 3 depicts selected in-memory computing building blocks. The use of IMDB technology for genome data analysis is driven by the declining cost developments for NGS and main memory modules as described in Section II.

In the following, we outline selected building blocks of in-memory computing and their relevance for real-time analysis of genomic data in the context of our work.

A. Combined Column and Row Store

Historically, separate database systems for processing of analytical and transactional data evolved. The former store and process data in a row-oriented format, i.e., attributes of one record are stored side by side, while analytical database systems are optimized to scan selected attributes of huge data sets rapidly, e.g., by maintaining pre-aggregated totals.

If complete data of a single row needs to be accessed, storing data in a row format is advantageous. For example, the comparison of two customers involves all of their database attributes, such as inquirer's name, time, and content need to be loaded. In contrast, columnar stores benefit from their storage format when only a subset of attributes needs to be processed. For example, adding up the gender ratio of patients treated in a certain period of time only involves the attributes date and gender, but the remainder, such as name and birth date, are not required. Using a row store for this purpose would require processing of all attributes, although only two of these attributes are required. Therefore, a columnar store benefits from accessing only relevant data.

Combining column and row stores improves any kind of analytical queries while keeping transactional response times low. In our case, the use of columnar stores supports the comparison of multiple genomes to identify common mutations in the blink of an eye.

B. Complete History

Keeping the complete history of values even after individual data points have been updated or changed is the purpose of the insert-only or append-only technique. Insert-only is a data management approach that stores

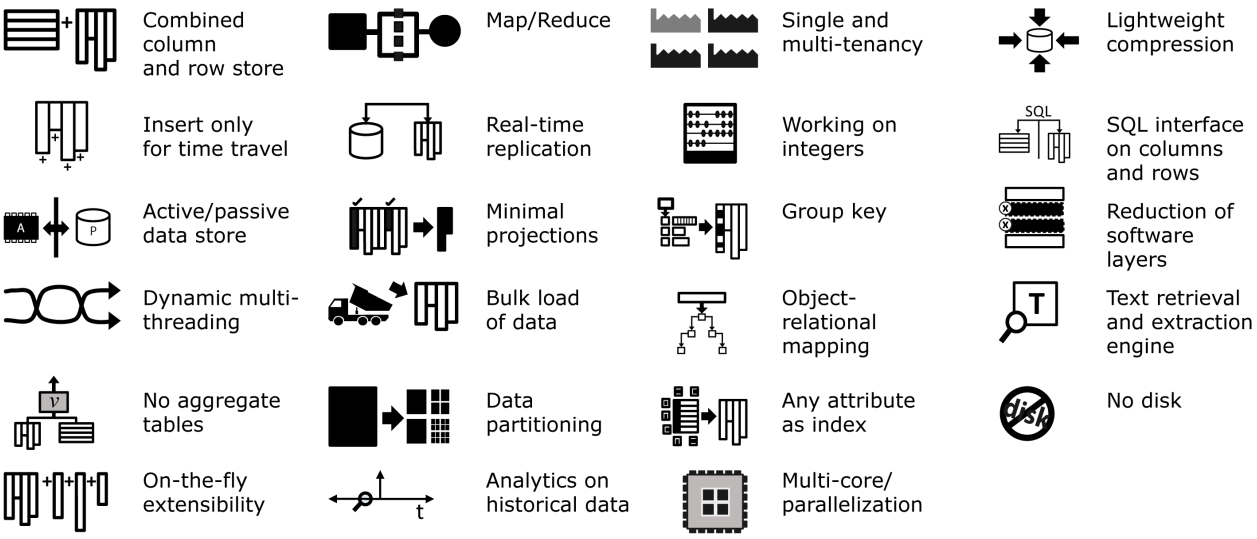

Figure 3. Selected in-memory computing building blocks.

data changes as new entries. Traditional database systems support four operations for data manipulation, i.e., insert, select, delete, and update of data. The latter two are considered as destructive operations since the original data is no longer available after their execution [20, Section 7.1]. In other words, it is neither possible to detect nor to reconstruct the values for a certain attribute after their execution since only the latest value is persistently stored in the database. Insert-only database tables enable storing the complete history of value changes and the latest value for a certain attribute [3]. This is the foundation of worldwide bookkeeping systems guaranteeing transparency.

Insert-only can also be used to trace decisions, e.g., in course of incident analysis. For example, consider a Clinical Information System (CIS) that is used to store latest decisions on medical dosages. If you directly replace the current value by a new value for the dosage, it is impossible to track when a patient received what dosage of a certain drug. Nowadays, updated dosages are stored as a new entry with a dedicated timestamp when they were applied. Using insert-only does not require this workaround and you can easily update the current dosage while the IMDB keeps a complete history of all changes. Thus, the IMDB is capable to reconstruct the global database state for any point in time using a specific database query.

C. Lightweight Compression

Lightweight compression techniques refer to a data storage representation that consumes less space than its original pendant [19]. A columnar database storage layout, as used in IMDBs, supports lightweight compression techniques, such as run-length encoding, dictionary encoding, and difference encoding [21]. Typically, values of a database attribute are within a limited subset of the attribute's full data domain, e.g., `male` and `female` for the gender type. The lightweight compression technique dictionary encoding, for example, maps all unique values to a uniform format, e.g., `male=1` and `female=2`.

The application developer can apply this technique during design time. However, IMDBs automatically perform lightweight compression optimized for the specific data to store. As a result, there is no longer an explicit need to map data from a human-readable format to an optimal storage representation since it is done transparently by the IMDB. Thus, the time to create new applications is reduced, the maintainability of the application code is improved since the source code is easier to understand, and any data stored in the database benefits from this kind of optimization without the need for explicit consideration in the application's code by the software developer.

For example, the International Code of Diseases (ICD) is identical for patients suffering from the same disease. Instead of storing the ICD redundantly in the database, dictionary compression stores it once and maps it to a smaller integer representation. Thus, only the corresponding integer value is stored in the database and all queries are rewritten to use the integer representation instead. The original representation is replaced just before the result set is returned to the client. As a result, the database executes all operations on compressed data without the need for explicit decompression, which improves cache-hit ratio since more compressed data fits into the same amount of cache memory [19].

D. Parallel Data Processing

Latest computer systems consist of multiple cores per individual Central Processing Unit (CPU), which is referred to as multi-core architecture [22, Chap. 2]. Additionally, a single server system can be equipped with multiple CPUs multiplying the amount of available computing cores, which is referred to as multi-CPU architecture [22, Chap. 2]. The hardware of a single computer system is designed to perform multiple processing tasks simultaneously. However, to use all available computing resources most efficiently software needs to incorporate specific instructions to explicitly make use of parallelization features, e.g., when adding up multiple values using the Parallel Addition (PADD) instruction [23, Chap. 5.3].

Parallelization can be applied to various locations within the application stack of software systems – from within the application running on an application server to query execution in the database system. For example, multiple clinical departments access the data of a single patient simultaneously. Processing multiple queries can be handled by multi-threaded applications, i.e., the application does not stall when dealing with more than one query at the same time. OS threads are a software abstraction that needs to be mapped to physically available hardware resources [24, Chap. 2].

A CPU core is comparable to a single worker on a construction area. If it is possible to map each query to a single core, the system's response time is optimal. Query processing also involves data parallelization, i.e., the database needs to be queried in parallel, too. If the database is able to distribute the workload across multiple cores, a single server works optimal. If the workload exceeds physical capacities of a single system, multiple servers or blades need to be installed for distribution of work to reach optimal processing behavior. From the database point of view, data partitioning supports parallelization since multiple CPU cores even on multiple servers can process data simultaneously [25, Chap. 6].

This example shows that multi-core architectures and parallelization depend on each other while data partitioning forms the basis for parallel data processing.

E. Data Partitioning

We distinguish between vertical and horizontal data partitioning [26].

Vertical partitioning refers to rearranging individual database columns. It is achieved by splitting columns of a database table in two or more sets of columns. Each of the sets can be distributed individually, e.g., on separate databases servers. This technique can also be used to maintain the same database column in different ordering to achieve better search performance for mixed workloads while guaranteeing high-availability of data [27]. Key to success of vertical partitioning is a thorough understanding of data access patterns. Attributes that are accessed in the same query should be located in the same partition since identifying and joining additional columns result in additional query processing overhead.

In contrast, horizontal partitioning addresses long database tables and how to divide them into smaller chunks of data. As a result, each portion of the database table contains a disjoint subset of the complete data. Splitting data into equivalent long horizontal partitions is used to support parallel search operations across all data of a database table and to improve scalability [19].

The identification of CpG Islands (CGIs) is a concrete application example: CGIs are known to represent unstable chemical compounds [28]. Their identification requires a full scan of the genome database table to identify positions where the bases cytosine and guanine are direct neighbors. Applying a horizontal partition per chromosome for the genome table enables scanning of all chromosomes in parallel. Furthermore, applying horizontal partitioning to each of the chromosome database tables enables processing of each individual chromosome by individual CPU resources, e.g., CPU cores.

F. Active and Passive Data

We distinguish two categories of data: active and passive. We refer to active data when it is frequently accessed and updates are expected to occur on regular basis, e.g., data of patients currently treated in a hospital. In contrast, passive data is neither updated nor accessed regularly. It is purely used for analytical and statistical purposes or in exceptional situations where specific investigations require this data. For example, tracking events of a certain pharmaceutical product that was sold five years ago can be considered as passive data. Firstly, from the business' perspective, the pharmaceutical can be consumed until the best-before date, which is reached two years after its manufacturing date. When the product is handled now, five years after it's manufacturing, it is not allowed to sell it any longer. Secondly, the product was most probably sold to a customer four years ago, i.e., it left the supply chain and is typically already used within its best-before data. Therefore, the probability that details about this pharmaceutical are queried is very low. Nonetheless, the tracking history is conserved and no data is deleted in conformance to legal regulations. As a result, the passive data can still be accessed but with a higher latency than active data. Thus, passive data results in a classification of data stores. For example, passive data can be used for reconstructing the path of a product within the supply chain or for a financial long-term forecast.

Dealing with passive data stores involves the definition of a memory hierarchy including fast, but expensive, and

slow, but cheap memory. A possible storage hierarchy is given by: memory registers, cache memory, main memory, flash storages, Solid State Disks (SSDs), Serial Attached SCSI (SAS) hard disk drives, Serial Advanced Technology Attachment (SATA) hard disk drives, and magnetic tapes [3].

Thus, active data that needs to be accessed in real-time can be separated from passive data that is ready for archiving. When data is moved to a passive data store, it frees fast accessible data stores, e.g., main memory.

To distinguish between active and passive data, rules for migration of data from one store to another need to be defined. We refer to them as data aging strategy or aging rules. We consider the process of aging, i.e., the migration of data from a fast to a slower medium as background task, which is performed regularly, e.g., once a month or once a week. Since this process involves reorganization of the entire database, it should be performed only during times of low database access, e.g., at night or on weekends.

G. Text Search and Text Mining

We distinguish the following categories of data:

- Structured data sources: We define structured data as data stored in a format, which can be used for automatic processing by computers. Examples for structured data are ERP data stored in relational database tables, tree structures, and arrays.
- Unstructured data sources: We define unstructured data as the opposite of structured data, which cannot be processed automatically, e.g., all data that is available as raw documents, such as videos or pictures. In addition, any kind of unformatted text, such as freely entered text in a text field, textual documents, or spreadsheets, are considered as unstructured data unless a machine-readable data model exists for automatic interpretation, e.g., a possible semantic ontology.

In the following, we outline selected features of text search that can be incorporated by IMDB technology.

Fuzzy search handles a specified level of fuzziness in search queries automatically, e.g., typing errors. It blows up the pool of words that are searched for by inverting pairs of letters or scrambling them. With these methods additional words can be found that are stored in a wrong format in the data set to search in. This is very helpful if humans added the data stored in the database, e.g., people, who search for terms, as well as people, who create textual content may add misspelled data. For example, a doctor's letter can contain various descriptions for the same result, e.g., "carcinoma", "karzinom", or "carzinoma". Fuzzy search helps to identify these entities as relevant for the same search query.

Synonym search addresses the challenge that different words can have identical meanings. These synonyms can be used in various contexts, but the search query typically only contains a single representation. For example, the medical abbreviation "ca." and "carcinoma" can be considered as synonyms. However, "ca." can also be the abbreviation for "circa". In other words, synonyms have individual meanings per context. To keep track of them, abbreviations should be considered by their probability in the active application context.

Entity and feature extraction refers to the identification of relevant keywords and names of entities from documents. This is comparable to tagging in online web blogs when certain additional meta information is associated to a document. Entity extraction can be customized by dictionaries and individual extraction rules. In this context, dictionaries are lists of entities with an assigned entity type that enable the database to recognize the listed entities in unstructured text. A dictionary contains one or more entity types, each of which contains any number of entities. Each entity in turn contains one standard form name and any number of synonyms. Extraction rules, define the entities of a specific type using a formal syntax. Such syntax allows formulating patterns that match tokens by using a literal string, a regular expression, a word stem, or a word's part-of-speech.

IV. High-Performance In-Memory Computing Platform

Figure 4 depicts the software system architecture of our high-performance in-memory computing platform with application, platform, and data layer as Fundamental Modeling Concepts (FMC) block diagram [29]. Our High-Performance In-Memory Computing Platform combines data from various data sources, such as patient-specific data, genome data, and annotation data within a single system. Thus, it enables flexible real-time analysis and combination of data in an interactive way for the first time. In the following, we share details about design decision and software components of our system.

A. Data Layer

The data layer holds all required data for performing processing and analyzing of genomic data. The data can be distinguished in the two categories master data and transactional data [30]. For example, human reference genomes and annotation data are referred to as master data, whereas patient-specific NGS data and Electronic Medical Records (EMR) are referred to as transactional data [31], [32]. Their analysis is the basis for gathering specific insights, e.g., individual genetic dispositions and to leverage personalized treatment decisions in course of precision medicine [2].

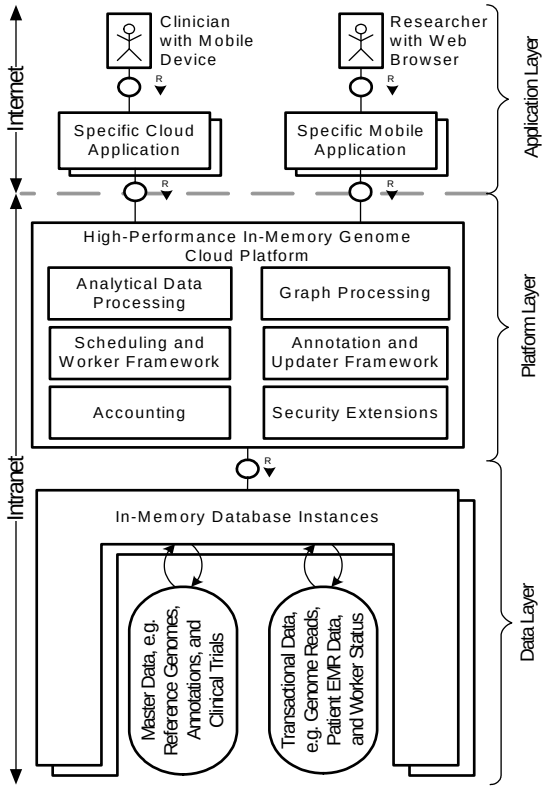

Figure 4. Our system architecture consist of application, platform, and data layer. Analysis and processing of data is performed in the platform layer eliminating time-consuming data transfer.

The actual step of analyzing the genetic data requires answering very specific questions. Thus, our application layer consists of specific applications to answer these questions. They make use of the platform layer to initialize and control data processing.

B. Application Layer

The application layer consists of special purpose applications to answer medical and research questions. You can access our cloud services online at http://www.analyzegenomes.com. We provide an Application Programming Interface (API) that can be consumed by various kinds of applications, such as web browser or mobile applications. Figure 4 depicts the data exchange via asynchronous Ajax calls and JavaScript Object Notation (JSON) [33], [34]. As a result, accessing data and performing analyses is no longer limited to a specific location, e.g., the desktop computer of a clinician. Instead, all applications can be accessed via devices connected to the Internet, e.g., laptop, mobile phone, or tablet computer. Thus, having access to relevant data at any time enhances the user's productivity. The end user can access our cloud applications via any Internet browser after registration. Selected cloud applications are our clinical trials search and our patient cohort

Figure 5. The patient-specific clinical trial search results based on the individual anamnesis of a patient. It extracts relevant entities from the free-text description of the clinical trial with the help of specific text-mining rules.

analysis, which are described in further details in the following [35].

1) Clinical Trials Application: Our clinical trials search assists physicians in finding adequate clinical trials for their patients. It analyses patient data, such as age, gender, preconditions, and detected genetic variants, and matches them with clinical trials descriptions from clinicaltrials.gov [36]. Furthermore, it incorporates details about the clinic a patient is treated in, e.g., to distinguish internal and external clinical trials to emphasize the link to colleagues from the same clinic. Our analysis incorporates more than 130,000 clinical trial descriptions, which are processed and ranked in real-time accordingly to the personal anamnesis of each individual patient. The ranked results are summarized on a single screen and provided to the researcher as depicted in Figure 5.

The clinical trials search incorporates the extraction of entities and features from the textual descriptions as described in Section III-G. We developed a set of specific dictionaries. For example, we use a dictionary for human gene identifiers with more than 120,000 gene names and synonyms and a dictionary for pharmaceutical ingredients with more than 7,000 entries. Our dictionaries incorporate a set of standardized vocabularies, e.g., the Metathesaurus Structured Product Labels (MTHSPL) of the Unified Medical Language System (UMLS) [37].

2) Patient Cohort Analysis: Figure 6 depicts our cohort analysis application. It enables researchers and clinicians to perform interactive clustering on the data stored in the IMDB, e.g., k-means and hierarchical clustering as shown in Figure 6 [38, Chap. 13]. Thus, they are able to verify hypotheses by combining patient and genome, and annotation data in real-time.

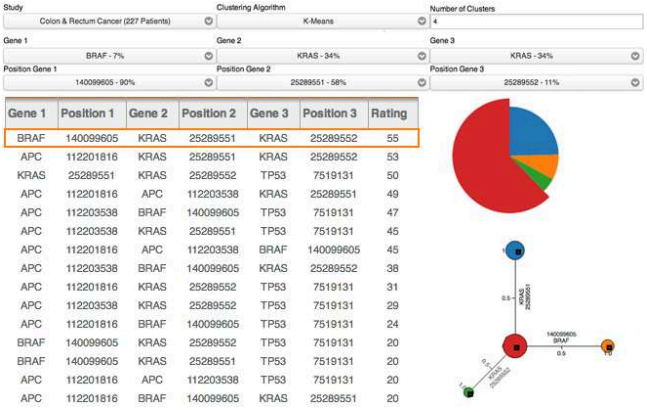

Gene 1	Position 1	Gene 2	Position 2	Gene 3	Position 3	Rating
BRAF	140099605	KRAS	25289551	KRAS	25289552	55
APC	112201816	KRAS	25289551	KRAS	25289552	53
KRAS	25289551	KRAS	25289552	TP53	7519131	50
APC	112201816	APC	112203538	KRAS	25289551	49
APC	112203538	BRAF	140099605	TP53	7519131	47
APC	112203538	KRAS	25289551	TP53	7519131	45
APC	112201816	APC	112203538	BRAF	140099605	45
APC	112203538	BRAF	140099605	KRAS	25289552	38
APC	112201816	KRAS	25289552	TP53	7519131	31
APC	112203538	KRAS	25289552	TP53	7519131	29
APC	112201816	BRAF	140099605	TP53	7519131	24
BRAF	140099605	KRAS	25289552	TP53	7519131	20
BRAF	140099605	KRAS	25289551	TP53	7519131	20
APC	112201816	APC	112203538	TP53	7519131	20
APC	112201816	BRAF	140099605	KRAS	25289551	20

Figure 6. Results of an interactive analysis of a cohort of 220 colon carcinoma patients using k-means clustering. It shows relevant combinations of genomic loci, such as gene KRAS on chromosome 12 at position 25,289,551, which are present in the majority of cohort members as depicted by the pie chart on the right.

C. Platform Layer

The platform layer holds the complete process logic and consists of the IMDB system that enables real-time data analysis. We developed specific extensions that support processing of high-throughput genome data and enables real-time analyses. Thus, we established selected system components as follows:

- Graphical modeling of workflow and analysis pipelines to improve reproducibility,
- Parallel execution of pipeline model instances to enable high-throughput processing,
- Prioritized scheduling of jobs,
- Integration of existing tools in our system and development of highly optimized tools for IMDB technology, and
- Always up-to-date access to international knowledge databases.

In the following, we outline details about selected components and their relevance for our computing platform.

D. Modeling of Genome Data Processing Pipelines

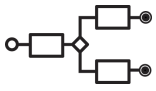

Specific processing and analysis tasks need to be performed to identify genetic variants from raw DNA data acquired from sequencing devices. Nowadays, various software tools are used for each step of the processing and analysis workflow while researchers and clinicians use individual setups and parameters for their experiments. These setups are commonly implemented as a number of software scripts depending on each other. We refer to a concrete implementation of a processing and analysis workflow as Genome Data Processing Pipeline (GDPP).

In the following, we define a subset of a standardized modeling notation for the definition of GDPPs to improve maintainability, ease of modeling, and to establish a common understanding of the workflow. Another goal of our modeling approach is to enable external scientists and physicians to model their pipelines accordingly to their individual needs and have them executed on a central computer cluster.

A specific runtime environment for GDPPs enables the translation of models into executable code as described in Section IV-E.

1) Requirements: We refer to the atomic unit of a GDPP as job. A job refers to a concrete script that can be executed to perform a specific task while activity refers to the abstract representation of a job in the process model. Thus, the most fundamental precondition for modeling of GDPPs is a representation of a number of jobs and their execution sequence. In order to allow reuse of a group of logically associated jobs in several pipelines, e.g., a specific combination of alignment algorithm and post-processing steps, the modeling system should support hierarchically nested inclusion of pipelines to form a new model.

Parallel data processing improves the execution time for the overall pipeline as described in Section IV-E. Therefore, the modeling approach should also support the explicit definition of activities that should be executed in parallel.

Some activities have a varying internal behavior or outcome depending on their defined input parameters. For example, an alignment job might support a dynamic parameter for the reference genome that is used for the alignment of chunks of DNA. Thus, modeling should support the definition of input parameters and the link to activities.

Additionally, the models should be stored in a standardized, machine-readable format, e.g., to ensure exchange and interpretation of models when sharing them across institutions.

We defined our GDPP modeling approach as a subset of Business Process Model and Notation (BPMN), which is a standardized and widely adopted modeling technique. In the following, we define the required subset and mapping to our GDPP modeling notation.

2) Business Process Model and Notation: The Business Process Management Initiative (BPMI) introduced BPMN standard in 2004. Since 2006, it is an official standard of the Object Management Group (OMG), which released BPMN version 2.0 in 2011. The actual work within a BPMN process is modeled by activity elements. They represent the atomic unit of a model that can be executed by either a human or a computer system. The logic of a BPMN flow is defined by so-called gateways, such as exclusive gateways representing a logical XOR and parallel gateways representing a logical AND. Each BPMN process is defined by a unique

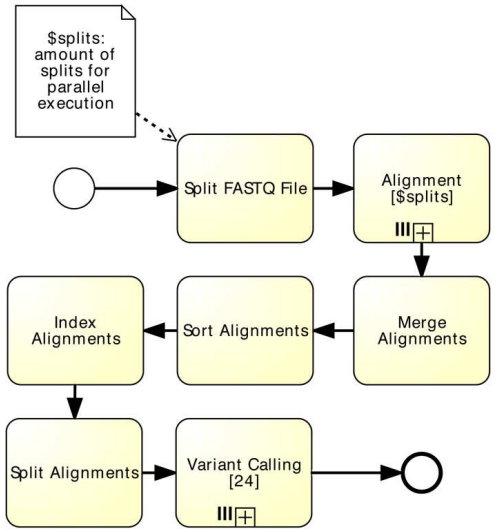

Figure 7. GDPP model of the general approach with file system as primary storage. The input FASTQ file is first split up for parallel processing during alignment. The outcome is merged again and prepared additional processing steps before it is split up per chromosome again for variant calling.

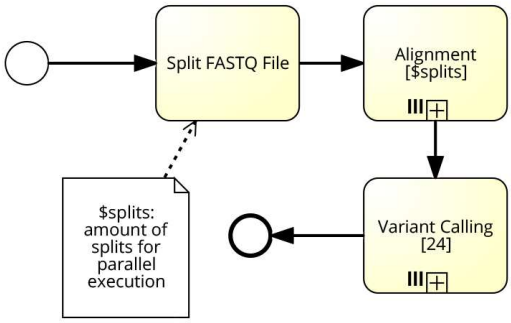

Figure 8. GDPP model incorporating an IMDB as primary storage. In contrast to using a file system as primary storage, the intermediate processing steps are not required anymore.

start event and at least one end event [39].

A widespread and well-defined XML-based representation of BPMN models is the XML Process Definition Language (XPDL). We incorporate the existing XPDL standard to store and exchange our GDPP models.

3) Hierarchy of Activities: GDPPs can be hierarchically nested to any level of depth. Any set of logically associated activities can be represented as a separate model containing a sub process model. Sub process activities are used as placeholders in the invoking process. An example is shown in Figure 7, which contains a sub process named `Alignment[$splits]` that is depicted in Figure 10. The names of the sub process and the corresponding process model are automatically replaced during runtime based on their name. Figure 10 depicts the concrete sub process for `Alignment[$splits]` in-

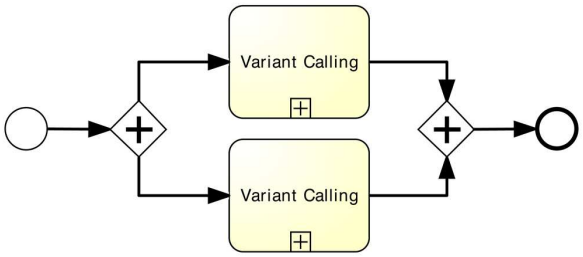

Figure 9. GDPP model using parallel gateways to perform variant calling two-times parallel.

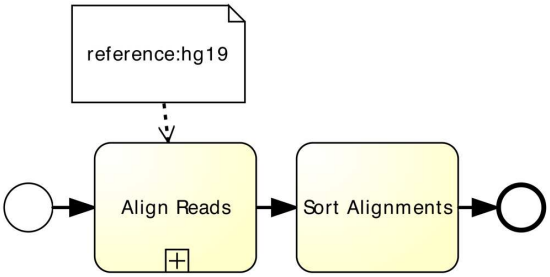

Figure 10. Modeling of parameters to acquire from end-users as input for an activity prior to its execution. Here, the reference to use during alignment is set to hg19.

cluded in the model depicted in Figure 7. The alignment step consists of multiple jobs to be performed, e.g., transformation steps or sorting the alignment results. In addition, each alignment algorithm modeled in our GDPP has its distinct sub process, which encapsulates further necessary transformation steps to receive output in the standard format.

4) Parallel Processing of Activities: Parallel execution of activities in BPMN can be defined as follows.

- Parallel multiple instances are modeled as an activity with three vertical lines at the bottom as depicted in Figure 7 for sub processes alignment and variant calling. The parallel multiple instance is executed as often as defined by the number defined in square brackets following the activity's name, e.g., variant calling is executed 24 times in parallel.
- Parallel gateways are an alternative way of modeling parallel workflows. They are used when no specification of quantity of parallelization exists. When a parallel gateway is signaled, all outgoing edges of the gateway are signaled as well. When the gateway consists of multiple incoming edges, the gateway only signals once all incoming edges were activated. Thus, the sequence flow can be split in two or more parallel strands and resynchronized if needed. Figure 9 illustrates an example for parallel gateways. This time, variant calling is executed by two activities in parallel.

5) Parameters and Variables: We distinguish between parameters and variables as follows. Parameters are set during design time of the GDPP model and cannot be changed afterwards. Variables are placeholders that are assigned at the latest point in time just prior to the execution of a GDPP model instance.

BPMN defines data objects for modeling of specific input parameters of activities [40]. A parameter is stored in a data object labeled as the parameter's name followed by its value separated by a colon. The parameter's name matches the input variable name of the corresponding activity. A data object can be associated to one or multiple activities.

We added support for variables in our GDPP models by using a specific data object identified by a dollar sign (`$`) followed by the variable's name. Figure 7 depicts the use of variables in a GDPP model, i.e., the variable `splits` has to be set to a concrete value prior to the execution of the concrete GDPP model instance.

Parameters and variables can be assigned to multiple activities. For example, Figure 8 depicts multiple usage of parameter `splits`. On the one hand, it is required by the first activity to know how many splits to create. On the other hand, the parameter defines the amount of alignment sub processes that will be executed in parallel.

E. Parallel Execution of Genome Data Processing Pipelines

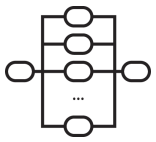

In context of precision medicine the aspect of high-throughput processing and analysis becomes essential to leverage a clinical solution. Thus, we focus on parallel execution of GDPPs and for that, we designed specific functionality within our platform.

A distributed set of computing nodes each running multiple workers forms our worker framework. Each worker is directly connected the IMDB database landscape to access their local portion of the database content. Relevant details about tasks that need to be executed are added to the tasks database table by the scheduler. Once a worker starts processing of a concrete task, it updates the current status of the task within the database. Incorporating the database for these purposes reduces the complexity of the individual worker code since specific exception handling can be processed by the database, e.g., using built-in database locks can prevent concurrent start of the identical task.

All workers and the scheduler use a specific communication protocol to exchange short messages between each other's, e.g., to reduce idle times. On the one hand, workers can exchange relevant status information about the load of a certain node and updated jobs. On the other hand, the scheduler sends a wakeup signal to all workers to inform about jobs ready to be executed. For further details about the scheduler component, please refer to Section IV-G.

F. Fair Use of Resources and Accounting

Processing and analyzing data consumes resources of our platform, such as computing time or hard disk storage. Thus, we have integrated a fine-grained accounting functionality to ensure fair usage of provided services and resources. The atomic measurement unit for any kind of service on our platform is called gene point. On the one hand, users can spend gene points on platform services or to access data provided by other users. On the other hand, users can acquire gene points by providing services or data to other users. This mechanism guarantees fair resource allocation for all users and encourages active data exchange. Furthermore, it builds the foundation for sharing intellectual property and enables compensation [3, Chap. 5].

The prioritized scheduling of jobs is the key concepts to implement fair use and accounting within our platform as discussed in the following.

G. Prioritized Task Scheduling

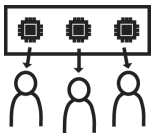

We created a single scheduler component coordinating the execution of multiple GDPPs. Thus, it enables resource allocation and distribution of workload across our cluster of worker machines. The scheduler stores its internal state permanently within the IMDB, e.g., for global communication, logging, and for maintaining statistics. We implemented specific scheduling algorithms optimized for throughput that analyze the complete execution history of all former runs in order to process shortest GDPP instances first.

The scheduler node is responsible for managing all aspects from reading the GDPP models to scheduling all relevant activities and linked jobs.

Every scheduling decision is persisted in the database prior to its executed, i.e., the database provides a consistent transaction log, which enables controlled recovery in case of a system failure.

We implemented specific scheduling policies to optimize scheduling decisions depending on various aspects. For example, we incorporate the Shortest Task First (STF) scheduling policy to minimize turnaround time and maximize throughput [24, Section 2.4.2].

Our STF scheduling policy is adapted to estimate the remaining execution time of all waiting tasks whenever a scheduling decision needs to be taken. The incorporated IMDB technology guarantees that the estimation can be processed in real-time and does not delay decision making significantly [3, Chap. 3].

The developed scheduler component is very generic and can easily be adapted to fit individual requirements, e.g., to prioritize the execution of tasks from a department or to keep a processing reserve for the very important users. Furthermore, individual scheduling policies can be developed to change the behavior of the scheduling system. Each scheduling policy can incorporate various input data, e.g., details about the overall system load provided by the load balancer as described in Section IV-H.

H. Load Balancing

The overall system load of all computing nodes incorporated by our computing platform depends on running jobs and their assignment to individual nodes. This becomes especially important if we assume a computing pool that consists of a heterogeneous hardware. Thus, we implemented a load balancer that incorporates the current system status of available worker nodes. The configuration of all attached worker nodes, e.g., how many workers are running on each of them or how many CPU cores are available, is stored in the configuration database table.

The detailed view of the load balancer can be incorporated by the scheduler component during its decision-making process as described in Section IV-G. For example, the scheduler still can postpone the execution of long-running jobs when short-running jobs are available.

I. Annotation Framework

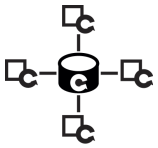

We consider the use of latest international research results as enabler for evidence-based therapy decisions [41]. Our annotation framework is the basis for combining international research results. It periodically checks all registered Internet sources, such as public FTP servers or web sites, for updated and newly added versions of annotations, e.g., database exports as dumps or characteristic file formats, such as Comma-Separated Values (CSV), Tab-Separated Values (TSV), and Variant Call Format (VCF) [42]. If the online version is newer than the locally available version, the new data is automatically downloaded and imported in the IMDB to extend the knowledge base.

The import of new versions of research databases is performed as a background job without affecting the system's operation. We import new data without any data transformations in advance. Thus, data becomes instantaneously available for real-time analysis [43], [44].

For example, the following selected research databases are regularly checked by our annotation framework: National Center for Biotechnology Information (NCBI), Sanger's Catalogue Of Somatic Mutations In Cancer (COSMIC), University of California, Santa Cruz (UCSC) [45], [46], [47].

J. Combined Search in Unstructured and Structured Data Sources

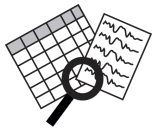

A significant amount of today's medical data is encoded in the form of unstructured natural language [48]. Scientific publications and patents, medical reports, as well as comments, keywords, or descriptions in database records use natural language to store information [48]. We consider this unstructured data as a substantial part of the world's medical knowledge. However, comprehension, analysis and searching of unstructured data are still challenging compared to structured data, such as experiment results or genomic variant data. So far, research to extract information either from structured or unstructured medical data does not investigate the advantages that can be gained by combining results from both sources.

For example, a physician could receive information contained in scientific publications that perfectly match her or his patient's current diagnosis. Additionally, researchers face the challenge to identify relevant information sources within a tremendously short timespan. With the help of our IMDB technology, we enable researchers to identify relevant data from structured and unstructured data sources. Our specific database extensions recognize relevant entities within text documents and extract them automatically.

This builds the foundation for applications that incorporate data from both worlds: structured and unstructured data. An example application that builds on the combined search in structured and unstructured data is our clinical trials search as described in Section IV-B1, which incorporates unstructured textual information from clinical trial descriptions and doctor letters as well as structured information obtained from the genetic biomarkers of a specific patient.

K. Development of Tools for In-Memory Computing vs. Integration of Existing Tools

Existing tools for genome data analysis can be directly integrated in our GDPPs. For that, we implemented a new job that invokes the corresponding tool via command line and adapted the pipeline model as described

in Section IV-D. This strategy facilitates an easy integration of new tools into our framework without caring for distribution and scheduling. However, this improves integrated algorithms only to a limited extent, e.g., since these tools still access data from files located on disk storage. Loading large files from disk into main memory for processing still consumes additional processing time prior to data analysis. In addition, the majority of tools do not exploit computational resources fully to optimize runtime performance. Analysis tools specifically designed for our in-memory computing platform benefit in terms of parallelization, compression, in-memory storage, and distribution across multiple machines.

1) Benefits of Optimized Tools for In-Memory Computing: Developing specific tools for genome data analysis as built-in functionality of our in-memory computing platform results in reduced setup and configuration in addition to improved data processing. Furthermore, the results of the data processing are directly available in our IMDB. Thus, you can apply any analysis tools directly to the results without the need for any data preparation. The different building blocks presented in Section III come along with further advantages that accelerate fast data processing as follows.

Lightweight Compression: Sequencing data consumes huge amounts of storage capacities, i.e., up to hundreds of GB per single human genome. Therefore, it is crucial to apply data compression techniques, e.g., as currently done in genome data analysis by converting the raw data from Sequence/Alignment Map (SAM) format into its Binary Alignment Map (BAM) format [49]. Our incorporated IMDB technology applies lightweight compression to genomic data in a transparent way. Thus, data remains in a human readable format, e.g., during database queries, while the storage footprint is automatically reduced.

Column Orientation: Storing data as complete tuples in adjacent blocks, i.e., row-wise, is advantageous if the complete data of a single row has to be accessed, for instance by comparing two complete table entries to each other. However, most often algorithms only require access to particular attributes of a data record for analysis. For example, when filtering read alignments in the first phase of variant calling, only data quality indicators need to be accessed such as mapping or base quality scores. If all records were stored row-wise as it is the case for files, all attributes need to be processed although only two of them might be relevant for computation. Storing data in columnar format, i.e., storing complete columns in adjacent blocks facilitates direct access only to relevant attributes and avoids cache misses [50], [51].

Multi-Core and Parallelization: When creating optimized analysis tools for our in-memory computing platform, we can profit from already existing functionality to apply parallelization and full exploitation of CPU resources. Thus, we can focus on optimizing algorithms instead of implementing resource management.

Data Partitioning: Regarding the optimization of analysis tools, in- and output data can easily be horizontally partitioned according to chromosomes and even chromosome regions to distribute data and it's processing to computing nodes. When working with current tools, distribution and selection of relevant data is a time-consuming task that is carried out by specific tools, e.g., SAMtools [49]. With data partitioning, the search space for accessing data of a particular chromosome or region reduces to only a small part of the original data set. This improves search operations and facilitates better scalability of our optimized algorithms.

2) Alignment on In-Memory Computing Platform: Our genome data alignment algorithm optimized for in-memory technology was designed with the following requirements in mind:

- Use available main memory for faster index structures that allow accelerating the lookup process,
- Minimize the cache miss ratio since cache misses are known to be a major cause for bad performance on modern hardware architectures, and
- Optimize parallel code execution, e.g., by minimize the need for process synchronization and avoid writing to shared data structures requiring locking.

We used a k-mer based index structure to find alignment position candidates and filled the unmatched gaps using heuristics optimized for low error rates and a variant of the Needleman-Wunsch and Smith-Waterman algorithms [52], [53].

Structure of the Index: The commonly used index structures based on the proposed techniques by Ferragina and Manzini (FM-index) have a very low memory impact, but require at least two cache misses on average per nucleotide even if only perfect matches are required [54]. k-mer-based indexes are less error tolerant since they usually require the whole k-mer to match the reference genome. They are much faster than FM-indexes though since complete k-mers can be identified by a single access to the index structure. The price to be paid is that the algorithm has to find sufficiently many perfectly matching k-mers to get a strong signal. FM-index-based algorithms are more tolerant in theory as deviations from the reference can be included into the search. But due to the large search space that has to be covered in order to achieve this tolerance, their efficiency on long reads is limited.

For example, 100 base pairs are nowadays standard and already cause major problems to this approach. Thus, additional assumptions need to be made, which are comparably restrictive as k-mer-based indexes.

While longer reads cause a stronger problem to FM-index search they help with finding sufficiently many k-mers without difference to the reference genome. Recent advances in sequencing quality improve this further and make k-mer indexes more attractive, which is the reason we prefer this approach.

Finding Optimal Positions: By comparing multiple k-mers from the read, the algorithm usually obtains many index hits per read of which some are true positives and others false positives. k-mers with too many hits are not very decisive and blow up the search space beyond their meaningful use. Therefore, k-mers with more than 256 hits are ignored. The search space can also be narrowed down by choosing longer k-mers, which is done whenever too few k-mers with few hits were found.

The possible matching positions from all k-mers are being matched with each other depending on the k-mer position within the read and the distances of their matches on the reference genome. The distance furthermore gives a lower limit for the number of insertions resp. deletions required for the match. The missing k-mers indicate that mismatches have appeared even if distances match. From this information, an optimistic score can be computed and the alignments are further processed starting with the best score. When each alignment is finalized, the actual score is known and can be compared to the optimistic score of the next alignment candidate. If the optimistic score is worse than the best actual score found, the alignment is done as no better alignment can be found anymore.

Filling the Gaps: To get a perfect alignment, all differences between the reference genome and the read need to be found similar to computing the edit distance, but with probabilistic scores for each deviation. They are traditionally computed by dynamic programming algorithms, which scale quadratic in read length. This problem is dramatically reduced by focusing on filling only the gaps in between the k-mer hits, .

Extending the matching parts into the gap until a difference compared to the reference genome is detected makes further improvements. If the remaining part is only a single nucleotide long both on the reference genome and on the read, it must be a substitution. If the gap on either the reference genome or the read is completely closed, it must be an insertion or deletion, respectively. Therefore, many of the differences can be resolved without the need for more complex algorithms due to lower error rates.

For the final step, we use a dynamic programming algorithm optimized for Single Instruction, Multiple Data (SIMD) based on the Needleman-Wunsch and Smith-Waterman algorithms adjusted to our boundary conditions [52], [53]. This allows alignments restricted on both ends by known k-mers and half open gaps for which a k-mer has only been found on one end.

Improvements for Mate-paired Reads: If a correlation in the alignment position on the reference genome is known beforehand (mate-pairing) the alignment finalization can be skipped for all positions that do not fulfill this correlation. Also the optimistic scores can already be computed for both reads simultaneously achieving a better estimate of the best alignment. This strategy excludes many possible matches at a very early stage. Thus, it reduces the amount of expensive full alignments and improves accuracy.

3) Variant Calling on In-Memory Computing Platform: We designed a variant calling approach to identify Single Nucleotide Polymorphisms (SNPs) that is directly executed within our in-memory computing platform. With respect to that, our approach has to meet the following requirements:

- Use available main memory capacity to store and process read alignments while eliminating access to slower file systems,
- Direct access to specific read alignment attributes without the need to traverse the complete data record, and
- Apply compression strategies to reduce memory footprint and to improve processing throughput.

Our SNP calling is divided in data preparation and genotype calling. We achieve parallelization by executing the algorithm in a MapReduce-like fashion, where the processing steps correspond to map phases. For each of them, data is split up into smaller subsets and processed in parallel [55]. After that, the result sets are merged in a reduce phase to be then again split up for the next map phase.

Data Preparation: During data preparation data is assembled and prepared for subsequent genotype calling. It comprises the data extraction and grouping phase.

The goal of the data extraction phase is to reduce the overall amount of data to process by filtering out irrelevant and low-quality data. During data extraction, we identify the sequences of a read alignment that are relevant for SNP calling. For that, we first eliminate reads that are not sufficient for processing, e.g., because necessary information is missing or data quality does not meet user-defined thresholds. Afterwards, we identify the relevant read alignment sequences. We receive the information about what parts of a read alignment are involved in single substitutions, insertions, or deletions from each read alignment's individual CIGAR attribute [56]. As we concentrate on the identification of SNPs in our approach, sequences of a read that are involved in insertions will be filtered from our data. The aim of the data-grouping phase is to rearrange the read alignment data for efficient genotype calling afterwards. The output received from the data extraction phase is

used to group all bases from relevant sequences of a read alignment according to the positions in the genome they have been aligned to. This way, each position in the genome has assigned four "piles" for the distinct bases Adenine (A), Cytosine (C), Thymine (T), and Guanine (G) that comprise information about base occurrences. At this time, we also extract relevant information about the data quality, e.g., base quality scores, as this information builds the computational basis for genotype calling in the subsequent processing step.

Genotype Calling: The goal of the genotype-calling step is to derive a concrete genotype for each particular position in the genome that is covered by the base pileups. For the actual computation, we apply a statistical model that is sensitive to input data quality. This includes that we have to compute the probability for each possible genotype, i.e., ten different genotypes for the diploid human organism, at a particular position in the genome. The genotype with the highest probability will be called in the end. To calculate the probability of a genotype, we apply a Bayesian framework as proposed by Nielsen et al. with two components called prior probability and genotype likelihood [57].

The prior probability of a genotype is its general chance to occur regardless of the given data. In our computations, we do not assign a unique prior probability to all genotypes. Instead, we distinguish genotypes according to their zygosity, i.e., homo- or heterozygous, and reference equality and make use of the assumptions stated by Li et al. [15].

The genotype likelihood of a genotype is its chance to occur with regard of the given data. We compute this value from all occurrences of a genotype at a particular position and incorporate the bases' quality scores. A base quality score indicates how likely the sequencing machine has detected a base correctly. We incorporate this value in our computations because the read alignments produced by those sequencing machines are error-prone up to one percent of the data [58], [59]. Thus, we give stronger weights to bases with a higher probability to be correct and downgrade low-quality bases.

After genotype calling, each derived genotype owns a quality value, which indicates the likelihood of the called genotype. All genotypes that differ from the reference genome and have a quality value that matches the user-defined threshold make up the set of emitted SNP calls.

V. Benchmarks

The aim of all conducted benchmarks was to minimize the overall execution time for a single GDPP run, i.e., to use the maximum of available computing resources and achieve highest throughput. Furthermore, we aim to compare selected alignment algorithms regarding their efficiency for varying file sizes. In the following, we share insights about our benchmarks conducted on our in-memory-based processing and analysis platform.

TABLE I. EXPERIMENT CONFIGURATIONS.

Experiment	Split Size	Primary Storage
A	1	File System
B	1	In-Memory Database
C	25	File System
D	25	In-Memory Database

TABLE II. DATA SET SPECIFICATIONS.

Data Set	Size [Gbp]	Size [GB]	Reads [Billion]
1	0.5	1.2	5.4
2	1.0	2.4	10.8
3	1.9	4.8	21.7
4	3.9	9.6	43.4
5	7.9	19.2	86.8
6	15.8	38.5	173.7
7	31.6	78.0	345.8

A. Setup

All benchmarks were performed on a computer cluster consisting of 25 identical computing nodes with a total of 1,000 cores provided the Future Service-Oriented Computing Laboratory at the Hasso Plattner Institute [60]. We incorporated this hardware setup to demonstrate the scalability of our in-memory computing platform. It should not be interpreted as minimum hardware resources required operating our contribution. Each of the nodes was equipped with four Intel Xeon E7-4870 CPUs running at 2.40 GHz clock speed, 30 MB Intel Smart cache, interconnected by 6.4 GT/s Quick Path Interconnect (QPI), and 1 TB of main memory capacity [61]. Each CPU consisted of 10 physical cores and 20 threads running a 64-bit instruction set. All computing nodes were equipped with Intel 520 series SSDs of 480 GB capacity combined using a hardware raid for local file operations [62]. The average throughput rate of the local SSDs was measured with 7.6 GB/s cached reads and 1.4 GB/s buffered disk reads. All nodes were interconnected via a Network File System (NFS) using dedicated 10 Gb/s Ethernet links and switches to share data between nodes.

Instead of using generated test data, we incorporated real NGS data for individual measurements, i.e., FASTQ files from the 1,000 genomes project [5]. We used the FASTQ file of patient HG00251 for our benchmarks, which consumes 160 GB of disk space, consists of approx. 63 Gbp, approx. 695 M reads with 91 bp individual read length, forming an average 20x coverage.

We implemented two GDPPs for our benchmarks. The first corresponds to the commonly followed approach of using a file system as primary storage. The distinct execution steps are modeled as GDPP notation in Figure 7. On the contrary, the second pipeline as

shown in Figure 8 uses an IMDB as primary storage, i.e., intermediate results are stored in our in-memory computing platform.

Our pipelines contain distinct parts for alignment and variant calling that are parallelized, e.g., by splitting up the input data. The alignment step is comprised of the alignment algorithm itself and file transformation and processing steps due to differing output formats per alignment algorithm. Furthermore, the GDPP using a file system as primary storage contains additional processing steps between alignment and variant calling, which are necessary to split up data per chromosome. These steps are not required for the IMDB-optimized GDPP since alignment results are already imported into the database and chromosome-wise splits are implemented using native database operations.

1) Burrows Wheeler Aligner: We used Burrows Wheeler Aligner (BWA) version 0.6.2 as alignment algorithm reference [63]. BWA was configured to use a maximum of 80 threads, which relates to the maximum available hardware resources of our benchmark infrastructure. The algorithm's output is a SAI file that needs to be converted to the SAM format. Therefore, we added format transformation directly after alignment to receive alignments in SAM format. For the GDPP models of Exp. A and C, we additionally have to carry out a transformation from SAM into BAM format and to sort the resulting BAM file as preparation for merging.

2) HANA Alignment Server: The second part of our benchmarks was performed on a GDPP integrating our own alignment algorithm as described in Section IV-K2. It is implemented directly within our in-memory computing platform, i.e., it can directly access native database operations. This algorithm was configured to use a maximum of 80 threads and emits alignments either in SAM or BAM format. As a result, additional format transformations, e.g., from SAM to BAM, are no longer required for both of our pipelines.

B. Experiments

We designed our benchmarks to compare the impact of the incorporated storage system and the level of parallelization on the overall execution time. Each of the experiment categories was conducted for the alignment algorithms BWA and HANA alignment server to evaluate the impact of the overall execution time for a specific GDPP. Exp. A and B were executed on a single computing node, while Exp. C and D were executed on 25 computing nodes to evaluate the impact of a fully parallelized execution environment as outlined in Table I. In addition, we derived subsets of the input data as shown in Table II.

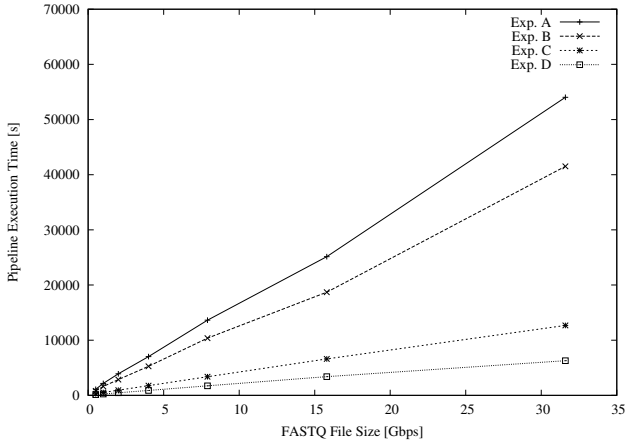

Figure 11. BWA: Development of overall execution times for varying file sizes and experiment setups.

C. Results

In the following, we present our obtained benchmark results. For each alignment algorithm, we measured the overall pipeline execution times t_x for Exp. x and derived the relative advance of execution time for Exp. x compared to Exp. A as $R_x = \frac{t_A - t_x}{t_A}$.

Table III shows the overall pipeline execution times incorporating BWA as alignment algorithm. The measured execution times indicate that the use of the IMDB as primary storage for intermediate results is beneficial for all selected file sizes. This pipeline optimization results in a reduction of the overall runtime by at least 25 percent on average.

Exp. C and D as shown in Table III document the impact of the parameter `splits`, i.e., the number of distributed computing nodes used for parallel execution as introduced in our pipeline models. Parallel execution of selected pipeline steps reduces the overall execution time by at least 74 percent on average for BWA. Additional improvement can be achieved by using the IMDB as primary storage. Figure 11 illustrates execution time behavior for GDPP with BWA as alignment algorithm. It clearly shows the improvements originating from parallelization and main memory as primary storage medium. For a GDPP using BWA as alignment algorithm, execution time can be reduced by at least 87 percent on average.

Table III shows the overall pipeline execution times for BWA and HANA alignment server. Execution times develop similarly to the results obtained for BWA pipelines. Table III depicts that runtime improves up to 50 percent when using an in-memory database as primary storage, and up to 75 percent when distributing the pipeline across 25 computing nodes.

Comparing the overall execution times amongst the different alignment algorithms used, we can see that

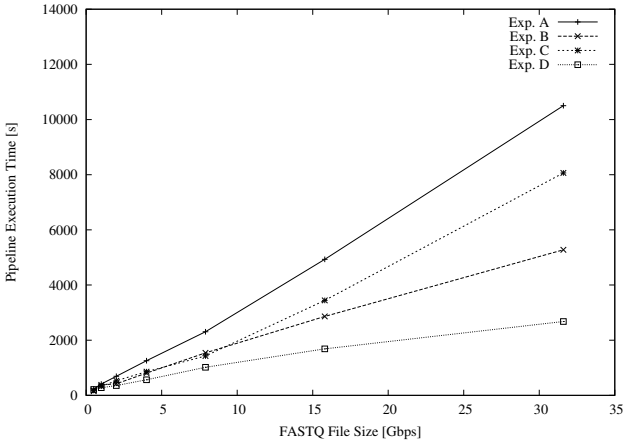

Figure 12. HANA alignment server: Development of overall execution times for varying file sizes and experiment setups.

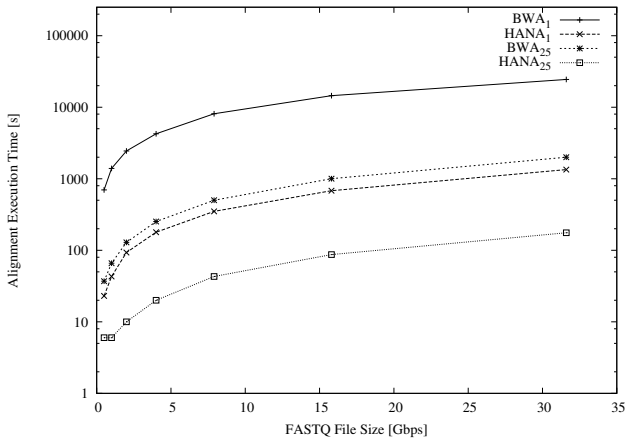

Figure 13. HANA and BWA alignment: Development of execution times for varying file sizes and split sizes.

runtime performance drops significantly when using HANA alignment server as alignment algorithm. From the alignment algorithms used, the pipelines applying HANA alignment server show best runtime performances throughout all runs, up to 85 percent faster than with BWA.

Figure 13 shows execution times for alignment with BWA and HANA for different file and split sizes. t_{Aln_1} and $t_{Aln_{25}}$ describes average processing times consumed by the alignment algorithm only with split sizes 1 and 25, respectively. Performing read alignment with BWA takes absolutely longer than HANA alignment server. We derived the speedup factor $S_{x:y} = \frac{t_x}{t_y}$ for BWA and HANA alignment server when applying parallelization. Performing BWA alignment in parallel on 25 nodes results in a speedup factor of up to 21x, which means the process has a great parallel portion that benefits from additional computing resources. HANA alignment server with 25 nodes results in a speedup factor of up to 9x. This can be explained by the very short execution time HANA alignment server consumes, i.e., there is a significant higher sequential portion of code that reduces the speedup.

For split size 1, HANA alignment server brings a relative runtime improvement of 97 percent on average as listed for $t_{1_{Aln}}$ in Table III. Relating these numbers to our overall execution times in Table III, the portion of alignment compared to the overall pipeline execution time is significantly reduced, e.g., to approx. five percent for HANA alignment server compared to approx. 20 percent for BWA alignment both processing the second-largest file size in Exp. D. In contrast when executing GDPPs with HANA alignment server instead of BWA at a split size of 25, the relative improvement rates drops below 90 percent, especially for the smallest file size with a relative improvement of 74 percent.

TABLE IV. INTERSECTION OF RESULT SET FROM HANA ALIGNMENT SERVER AND BWA. IN TOTAL, HANA ALIGNMENT SERVER CREATES APPROX. 16M MORE ALIGNMENTS THAN BWA WHILE LEAVING ONLY HALF THE READS UNALIGNED.

	Total (#)	Aligned (#)	Unaligned (#)
BWA∩HANA	274,785,274	254,223,773	20,561,501
BWA	329,338,990	286,491,783	42,847,207
HANA	345,805,881	324,241,424	21,564,457

Table IV shows result set intersections of read alignment output from BWA and HANA alignment, respectively. We concentrate on a quantitative analysis of our obtained results since the selected benchmark data was taken from the 1,000 genome project [5]. Thus, it is no gold standard available that could be used to validate obtained alignment results.

The result set produced by BWA contains less read alignments than HANA alignment server, which includes the exact amount of read alignments from the input file listed as data set 7 in Table II. Both alignment algorithms share the majority of joint read alignments, i.e., approx. 274M reads. From them, a small proportion is made up from unaligned reads, i.e., reads for which the alignment algorithm could not find a suitable position in the genome. BWA leaves more than 42M reads unaligned, which is about twice as much as HANA alignment server. Thus, HANA maps a total of 324M read alignments, i.e., about 18M more read alignments than BWA with only 286M.

VI. Evaluation and Discussion

Our conducted benchmarks verify two hypotheses. Firstly, the usage of the IMDB as primary storage system is beneficial for integrating established alignment algorithms, such as BWA, as well as optimized alignment algorithms for IMDB technology, such as HANA

TABLE III. COMPARISON OF INDIVIDUAL EXECUTION TIMES FOR BWA (I) AND HANA (II) ALIGNMENT (R = RELATIVE IMPROVEMENT, S = SPEED UP).

	I	II	I	II	I	II	I	II	I	II	I	II	I	II
Size [Gbp]	0.5		1.0		2.0		4.0		7.9		15.8		31.6	
$t_A[s]$	1,100	231	2,159	409	3,900	690	7,029	1,256	13,626	2,305	25,147	4,931	54,034	10,503
$t_B[s]$	808	153	1,622	377	2,860	421	5,259	806	10,364	1,542	18,707	2,861	41,520	5,276
$t_C[s]$	283	178	520	330	943	529	1,761	860	3,377	1,427	6,609	3,443	12,673	8,064
$t_D[s]$	130	212	245	278	470	355	893	566	1,733	1,016	3,387	1,685	6,275	2,676
$R_B[\%]$	27	34	25	8	27	39	25	36	24	33	26	42	23	50
$R_C[\%]$	74	23	76	19	76	23	75	32	75	38	74	30	77	23
$R_D[\%]$	88	8	89	32	88	49	87	55	87	56	87	66	88	75
$t_{1_{Aln}}[s]$	699	23	1,395	43	2,446	93	4,250	179	8,099	350	14,504	680	24,417	1,342
$t_{25_{Aln}}[s]$	37	6	66	6	129	10	252	20	501	43	1,001	87	2,000	176
$R_{1:25}[\%]$	95	74	95	86	95	89	94	89	94	88	93	87	92	87
$S_{1:25}$	19x	4x	21x	7x	19x	9x	17x	9x	16x	8x	14x	8x	12x	8x
$R_{1_{I:II}}[\%]$	97		97		96		96		96		95		95	
$R_{25_{I:II}}[\%]$	84		91		92		92		91		91		91	
$S_{1_{I:II}}$	30x		32x		26x		24x		23x		21x		18x	
$S_{25_{I:II}}$	6x		11x		13x		13x		12x		12x		11x	

alignment server. Secondly, our platform supports the parallel execution of intermediate process steps across multiple computing nodes, which results in an additional performance improvement compared to the execution on a single computing node.

We observed the best relative improvement for GDPP using the IMDB as primary data storage and BWA as alignment algorithm with at least 74 percent on single computing node and up to 89 percent on 25 computing nodes. Thus, the overall pipeline execution time with BWA as alignment algorithm correlates to the number of base pairs contained in the FASTQ file in a linear way. However, improvements when using 25 nodes is still below our expectation of a factor 25 due to the use of traditional tools, e.g., SAMtools, which partially operate in a single threaded way.

Relative improvement observed for pipelines using HANA alignment server remain below the numbers achieved by pipelines using BWA. For the three largest file sizes, we achieve relative improvements between 33 and 42 percent on a single computing node and between 55 and 66 percent on 25 computing nodes. For this pipeline, runtime limitations from third-party tools, such as SAMtools, apply. Using HANA alignment leads to a significant reduction of overall execution times. Thus, it results in a detrimental shift of the ratio between time overhead needed for setting up parallelization, i.e., splitting and merging, and the time improvement due to parallelization. For example, the time needed for merging intermediate results in GDPPs using file storage as primary storage medium increases up to 10x when distributing pipeline execution across 25 computing nodes. It shows almost no impact for BWA alignment as the majority of time is spent on alignment. In contrast, HANA alignment reduces the proportion of time needed for alignment significantly, so that the impact of remaining operations, e.g., merging of partial results, on the overall runtime duration increases. In addition, HANA alignment reaches its minimum execution time of approx. 6 seconds when operating on the small benchmark files, leading to worse relative improvement rates compared to BWA.

As a result, GDPPs using HANA alignment have a worse speedup compared to BWA alignment while the overall execution time is significantly smaller because of its near optimal use of parallelization. In addition, pipeline execution times reach a lower boundary that reduces relative performance improvements for the three smallest files. For example, the time needed for alignment of the smallest benchmark data set drops below ten seconds on a single node.

Scaling factors for the overall execution time across all experiments and file sizes indicate a constant and predictable system behavior of our system for varying input file size. Thus, we are able to predict execution time, which helps to supervise the correct system functionality, e.g., to detect broken computing resources. We do not elaborate on costs emerging when using the cluster as it remains available during pipeline execution to other users that can start their own pipelines or use one of our other applications, e.g., patient cohort analysis.

Furthermore, our results stress the benefits of using an IMDB for operating on intermediate results of the pipeline execution. The pipeline optimized for the IMDB no longer uses individual tools operating on files for specific process steps, such as sorting, merging, and indexing. These operations are directly performed as an integral operation of the incorporated IMDB without the need to create intermediate files in the file system at all.

VII. Conclusion

In our contribution, we shared details about building blocks of in-memory computing and proofed the applicability of the IMDB technology for genome data

processing and its real-time analysis. For that, we conducted expressive benchmarks, which underline that our computing platform improves the overall runtime by enabling a) scale-out, b) seamless integration of existing tools, such as BWA, and c) development of specific algorithms, such as HANA alignment and variant calling, which are directly embedded as core components in the incorporated IMDB.

We shared insights in specific system components of our technology stack, such as task scheduling, worker and annotation framework, which build the foundation for consistent and scalable high-throughput data processing. To enable reproducible genome data analysis, we shared details about our GDPP modeling notation for processing and analysis pipelines based on BPMN.

Ultimately, we linked our technology building blocks to concrete requirements for specific applications in the context of precision medicine and clinical research, e.g., cohort analysis and search in unstructured clinical trial documents. These applications are the results of interdisciplinary cooperation with researchers, clinicians, and medical experts. As a result, we were able to monitor improvements in the daily working routine of these target audiences by providing them our cloud applications.

Our future work focuses on integration of additional tools and services into our in-memory computing platform to further support researchers and clinicians in the course of precision medicine. In addition, our future research will focus on patients to support them in explore latest international medical knowledge about critical diseases and possible treatments, such as cancer disease.

References

[1] M.-P. Schapranow, F. Häger, and H. Plattner, "High-Performance In-Memory Genome Project: A Platform for Integrated Real-Time Genome Data Analysis," in Proceedings of the 2nd Int'l Conf on Global Health Challenges. IARIA, Nov 2013, pp. 5–10.

[2] K. Jain, Textbook of Personalized Medicine. Springer, 2009.

[3] H. Plattner and M.-P. Schapranow, Eds., High-Performance In-Memory Genome Data Analysis: How In-Memory Database Technology Accelerates Personalized Medicine. Springer-Verlag, 2014.

[4] I. Bozic et al., "Accumulation of Driver and Passenger Mutations during Tumor Progression," Proceedings of the National Academy of Sciences of the United States of America, vol. 107, no. 43, Oct. 2010, pp. 18 545–50.

[5] The 1,000 Genomes Project Consortium, "A Map of Human Genome Variation from Population-scale Sequencing," Nature, vol. 467, no. 7319, Oct. 2010, pp. 1061—1073.

[6] Illumina, "HiSeq 2500 Sequencing System," http://res.illumina.com/documents/products/datasheets/datasheet_hiseq2500.pdf [retrieved: May 30, 2014], Jan 2014.

[7] National Human Genome Research Institute, "DNA Sequencing Costs," http://www.genome.gov/sequencingcosts/ [retrieved: May 30, 2014], Apr 2013.

[8] J. C. McCallum, "Memory Prices (1957-2013)," http://www.jcmit.com/memoryprice.htm [retrieved: May 30, 2014], Feb 2013.

[9] W. J. Ansorge, "Next-Generation DNA Sequencing Techniques," New Biotechnology, vol. 25, no. 4, 2009, pp. 195–203.

[10] S. Pabinger et al., "A Survey of Tools for Variant Analysis of Next-generation Genome Sequencing Data," Brief Bioinform, Jan. 2013.

[11] S. Wandelt et al., "Data Management Challenges in Next Generation Sequencing," Datenbank-Spektrum, vol. 12, no. 3, 2012, pp. 161–171.

[12] V. Fusaro, P. Patil, E. Gafni, D. Wall, and P. Tonellato, "Biomedical cloud computing with amazon web services," PLoS Comput Biol, vol. 7, no. 8, Aug 2011, p. e1002147.

[13] B. Langmead, M. C. Schatz, J. Lin, M. Pop, and S. L. Salzberg, "Searching for SNPs with Cloud Computing," Genome Biol, vol. 10, no. 11, 2009, p. R134.

[14] B. Langmead, C. Trapnell, M. Pop, and S. L. Salzberg, "Ultrafast and Memory-efficient Alignment of Short DNA Sequences to the Human Genome," Genome Biol, vol. 10, no. 3, 2009, p. R25.

[15] R. Li et al., "SNP Detection for Massively Parallel Whole-Genome Resequencing," Genome Research, vol. 19, no. 6, 2009, pp. 1124–1132.

[16] J. Goecks, A. Nekrutenko, and J. T. The Galaxy Team, "Galaxy: A Comprehensive Approach for Supporting Accessible, Reproducible, and Transparent Computational Research in the Life Sciences," Genome Biology, vol. 11, no. 8, Aug 2010, p. R86.

[17] M. Reich et al., "Gene Pattern 2.0," Nat Genet, vol. 38, no. 5, May 2006, pp. 500–501.

[18] B. Néron et al., "Mobyle: A New Full Web Bioinformatics Framework," Bioinformatics, vol. 25, no. 22, Nov 2009, pp. 3005–11.

[19] H. Plattner, A Course in In-Memory Data Management: The Inner Mechanics of In-Memory Databases, 1st ed. Springer, 2013.

[20] M.-P. Schapranow, "Transaction Processing 2.0," Master's thesis, Hasso Plattner Institute, 2008.

[21] P. Svensson, "The Evolution of Vertical Database Architectures – A Historical Review," in Proceedings of the 20th Int'l Conf on Scientific and Statistical Database Management. Springer-Verlag, 2008, pp. 3–5.

[22] A. Vajda, Programming Many-Core Chips. Springer, 2011.

[23] A. Clements, Computer Organization & Architecture: Themes and Variations. Cengage Learning, 2013.

[24] A. S. Tanenbaum, Modern Operating Systems, 3rd ed. Pearson Prentice Hall, 2009.

[25] J. M. Hellerstein and M. Stonebraker, Readings in Database Systems, 4th ed. MIT Press, 2005.

[26] S. S. Lightstone, T. J. Teorey, and T. Nadeau, Physical Database Design: The Database Professional's Guide to Exploiting Indexes, Views, Storage, and more. Morgan Kaufmann, 2007.

[27] J. M. Hellerstein, M. Stonebraker, and J. Hamilton, Architecture of a Database System, Foundation and Trends in Databases. now Publishers, 2007, vol. 1.

[28] M. Gardiner-Garden and M. Frommer, "CpG Islands in Vertebrate Genomes," Mol Biol, vol. 196, no. 2, July 1987, pp. 261–282.

[29] A. Knöpfel, B. Grone, and P. Tabeling, Fundamental Modeling Concepts: Effective Communication of IT Systems. John Wiley & Sons, 2006.

[30] T. K. Das and M. R. Mishra, "A Study on Challenges and Opportunities in Master Data Management," Int'l Journal of Database Mgmt Syst, vol. 3, no. 2, May 2011.

[31] The Genome Reference Consortium, "Genome Assemblies," http://www.ncbi.nlm.nih.gov/projects/genome/assembly/grc/data.shtml [retrieved: May 30, 2014].

[32] A. Rector, W. Nolan, and S. Kay, "Foundations for an Electronic Medical Record," Methods of Information in Medicine, 1991, pp. 179–186.

[33] A. T. Holdener, AJAX: The Definitive Guide, 1st ed. O'Reilly, 2008.

[34] D. Crockford, "RFC4627: The application/json Media Type for JavaScript Object Notation (JSON)," http://www.ietf.org/rfc/rfc4627.txt [retrieved: May 30, 2014], July 2006.

[35] M.-P. Schapranow, "Apps of analyze genomes," http://we.analyzegenomes.com/apps/ [retrieved: May 30, 2014], March 2014.

[36] U.S. National Institutes of Health, "Clinicaltrials.gov," http://www.clinicaltrials.gov/ [retrieved: May 30, 2014], 2013.

[37] U.S. National Library of Medicine, "Unified Medical Language System (UMLS)," http://www.nlm.nih.gov/research/umls/ [retrieved: May 30, 2014], Jul 2013.

[38] S. Krawetz, Bioinformatics for Systems Biology. Humana Press, 2009.

[39] M. Weske, Business Process Management - Concepts, Languages, Architectures. Springer, 2007.

[40] M. Owen and J. Raj, "BPMN and Business Process Mgmt," http://www.omg.org/bpmn/Documents/6AD5D16960.BPMN_and_BPM.pdf [retrieved: May 30, 2014], 2003.

[41] M.-P. Schapranow, H. Plattner, and C. Meinel, "Applied In-Memory Technology for High-Throughput Genome Data Processing and Real-time Analysis," in System on Chip (SoC) Devices in Telemedicine from LABoC to High Resolution Images, 2013, pp. 35–42.

[42] The 1000 Genomes Project Consortium, "VCF (Variant Call Format) Version 4.1," http://www.1000genomes.org/wiki/Analysis/Variant+Call+Format/vcf-variant-call-format-version-41 [retrieved: May 30, 2014], Oct. 2012.

[43] A. Bog, K. Sachs, and H. Plattner, "Interactive Performance Monitoring of a Composite OLTP and OLAP Workload," in Proceedings of the International Conference on Management of Data. Scottsdale, AZ, USA: ACM, 2012, pp. 645–648.

[44] F. Färber et al., "SAP HANA Database: Data Management for Modern Business Applications," SIGMOD Rec., vol. 40, no. 4, Jan. 2012, pp. 45–51.

[45] National Center for Biotechnology Information, "All Resources," http://www.ncbi.nlm.nih.gov/guide/all/ [retrieved: May 30, 2014].

[46] S. A. Forbes et al., "The Catalogue of Somatic Mutations in Cancer: A Resource to Investigate Acquired Mutations in Human Cancer," Nucleic Acids Research, vol. 38, 2010.

[47] L. R. Meyer et al., "The UCSC Genome Browser Database: Extensions and Updates 2013," Nucleic Acids Research, 2012.

[48] M. Krallinger, A. Valencia, and L. Hirschman, "Linking Genes to Literature: Text Mining, Information Extraction, and Retrieval Applications for Biology," Genome Biology, vol. 9, supplement 2, 2008, p. S8.

[49] H. Li et al., "The Sequence Alignment/Map Format and SAMtools," Bioinformatics, vol. 25, no. 16, 2009, pp. 2078–2079.

[50] M. Stonebraker et al., "C-store: A Column-oriented DBMS," in Proceedings of the 31st International Conference on Very Large Data Bases. VLDB Endowment, 2005, pp. 553–564.

[51] G. P. Copeland and S. N. Khoshafian, "A Decomposition Storage Model," in ACM SIGMOD Record, vol. 14, no. 4. ACM, 1985, pp. 268–279.

[52] S. B. Needleman and C. D. Wunsch, "A General Method Applicable to the Search for Similarities in the Amino Acid Sequence of Two Proteins," Mol Biol, vol. 48, no. 3, Mar. 1970, pp. 443–53.

[53] T. F. Smith and M. S. Waterman, "Identification of Common Molecular Subsequences," Journal of molecular biology, vol. 147, no. 1, Mar. 1981, pp. 195–7.

[54] P. Ferragina and G. Manzini, "Opportunistic Data Structures with Applications," in Proceedings of the 41st Annual Symposium on Foundations of Computer Science. IEEE, 2000, pp. 390–398.

[55] J. Dean and S. Ghemawat, "MapReduce: Simplified Data Processing on Large Clusters," in Proceedings of the 6th Symposim on Operating Systems Design and Implementation, 2004, pp. 137–150.

[56] A. Stabenau et al., "The Ensembl Core Software Libraries," Genome Research, vol. 14, no. 5, 2004, pp. 929–933.

[57] R. Nielsen et al., "Genotype and SNP Calling From Next-generation Sequencing Data," Nature Reviews Genetics, vol. 12, no. 6, 2011, pp. 443–451.

[58] D. R. Bentley et al., "Accurate Whole Human Genome Sequencing Using Reversible Terminator Chemistry," Nature, vol. 456, no. 7218, 2008, pp. 53–59.

[59] M. Margulies et al., "Genome Sequencing in Microfabricated High Density Picoliter Reactors," Nature, vol. 437, no. 7057, 2005, pp. 376–380.

[60] Hasso Plattner Institute, "Future SOC Lab," http://www.hpi.uni-potsdam.de/forschung/future_soc_lab.html [retrieved: May 30, 2014], Feb 2014.

[61] Intel Corporation, "Intel Product Quick Reference Matrix," http://cache-www.intel.com/cd/00/00/47/64/476434_476434.pdf [retrieved: May 30, 2014], Apr 2011.

[62] ——, "Intel Solid-State Drive 520 Series," http://www.intel.com/content/dam/www/public/us/en/documents/product-specifications/ssd-520-specification.pdf [retrieved: May 30, 2014], Feb 2012.

[63] H. Li and R. Durbin, "Fast and Accurate Short Read Alignment with Burrows-Wheeler Transformation," Bioinformatics, vol. 25, 2009, pp. 1754–1760.

Comparing Local, Collective, and Global Trust Models

Charif Haydar, Azim Roussanaly, and Anne Boyer
Université de Lorraine
Laboratoire Loria, Nancy, France.
{charif.alchiekhhaydar, azim.roussanaly, anne.boyer}@loria.fr

***Abstract*—Today, trust modelling is a serious issue on the social web. Social web allows anonymous users to exchange information without even knowing each other beforehand. The aim of a trust model is to rerank acquired information according to their reliability, and to the trustworthiness of their authors. During the last decade, trust models were proposed to assist the user to state his opinion on the acquired information, and on their sources. We identify three paradigms for trust modelling: the first relies on evaluating previous interactions with the source (individual trust), the second relies on the word of mouth paradigm where the user relies on the knowledge of his friends and their friends (collective trust), and the third relies on the reputation of the source (global trust). In this paper, we propose and compare three trust models, each of which represent one of the precedent paradigms. All three models make use of subjective logic (SL). SL is an extension of probabilistic logic that deals with the cases of lack of evidence. It supplies framework for modelling trust on the web. The comparison includes three axes: the precision, the complexity and the robustness to malicious attacks. We show that each of the three models has a weak point in one of the three axes.**

***Index Terms*—Trust modelling; Subjective logic; Collective trust; global trust; local trust; reputation.**

I. Introduction

This paper provides an extension of work presented at the third International Conference on Social Eco-Informatics in Lisbon in November 2013 [1]. The work centres on modelling trust in the stackexchange [2] question answering platform, and compares the precision of two models, one is based on individual opinions, and the other is based on collective opinions. This extended work integrates more trust models, and uses further analysis of the robustness, the complexity, and the precision of models.

Web 1.0 provided a popular access to the largest data store ever existed (Internet). The major difficulty resided in extracting relevant information and resources from the huge mass of data available for most queries. Information retrieval (IR) came out to yield Internet more efficient and exploitable by ranking resources according to their relevance to queries. Then, web 2.0 arrived with more interactive tools such as forums and social networks. Numerous people who were only spectators in web 1.0, became the actors in web 2.0. They are now able to share their own opinions and knowledge. Collaborative IR and social recommender systems (RS) [3] are now used to rank these kinds of resources.

Web 2.0 provides a highly connected social environment. It allows data exchange among anonymous people from all around the world. Acquiring information from such sources raises the question about its reliability and trustworthiness. Modelling social trust into computational trust appeared to overcome the trustworthiness problem (for both information and resources). Today, computational trust is integrated in many domains and contexts such as social networks, recommender systems [4], [5], file sharing [6], multi-agents systems [7] etc.

We consider social trust as the belief of an individual, called truster, that another individual, called trustee, has the competence and the willingness to either execute a task in favour of the truster, or to assist him to execute it. The assistance can simply be recommending another individual to execute the task. The truster tries to acquire information and constructs his own belief about the trustee before deciding to cooperate with him [1].

Building truster's opinion on the trustee is mainly derived by three means; the first is by exploiting previous interactions between both of them, so the truster relies on his own knowledge about the trustee (individual opinion). The second uses the word of mouth mechanism, where the truster exploits the collective knowledge of his trustee friends and their friends (collective opinion). The third is by relying on a global reputation score associated to the trustee (global opinions).

Our objective in this paper is to propose and compare three trust models based on the three types of opinions. A local trust model that uses the individual opinions when they are available, and otherwise collective opinions. A collective trust model that uses strictly collective opinions. A global trust model that uses only global opinions. We evaluate these three models from the perspective of precision, complexity, and robustness to malicious attacks. All our models use a framework of subjective logic (SL) [8], which is an extension of probabilistic logic, based on the belief theory [9], [10]. SL provides a flexible framework form modelling trust [1], [11].

The object of our comparison is the dataset stackexchange. It is a social website based on a question answering platform to assist users to find answers to their questions in diverse domains (programming, mathematics, English language, cooking, etc.). We assume that proposing an answer is proof of willingness to assist the person asking. Therefore, our objective is to find the user capable to provide the most relevant answer.

The paper is organized as follows: in Section II, we explain the general framework, by presenting social trust and computational trust. In II-C, we introduce subjective logic and some of its operators. In Section III, we detail the three proposed models. In Section IV, we describe the used dataset, and present our interpretation of the success and the failure of an interaction according to current data structure. In Section V, we discuss the results of the three axes of comparison. Finally, in Section VI, we resume our conclusions and future work.

II. General Framework

The objective of trust is to find the appropriate person to cooperate with in order to achieve a given task. Truster's decision to cooperate or not is influenced by many factors such as: the context, the completeness of his opinion about the trustee, the reputation of the trustee, the emergency of the task for him, and many more. In the following section, we present a real life example about trust in order to explain this phenomena, and some factors that can influence the cooperation decision.

Suppose that Alice wants to paint her house. She advertises this information and receives estimates from three professional candidates (Eric, Fred and George) *willing* to do the job for her. She already knows Eric because he painted her clinic sometime ago. Alice does not know neither Fred nor George. If Alice is satisfied with Eric's job in her clinic, she might hire him for the house directly, and ignore the offers of Fred and George. Nevertheless, if Alice is a perfectionist, she will investigate on their work. Alice can ask her friends (Bob and Caroline) about Fred and George. She might also use a referential organization that classifies painters, or any other means to acquire information about the reputation of the three painters.

Suppose that Bob says that Fred is a good professional. Caroline says that she recently hired George to paint her house and she is not satisfied with his work, whereas her sister Diana has hired Fred and was satisfied. Alice trusts Bob and Caroline but not as painters, because she thinks they lack competence in that domain. Even so they are still capable of playing an important role as advisers or recommenders.

After the suggestions of Bob and Caroline, Alice will eliminate George and choose between Eric and Fred.

In this scenario, Alice asked her friends only about the candidates that she herself does not know. But the scenario could have been changed if she asked them also about Eric. Bob could say for example that Eric is good for concrete walls used in Alice's clinic, but he is not very competent for wooden walls like those of Alice's house. This information can be sufficient to convince Alice to hire Fred instead of Eric.

This example shows the limit of direct interactions manner, and that the word of mouth may be useful to enrich the knowledge of the truster about the trustee. It can lead to sharpen his decision even when he thinks that his own acquired knowledge is sufficient to make a decision.

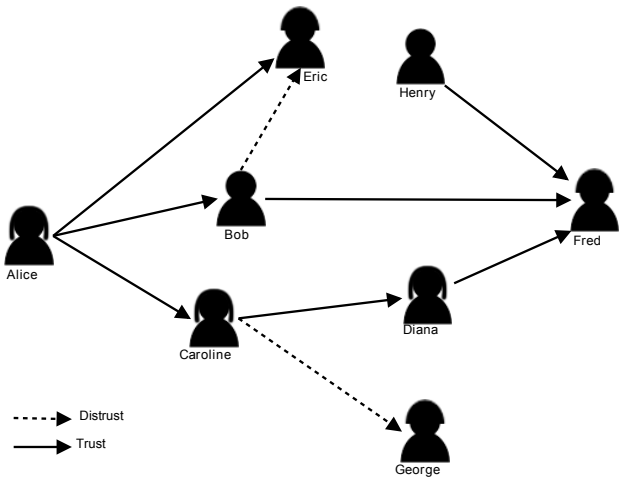

Fig. 1: Trust network.

In another scenario, Alice could simply search for the best ranked painter referenced by specialised magazine, syndicate, or other organization. Usually, these rankers track all the interactions of their target, and use its entire history to perform their ranking. As we can see in Fig. 1, neither local nor collective trust model would allow Alice to use the interaction of Henry with Fred, as no path connects her to Henry. The global trust models use the opinions of all the users about Fred regardless if Alice trusts them or not. Global opinions are based on a larger number of interactions. Note that the active user has no control on the users who participate in building this kind of opinion for him. His own opinion about participants is not considered.

Furthermore, the current example allows us to distinguish four types of trust relationships; these types are also discussed in [12]:

1) Direct trust: is the result of interactions between exactly the truster and trustee, such as the relations "Alice Bob" and "Alice Eric".
2) Indirect trust: the two persons do not know each other. Trust is established due to trustee intermediate persons, such as the relation "Alice Fred".
3) Functional trust: the expectation of the truster is that the trustee accomplishes the task himself, such as the relation "Alice Eric", "Alice Fred" and "Alice George".
4) Referential trust: the expectation of the truster is that the trustee will recommend someone to accomplish the task, such as the relation "Alice Bob" and "Alice Caroline". Note that the recommendation of Caroline is also based on her referential trust in her sister Diana. In other words, no obligation for the trustee in referential trust to base his recommendation on a functional trust relation. Normally, a series of referential trust relations must end with one functional trust relation [13].

Fig. 1 illustrates the trust network used by Alice to make her decision.

In the next section, we discuss the formalization of social

trust for the social web, and compare the different models that exist.

A. Computational trust

Computational trust raised in the last decade to ensure trust awareness in intelligent systems, usually consists of a formalization of social trust adjusted to specific context and application. Basically, computational trust has three axes [14]:

- Quantitative, also called global-trust or reputation: the system computes a score for each user, this score represents his global trustworthiness. This score is considered when any other user needs to interact with this user [15].
- Qualitative, also called local-trust or relationship: takes into account the personal bias. It is represented as user to user relationship. It is the trustworthiness of a user Y from the point of view of one single user X [15].
- Process driven (system): represents the trust of the users in the system [14].

This work focuses on the qualitative and quantitative axes. Most local trust models [4], [16], [17], [18] tend to formulate it as a trust network. A trust network is a directed weighted graph where vertices represent users, and edges represent trust relationships. Models differ by their notation of edges, and their strategies in traversing the network to compute trust between two unconnected users. This operation is called Trust propagation. It is fundamental in local trust models, as it allows to estimate how much a user A (called source node) should trust a user B (called destination node).

Global trust models [19], [6] associate a score of reputation to each user. This same score is used in all the interactions where this user is implicated as a trustee. These models do not take the personal bias into consideration. Hence, when a user is judged reputed/non-reputed, he is seen so by everybody.

Local trust models suffer from a cold start problem, they can not deal neither with new users nor with users having no friends [11]. Global trust models are not concerned by this problem. Nevertheless, it is difficult for new users to build their own reputation in a global trust model, since ancient reputed users are usually more susceptible to be recommended by the system.

As most social applications, social recommender systems are exposed to different types of malicious attacks [20], [21]. Malicious attackers aim to take the control over the recommender system for different purposes, such as driving the system to recommend or to oppose the recommendation of given items, inserting viruses, spam or advertisements, etc.

Trust-aware recommenders are more robust than other recommenders for most attacks [22]. Nevertheless, they are not completely immune to all kinds of malicious attacks, such as group attacks [23] which is always possible in some trust models.

Computational trust is applied to many fields in artificial intelligence, recommender systems, file sharing, Spam detection, networks security, etc. Most computational models are fitted to their application fields and context. Basically, we identify two categories. Models dealing only with trust relationships, and models dealing with trust and distrust relationships.

The first category contains numerous models such as [24], [25], [26], [27], [28], [29]. The main disadvantage of this category is that models do not distinguish between distrusted and unknown persons. Social systems have to give chances to new and unknown users to prove their trustworthiness, whereas it must be more severe in blocking distrusted and malicious users [30]. Unknown users are often new users, a system unable to distinguish them from distrusted users risks being very severe with them, so discourage the evolution of the trust network, or being too tolerant with distrusted users, which make it less efficient.

Models in the second category distinguish between unknown and distrusted people. Models in [31], [32], [33], [12], [34], identify three possible cases: trust, distrust and ignorance. Authors in [34] classify these models into two groups; gradual models [31], [32], [34] and probabilistic models [33], [12]. Gradual representation of trust is more similar to the human way in expressing trust, whereas probabilistic representation is more meaningful mathematically.

We use SL [12], [8] in our models. Our choice is motivated by many factors. SL considers trust ignorance and distrust relationships, which is compatible with our need to distinguish between unknown and distrusted people. Most other trust models consider the creation and the evolution of trust links as an external issue, they describe and deal with existing links. SL is more transparent about this issue, trust relationships in SL are based on the accumulation of interactions between a couple of users. It proposes many operators that allow to integrate many aspects and factors of trust, which make it one of the most generic and flexible trust models.

It is based on the belief theory [9], [10], which offers the capacity to aggregate many beliefs coming from many sources (even contradictory ones), which corresponds to the case when a user needs to aggregate the opinions of many of his friends on a given issue.

Nevertheless, we compare them to referential model called MoleTrust [4]. This model has been frequently used in the trust based recommendation, and proved its quality in this domain, and surpassed the collaborative filtering in the term of performance. We explain this in the following Section II-B, before proceeding to the Section II-C which is dedicated to explain the structure and some operators of subjective logic.

B. MoleTrust

Moletrust was presented in {massa04. It considers that each user has a domain of trust, to where he adds his trustee friends. User can either fully trust other users, or not trust them at all. The model considers that trust is partially transitive, so its value declines according to the distance between the source user and the destination user. The only initializing parameter is the maximal propagation distance d.

If user A added user B to his domain, and B added C, then the trust of A in C is given by the equation:

$$Tr(A,C) = \begin{cases} \frac{(d-n+1)}{d} & \text{if } n \leq d \\ 0 & \text{if } n > d \end{cases} \quad (1)$$

Where n is the distance between A and C ($n = 2$ as there are two steps between them; first step from A to B, and the second from B to C).
d is the maximal propagation distance.

Consider $d = 4$ then: $Tr(A,C) = (4-2+1)/4 = 0.75$.

We consider that when a user A accepts an answer of another user B, that A trusts B. A Moletrust link between both users is created. While the algorithm is not aware to distrust so no interpretation exists for unaccepted answers.

C. Subjective logic

Subjective logic (SL) [8] is an extension of probabilistic logic, which associates each probability with a degree of uncertainty. Subjective logic allows to build models that treat situations of incomplete evidences.

Belief theory [9], [10] is a special case of probability theory dedicated to treat incomplete knowledge. The sum of probabilities of possible cases can be less than 1. Subjective logic [35] offers a belief calculus using a belief metrics called opinion. The opinion of an individual U about a statement x is denoted by:

$$\omega_x^U = (b, d, u, a)$$

where: $b, d, u \in [0, 1]$ are respectively the belief, disbelief and uncertainty of U about x. The sum of the three values equals to one (i.e $b + d + u = 1$). Base rate $a \in [0, 1]$ is the prior probability. Basically, base rate is a statistical measure applied in cases of evidence absence. For example, when we know that the percentage of a disease x in a given population is 1%, then the base rate of x's infection is 1%. When we meet a new individual who did not make a test for the disease, a priori we assume that the probability that he is infected is 1%. In social trust cases, while no a priori statistics are present, we consider that unknown person has a half chance to be trustworthy. So we use a base rate $a = 0.5$. In subjective logic, the base rate steers the contribution of the uncertainty in the computation of the probability expectation value according to 2:

$$E(\omega_x^U) = b + a \times u \quad (2)$$

The opinion in subjective logic is based on the accumulation of successful and failed experiences. After each experience, U updates his opinion about x consistently with experience's outcome. According to this description, opinion can be represented as a binary random variable. Beta distribution is normally used to model the behaviour of this kind of variables. By consequence, the opinion corresponds to the probability density function (PDF) of beta distribution. PDF is denoted by two evidence parameters α and β that can be written as functions of the number of successful and failed experiences respectively.

TABLE I: Opinion evolution with successive interactions.

No	state	r	s	belief	disbelief	uncertainty
0	no interaction	0	0	0	0	1
1	successful interaction	1	0	1/3	0	2/3
2	failed interaction	1	1	1/4	1/4	2/4
3	successful interaction	2	1	2/5	1/5	2/5

$$\begin{aligned} \alpha &= r + W \times a \\ \beta &= s + W \times (1 - a) \end{aligned} \quad (3)$$

where r is the number of successful experiences (evidences). s is the number of failed experiences. W is the non-informative prior weight that ensures that the prior (i.e., when $r = s = 0$) Beta PDF with default base rate $a = 0.5$ is a uniform PDF (normally $W = 2$).

The expectation value of beta PDF is:

$$E(Beta(p|\alpha, \beta)) = \frac{\alpha}{\alpha + \beta} = \frac{r + Wa}{r + s + W} \quad (4)$$

In subjective logic, the mapping between the opinion parameters and the beta PDF parameters is given as follows:

$$b = \frac{r}{(r + s + W)} \quad (5)$$

$$d = \frac{s}{(r + s + W)} \quad (6)$$

$$u = \frac{W}{(r + s + W)} \quad (7)$$

Table I shows an example of the evolution of an opinion with successive interactions.

In the first line of Table I, we see the case of absence of evidence (experiences). The opinion is completely uncertain ($u = 1$). In this case, according to 2, the expectation value equals to the base rate value. The arrival of new experiences, will make the uncertainty decrease, regardless if these experiences are successful or not. Successful experiences will augment the belief, whereas failed experiences will augment the disbelief.

Subjective logic opinions can be illustrated in the interior of an equilateral triangle. The three vertices of the triangle are called belief, disbelief, and uncertainty. The uncertainty axis links the uncertainty vertex with the opposite edge (the belief-disbelief edge), the uncertainty value of the opinion is plotted on this axis considering that its contact with the edge belief-disbelief represents the value 0, whereas the contact with the uncertainty vertex represents the value 1. In the same way, we describe the belief and the disbelief axis.

The opinion is represented by the intersection point of the three projections on the three axis (belief, disbelief and certainty) as shown in the example in Fig. 2. The bottom of the triangle is the probability axis, the probability expectation value is the projection of the opinion point on the probability axis with respect to the line linking the uncertainty vertex with the base rate point on the probability axis. Fig. 2 illustrates an example of opinion mapping in subjective logic. The opinion

is represented by a point inside the triangle. The point is the intersection of the projection of the three values b, d, and u on the axis of belief disbelief and uncertainty, respectively. The probability expectation value $E(x)$ is the projection of ω_x on the probability axis directed by the axis linking a_x with the uncertainty edge.

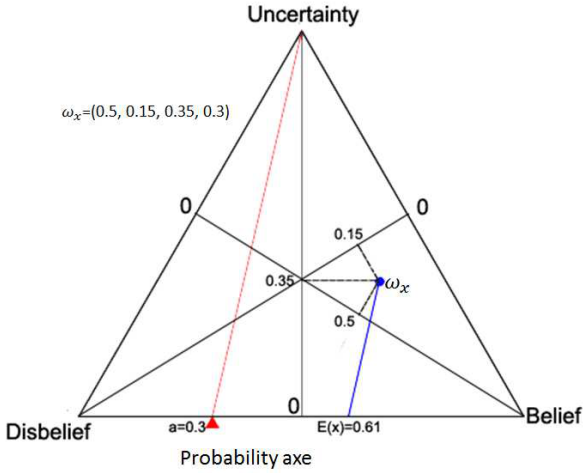

Fig. 2: Subjective logic Opinion.

Note that changing the value of base rate can make people more reckless or more cautious.

After defining the structure of the opinion in subjective logic, we need to explain some of subjective logic operators that are useful for building trust network. Local trust networks are usually represented by a direct graph, where vertices represent users, and edges represent trust relations. Consequently, computing trust value between two users is reduced to finding a path or more connecting them to each other.

1) Trust transitivity: If an individual A trusts another individual B, and B trusts C, trust transitivity operator is used to derive the relation between A and C.

Subjective logic proposes the uncertainty favouring transitivity. This operator enables the user A to receive the opinion of a friend C of his trustee friend B, or to ignore the opinion of B in case of A distrust B. Formally the operator is given by (8).

$$\omega_B^A = (b_B^A, d_B^A, u_B^A, a_B^A)$$
$$\omega_C^B = (b_C^B, d_C^B, u_C^B, a_C^B)$$

$$\omega_B^A \otimes \omega_C^B = \begin{cases} b_C^{A:B} = b_B^A.b_C^B \\ d_C^{A:B} = b_B^A.d_C^B \\ u_C^{A:B} = d_B^A + u_B^A + b_B^A.u_C^B \\ a_C^{A:B} = a_C^B \end{cases} \quad (8)$$

The belief of A in C is the union of his belief in B, and that of B in C. The disbelief of A in C is the union of his belief in his friend B, and the disbelief of B in C. The uncertainty of A in C is the sum of his uncertainty and disbelief in B, and the union of his belief in B and the uncertainty of B about C.

2) Opinion fusion: Suppose in the previous example that A has another trustee friend D who also trusts C. A has two separate sources of information about C.

Subjective logic proposes two main types to fuse B's and D's opinions about C:

$$\omega_B^C \underline{\oplus} \omega_D^C = \begin{cases} b_{B\diamond D}^C = \frac{b_B^C.u_D^C + b_D^C.u_B^C}{u_B^C + u_D^C - u_B^C.u_D^C} \\ d_{B\diamond D}^C = \frac{d_B^C.u_D^C + d_D^C.u_B^C}{u_B^C + u_D^C - u_B^C.u_D^C} \\ u_{B\diamond D}^C = \frac{u_B^C + u_D^C}{u_B^C + u_D^C - u_B^C.u_D^C} \end{cases} \quad (9)$$

This operator allows the user to aggregate the opinions of his trustee friends, regardless of their possible contradictory opinions.

III. Proposed Models

The aim of our models is to predict the most relevant answer to a given question within a list of answers. Basically, trust models consider that the person asking tends more to accept answers written by trustworthy people, so trust models try to retrieve these users. We have developed three trust aware models. All of them are based on subjective logic. We refer to them as local trust model (LTM), which is a classical local trust model, so it exploits only individual opinions when they are available, otherwise it exploits collective opinions. Collective trust model (CTM) which exploits collective opinions all the time, and global trust model (GTM), which depends on context-aware reputation scores.

A. Local trust model

This model is basically based on the model proposed in [12]. It consists of building a local trust network between users. The edges of this network are SL opinions of users about each other. Formally, we represent the trust network as a graph $G = (V, E)$, where V represents the set of vertices (users), and E represents the set of edges (direct trust relationships). Suppose that a user a asks a question q, a set of users $\mathcal{R}$ will propose many answers. The aim of the trust model is to compute a score for each user $r \in \mathcal{R}$ using the trust network. The trust model estimates that a will accept the answer proposed by the highest score member of $\mathcal{R}$. Local trust computes the score according to (10):

$$score(r) = \begin{cases} e(a,r) & \text{if } e(a,r) \in E \\ \sum_j \underline{\oplus}[e(a,f_j) \otimes e(f_j,r)] & \text{elsewhere} \end{cases} \quad (10)$$

where: $e(a,r)$ is the direct opinion (edge) of a in r.
f_j is a member of F, the set of the direct friends of a, formally: $f_j \in F : \Longleftrightarrow\ e(a,f_j) \in E$.
$\Sigma_{0\leq j\leq N}\underline{\oplus}$ is the aggregation of multiple (exactly N) opinions. Note that $e(f_j,r)$ itself can be composed of the opinions of the friends of f_j.

To predict the accepted answer of a given question q asked by the user A, we identify $\mathcal{R}$ the set of users who contributed

1: **procedure** INDIVIDUALTRUST(A, B)
2: **if** $(e(A,B) \in E)$ **then**
3: **return** $e(A,B)$
4: **else**
5: $e(A,B) \leftarrow e(0,0,1)$ ▷ a neutral opinion
6: **for all** $f \in A.friends$ **do**
7: $e(A,B) \leftarrow e(A,B) \underline{\oplus} [e(A,B) \otimes e(f,B)]$
8: **end for**
9: **return** $e(A,B)$
10: **end if**
11: **end procedure**

Fig. 3: Individual trust function.

answers to the current question. Then, we traverse the graph (trust network) to compute the local trust between person asking and each of them. We assume that A will accept the answer of the most trustee user within $\mathcal{R}$. According to this model, A consults his friends only about members of $\mathcal{R}$ with whom he has no direct interactions, otherwise considers only his own opinion. Consulted friends repeat the same strategy in consulting their friends. The drawback of this model is when A has only one interaction with a member r of $\mathcal{R}$, this might be not enough to evaluate him. A may have a friend B who has had many interactions with r so more apt to evaluate r. According to this model A will not ask B about his opinion in r.

The aim of A is to rank $\mathcal{R}$ by the trustworthiness of its members. Whenever he has no information about a member r of $\mathcal{R}$, A will ask his friends their opinions on this very member. So the task of friends is to evaluate r without any farther information. The more A is connected, the faster is the model, since the probability to have direct relationships with the members of $\mathcal{R}$ becomes higher. The pseudo code 3 shows how this model works in demanding friends' opinions.

B. Collective trust

This model is based on collective opinions instead of personal opinions. In the previous model, collective opinions were used only in the case of absence of personal opinions. In this model, collective opinions are used in all cases. This semantically means that A will ask his friends about all the members of $\mathcal{R}$, so even those whom he already knows. Formally:

$$score(r) = \begin{cases} (a,r) \underline{\oplus} \sum\limits_j \underline{\oplus} [e(a,f_j) \otimes e(f_j,r)] \\ \text{if } e(a,r) \in E \\ \\ \sum\limits_j \underline{\oplus} [e(a,f_j) \otimes e(f_j,r)] \\ \text{elsewhere} \end{cases} \quad (11)$$

This model assumes that direct interactions are frequently unable to assure sufficient information about users. In the previous model, a user could supply a personal opinion about another user once he has at least one interaction with him. We think that this affects the quality of the opinion, because of the lack of experience. In the current model, user aggregates his opinion with the his friends' opinions, each friend's opinion is conditioned by the trust given to him by the active user. This means that we always need to traverse the graph, which can be time consuming in large graphs. We alleviate this problem by building a graph by domain in our data.

1: **procedure** COLLECTIVETRUST($(A, \mathcal{R})$)
2: Declare $scores[\mathcal{R}]$
3: **for all** $score \in scores$ **do** $score = e(0,0,1)$ ▷ neutral opinion
4: **end for**
5: **for all** $(r \in \mathcal{R}$ **do**
6: **if** $opinion(A,r) \in E$ **then**
7: $scores[r] = e(A,r) \otimes scores(r)$
8: **end if**
9: **end for**
10: **for all** $f \in A.friends$ **do**
11: $fscore = collectiveTrust(f, \mathcal{R})$
12: **for all** $r \in \mathcal{R}$ **do**
13: $scores[r] = scores[r] \underline{\oplus} fscore[r]$
14: **end for**
15: **end for**
16: **return** $scores$
17: **end procedure**

Fig. 4: Collective trust function.

Example:

Back to the same example in Section II. Fig. 5 illustrates trust network extracted from the described relations in the example. So when A asks a question to which she get replies from E, F and G, then $\mathcal{R} = E, F, G$. A needs to rank the members of $\mathcal{R}$ to identify the most trustworthy member.

For the individual trust model, scores are computed as follows:

$$score(E) = e(A,E)$$

$$score(F) = [e(A,B) \otimes e(B,F)] \underline{\oplus} [e(A,C) \otimes e(C,D) \otimes e(D,F)]$$

$$score(G) = e(A,C) \otimes e(C,G)$$

As for the collective trust model, the scores of F and G do not change, but the score of E becomes as follows:

$$score(E) = [e(A,E)] \underline{\oplus} [e(A,B) \otimes e(B,E)]$$

Now let us add a link between C and F, and see the effect of such a link:

In individual trust model:

$$score(F) = [e(A,B) \otimes e(B,F)] \underline{\oplus} [e(A,C) \otimes e(C,F)]$$

In collective trust model:

$$score(F) = [e(A,B) \otimes e(B,F)] \underline{\oplus} [[e(A,C) \otimes e(C,F)] \underline{\oplus} [e(A,C) \otimes e(C,D) \otimes e(D,F)]]$$

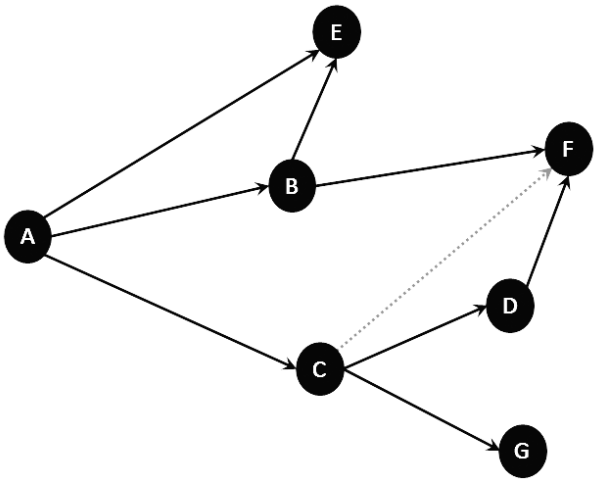

Fig. 5: Trust graph.

Once again, we see that in the local trust model, as C has a direct link with F, so when A asks him about his opinion on F, C sends back his response relying only on his own opinion on F. Whereas in the collective trust model, for the same case, C asks D his opinion on F, and aggregate the response of D with his own opinion before sending back the result to A.

C. Global trust model (GTM)

Each question in stackexchange has a set of associated keywords. We use these keywords to build a new global trust model (GTM), that exploits the reputation of users towards keywords. When a user A accepts the answer of a user B to his question, a link is created or updated between B and each of the keywords associated with the question, so we do not use neither a graph nor user to user connections. The semantic signification of the links between users and keywords is the experience of the user towards the keyword, so a reputed user towards a keyword can also be called expert. The profile of a user is represented by a hashtable where keys are the keywords and the values are subjective logic opinions to express his experience related to the keywords.

To predict the accepted answer of a given question Q asked by the user A, we identify $\mathcal{R}$ the set of users who contributed answers to the current question, and the set K of keywords associated to the question. We compute the average reputation score to each member of $\mathcal{R}$ towards the elements of K. The member with the highest average score is chosen to be the owner of the accepted answer.

In (LTM) and (CTM) only friends and their friends can influence the decision of the person asking, and their influence is limited by the trust that the person asking accord to each them. In the current model, all the users in the dataset can influence the reputation score of the members of $\mathcal{R}$ without conditions. This can affect the robustness of the model to malicious attacks.

IV. Experimental work

We use the dataset of the website stackoverflow. The website offers a question answering forum for multiple domains, mainly but not limited to computer science. The available data contains 30 domains. Users subscribe to the website by domain, so one user can have multiple accounts, according to the number of domains in which he participates. The total number of accounts is 374,008 for about 153,000 users.

The user asks a question in a given domain, and associates a set of keywords to his question, then he receives many answers. He chooses the most relevant answer and attributes an "accepted answer" label to it. Nevertheless, users can keep proposing new answers. Subsequent users who have the same problem as the person asking can take advantage of the answers and rate them on their usefulness by attributing thumb-up or thumb-down. In the available dataset, we have access to only the total number of thumbs-up and the total number of thumbs-down an answer receives, but no information about suppliers' identities. The website offers the possibility to order answers by relevance, where the accepted answer is put in the top of the list, followed by the other answers ordered by the difference between thumbs-up count and thumbs-down count. Our work aims to use trust based models to predict the accepted answer over the set of available answers. Total number of questions in current dataset equals to 371,594, for a total number of answers 816,487. We divide the questions of each domain in five equivalent sets. Then, we apply a crossing test in five iterations, in each iteration we use four sets for learning and building the trust network and the fifth for testing the prediction quality.

A. Interpreting interactions

In stackoverflow, when a user A asks a question, he receives a list of answers from many users. A can accept only one answer. Unaccepted answers are not necessarily bad ones. They might be simply not good enough compared to the accepted one. They might even be better but arrived too late and A has already accepted another satisfactory answer. Basically, while we do not have an explicit reaction from A towards the unaccepted answers, we suppose four hypotheses to treat them:

1) rigorous hypothesis: unaccepted answers are considered as failed interactions.
2) ignoring hypothesis: unaccepted answers are not considered at all.
3) independent subjective hypothesis: in both previous methods, the interaction value is either +1 (successful), or -1 (failed). In this method, we introduce relatively successful/failed interactions. We use the rates of community towards the answer to estimate a subjective successful/failure of the interaction. In fact, the thumb-up represents a successful interaction with an unknown user, same thing for the thumb-down with a failed interaction. The global reaction of the community towards the answer is subjective opinion resulting from

members' interactions with the answer. We consider the expectation value of the community's opinion as the value of the partially successful/failure of the interaction between the person asking and the replier.

4) dependent subjective hypothesis: regarding to the fact that a user can give a thumb-up for an answer because it is better/worse than others, the attribution of thumb-up and thumb-down can be relative too. The reason why we propose another subjective method where our certainty is influenced by the global number of thumb-up and thumb-down attributed to all answers of the same question. In this case, the opinion about an answer is dependent on the the other opinions about the other answers.

$$Certainty_j = \frac{\sum_j th}{2 + \sum_{i=an_0}^{an_n} \sum_i th}$$

where th is an absolute value of thumb (up or down).
j is the current answer.
n is the number of answers of the current question.
The default non-informative prior weight W is normally defined as W = 2 because it produces a uniform Beta PDF in case of default base rate a = 1/2.
The three components of the opinion are:

$$belief_j = uncertainty_j \times \frac{\sum_j th_{up}}{\sum_j th}$$

where $\sum_j th_{up}$ is the number of thumbs up attributed to the answer.

$$disbelief_j = uncertainty_j \times \frac{\sum_j th_{down}}{\sum_j th}$$

where $\sum_j th_{down}$ is the number of thumbs down attributed to the answer.

$$uncertainty_j = 1 - certainty_j$$

Finally, we compute the expectation value of the resulting opinion and consider it as the value of the relative success/failure interaction.

V. Evaluation

Our comparison includes three axes. The first one is the precision of prediction. The second is the complexity, which indicates the execution time of each model. The third is the robustness to malicious attacks.

A. Precision

Evaluation Metrics: We consider the problem of finding the accepted answer as a list ranking problem with one relevant item. Mean reciprocal rank (MRR) is a quality metrics used to evaluate systems that have to give out a ranked list with only one relevant item. Reciprocal rank (RR) of question is $1/r$ where r is the rank given by the evaluated algorithm to the accepted answer. Mean reciprocal rank is the mean value of RR's to all questions. The value of this metrics varies between 0 and 1, where 1 is the best precision score.

TABLE II: MRR results.

method	MoleTrust	Local trust	Collective trust	Global trust
Rigorous	-	0.57	0.88	0.884
Ignoring	0.53	0.58	0.75	0.7
Dependent probabilistic	-	0.62	0.87	0.815
Independent probabilistic	-	0.617	0.86	0.78

TABLE III: MPLR results.

method	MoleTrust	Local trust	Collective trust	Global trust
Rigorous	-	0.37	0.85	0.85
Ignoring	0.3	0.36	0.69	0.6
Dependent probabilistic	-	0.442	0.84	0.76
Independent probabilistic	-	0.438	0.83	0.73

MRR is a good indicator to the performance of prediction algorithms for ranked lists. Nevertheless, we think that it is not perfectly adapted to our case. MRR is usually used for systems that have to predict a list of items within which a relevant item exists. We are trying to find the accepted answer by re-ranking an existing list of answers. Remark the case when the algorithm ranks the relevant item in the last position of the list, the algorithm is recompensed for at least having chosen the item within the list. In our case, the list is predefined, so the algorithm should not be recompensed for ranking the relevant item at the end of the list. The range of RR values is $[1/r, 1]$, we propose a modified version where the value varies between 1 if the relevant item is in the top of the list, and 0 if it is at the end of the list. We call this metrics mean predefined lists rank (MPLR), where predefined lists rank PLR is given by the formula 12:

$$PLR = \frac{N - r}{N - 1} \tag{12}$$

where: N is the size of the list.

MPLR is the average of PLRs for all questions. We employ a modified competition ranking strategy, so the ranking gap is left before the *ex aequo* items. For example, if two items on the top of the list have the same score, they are considered both second, and no item is put at the top of the list.

Results and discussions: Only questions with accepted answers and more than one proposed answer are appropriate for our test. The corpus contains 118,778 appropriate questions out of the 371,594 questions of the corpus.

As MoleTrust is not probabilist and does not consider the distrust, only the ignoring hypothesis is applicable on it. Table II illustrates the MRR scores of the four models, and Table III illustrates MPLR scores. MPLR scores are, of course, lower than those of MRR. Nevertheless, both tables lead to the same conclusions.

Obviously, all the SL models are more precise than MoleTrust, which guarantee certain improvement to the SL compared to the referential model.

Concerning the SL models, it is obvious that the precision of CTM and GTM surpass widely that of LTM.

Basically, the truster in LTM builds his belief by mainly exploiting his own interactions. Whereas, CTM leans fully on collective opinions that rely on more complete evidences than individual ones. Trustee friends enrich collective opinions by more knowledge, that make them more reliable and accurate. These results show the limit of individual opinions and local relationships, because direct interactions can be poorly informative, and relying only on them can lead to inaccurate decisions. A fellow in a social environment always needs to integrate and interact within communities to be more informed, and more capable to adjust his decisions.

GTM offers a larger archive of interactions to the trusters. A truster in GTM has access to all the past interactions of the trustee, so constructs a more elaborate belief about him. The performance of GTM is largely better than LTM. On the other hand, it is less precise than CTM even though it makes use of more evidences. We assume that sometimes these supplementary evidences cause information overload, and tend to be noisier than profitable. In addition, GTM accord the same weight to the opinions of all participants, whether they were trustees or not to the active user.

We would refer to the difference in context consideration. LTM and CTM consider the domain of the question as a context. GTM considers a more refined interpretation of the context, based on a sub-domain defined by the tags associated to the question. The context in GTM is very adaptive, this leads to a more specific person having competences in this exact context. The presence of this person in the list of people who answered the question proves his willingness to assist the person asking, his competence and mastery of subject lead him to be the owner of the accepted answer. For example, if B was able to answer a question of A about Java programming language, this does not mean that he would be able the next time to reply to a question about C++ programming language, although it is still the same domain (context) for LTM and CTM. So even within the same domain, people might be experts in narrow sub-domains, while having a general or even weak knowledge about the other parts of the domain. If A tried to reply the question of B about C++, only GTM will detect that he is not the best person to reply in the domain of "c++ programming", whereas LTM and CTM will consider him a good candidate because he is a trustee in the domain of "programming". Current precision score do not allow to evidently evaluate the influence of both considerations.

In real life, regret can assist to re-establish trust. The structure of local trust systems does not possess any mechanism to reconsider relationship after a bad integration with a destination user (which can be occasional), collective opinions allow the reconsideration of the relation with this user if he was trustee by intermediate friends of source user.

Regarding the four hypotheses about treating unaccepted answers in LTM, we find that probabilistic methods are slightly better than both rigorous and ignoring hypotheses. In CTM and GTM, the three hypotheses that try to infer from unaccepted answers surpass the performance of the fourth that neglects this information (ignoring hypothesis). We conclude that unaccepted answers can be profitable, and then should not be neglected. Extracting information from these answers is possible thanks to the flexibility of subjective logic. This framework proves again its capability to deal with incomplete evidence cases.

B. Complexity

Complexity is an important issue to evaluate algorithms. The importance of complexity evaluation is to estimate the time needed for each model to be executed. A good recommender must be able to generate recommendation in a reasonable delay.

Algorithm complexity is a function of $t(n)$, where n is the input size. The complexity function gives a clue about the expected execution time of the algorithm given an input of size n. Complexity calculus is independent from the hardware, the programming language, the compiler and the implementation details. It takes in consideration only the elementary operations of the algorithm such as: variable assignment $(t(n) = 1)$, comparison $(t(n) = 1)$, loop on a list of size n $(t(n) = n)$, comparing all the values of an array to each other $(t(n) = n^2)$, traversing a graph $(t(n) = V + E)$, where V is the number of vertices, and E is the number of edges).

The big O notation is used to refer to the complexity, this notation keeps only the elementary element that maximize the algorithm complexity. For example, having an algorithm with $(t(n) = n^2 + 4 \cdot n + 2)$, the equivalent in big O notation is $O(n) = n^2$.

Generally, the evaluation of complexity takes into account the worst case and the average case. The worst case represents the upper bound of time needed to execute the algorithm, and the average case is the lower bound.

Graph traversal complexity equals to $O(V+E)$. In the worst case, MoleTrust, LTM and CTM have to execute this operation R times, where R is the number of users who have proposed answers to the question. By consequence, the complexity of these three models equals to $O(R \cdot (V + E))$. The complexity of the GTM is $O(R \cdot L)$, where L is the size of the list of keywords with which the member of R has a reputation score.

In the worst case, MoleTrust, LTM and CTM have the same complexity. We can consider that the GTM is less complex whereas L is usually smaller than $V + E$.

As the worst case is mostly infrequent, it is usually accompanied by the average case complexity. We define R' as the subset of R that contains the users having no direct trust relationship with the active user, so $R' \subseteq R$. The average complexity of LTM is $O(R' \cdot (V + E))$. It is obvious that average complexity of CTM is the same as its worst case complexity. The average complexity MoleTrust is less than LTM and CTM, because it stops searching when it finds the first member of R. Basically the average complexity of the GTM equals also to $O(R \cdot L)$ when using lists. The average complexity of hashtables is $O(1)$.

Finally, from the perspective of complexity we find that GTM is the less complex, followed by LTM, and CTM is the most complex one, so the most time consuming. This complexity analyses illustrates the limitation of CTM for the applications with huge graphs.

C. Robustness against malicious attacks

In a malicious group attack scenario, we distinguish three groups of users. The attackers who participate in the execution of the attacks. The affected users whose recommendations are contaminated because of the attack. And the pure users who are untouched by the attack.

In the group attack many profiles cooperate to achieve the attack's goal. These profiles can be possessed by one or more user, they unite to improve the score of one or more of them to a point that they can control the recommendations generated to other users. In the current application a group of profiles might ally together to execute a group attack. The members of the group keep mutually inserting questions, answering them, and accepting each others' answers. While the application is contextualized, and the trust models treat the domains separately, attackers must target a given domain or repeat the same operation for each domain.

GTM is weak for this kind of attacks. The group can augment the reputation score of its members for chosen keywords, and contaminate them. Hence, when any pure user asks a question containing contaminated keywords, he will become affected and receive a contaminated recommendation from the attackers.

In MoleTrust, the local and the collective models, the topology of the graph assists to isolate the group of attackers. The communitarian behaviour will make them highly connected to each other but weakly connected to other users. Hence, a pure user can not be affected unless he decides himself to trust one or more attackers, which is very unlikely. Even if this happens once by accident, the resulting link is not strong enough (especially in CTM), because it is based on one interaction, and it will be more uncertain than other links, so with weak influence.

In [23], the authors propose the bottleneck property to state about the robustness of a trust model to the group attack. The meaning of the bottleneck property is that when having a trust relation $s \rightarrow t$, where s is a pure user and t is an attacker, this relation is not significantly affected by the successors of t. Fig. 6 illustrates an attacked graph with a bottleneck property.

The edges in our models are formed of SL opinions. So the only way to strengthen this relation, is by more successful interactions between s and t, which is decided by s himself. To summarize, in local and collective model, the attack can succeed only when pure users decide deliberately to trust attackers.

The conclusion of this analysis is that the global model is weaker than the local and the collective models against malicious group attacks.

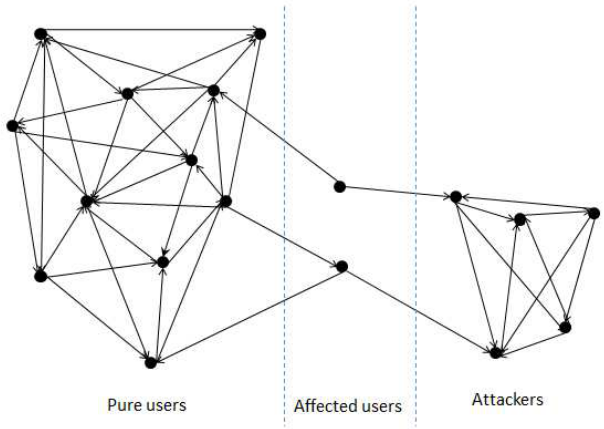

Fig. 6: The bottleneck phenomena in the trust graph.

VI. Conclusion and Future Works

In this paper, we compared three different interpretations of computational trust model.

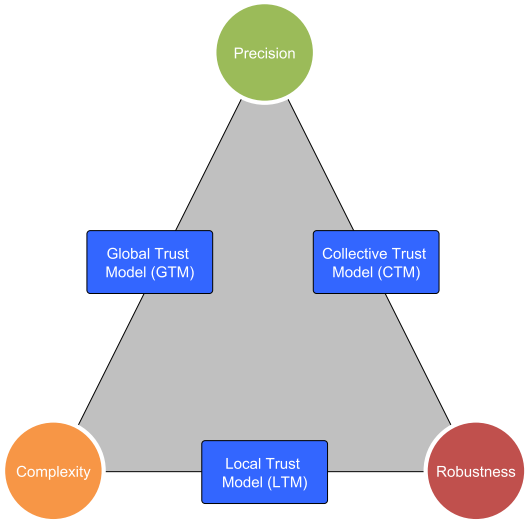

Fig. 7: The triple evaluation of the three trust models.

We effected a comparison that consists of three axes (precision, complexity, and robustness). Fig. 7 resumes the conclusions. In terms of precision, we showed the limits of individual opinions compared to collective and global ones. Using opinions based on evidences from multiple resources is more fruitful, with some reservations to information overload limits. We represent that in Fig. 7, by putting CTM and GTM closer to the precision circle than LTM.

Although CTM has the best precision score, it still the most complex model among the three studied model. In Fig. 7, GTM and LTM are closer to the circle of complexity, because they have a better (lower) complexity. Even though GTM is less complex than LTM.

GTM forms a compromise between precision and complexity. Yet, its weak point is in the robustness axe. It is

theoretically weaker than the other two models. In Fig. 7, it is located far from the robustness circle.

Our study puts the light on a weak point of each model. So the choice of a model is still dependant on the type application, the context and the desired characteristics.

Some of our results are theoretically inferred (the robustness issue). We are interested in proving that empirically, by simulating malicious attacks on the dataset, in order to measure the influence of these attacks on the precision of each model.

REFERENCES

[1] C. Haydar, A. Roussanaly, A. Boyer *et al.*, "Individual opinions versus collective opinions in trust modelling," in *SOTICS 2013, The Third International Conference on Social Eco-Informatics*, 2013, pp. 92–99.

[2] "Stack overflow website (data collected in sep 2011)." http://stackexchange.com/, Sep. 2013, [Online; accessed 2014-05-30].

[3] T. Zuva, S. O.Ojo, S. Ngwira, and K. Zuva, "A survey of recommender systems techniques, challenges and evaluation metrics," *International Journal of Emerging Technology and Advanced Engineering*, 2012.

[4] P. Massa and B. Bhattacharjee, "Using trust in recommender systems: an experimental analysis," *Trust Management*, pp. 221–235, 2004.

[5] J. A. Golbeck, "Computing and applying trust in web-based social networks," Ph.D. dissertation, University of Maryland at College Park, College Park, MD, USA, 2005, AAI3178583.

[6] S. D. Kamvar, M. T. Schlosser, and H. Garcia-Molina, "The eigentrust algorithm for reputation management in P2P networks," in *Proceedings of the 12th international conference on World Wide Web*, ser. WWW '03. New York, NY, USA: ACM, 2003, pp. 640–651.

[7] S. D. Ramchurn, D. Huynh, and N. R. Jennings, "Trust in multi-agent systems," *The Knowledge Engineering Review*, vol. 19, 2004.

[8] A. Josang, "Subjective logic," http://folk.uio.no/josang/papers/subjective_logic.pdf, Sep. 2013, [Online; accessed 2014-05-30].

[9] A. Dempster, "The DempsterShafer calculus for statisticians," *International Journal of Approximate Reasoning*, vol. 48, no. 2, pp. 365–377, 2008.

[10] R. R. Yager, J. Kacprzyk, and M. Fedrizzi, Eds., *Advances in the Dempster-Shafer theory of evidence*. New York, NY, USA: John Wiley & Sons, Inc., 1994.

[11] C. Haydar, A. Boyer, and A. Roussanaly, "Local trust versus global trust networks in subjective logic," in *Web Intelligence (WI) and Intelligent Agent Technologies (IAT), 2013 IEEE/WIC/ACM International Joint Conferences on*, vol. 1. IEEE, 2013, pp. 29–36.

[12] A. Josang, R. Hayward, and S. Pope, "Trust network analysis with subjective logic," in *Proceedings of the 29th Australasian Computer Science Conference-Volume 48*, 2006, pp. 85–94.

[13] A. Josang and S. Pope, "Semantic constraints for trust transitivity," in *Proceedings of the 2nd Asia-Pacific conference on Conceptual modelling-Volume 43*, 2005, pp. 59–68.

[14] M. Kwan and D. Ramachandran, "Trust and online reputation systems," in *Computing with Social Trust*, ser. HumanComputer Interaction Series, J. Golbeck, Ed. Springer London, Jan. 2009, pp. 287–311.

[15] C. N. Ziegler and G. Lausen, "Spreading activation models for trust propagation," in *e-Technology, e-Commerce and e-Service, 2004. EEE'04. 2004 IEEE International Conference on*, 2004, pp. 83–97.

[16] A. Abdul-Rahman and S. Hailes, "Supporting trust in virtual communities," in *Proceedings of the 33rd Annual Hawaii International Conference on System Sciences, 2000*, Jan. 2000, pp. 6007–6016.

[17] K. Krukow, *Towards a Theory of Trust for the Global Ubiquitous Computer: A Dissertation Presented to the Faculty of Science of the University of Aarhus in Partial Fulfilment of the Requirements for the PhD Degree*. Department of Computer Science, University of Aarhus, 2006.

[18] L. Mui, *Computational Models of Trust and Reputation: Agents, Evolutionary Games, and Social Networks*. PhD Thesis, Massachusetts Institute of Technology, 2002.

[19] K. McNally, M. P. O'Mahony, B. Smyth, M. Coyle, and P. Briggs, "Towards a reputation-based model of social web search," in *Proceedings of the 15th International Conference on Intelligent User Interfaces*, ser. IUI '10. ACM, 2010, pp. 179–188.

[20] B. Mobasher, R. Burk, R. Bhaumik, and C. Williams, "Toward trustworthy recommender systems an analysis of attack models and algorithm robustness," *ACM Transactions on Internet Technology (TOIT)*, vol. 7, no. 4, 2007.

[21] A. Jøsang and J. Golbeck, "Challenges for robust trust and reputation systems," in *Proceedings of the 5th International Workshop on Security and Trust Management (SMT 2009), Saint Malo, France*, 2009.

[22] P. Massa and P. Avesani, "Trust-aware collaborative filtering for recommender systems," *On the Move to Meaningful Internet Systems 2004: CoopIS, DOA, and ODBASE*, pp. 492–508, 2004.

[23] R. Levien, "Attack resistant trust metrics," Tech. Rep., 2004.

[24] W. Tang, Y.-X. Ma, and Z. Chen, "Managing trust in peer-to-peer networks," *Journal of Digital Information Management*, vol. 3, no. 2, pp. 58–63, 2005.

[25] M. Richardson, R. Agrawal, and P. Domingos, "Trust management for the semantic web," in *Proceedings of the second international semantic web conference*, 2003, pp. 351–368.

[26] I. Zaihrayeu, P. P. D. Silva, D. L. Mcguinness, I. Zaihrayeu, P. Pinheiro, S. Deborah, and L. Mcguinness, "IWTrust: improving user trust in answers from the web," in *Proceedings of 3rd International Conference on Trust Management (iTrust2005*. Springer, 2005, pp. 384–392.

[27] R. Falcone, G. Pezzulo, and C. Castelfranchi, "A fuzzy approach to a belief-based trust computation," in *Lecture Notes on Artificial Intelligence*. Springer-Verlag, 2003, pp. 73–86.

[28] F. Almenrez, A. Marn, C. Campo, and C. G. R, "PTM: a pervasive trust management model for dynamic open environments," in *First workshop on pervasive security, privacy and trust PST04 in conjuntion with mobiquitous*, 2004.

[29] J. O'Donovan and B. Smyth, "Trust in recommender systems," in *Proceedings of the 10th international conference on Intelligent user interfaces*, 2005, pp. 167–174.

[30] R. Burke, B. Mobasher, R. Zabicki, and R. Bhaumik, "Identifying attack models for secure recommendation," in *Beyond Personalization: A Workshop on the Next Generation of Recommender Systems*, 2005.

[31] M. De Cock and P. P. da Silva, "A many valued representation and propagation of trust and distrust," in *Proceedings of the 6th international conference on Fuzzy Logic and Applications*, ser. WILF'05. Berlin, Heidelberg: Springer-Verlag, 2006, pp. 114–120.

[32] R. Guha, R. Kumar, P. Raghavan, and A. Tomkins, "Propagation of trust and distrust," in *Proceedings of the 13th international conference on World Wide Web*, 2004, pp. 403–412.

[33] U. Kuter and J. Golbeck, "Using probabilistic confidence models for trust inference in web-based social networks," *ACM Trans. Internet Technol.*, vol. 10, no. 2, pp. 8:1–8:23, 2010.

[34] P. Victor, C. Cornelis, M. D. Cock, and P. P. D. S. B, "Gradual trust and distrust in recommender systems. fuzzy sets and systems," in *press*, 2009.

[35] A. Josang, "A logic for uncertain probabilities," *International Journal of Uncertainty, Fuzziness and Knowledge-Based Systems*, vol. 9, no. 03, pp. 279–311, 2001.

Synthetic Standards in Managing Health Lifecycles and Cyber Relationships

Simon Reay Atkinson
Complex Civil Systems Research Group
The University of Sydney
Sydney, Australia
simon.reayatkinson@sydney.edu.au

Amanda Goodger
Engineering Design Centre
The University of Cambridge
Cambridge, England
acg66@cam.ac.uk

Seyedamir Tavakoli Taba
Complex Civil Systems Research Group
The University of Sydney
Sydney, Australia
seyedamir.tavakolitabaezavareh@sydney.edu.au

Nicholas H.M. Caldwell
School of Business, Leadership and Enterprise,
University Campus Suffolk
Ipswich, England
n.caldwell@ucs.ac.uk

Liaquat Hossain
Information Management Division
Information and Technology Studies
The University of Hong Kong
lhossain@hku.hk

***Abstract*—This paper considers connected strands of thinking in the area of socio info techno systems emerging from Sydney University, Complex Civil Systems Group, the Advanced Research and Assessment Group (ARAG), Cambridge University, Engineering Design Centre, the Information Management Division at the University of Hong Kong and the School of Business, Leadership and Enterprise at University Campus Suffolk. The paper is divided into six sections. First, it examines the synthesis of the machine and the organization in what has been termed mechorganics; then, it identifies the Lodestone concept as a means for instrumenting social awareness; before considering the role variety plays in collaboratively influencing complex systems, over time, and coordinating and controlling them, in time. Having established the bases, the paper then develops a lifecycle model applied, in this instance, to the health sector. Finally, it examines the needs for assaying information and data as a means of providing the social transparencies needed for real time verification and validation. From this, it posits the needs for simple empirical standards and setting/vetting organizations that encourage good behavior and discourage bad. These standards' organizations provide for the governance and assurances necessary for packet-markets to form where transactions / prices can be assured, products verified, exchanges made and fees / taxes abstracted.**

Keywords-mechorganics; lodestone; instrumenting; packet-markets; governance; metadetics; synthetic ecology; assaying.

I. INTRODUCTION

This paper is developed from a paper presented at SOTICS 2013 entitled The Need for Synthetic Standards in Managing Cyber Relationships [1]. In this paper, we consider Cyber may consist of two sub-systems identified and classified as being **"**Coordination Rule and Control (CRC)" and "Collaboration and Social Influence (CSI)" [2, 3]. These system attributes provide the necessary and "requisite variety" [4] to enable both control, "in time", and influence [5]-[9], "over time". In this regard, Cyber may consist of two poles:

> A technologically bounded, largely immeasurable, strongly scientific, stochastic *coordination*, *rule* and *control* space; comprising virtual-media and the display of data dealing with the *real* communication of *facts*; and the *conceptualization* of alternative possibilities, themselves capable of generating hard physical and soft more *social* effects and *collaboratively influencing* them [10].

"Mechorganics" is postulated to have 1) a thematic *systems* identity (defined by its *networked* disciplines) and 2) a *critical* and *functional* education base [11,12]. It is not seen either as 'a reversion of digital data back to an analogue form' [13] or some form of 'Golem' warned of by Wiener [14]. Mechorganics is based on "designing humanity back into the loop" [15,16] and: 'the *synergistic* combination of *civil* mechanical *systems* engineering, social network dynamics, ICT and the management of *interconnected* knowledge, information (and data) *infrastructures* in the *designing* and *composing* of *adaptive* (resilient and sustainable) organizations' [15].

The "Lodestone" concept arose from a concern that the "Cyber-pole" applying Coordination, Rule and Control (CRC) was being emphasized at the expense of the whole and specifically the pole dealing with collaboration and social influence. The result, it was conjectured, was twofold: first, that government was becoming irrelevant to many social-media users and, secondly, that this was creating a vacuum in which less benign influences might flourish. For example, studies of social networking and identity have shown that there is a strong tendency to connect like-to-like [17]. This narrowing focus potentially reduces societal *variety* and makes people less tolerant to alternative ideas

and *ontologies* than their 'non-digital forebears'. They may, in actual fact, become non-democratic, *xenonetworks* (from xenophobia, xenonetworks are 'social networks with a strong dislike or fear of other networks or ideas that appears foreign or strange to them') [3], extremely hostile to alternative ideas (and that they might be wrong). Discussion at the time was focused (as it remains largely today) on finding information 'keystones', 'architectures', 'protocols' or 'gateways' not so much to assist people identify good information from bad but to control. A problem with each of these concepts is that they obtrusively and exclusively focus on the stable, static (hence keystone) and ergodic, as opposed to the dynamic and non-ergodic. The "Information Lodestone" concept recalled the semi-mythical lodestones of antiquity that enabled ancient mariners both to determine / 'fix' their position and simultaneously steer a safe course. The objective is to design a non-obtrusive, dynamic instrument. In this respect, we are commencing work with Health and manufacturers of sensitive materials, to model and identify data / information flows and the potential for leaks along complicated, sensitive lines-of-communication in which knowledge assurances, e.g., for operating on patients, are essential. Other work is being undertaken to teach life systems management skills to young people, with an emphasis on either *metamatics* (the mathematics of cyber-social and cyber-physical systems) or *metadetics*, as defined in this paper. We consider this to be exciting work, on the cutting edge of our science, essential to enabling the emerging Knowledge Enterprise Economies of the 21st Century.

This paper is divided into six sections. In Section II, the cyber-system is considered as it relates to the individual and at the social level. In the next section, means for instrumenting the Cyber are posited from which we then posit the types of setting and standards that might apply. This is then used as the bases for modeling a health life system as applied to the Australian Radiologist profession. Finally, inclusive designs and *standards* to enable people to *sensemake* within new and emerging cyber and synthetic ecologies are posited.

II. Cyber as a Social Being

The informal motto of the Lodestone Project was suggested as 'conscius in res' or "sense-in-being", relating to Badiou's [18] understanding of "being", when he states: 'what happens in art, in science, in true (rare) politics, and in love (if it exists), is the coming to light of an indiscernible of the times, which, as such, is neither a known or recognized multiple, nor an ineffable singularity, but that which detains in its *multiple-being* all the common traits of the collective in question: in this sense, it is the *truth* of the *collective's being*'. The idea of *multiple-beings* holds within it the traits of the social being at the heart of most systems and organizations. It is their truths and trusts that "detain the common traits of the collective in question". When these trusts dissipate or are allowed to wither, the organization may remain as a physical entity (when a building becomes statue) but its essence and being – its "ineffable singularity" – is no longer [19]. It is conjectured that, by dealing with cyber exclusively as an info-techno construct, many organizations lost sight of their "social being".

Considering the Cyber as two poles, it is suggested that one has more info/techno-socio traits; the other more socio-info/techno, in which, building on work by Harmaakorpi et al. [20], [17], it is posited that: 'Info-Techno-Socio systems seek to program (as opposed to programme) the relationship between technical *processes* and humans by *digitizing performance fidelity* and coding for repeatable *risk free* procedures in computer-control-spaces so that *data* and *communication* do not [temporally] contradict each other ' [21]. By contrast: 'Socio-Info-Techno systems stress the *reciprocal interrelationship* between humans and computers to foster *improved shared awareness* for *agilely* shaping the *social programmes of work*, in such a way that *humanity* and *ICT [control] programs* do not contradict each other '[21].

The two systems are also considered in terms of their signatures, where I-T-S systems are considered as strong-signal systems [22]-[25], in which: '*Control* (through *switching*) of Information, Data and Communication are the key variables' after, Castells [26] and Sokol [27]. And weak-signal S-I-T systems [22]-[25], in which: 'Influence (through *shared awareness*) of Information and abstracted social Knowledge are the key variables', after Castells [26].

Most of us intuitively know the type of organization we would wish to be working for. Warren and Warren (1977) considered this in terms of "organizational health" and concluded that 'healthy organizations' have 'a critical capacity for solving problems', [28]. They identified three dimensions of *connectedness* (see also Thibaut and Kelley [29]): *identification* with the organization (they referred to as neighborhood); interstitial *interaction* within the organization and existential *linkages* outside the organization.

Considerations of health apply equally to organizations working with/in the Cyber and their capacity for "problem solving" and so controlling, in time, and influencing, over time. This research is developed further in Section V. It is contended that successful companies are constantly "balancing" between the *exploitative* (delivered *in time* by coordination, rule and control) and the *explorative* (delivered *over time* through collaborative social influence). The capacity for balancing between coordination & control (the exploitative) and collaboration and influence (the explorative) to keep an organization "in kilter" is known as "ambidexterity" [30]. It is suggested that this ability to *dynamically balance* between the *exploitative* and the *explorative* is indicative of a systems ability to "problem solve" and, therefore, of its health.

As humans learn, it is thought that they develop a critical capacity for problem solving based upon their individual social system model. This capacity for systems and critical thinking can be taught and is seen as a necessary pre-requisite for understanding and dealing with complexity. In this regard, from Lever et al. [31], it is considered that:

> **Systems Thinking** may be the ability to determine appropriate options for leading, managing, designing, engineering and modeling complex systems, taking adequate *empirical* account of different system types, configurations, dynamics and constraints, and
>
> **Critical Thinking** may be the ability to ask the right questions and make useful sense of information that is technically complex, incomplete, contradictory, uncertain, changing, *non-ergodic* and subject to competing claims and interests.

After Dreyfus & Dreyfus [32], it is suggested we all have an individual 'meta-datum' that *reference* what is posited as our "metadetic spheroid" [32]-[34]. This gives rise to concepts of "metadetic-datum", with similarities to a geodetic datum used to "reference" the spheroidal model of the earth being applied, e.g., World Geodetic System (WGS) 84. Individual metadetic spheroids may be broadly similar. How they are referenced – in other words their datum – is seen to affect how humans' process information and what they perceive. A metadetic-spheroid is an individual's model (no matter how incomplete) of the sociodetic-spheroidal "beings" / organizations they inhabit; see Fig. 1. The meta-datum achieves the best "fit" of an individual's metadetic-spheroid to what may be thought of as its "sociodetic-spheroid" describing the overall model of the related social system.

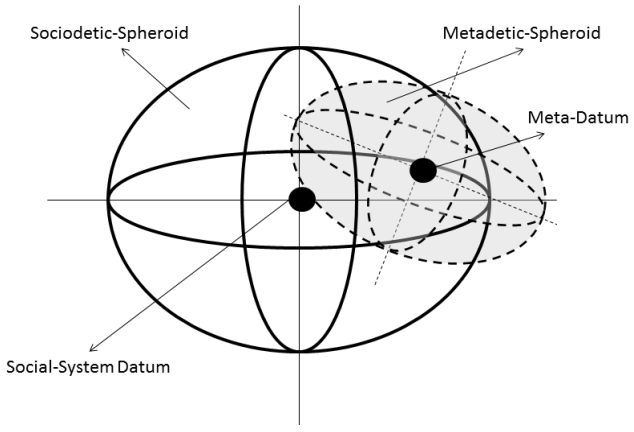

Figure 1. Sociodetic / Metadetic Spheroids and Datums

Bunge [35] maintains that 'perception is personal; whereas knowledge is social'. An individual's perception of their "sociodetic spheroidal system" is incomplete. Only by "collaboratively connecting" with "others" metadetic spheroids may an individual begin to "map" the sociodetic spheroidal whole. It is this process of "collaborative sensemaking" that moves what is effectively static, positional information and data to the social and dynamical knowledge of "being".

Markov chains applied within Bayesian Belief Networks [36] were considered by Logan and Moreno [37] in terms of 'Meta-State-Vectors' referenced to 'Meta-Data' [32]-[34]. Meta-State-Vectors (MSVs) relate to the idea of some information containing "indicators" that will be identified immediately against an individual's metadetic-datum without the need for preamble / additional processing. MSVs are therefore distinguishable from serial information; from which 'expert' human processors 'can form diagnostic hypotheses and draw rational conclusions from system patterns [and] *critical* reflection of their own meta-datum' [32]. In terms of collaboration and shared awareness, this should enable individuals to 'make better use of one another's expertise' [39], particularly if 'authenticated' [39], validated and verified.

In a social system, there also exists the risk of knowledge blindness or "blind knowledge" [40,41]. Models of "info/techno-socio exchange" and "socio-info/techno knowledge capture" therefore need to differentiate 'between the active physical and technological capture of data and information' [42, 43] and the socio-info/techno exchange of knowledge [44]-[49]. To understand how the best "fit" is to be achieved between the info/techno-socio "machine" and the socio-info/techno organizational "being", it is necessary to identify the system's ecology and its purpose / role within it. If an organization's purpose is to problem solve, then how it maps its sociodetic spheroid and positions its datum will determine its health and future fitness judged by its ability to 'test for both success and failure' [50].

III. INSTRUMENTING THE CYBER

At the turn of the millennium, the old UK Defence Research Agency (DERA) was undertaking trials of networked soldiers at the British Army Training Unit in Suffield (BATUS), Canada. Soldiers had all been issued with GPS. As reported to the first author, the result was "digital" in terms of the troops' movement, which was recorded as being "stop and go". Troops would stop, find out where they were, report their position and then move. The researcher removed GPS from the soldiers and caused them to return to map and compass. The result was dramatic. Soldiers began to interpret their datum against the map and to use their senses to determine progress. They used the compass to provide analogue direction and their bearing to dynamically align their datum.

After the Heisenberg principle, Price [51] suggests that 'it is impossible to determine simultaneously both the position and momentum of a particle with any great degree of accuracy or certainty'. This led the first author to surmise a potential metaphor for the modern age: 'that we *know*

precisely where we are but we no longer *know* where we are going'. Although causality is hard to attribute [52], it may be possible to apply the Heisenberg principle as a useful rule-of-thumb when designing dynamic (non-ergodic) systems by suggesting that:

> 'the more precisely one measures a position, the less able one may *identify* change, over time, and vice versa' [19].

This has specific implications for system designs noting the predilection in recent years to emphasize metrication and the setting of targets / goals etc. for managing organizations. Reported separately [19],[53], instead of improving shared awareness, the excess of information and targets required as a form of control can detract from work [54] and so collaboration and shared awareness. This suggested that reducing collaborative and shared awareness impacts negatively an organization's ability to problem solve. *Ipso facto*, these *exploitative* type organizations become unhealthy and potentially, even, risky places to be.

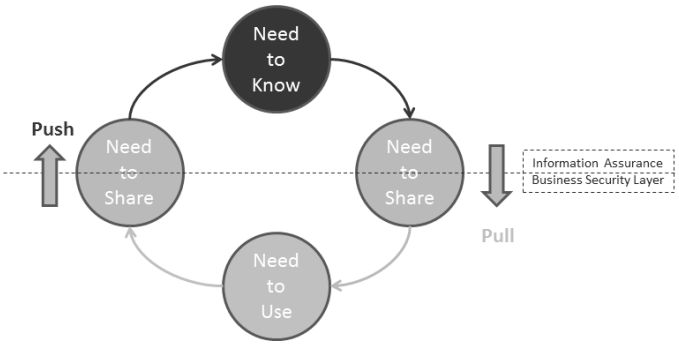

Figure 2. Three Needs Model (3NM)

In addressing the failures of government and collective (collegial) intelligence prior to 9/11 and the Iraq War, the US 9/11 Commission [55] and the (Lord) Butler Enquiry [56] in the UK identified the failure of governance specifically in terms of the *digital ecologies*, then in existence. What they saw was that essential information existed, but that it was being missed, mislaid and, critically, not *shared*. Furthermore, they saw confusion between data, information and communication networks (essentially ICT) and what was being identified and abstracted in terms of *knowledge* and actionable intelligence that could be appropriately *shared* and *used* across government, in real time. Busy Secretary's of State, Ministers, government officials / business / industry / financial leaders and project / programme directors, managers, administrators, users, agents and other consumers of *actionable intelligence* were being overwhelmed in a deluge of data and information technology, process and methodology that was quite literally *blinding them* to what was vital; what was strategic; what was operational; what was routine; what was base level knowledge (against which change and perturbations might 'show up' (be *envisioned*)) and what was simply background *noise*. Organizational structures had not simply atrophied but had become 'tuned out' – no longer able to select between the vital *weak-signals* of innovation, adaptation and change (as threat or opportunity) and the *strong-signals* of method and process [22]-[24],[57],[58]. Recommendations arising from 9/11 [55,56] and the Global Financial Crisis were three fold: firstly has been to require greater transparency, e.g., between the banks, investors, borrowers and governments; secondly, has been to demand greater regulation and thirdly, to move away from the need to know control model towards what has been described as the three needs model – need to know; need-to-share; need-to-use (3NM) [43].

Knowledge blindness [41] was also seen in the run-up to the Global Financial Crisis (GFC), when public and private organizations / individuals capable of identifying alternative *futures* were no longer able to communicate / be listened to: 'It is remarkable that the advanced research and assessment group…put the danger of a global financial collapse into the [UK] draft national security strategy [in 2005/6], but were told to take it out, presumably for political reasons, before it occurred' [59].

In this respect, Szilard's warning that 'information is expensive to acquire and use' [60] and Bunge's recognition that 'knowledge is social' [35] had been potentially lost in the *noise* of new IT, methods and processes. The Lodestone project was conceived from this confusion and a recognition that 'today's economy and society is totally reliant on technology as an enabling force for all economic and societal activities' [61]. It identified the potential of societal cascades in which 'a failure of a very small fraction of nodes in one network may lead to the complete fragmentation of a system of several interdependent networks' [62].

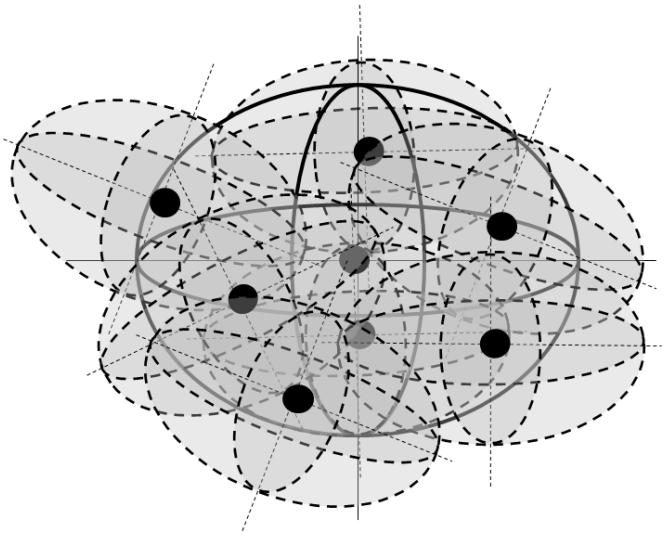

Figure 3. Multiple Meshed Sociodetic / Organisational System Model

The series of cascades considered at the time (2009/10) included UK strategic failure in Iraq and Afghanistan [63] and the global financial crisis. Significantly, an undermining in binding societal trusts and assurances were seen simultaneously to be occurring / had the potential to occur, such as the UK MPs honors and expenses scandals; connecting to the phone hacking scandal that implicated media, police and politicians; to the failure of the BBC to protect young and vulnerable people; to the 2010 UK student riots and the 2011 "London" riots. Each of these cascades began / was exacerbated in the Cyber as, potentially, they will also be resolved. Consequently, it was seen as being necessary 'to protect…information infrastructure technologies…a strategic core [of] which must be maintained, i.e., the Critical National Infrastructure (CNI) / Critical Information Infrastructure (CII)'.

It was recognized that 'small incremental changes and / or large-scale modifications can drastically shape and reshape both the economy and its society with known and often unknown consequences, due to ever-increasing interconnectivities and growing complexities … especially, the information technologies that have come to pervade virtually all aspects of life' [64] – hence "societal cascades". This led to the development of an 'Assurance Case Approach methodology for individual CII assets to input into the larger Business Information Environment', 'the development of a *Mesh* case that can be visualized as the 3-D atomic structure of a molecule' and which 'provides a lateral approach for interdependencies between individual assurance cases' [61]. The "multiple" mesh envisioned represents the sociodetic spheroidal "being" described by Fig. 3 and relates to both interdependencies and assurances to provide overarching confidence in the system whole. Protecting the system whole and providing for resilience and responsiveness required a flexible, adaptive and *ambidextrous* CSI 'approach over time and real-time', CRC mechanisms for interacting directly with 'dynamic information ecosystems' [61], in time.

IV. Setting Cyber Standards

Regulations and controls can be antithetical to creating a shared aware and collaborative ecology and enabling the necessary transparencies for encouraging good behavior and discouraging bad [53]. The three needs model aims to create an information assurance / business security layer between the user (pull) and the knowledge (push) custodian [43], see Fig. 2. There are significant challenges to the managing of information and data allowing for successful, inclusive means for identifying / testing when information and data has been tampered with, changed, added to or where leakage points may occur. Examples include the loss (probably through accounting errors and multiple packet switching) of sensitive materials, e.g., in the explosives industry for products that have to be accounted for to the milligram. Similarly, limited information and data tracking (including asset tracking), e.g., in the health service, means that safety critical equipment can become mislaid or misapplied; so placing patients at risk. During the recent Europe-wide meat scandal an inability to track information and data and test / verify it for validity at key stages of the supply chain, enabled graft and fraud to take place across the whole.

Throughout history, successful economies have been based upon the accurate and reliable "assaying" of materials, such as metals (gold) and food. These social transfer points also became the opportunity for reliable trade and pricing moments and so taxation. Scales and weights were regularly tested and subject to daily public scrutiny – they created *transparencies* for encouraging good behavior and identifying bad. Similar open-social "assaying standards" that can be used to assess information and data in terms of its goodness, purity and proof are harder to find. And there is not a simple and readily available *instrument* such as a "scale and weights" or "map and compass" that can be applied unobtrusively at different stages of often complex supply chains to verify and validate information & data flows and leakages. This does four things: it limits transparencies; so encouraging graft / crime; consequently reducing the opportunities for legitimate business / taxation and discouraging good behavior.

In his theory of the firm, Coase [65] argues that the reason for firms forming is to enable 'employer and employee relations with regard to cost', which 'were necessary to understanding the working of firms and organizations'. He suggested that 'governance is chosen in a cost effective degree to infuse order, thereby to mitigate conflict and realize mutual gain' [65]. It follows that regulations and controls that fail to 'mitigate conflict and realize mutual [collaborative] gain' create unhealthy ecologies by limiting organizational problem solving capacities [53]. In his Law of Requisite Variety, Ashby [4] maintains that 'only variety can *control* variety' and that 'for every control one needs a controller'. Reported separately [19],[53],[66], 'organizations under control, may never be more shared aware than the sum of their links'. By contrast, organizations that enable collaborative social influence can 'generate, on average, 12.5% more [linkages] than formally specified' [19]. Furthermore, these organizations can adapt, over time, to different levels of control. In other words, these 'new' linkages also provide the 'variety necessary to *control* variety' – so meeting Ashby's Law of Requisite Variety.

V. A Sociodetic Health Life-System

Law & Callon state that 'the *technical* thus is *social*' [67]. Not only may the technological be social but, as previously noted, Bunge [35] attests, '*knowledge* is social' also. A key conclusion to be drawn from this is that *mechorganic* designs that consider the social as technical and remove from the technical its social knowledge, strip from an

organization its heart and very 'being' [18],[68] – hence knowledge stripping [21].

Given its highly socialized technical setting, the Radiology specialization was identified as being an early indicator – a *canary* – for the "health" of the medical profession [69]-[71]. Representing approximately 6% of graduating medical students in Australia, the 12 year education programme (from commencing medical studies) is one of the longest specialist professional pipelines [72]. Compared to a graduate employee, radiologists spend three times as long in Higher Education, Table I, and for every year in education; 1.2 years working. Given these constraints, the profession may be highly susceptible to minor changes in recruiting and retention flows. It is also possible that a 6% radiologist-extraction rate (from medical schools / universities) represents a long term constant. In which case, based on US Figures [73], for every extra radiologist an additional 20 medical students (allowing for drop-outs) would need to start at Medical School – but such a simple measure may not reflect those medical students actually wanting / desiring to become radiologists.

TABLE I. HIGHER EDUCATION WORKING PARAMETERS

	Educ-ation (E)	Higher Educ-ation (HE)	Work-ing Life (WL)	E: WL %	HE: WL %
Graduate	17yrs	4yrs	43yrs	40%	9%
Medical	20yrs	7yrs	40yrs	50%	18%
Radiol-ogist	25yrs	12yrs	35yrs	71%	34%

A question asked of the profession was that of its *sociodetic* 'face' in terms of its profile and age. In other words, 'what is the face of the Australian Radiology profession today and what does the profession think it should be?' Noting the sensitivity of the profession to changes in its supply pipeline, another question may be 'what is a sustainable professional age profile?' From the RANZCR Radiology Workforce Report [72], it was possible to model the Radiologist Age Profiles for 2000, when the 35-44 year age group was the largest, compared to 45-54 years in 2010, when the average age was 50.7 (median, 48 years) [72].

Figure 4 considers three faces: the 2010 profile (average age 50); the 2021 population allowing for the ageing of the Baby Boomer / X Generations (~ 1945-1959 / 1960-1974 [74]) with the same numbers as 2010 and, thirdly, allowing for population growth to two thousand (2062) active radiologists based on the same profile. In the first instance, the 2021 profiles show the radiologist 'face' continuing to grey – from 50 to 53. The impact of an ageing tail on opportunities at the start-of-career is significant, which may act unintentionally as a position / job blocker in later years. New positions reduce from about 90 in 2000; to 80 in 2010 and 70 in 2021. Only by growing and changing the population profile to two thousand in 2021 (through a targeted *re-aggregation* program), do start-of-career opportunities increase significantly (to ~125 places compared to between 75 today and 100 in 2021, based on ageing the current population), while the average age or face of the profession reduces to 45 [72].

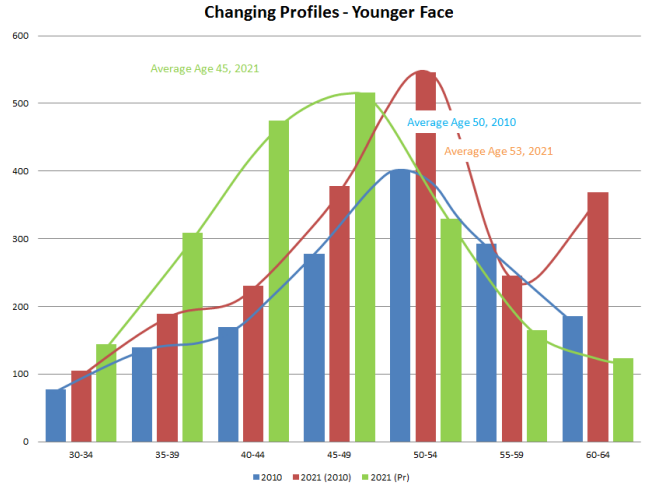

Figure 4. Radiologist New Age / Face Profiles 2010 & 2021

A complex system necessarily manages both growth and decline and 'hunts' for its equilibria positions. Nevertheless, it cannot always grow in order to sustain vacancies and opportunities at start-of-career. This may indicate that the current *sociodetic* model may be inherently unstable and potentially unsustainable (either interstitially or existentially) over the longer term.

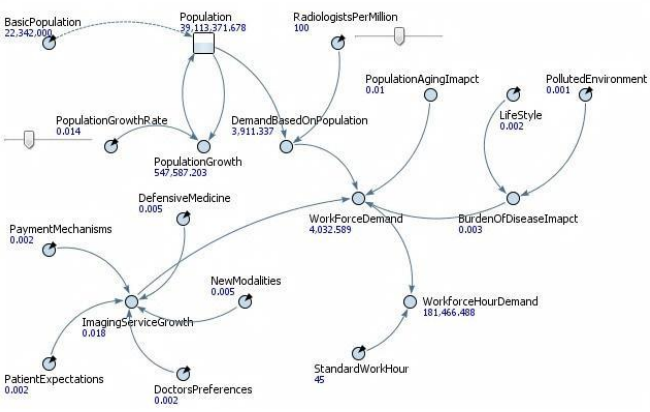

Figure 5. Demand for Radiologists in Working Hours, 2050

Based upon changing Australian demographics to 2050, a *sociodetic* study was undertaken and a *synthetic ecology* model of the profession developed [19],[71]. In this respect, we humbly propose a *Synthetic Ecology* to be:

> 'A system (being or entity) that *adapts*, over time, by combining, through design and by natural processes, two or more *dynamically* interacting networks, including *organisms*, the communities they make up, and the non-living (physical and technological) *mechanical* components of their environment'.

Continuing with the *sociodetic* examination of the Radiologist workforce, a number of factors were considered, including feminization linked to increases in part-time working (more notably amongst female practitioners); reducing working ages and population growth and ageing [72]. On feminization, much research over the last decade [75]-[79] has examined this significant trend in medicine. In this regard, after Douglas [80], Ferguson [81] and Fondas [82], Feminization is considered to be:

> 'the spread of socio traits or qualities that are traditionally associated with females to things (e.g., technologies) or people (professions) not usually [/ previously] described that way; including the shift in gender roles towards a focus upon the feminine, as opposed to the *pre-modern* cultural focus on masculinity' [71].

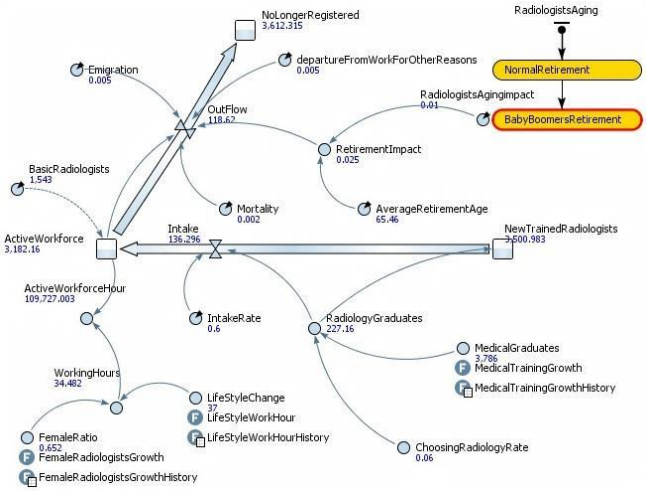

Figure 6. Supply of Radiologists in Working Hours, 2050

Feminization of the medical workforce appears to be a global trend [83]. The 2010 RANZCR Radiology Workforce Report [72] shows that females were 17.1% of radiologists in 1998; 23.6% in 2010 and anticipated to be 34% in 2020. Based on historical data, a function of the *sociodetic* model was designed to consider the future growth of female radiologists reaching a maximum of 65% female by 2050, based upon current European trends. This may have a significant impact on the system impacting, as it does, on the face and age of the population. On average, the working life of a female doctor may be 60% that of male doctors [84]. We hasten to add that we see *feminization* as a good - and one that we need to understand if we are to better *fit* our people to the *sociodetic* systems they work within. There is also an impact upon part time working, in that – quite unexceptionally – 17.3% of Australian female radiologists may be working part-time; compared with 6.7% of male employees [72].

The trend toward reduced working hours is also increasing among Australian radiologists. Studies show in 2010, 34 per cent (c.f. 20 per cent in 2000) planned to decrease their working hours, while only 8.7 per cent (16 per cent in 2000) planned to increase their hours [72]. The function in the *sociodetic* model expects the working hours in the future to be based on a dynamic full-time working profile (that assesses 37 hours per week as a minimum full-time equivalent).

Population growth and ageing is also likely to place potentially extraordinary demands on health services [71]. Changes to the workforce may also have the same demographic impact. The Australian Bureau of Statistics quoted by RANZCR [72] estimates that the 'Australia's civilian labor force aged 15 and over [will] grow to 10.8 million in 2016, an increase of 1.5 million or 16% from the 1998 labor force of 9.3 million'. Yet, the 'average annual growth rate of 0.8% between 1998 and 2016' is less than half that for 1979 to 1998.

Figure 7. Radiologists Working Hours Demand and Supply (2010-2050)

Figure 7 shows the demand and supply of radiologists in a dynamic model over 40 years between 2010 and 2050. It appears that even if the radiology training programme grows at a higher rate (above the medical training growth rate) than its historical growth rate, the system would never be able to meet demand. It suggests that the 6% intake rate of first year registrars is insufficient and industry absorption will need to grow at a higher rate than the radiology specialist training programme. If the system is not able to increase the intake rate faster than the new radiologists supply rate (coming from the national training programmes and immigration) the profession may face two crises. First, supply and demand at current rates will never balance, Figure 7. Secondly, the number of trained, qualified radiologists who fail to enter the profession through the supply pipeline (un-employment in the occupation) may account for more than 3500 specialists over 40 years. Figure 7 indicates that the difference between

demand and supply in active working hours is not simply about increasing the numbers of radiologists. The effects of factors such as feminization and lifestyle changes become more evident. A side-effect (pressure on active radiologists to become more efficient (more for less)) of this imbalance may result in the reduction of imaging services quality – a potential 'third crisis'.

Technological advances in medical imaging have been one of the key factors in the expansion of radiological examinations and procedures since the 1970s. Recent research [71] has shown that rather than necessarily acting as an *aid* to knowledge transfer between GPs, Radiographers and Radiologists that, while the amount of information transfer (20 times as many digitized images compared to old 'films') has increased, the all-important opportunities for collaboration between practitioners and patients (necessary for social knowledge transfer) has potentially reduced. Indeed, radiologists, nurses and radiographers meet to transfer notes, today, far less frequently – and the *weak* signals of 'influence and abstracted social Knowledge' are often lost / drowned out by *strong-signals* of information / data transfers. It was concluded that 'new technologies can result in more efficient productivity (measured by information transfer) but that they can also carry risk if incorrectly applied' [71].

Research identified that Australia, like many other developed countries, e.g., the US and Germany, is facing a dénouement: traditional models of health care, specifically in radiology, are unsustainable based on growing demand for health care services [72]. As a result of unique, interstitial demands on the Australian health system, it is suggested that the existing radiology provisions model needs to consider the *sociodetic* development of patient care, patient safety and quality of service in addition to increasing the number of radiologists and radiographers and changing information communication technologies – the socio-info-techno and the info-techno-socio [71].

Conventional responses in Australia and many developed countries have been to increase the number of radiologists. Since 2007, medical radiation science programs expanded and offered more places at universities. Although students with high entrance scores enter the Australian undergraduate medical imaging programs, it appears that significant numbers retire / leave the profession soon after graduation. This *leakage* may be partly due to the lack of clinically-oriented career development opportunities [85]. The other reason for leakage might be the oversupply of radiographers into the current employment model and its inability to use them appropriately, see Figure 4. The successful implementation of this concept – authorizing diagnostic radiographers to take new practice roles beyond traditional ones – was noted. Caution was also suggested – at the unit and operational level this may offer potentially attractive opportunities for optimization and fractionation as a way of reducing costs by reducing skill contribution and, thereby, investment in the individual [86]. At the system level, this type of 'Just-in-Time' [87] approach can cause problems to the development of skill sets 'over-time' – particularly in a tightly coupled system such as exists between radiographers and radiologists [72].

The appropriate application of part time workers, if managed at the system level, could enable the necessary flows into and out of the profession, while maintaining on-entry positions and the generation of expertise and experts later in the profession. Fragmented and fractionated [88] as the profession may have been managed to date, the projected increase in Part Time workers may negatively impact these positions through 'job-blocking' and reducing the all-important flows into, out of and through the profession [72].

Another tightly coupled relationship is that between the private and the public sectors. By and large, the private sector is interested in recruiting with established proficiency [89], such as radiologists with ten or more years' experience in the field. This can put pressure on employed numbers in the public sector – so creating a vicious circle of reducing numbers; increasing costs to the private sector and reducing levels of in-house expertise.

To increase *sociodetic* / system level performance in various clinical departments, *ecological* identification and classification of 'patients' characteristics' and available technologies may as well be necessary, specifically in 'redesigning scheduling schemes' [90]-[92]. After Walter [93] and Huang and Marcak [94], it is suggested that patient classification in a hospital radiology department may help to improve patient access to care. This may then enable the optimizing of medical resource utilization of socio-info-techno applications by better balancing the time of available doctors and specialists with patients [71].

VI. A New Metadetic

In this paper, we undertook an *ecological identification* (as opposed to system identification) of the Radiologist Profession. We did this in order to develop the *synthetic ecology* in which the highly socialized, technical setting of the radiology profession exists, today. To undertake the *ecological* modelling, we constructed a *sociodetic* model of the profession based upon the age of the profession and the factors affecting its previous, current and future supply and demand. We then used these '*dynamically* interacting networks' to construct and test models of the profession as it may vary (depending on supply and demand inputs), over time. In undertaking this research, we suggested what a *Synthetic Ecology* might 'be'. Given its early application of ICT imaging and data / information management technologies, we saw the Radiologist profession as increasingly operating within the Cyber. This poses challenges if the profession is to: retain knowledge; learn, over time; respond to relatively rapid changes in supply and

demand; while preserving quality of health care provision. We identified that the current model was failing and that, unless change was addressed at the socio-info-techno system level, the profession would fail to meet projected population demands. We concluded that new *inclusive* standards were required in managing health care provision and relationships – specifically between specialists, practitioners, patients and new technologies – that will, increasingly occur, *exclusively* within the Cyber.

In setting Cyber Standards, the issue appears two fold. First, to create inclusive standards through 'the *synergistic* combination of *civil* mechanical *systems* and the management of *interconnected* knowledge, information (and data) *infrastructures* in the *designing* and *composing* of *adaptive* (resilient and sustainable) organizations' [15], that readily encourage openness and transparencies and can be easily *assayed*. Secondly, is for these standards to encourage collaborative shared awareness, from which new controls and pricing opportunities and markets may emerge. Thus, inclusive standards for information / data "packet-switching" may create opportunities for "packet-marketing" and so for pricing and taxation. This returns to *standards* acting as social *instruments* that, through their very "being", can *synthesize* the info-techno and socio to create opportunities both for collaborative *exploration* and *exploitative* control – or *ambidexterity*. It is posited that creating socially inclusive and acceptable *standards* for *assaying* the goodness of information and data enables this *synthesis*. This leads potentially into a third area to do with the synthesizing of Cyber Standards, introduced in Section III and by Figs. 1 and 3 and to a concept for Synthetic Ecologies introduced in Section V. Finally, applying the *sociodetic* model developed for the Australian Radiologist profession, it is suggested that how social reference-standards are designed to be inclusive of the machine and the organization and are best "fitted" to their organizational (*sociodetic*) systems, may potentially be considered as the subject of "metadetics".

ACKNOWLEDGMENT

UK Admiralty and Defence Research Establishments 1842-1991. Advanced Research Assessment Group (ARAG) 2003-2009. CESG. Centenary of Royal Australian Navy (1913-2013).

REFERENCES

[1] S. Reay Atkinson, S.Tavakoli Taba, A.M.C. Goodger, N.H.M. Caldwell, and L. Hossain, "The need for synthetic standards in managing cyber relationships," the Third International Conference on Social Eco-Informatics (SOTICS), 18-20 Nov. 2013, Lisbon, International Academy, Research and Industry Association (IARIA), pp. 1-7.

[2] D. Walker, S. Reay Atkinson, and L. Hossain, "Collaboration without rules - a new perspective on stability operations," IEEE Cyber Conference, 14-16 Dec, 2012, IEEE: Washington.

[3] S. Reay Atkinson, S. Feczak, A. Goodger, N.H.M. Caldwell, and L. Hossain, "Cyber-internet: a potential eco-system for innovation and adaptation," in European Alliance for Innovation: Internet as Innovation Eco-System Summit and Exhibition, 4-6 Oct. 2012, EAI, Riva del Garda: Italy.

[4] R. Ashby, An Introduction to Cybernetics, 1957, London: Chapman and Hall.

[5] D. Cartwright, "Influence, leadership, control," in Handbook of Organizations, J.G. March, Editor, 1965, Rand McNally: Chicago, pp. 1-47.

[6] P.A. David, "Path dependence - a foundational concept for historical social science," Cliometrica - The Journal of Historical Economics and Econometric History, 2007, vol. 1, no. 2, Summer 07.

[7] R.A. Dahl, "The concept of power," Behavioral Science, 1957, vol. 2, issue 3, July: p. 201.

[8] L. Hossain, M. D'Eredita, and R.T. Wigand, "Towards a product process dichotomy for understanding knowledge management, sharing and transfer systems," in Organizations, submitted to Information Technology and People, 2002.

[9] D.H. Wrong, "Some problems in defining social power," the American Journal of Sociology, 1968, vol. 73, no. 6 (May), pp. 673-681.

[10] S. Reay Atkinson, "Cyber-: envisaging new frontiers of possibility," UKDA Advanced Research and Assessmnent Group, 2009, unpublished, Occasional Series, 03/09.

[11] L.O. Dahlgren, "Undervisningen och det meningsfulla lärandet (the teaching of meaningful learning)," 1995, Linköping University.

[12] M. Grimheden and M. Hanson., "Mechatronics - the evolution of an academic discipline in engineering education," Mechatronics, 2005, vol. 15, pp. 179-192.

[13] K.D. Bollacker, "Avoiding a Digital Dark Age," American Scientist, 2010, vol. 98, pp. 106-110.

[14] N. Wiener, God and Golem, Inc., 1964, Cambridge, MA: MIT Press.

[15] L. Hossain, S. Reay Atkinson, M. D'Eredita, and R.T. Wigand. "Towards a mech-organic perspective for knowledge sharing networks in organizations," in UK Academy for Information Systems, 2013, Worcester College University of Oxford, 18-20 March.

[16] S. Reay Atkinson, "An age of evolutionary step change," in Think-Piece, 2012, University of Sydney: Complex Civil Systems Research Group.

[17] M.C. Larsen, "Understanding social networking: on young people's construction and co-construction of identity online," in Proceedings of Internet Research 8.0, Lets Play, 2007, Association of Internet Reserearchers: Vancouver.

[18] A. Badiou, Being and Event, ed. T.O. Feltham, 2005, London: Continuum.

[19] S. Reay Atkinson, "Engineering design adaptation fitness in complex adaptive systems", 2012, PhD Thesis, Cambridge University Engineering Department, EDC: Cambridge, UK.

[20] V. Harmaakorpi, I. Kauranen, and A. Haikonen, "The shift in the techno-socio-economic paradigm and regional competitiveness," in The 43rd Conference of European Regional Sciences Association (ERSA), 27-31 Aug. 2003, Helsinki University of Technology: Lahti Center, Jyväskylä, Finland.

[21] S. Reay Atkinson, A. Goodger, N.H.M. Caldwell, and L. Hossain, "How lean the machine: how agile the mind," the Learning Organization, 2012. vol. 19, issue 3, pp. 183 - 206.

[22] H.I. Ansoff, "Managing strategic surprise response to weak signals," California Management Review, 1975, vol. XVIII, no. 2, pp. 21-33.

[23] B. Coffman, "Weak signal research, Part I: Introduction," 1997, [cited 2010 13 Oct]; available from: http://www.mgtaylor.com/mgtaylor/jotm/winter97/wsrintro.htm, last accessed May 2011.

[24] E. Hiltunen, "Weak signals in organizational futures learning," 2010, Helsinki School of Economics, A-365.

[25] E. Hiltunen, "Good sources of weak signals: a global study of where futurists look for weak signals," Journal of Futures Studies, 2008, vol. 12, no. 4, pp. 21-44.

[26] M. Castells, "The information age. Economy, society and culture," in vol. I, The Rise of the Network Society, 1996, Blackwell Publishers: Oxford.

[27] M. Sokol, "The knowledge economy: a critical view," in paper presented at the Regional Studies Association International Conference Pisa, 12-15 April, 2003.

[28] R.B. Warren and D.I. Warren, The Neighborhood Organizer's Handbook, 1977, South Bend, Ind: University of Notre Dame Press.

[29] J.W. Thibaut and H.H. Kelley, The Social Phsychology of Groups, 1959, New York, London: John Wiley, Chapman Hall.

[30] Z-L. He and P-K. Wong, "Exploration vs. Exploitation: an empirical test of the ambidexterity hypothesis," Organization Science, 2004, vol. 15, no. 4, July-August, pp. 481-494.

[31] T. Lever, H. Ainsworth, G. McGarry, S. Ludewig, and S. Reay Atkinson, "Project management professional and academic, complex critical and systems thinking competency matrix (CCSTCM™)," in Unpublished, CCSTCM™, S. Reay Atkinson, Editor, 2012, Complex Civil Systems Research Group and Project Management Programme: University of Sydney, Faculty of Engineering and IT, School of Civil Engineering.

[32] H.L. Dreyfus and S.E. Dreyfus, Mind Over Machine, 1987, New York: The Free Press.

[33] G. Chaitin, Meta Math, 2005, New York: Pantheon Books.

[34] P.A. Corning, "From complexity to life: on the emergence of life and meaning," Book Review Essay, in Technological Forecasting and Social Change (2003), N. Gregersen, Editor, 2004, OUP: Oxford.

[35] M.A. Bunge, "Ten modes of individualism - none of which works - and their alternatives," Philosophy of the Social Sciences, 2000, vol. 30, no. 3, pp. 384-406.

[36] S. Russell and P. Norvig, Artificial Intelligence A Modern Approach, 1995, Upper Saddle River, New Jersyey: Prentice Hall.

[37] B. Logan and P.J. Moreno, "Factorial hidden models for speech recognition: preliminary experiments, in technical report series," CDR 97/7, September, Cambridge Research Laboratory, 1997, Cambridge University: Cambridge.

[38] H. Mintzberg, D. Dougherty, J. Jorgensen, and F. Westley, "Some surprising things about collaboration - knowing how people connect makes it work better," Organizational Dynamics, 1996, Spring, pp. 60-71.

[39] R.L. Ackoff, "From data to wisdom," Journal of Applied Systems Analysis, 1989, vol. 15, pp. 3-9.

[40] R. Dawkins, The Blind Watchmaker, 1986, London: Penguin Books.

[41] L. Perros-Meilhac, P. Duhamel, P. Chevalier, and E. Moulines, "Blind knowledge based algorithms based on second order statistics," in ICASSP, IEEE Proceedings, vol. 5, Mar. 1999, pp. 2901-2904, Phoenix, Arizona.

[42] D. Rus and D Subramanian, "Customizing information capture and access," ACM Transactions on Information Systems, vol. 15, no. 1, Jan.1997, pp. 67-101.

[43] S. Reay Atkinson, S. Lesher, and D. Shoupe, "Information capture and knowledge exchange: the gathering testing and assessment of information and knowledge through exploration and exploitation," in 14th ICCRTS: C2 and Agility, 2009, CCRP: Washington.

[44] W. Bijker, T. Hughes, and T. Pinch, "The social construction of Technological Systems," 1987, Cambridge, MA: MIT Press.

[45] K. Henderson, On Line and On Paper, 1999, Cambridge, MA: MIT Press.

[46] A. Martinelli, M. Meyer and N. von Tunzelmann, "Becoming an entrepreneurial university? A case study of knowledge exchange relationships and faculty attitudes in a medium-sized, research-oriented university," Journal of Technology Transfer, 2007 (2008), vol. 33, DOI 10.1007/s10961-007-9031-5, pp. 259-283.

[47] Y. Cengeloglu, S. Khajenoori, and D. Linton, "A framework for dynamic knowledge exchange among intelligent agents," in AAAI Technical Report FS-94-02, 1994, AAAI: Palo Alto, CA.

[48] S. Hagen, "From tech transfer to knowledge exchange," Ch. 10, in European universities in the marketplace, the Authors Volume Compilation, 2008, Portland Press Ltd.

[49] B. Latour, "Visualization and cognition: thinking with eyes and hands," Knowledge and Society, 1986, Studies in the Sociology of Culture of Society Past and Present, vol. 6, pp. 1-40.

[50] J.K. DeRosa, A-M. Grisogono, A.J. Ryan, and D.O. Norman, "A research agenda for the engineering of complex systems," in IEEE International Systems Conference, SysCon, 2008, IEEE, pp. 15-22.

[51] H. Price, Time's Arrow: New Directions for the Arrows of Time, 1996, Oxford, UK: OUP.

[52] H. Price, Causation, Physics, and the Constitution of Reality: Russell's Republic Revisited, 2007, Ed. R. Corry, Oxford, UK: OUP.

[53] S. Reay Atkinson, S. Tavakolitabaezavareh, D. Walker, L. Liu, and L., Hossain, "Securing the bolts before the horse has bolted: a new perspective on managing collaborative assurance," in IEEE, 2013, Conference on Security Management, Aug.2013, Las Vegas.

[54] L. Dabbish and R. Kraut, "Controlling interruptions: awareness displays and social motivation for coordination," in ACM Conference on Computer-Supported Cooperative Work, 2004, Chicago, USA.

[55] National Commission of Terrorist Attacks (NCTA), "9/11 Commission Report," 2004 [cited 2007 June], Available from: http://www.9-11commission.gov/report/911Report.pdf., last accessed Mar. 2010.

[56] Lord Butler, "Review of intelligence on weapons of mass destruction," in Report of a Committee of Privy Counsellors, Chairman, the Rt Hon, the Lord Butler of Brockwell KG GCB CVO, 2004, Ordered by the House of Commons, 14 July: London.

[57] M. Granovetter, "The strength of weak ties," American Journal of Sociology, 1973, vol. 78, no. 6, pp. 1360-1380.

[58] M. Hansen, "The search-transfer problem: the role of weak ties in sharing knowledge across organization subunits," Administrative Science Quarterly, 1999, pp. 82-111.

[59] B. Jenkin MP, "Speaking in the House of Commons," Hansard, 2010. Column 699,1 Mar, http://www.publications.parliament.uk/pa/cm200910/cmhansrd/cm100301/debtext/100301-0010.htm, last accessed June 2013.

[60] L. Szilard, "On the Increase of entropy in a thermodynamic system by the intervention of intelligent beings - the critique," (Rapoport A. and M. Knoller trans.), Behavioral Science, 1964 (1929), vol. 9, pp. 302-310.

[61] A.C. Goodger, N.M.M. Caldwell, and J.T. Knowles. "What does the assurance case approach deliver for critical information infrastructure protection in cybersecurity?," in System Safety, The 7th International IET System Safety Conference, incorporating the Cyber Security Conference, Edinburgh, 15 Oct.2012, IET.

[62] S.V. Buldyrev 2, R. Parshani, G. Paul, H.E. Stanley, and S. Havlin, "Catastrophic cascade of failures in interdependent networks," Nature, 2012, vol. 464, 15 April, pp. 1025-1028.

[63] Public Administration Select Committee (PASC), "Who does UK national strategy?," in PASC, 12 Oct., 2010, House of Commons London.

[64] P. Dickens, Global Shift - Reshaping The Global Economic Map in the 21st Century, 2003, London: Sage Publications.

[65] R.H. Coase, "The nature of the firm," Economica, 1937, New Series, vol. 4, no.16, Nov., pp. 386-405.

[66] S. Reay Atkinson, A.M. Maier, N.H.M. Caldwell, and P.J. Clarkson, "Collaborative trust networks in engineering design adaptation," in International Conference of Engineering Design, ICED11, 2011, Technical University of Denmark, Lyngby.

[67] J. Law and M. Callon, "Engineering and sociology in a military aircraft project: a network analysis of technological change," Social Problems, Special Issue, the Sociology of Science and Technology, 1988, vol. 35, no. 3, June.

[68] M. Heidegger, Sein und Zeit (Being and Time), translated by J. Macquarrie and E. Robinson, vol. 2, 1927(1962), London: SCM Press.

[69] D.S. Randolph, "Predicting the effect of extrinsic and intrinsic job satisfaction factors on recruitment and retention of rehabilitation professionals," Journal of Healthcare Management, American College of Healthcare Executives, 2005, vol. 50, no. 1, p. 49.

[70] Z.M. Daniels et al., "Factors in recruiting and retaining health professionals for rural practice," the Journal of Rural Health, 2007, vol. 23, no. 1, pp. 62-71.

[71] S. Tavakolitabaezavareh, K.S. Chung, S. Reay Atkinson, M.W. Pietrzyk, and S. Lewis, "A systems life-cycle approach to managing the radiology profession – an Australian perspective," unpublished work in course of submission, 2013.

[72] RANZCR, "Radiology Workforce Report, 2011," The Royal Australian and New Zealand College of Radiologists (RANZCR), 2010, Canberra.

[73] G. Garrison, C. Mikesell, and D. Matthew, "Medical school graduation and attrition rates," Analysis in Brief, April, 2007, vol. 7, no. 2.

[74] S. Reay Atkinson, S.Tavakolitabaezavareh, M. Harré, R.T. Wigand, and L. Hossain, "Towards a new social philosophy of the physical sciences," in the Third International Conference on Business Sustainability, Management, Technology and Learning for Individuals, Organisations and Society in Turbulent Environme, 2013, Póvoa de Varzim, Portugal, Nov. 20-22.

[75] B. Meyboom-de Jong, "Feminiscring van de geneeskunde," Nederlands tijdschrift voor geneeskunde, 1999, 143, pp. 1134-1135.

[76] JAMA, "The feminization of medicine critical women's health issues in the 21st century saints and sinners: women and the practice of medicine throughout the ages, why aren't there more women surgeons? encouraging the advancement of women," the Journal of the American Medical Association (JAMA), 2000, vol. 285, no. 5, pp. 666-666.

[77] S.P. Phillips and E.B. Austin, "The feminization of medicine and population health," the Journal of the American Medical Association, 2009, vol. 301, no. 8, pp. 863-864.

[78] C. Teljeur and T. O'Dowd, "The feminisation of general practice – crisis or business as usual?," the Lancet, 2009, vol. 374 , issue 9696, p. 1147.

[79] N. Weizblit, J. Noble, and M.O. Baerlocher, "The feminisation of Canadian medicine and its impact upon doctor productivity," Medical Education, 2009, vol. 43, no. 5, pp. 442-448.

[80] A. Douglas, The feminization of American Culture, 1977, Farrar Straus & Giroux.

[81] K.E. Ferguson, "The feminist case against bureaucracy," 1985, Philadelphia: Temple University Press.

[82] N. Fondas, "Feminization unveiled: management qualities in contemporary writings," Academy of Management Review, 1997, vol. 22, no. 1, pp. 257-282.

[83] C.E. Yelland and M.E. Yelland, "Women in medicine: two generations," the Medical Journal of Australia, 2001, vol. 174, no. 1, p. 52.

[84] P.M. Brooks, H.M. Lapsley, and D.B. Butt, "Medical workforce issues in Australia: tomorrow's doctors-too few, too far," the Medical Journal of Australia, 2003, vol. 179, no. 4, pp. 206-208.

[85] T. Smith and S. Lewis, "Opportunities for role development for medical imaging practitioners in Australia: Part 1-rationale and potential," Radiographer: the Official Journal of the Australian Institute of Radiography, 2002, vol. 49, no. 3, p. 161.

[86] L.E. Davis, "The coming crisis for production management: technology and organization," the International Journal of Production Research, 1971, vol. 9, no. 1, pp. 65-82.

[87] T. Ōno, Toyota Production System: Beyond Large-Scale Production, 1988, Productivity Press.

[88] J. Kim and P.J. Bentley, "Immune memory in the dynamic clonal selection algorithm," in Proceedings of the First International Conference on Artificial Immune Systems ICARIS, 2002, Citeseer.

[89] H. Dreyfus and S.E. Dreyfus, Mind over Machine, 2000, New York: The Free Press.

[90] I. Adan and J. Vissers, "Patient mix optimisation in hospital admission planning: a case study," International Journal of Operations & Production Management, 2002, vol. 22, no. 4, pp. 445-461.

[91] T. Cayirli and E. Veral, "Outpatient scheduling in health care: a review of literature," Production and Operations Management, 2003, vol. 12, no. 4, pp. 519-549.

[92] B. Cardoen, E. Demeulemeester, and J. Beliën, "Operating room planning and scheduling: a literature review," European Journal of Operational Research, 2010, vol. 201, no. 3, pp. 921-932.

[93] S. Walter, "A comparison of appointment schedules in a hospital radiology department," British Journal of Preventive & Social Medicine, 1973, vol. 27, no. 3, pp. 160-167.

[94] Y-L. Huang and J. Marcak, "Radiology scheduling with consideration of patient characteristics to improve patient access to care and medical resource utilization," Health Systems, 2013.

Modeling of the Organ of Corti Stimulated by Cochlear Implant Electrodes and Electrodes Potential Definition Based on their Part inside the Cochlea

Umberto Cerasani and William Tatinian
University Nice Sophia Antipolis
LEAT UMR CNRS-UNS 6071
Valbonne, France
Email :
umberto.cerasani@unice.fr william.tatinian@unice.fr

***Abstract* – Cochlear implants are used by deaf people to recover partial hearing. The electrode array inserted inside the cochlea is an extensive area of research. The aim of the electrodes array is to directly stimulate the nerve fibers inside the Organ of Corti. The electrical model of the physical system consisting of Organ of Corti and the electrodes is presented in this paper. This model allowed to run SPICE simulations in order to theoretically detect the minimal voltage sufficient for nerve fiber stimulation as well as the impact of the electrode voltage on the duration of nerve fibers stimulation. Besides, to ensure functional sound perception, the electrode potential should depend on their position inside the cochlea. A afferent nerve fiber repartition map over the cochlea position, considering the frequency sensitivity of the different parts of the ear was created. This projection allowed to propose a theoretical electrodes potential correction based on their cochlea position.**

Keywords: cochlear implant, electrical analog, transient simulations, afferent nerve fibers repartition, spiral ganglions

I. INTRODUCTION

Cochlear implants are an electrical device used by severely deaf people to gain or recover partial audition. They allow direct stimulation of the auditory fibers using an electrodes array designed to reproduce the stimulus that would be generated by a healthy cochlea.

To do so, an external part of the hearing devices is located outside the ear and contains a microphone that captures the acoustic waves and transforms them into an electrical signal used by the data processing unit. Then, this signal is transmitted to the receiver, located within the patient's head, close the skull. The receiver is composed of a demodulator and a set of electrodes driven by electrical signals that will contract the cochlea and stimulate the auditory nerve [1], [2], [3].

Cochlear implants directly stimulate the nerve fibers inside the cochlea, and requires surgery to pull the electrodes array inside the scala tympani (Figure 1).

The connection between the electrodes in the scala tympani and the auditory nerve fibers is critical for efficient nerve fibers stimulation.

In an healthy ear, when a sound wave is produced, it strikes the eardrum and this vibration is reported in the oval window using ossicles. The oval window is the very first part of the cochlea. This oval window vibration creates a wave propagating inside the scala vestibuli, which is filled with perilymph.

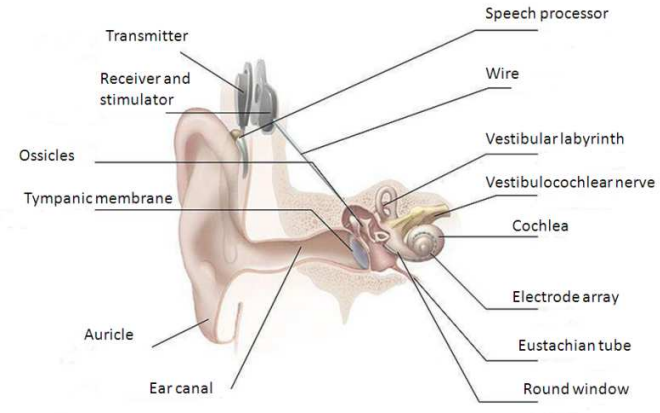

Figure 1. Cochlear implant device [3]

According to biophysical theories [4], [5] when a mechanical wave propagates inside the cochlea, the Basilar Membrane (BM) distorts to absorb the wave energy, resulting in a height variation of the BM, which compresses the organ of Corti. As shown in Figure 2, the organ of Corti is composed of Hair Cells (HC) (Outer Hair Cells (OHC) and Inner Hair Cells (IHC)), which have stereocilia at their end. When BM vibrates, stereocilia position change allowing potassium channels to open [6, 7]. Opening of the potassium channels creates the depolarization of the HC allowing complex mechanisms to take place (reviewed in [8], [9], [10]), and finally, resulting in neurotransmitter released in the synapse. Once released, these neurotransmitters travel to the post synaptic cell (the nerve fiber) and creates the depolarization of the nerve fiber. This depolarization, if sufficiently important, generates an Action Potential (AP) running through the nerve cell membrane [11], [12].

The aim of the electrodes array of the cochlear implant is to generate an AP once a sound is perceived.

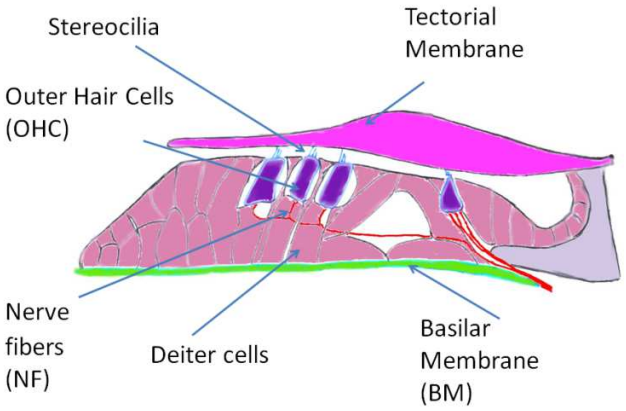

Figure 2. Organ of Corti

Consequently, to obtain the same Action Potential at the nerve fiber using only electrode stimulation, two possibilities exist. First the direct nerve fiber stimulation can be made by changing the nerve membrane potential in order to produce a membrane depolarization above the threshold of Voltage Sensitive Na+ Channels (Na_v) to create an AP [13]. The second solution consists in opening the potassium channels of the stereocilia to recreate the complete stimulation process. As HC or stereocilia are disfunctionning in the vast majority of implanted patients, only the first mechanism is considered in this paper.

Electrical model of electrodes inserted within the cochlea have been proposed by Hartmann et al. [14], where the spatial distribution of electrical potential was measured for intracochlear stimulation. In addition, electronic model of electrode/neuron coupling is available in [15] in order to reveal the most efficient coupling conditions. However, both models lack of physical connection with AP generation. In this paper, we present an electrical description of the electrode and organ of Corti in order to obtain theoretical minimal stimulation voltage sent to the electrodes for AP generation. Furthermore, this model allowed us to link the stimulation voltage with the duration of the nerve fibers stimulation. Then the impact of surrounding electrodes were theoretically investigated.

The next section presents the theoretical model developed for the Organ of Corti associated with the electrodes. Thereafter, simulation results from SPICE software are presented.

The threshold of hearing [16] describes the minimum power of the acoustic vibration required to perceive a sound related to the sound frequency. This relation is not linear for mammals, indicating that various physical properties of the ear ensure this frequency selectivity. As the Central Nervous System (CNS) interprets the message sent by the afferent nerve fibers, this frequency selection has to be recreated in cochlear implants where the afferent nerve fibers are directly stimulated. In that intent, we used two topographic maps of the cochlea: one describing the repartition of the afferent nerve fibers (also called Spiral Ganglion Cells (SGC) (cf Section V)) over their place inside the cochlea and another one describing the same repartition but weighted by a threshold of hearing related function. By comparing the number of afferent nerve cells stimulated in both maps, we defined corrective coefficients. These coefficients were used to correct the potential sent to the electrodes and may permit better sound reconstruction by the brain.

Finally, the conclusion and future work direction are presented.

II. ORGAN OF CORTI ELECTRICAL ANALOG

The electrical equivalent circuit of human tissue used in this paper is the one presented in Figure 3 and extracted from Cole and Cole impedance model [17], which has been shown to fit experimental data. The human tissues considered were the one present in Figure 2. The value of R_s, R_p , C_h and C_p were obtained using a gain response extraction over frequencies analysis.

The electrical analog model is based on the impedance response over frequencies. R_s and C_h model the tissue impedance at low frequencies. As the maximum hearing frequency is 22khz, it was considered in this paper that R_p and C_p could be neglected as their model the energy loss and tissue response in high frequencies.

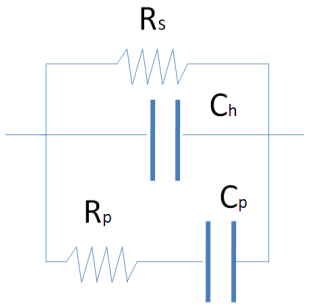

Figure 3. Human tissue electrical analog [17]

To obtain the numerical values for R_s and C_h for all the tissues or interfaces, we use the physical equations for the capacitance (parallel-plate capacitor) and for the resistance computation (cylindrical resistance model) [18], [19].

The values of the relative permeability and electrical conductivity for the nerves were extracted from [20] or from [21] for platinum as electrodes are mainly composed of it. However as far as the authors know, no relative permeability or electrical conductivity was available for Deiter cells or Basilar Membrane tissue. As Deiter cells are mainly composed of microtubules [22], which are involved in mechanical transport as actin proteins found in muscles cells and because the width of the BM is negligible compared to the Deiter cell height, we chose to take the relative permeability and electrical conductivity of muscle cells to characterize those two tissues.

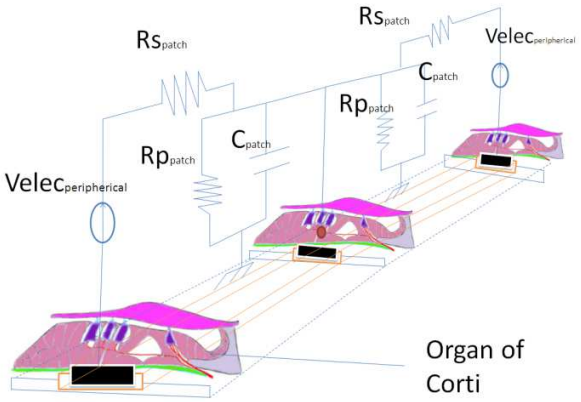

Figure 4. Two surrounding electrodes influences the nerve fibers targeted.

On the other hand, the computation of the capacitance and the resistances (C_{patch}, Rp_{patch}, Rs_{patch}) between two electrodes is more complex, as highlighted Figure 4, those variables depend on the distance between the two electrodes. The Cable Model Theory was used to compute those variables as the space between two electrodes is composed of various tissues rendering the Cole and Cole model implementation difficult. We simplified the tissue between two electrodes as only made of Deiter cells, then we implemented the Cable Model Theory in order to obtain a general impedance depending on the electrodes distance.

To compute Rs_{patch}, the cylindrical model of resistance was considered. The cylinder going from the first electrode to the second electrode, as defined in Figure 5.a, was used to compute Rs_{patch} (expressed in (1)):

$$R_{spatch} = \frac{1}{\sigma_M} * \frac{l_{spatch}}{S_{spatch}}$$

$$\text{with} \quad l_{spatch}(y) = \int_0^{Y_{tot}} y * dy$$

$$\text{and} \quad S_{spatch}(y) = \int_0^{2*\pi} \int_{-\frac{X1}{2}}^{\frac{X1}{2}} \rho * d\rho * d\theta \qquad (1)$$

where σ_M is the electrical conductivity of muscle cells, Y_{tot} is the distance between the two electrodes, X_1 is the distance between one electrode and the corresponding nerve fibers. Those values were respectively extracted from [23] and [24]. y is the variable shown in Figures 5.a, 5.b and 5.c.

Rp_{patch} models the resistance between the two longitudinal edges of the cylinder defined previously. Hence, this computation changes as expressed in (2), as it models all the losses through the ground from one electrode to another one.

$$R_{ppatch} = \frac{1}{\sigma_M} * \frac{l_{ppatch}}{S_{ppatch}}$$

$$\text{with} \quad l_{ppatch}(y) = \int_0^{Z1} dz$$

$$\text{and} \quad S_{spatch}(y) = \int_0^{2*\pi} \int_0^{y} \rho * d\rho * d\theta \qquad (2)$$

where Z_1 is the distance between the electrode and the nerve fibers and we supposed Z_1 equal to X_1 for simplification purposes.

We defined Cp_{patch} as a squared parallel plate capacity (Figure 5.c) (developed in (3)):

$$C_p = \mathcal{E}_0 \mathcal{E}_M \frac{A_{patch}}{d_{patch}}$$

$$\text{with} \quad d_{patch}(y) = \int_0^{Z_1} dz$$

$$\text{and} \quad A_{patch}(y) = \int_0^{y} dy_1 \int_0^{X_1} dx \qquad (3)$$

Where $\mathcal{E}_0$ is the vacuum permeability and $\mathcal{E}_M$ is the muscle relative permeability.

For reader's convenience, the value of the capacitance and resistance described previously are summarized in Table I.

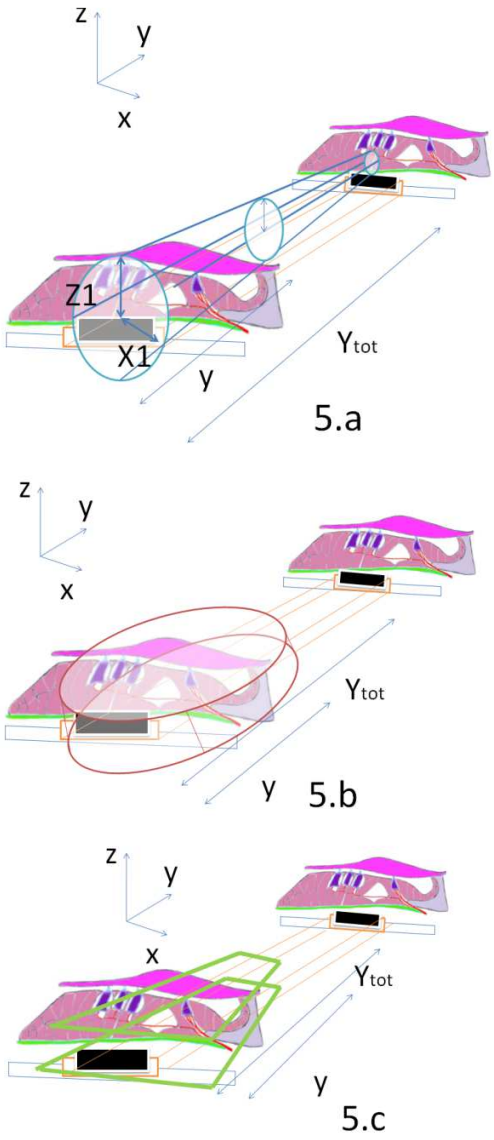

Figure 5. Physical model of Rs_{patch} (5.a), Rp_{patch} (5.b) and Cp_{patch} (5.c)

The electrical description containing only a single electrode is shown Figure 6.a. The input voltage generator is directly connected to the electrodes analog model (low frequencies model), which can be eventually considered as a perfect conductor compared to the other resistance values. Then the current can flow to the nerve cell or can go back to the ground. The current loss through the physical isolation between the electrode and the ground is neglected as the insulator has a low loss tangent (high resistivity). The membrane rest potential of a nerve cell is around -70mV, explaining the two -70mV voltage generators, in Figure 6.a. We defined the analog equivalent circuit of a nerve cell using a resistance (R_n) in parallel with a capacitor (C_n) (this electrical description should not be confused with the Hodgkin-Huxley model [25], which is used to model ions flow through the nerve cell membrane and not the electron flow).

In addition, the electrical description of the system starting from the nerve and going through all the body to the earth was not considered because very little electrical current is going through this pathway.

TABLE I. RESISTANCES AND CAPACITANCES USED IN THE ELECTRICAL MODEL

Electrodes	**Re= 1.5 Ω, Ce=11 fF**
Basilar Membrane and Deiter cells	R_{bc}= 933 Ω, C_{bc}= 300 nF
Nerve fibers	R_n= 1076Ω, C_n= 3µF
Cable Model Theory	Rs_{patch}= 8 MΩ, Rp_{patch}= 1265 Ω Cp_{patch}= 92.6 nF

Figure 6.b exhibits the electrical description of the overall system with two surrounding electrodes added. They are composed of a voltage generator, the platinum electrode equivalent circuit and the cable model (Rs_{patch}, Rp_{patch} and C_{patch}), to connect the peripheral electrodes with the nerve fiber that we want to activate.

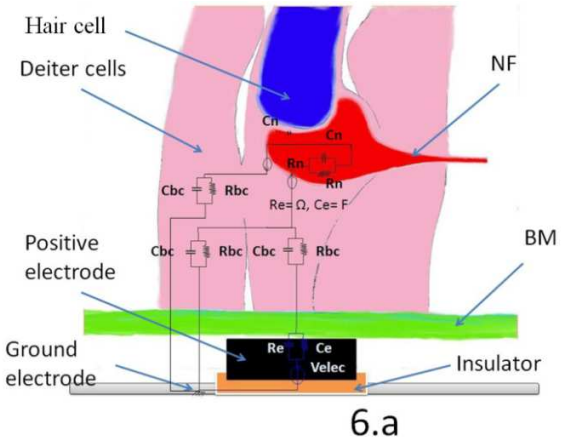

Figure 6.a. Electrical analog of the electrode and nerve.

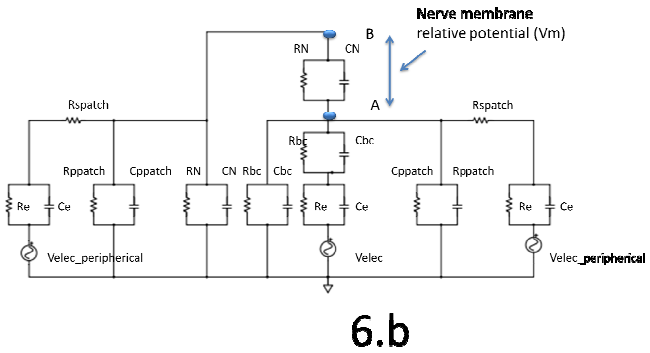

Figure 6.b. Electrical analog with three electrodes

The main goal of the addition of the two surrounding electrodes was to study theoretically the influence of these on the stimulation of selected nerve fibers (or more precisely of the packet of nerve fibers that should only be stimulated by the central electrode). These perturbations, if significant, could make the sound reconstitution inaccurate.

III. INTERPRETATION OF THIS ELECTRICAL ANALOG

The membrane potential (Vm) (which corresponds to the difference of potential between point A and point B in Figure 6.b) had to vary of 30mV to generate an AP. The electrode stimulation (Velec) was made using a DC source. Neglecting the effect of the capacitors, Vm varied linearly with Velec and the variation of 30mV was reached for an electrode stimulus around 0.9V.

When a nerve fiber is stimulated constantly, it will not produce an AP indefinitely but rather produce a succession of randomly spaced AP called spike trains. The spike train length that could be produced by a sound of given intensity has to be reproduced with the electrodes of the cochlear implant. We performed transient simulation including the capacitors effects by injecting a square voltage with a period of 150ms. This experiment was repeated for input square voltages varying from 1V to 5V (Figure 7.a). The aim of this simulation was to study if the voltage amplitude sent to the electrode would affect the spike train duration and starting time. Figure 7.b reveals that the delays for Vm potential to reach its maximum value were around 0.1µs, which were small compared to the duration of a nerve AP (few ms). This result pointed out that theoretically the electrode voltage magnitude had a very insignificant effect on the spike train duration. In addition, the recreated spike train starting time has negligible delay with the electrode stimulation starting time.

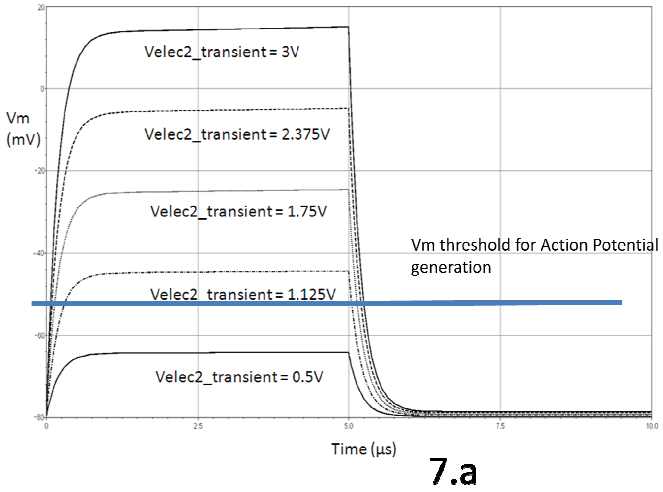

Figure 7.a. Transient simulation with different electrode voltage as input and Vm voltage as output.

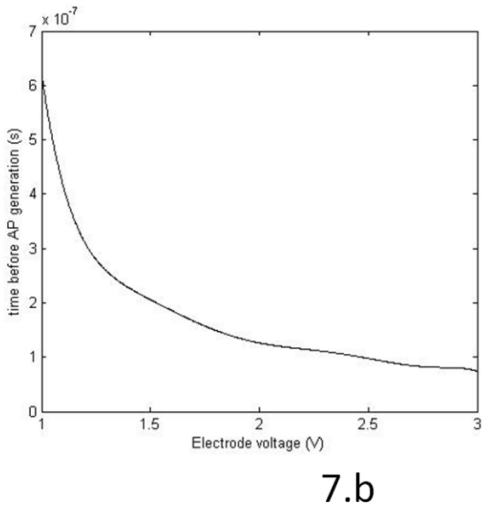

Figure 7.b. Time before AP generation depending on the elctrode voltage

A general overview of the spike train related to the Vm amplitude is presented in Figure 8. The AP generated were obtained from basic mathematical functions in order to model the

nerve fiber AP created after square voltage electrode stimulation. The interspike time was taken randomly and greatly depends on the amplitude of the stimulus [26]. However, the electrical analog presented in this paper does not account for this effect.

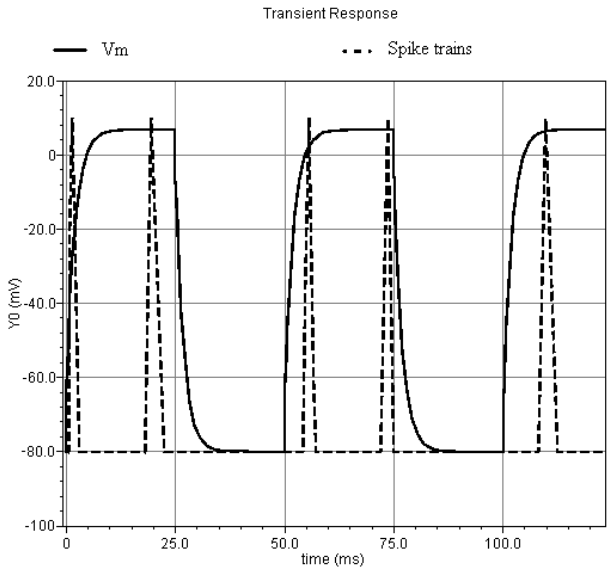

Figure 8. Spike train generated by the electrode input voltage

We performed also a parametric simulation using the electrical description of Figure 6.b, where the surrounding electrodes are added. The central electrode had a DC voltage of 1V and we varied the voltage of the surrounding electrodes between 0.9 and 5V. According to resistances and capacitances values used in Figure 6.b, analytical computation showed that when the voltage of the surrounding electrodes was maximum (5V), the nerve fibers (above the central electrode) membrane potential Vm variation was 0.5mV, which was not high enough to stimulate these nerve fibers (the ones that should be stimulated only by the central electrode).

The overall system consumption is a great significance as cochlear implants are not convenient for the user to recharge. The study of the power consumption is presented Figure 9.

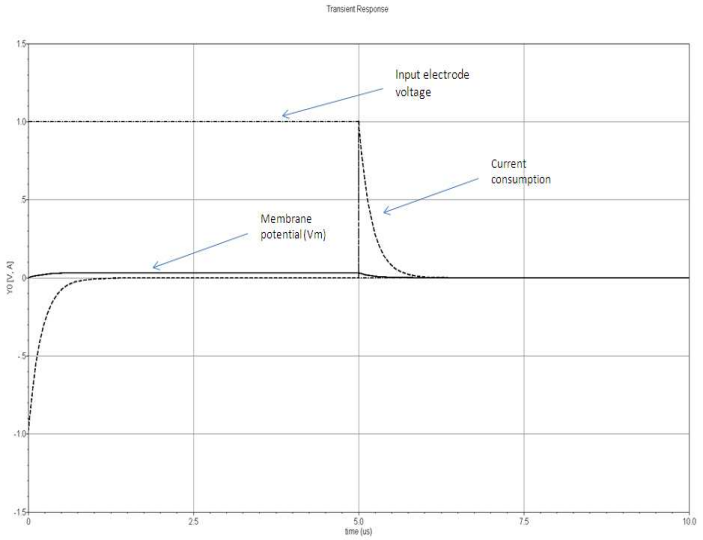

Figure 9. Current consumption during one stimulation period

The current peaks during each input signal transitions could reach 1A. Consequently, the maximum power consumed during a square input signal generation by the electrodes was around 1W (peak value), whereas the mean power consumed per period was around 50mW. These results may be used for the electrode array design to define battery size as well as electrode minimum width.

IV. NERVE REPARTITION MAP

The biomechanical most widespread theory of BM vibration is the Traveling Wave theory: following acoustic vibrations, the BM is excited and vibrates at a particular place inside the cochlea. This place depends on the sound wave frequency as well as sound amplitude [27], [28]. Cochlear implants aim to recreate the neural stimuli of an healthy cochlea using an wired electrodes array inserted inside the scala tympani, close to the BM. As each electrode is at a fixed place inside the cochlea, electrode stimulation will excite only a limited region of the cochlea which will be further interpreted in the brain as a sound of a certain frequency as indicated in Figure 10. Consequently, sound division into single frequency (using the Fast Fourier Transform (FFT) algorithm for instance) is necessary to select the right electrode to activate which then stimulates its surrounding nerve fibers.

In order to only select the nerve fibers associated with the resonating IHC, we created an afferent nerve fiber map of the cochlea including the frequency selective mechanisms of the ear.

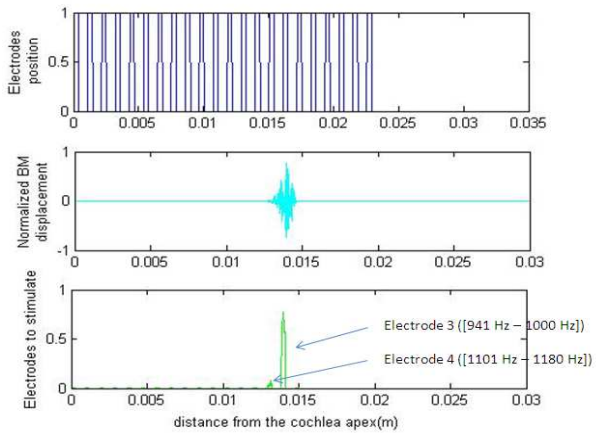

Figure 10. The auditory nerve fibers position stimulated by the electrodes array (a), BM displacement for a 1250Hz sine wave (b), Resulting electrodes stimulated by the 1250 Hz sine wave based on the BM displacement theory (c).

V. SPIRAL GANGLIONS

There are between 30000 to 40000 nerve fibers in the cochlea of a normal adult [29]. Three types of nerve fibers innervate the cochlea: autonomic, which are associated with blood vessel and other physiological functions, afferent (conducting information from the cochlea to the brain) and efferent (conducting information from the brain to the cochlea, especially to the Outer Hair Cells). Afferent nerve fibers are produced by Spiral Ganglions Cells (SGC) [30]. Spiral ganglions are synaptically connected to the IHC and OHC as indicated in Figure 11.

Type I SGC represent 95% of the SGC and each one connects to a single IHC whereas a single IHC is connected to 10-20 type I SGC [30].There are around 15 nerve fibers per IHC in the lower second turn of the cochlea and this number changes from the base

to the apex, most probably slightly contributing the cochlea sensitivity toward certain frequencies [31], [32], [33].

Type II spiral ganglions are smaller and unmyelinated and mostly connect OHC.

It may be deduced that IHC are surrounded by almost all the afferent nerve fibers, therefore, they are thought to function primarily as sensory receptors [34]. OHC otherwise are more connected with motor properties of the stereocilia [35], they may permit an higher accuracy in sound perception.

In [36], the spiral ganglions repartition over the cochlea distance from the base is presented for cats. We assumed that the spiral ganglions cochlea distribution for other terrestrial mammal species was similar [37], [38] (this assumption may be used as first approximation).

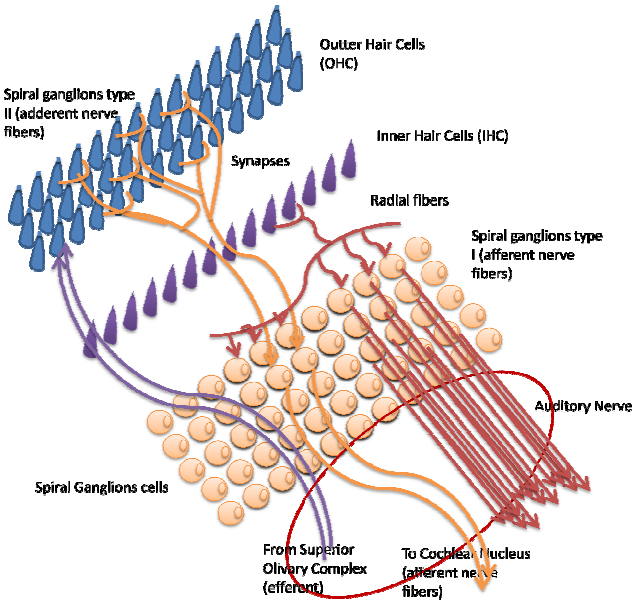

Figure 11. Auditory Nerve fibers and hair cells. Redrawn from [39]

As type II SGC function in hearing sensation has been partially understood and because their number is limited compared to type I SGC number, we neglected type II SGC, and supposed in this model that:

- the total SGC number and repartition was entirely defined by type I SGC.
- the total afferent nerve cell number and repartition inside the cochlea was therefore similar to type I SGC number and repartition.

VI. EAR FREQUENCY SENSITIVITY HYPOTHESIS

When the eardrum is stimulated, the nerve response over frequency presents a peak amplitude around 4KHz [40]. The human ear is composed of the outer ear, the medium ear and the inner ear (where BM makes the Organ of Corti oscillates) [41]. This particular human hearing frequency sensitivity may result from the combined effects of outer ear resonance, the middle ear resonance and the cochlea sound filtering and amplification.

It has been suggested that the outer ear and the medium ear contributes to frequency sensitivity in mammalian hearing, especially for frequencies around 3KHz [42], [43], [39], [44] [45].

The cochlea frequency sensitivity may also result from others various mechanisms still controversial. Considering only the cochlea biophysics, the intracochlear/eardrum magnitude of the scala tympani over frequency found in [46] may indicate varying vibrations amplitude depending on the sound wave frequency. The BM displacement, when stimulated by a mechanical wave, contributes to produce the frequency sensitivity of the cochlea due to the BM different physical properties (stiffness, etc.) inside the cochlea (distance from the base).

The cochlea sensitivity toward certain frequencies may be further affected by other physiological factors, such as different afferent nerve fibers repartition and stimulation, depending on the position on the cochlea. Several mechanisms have been proposed such as:

- IHCs frequency response (similar to a low pass filter with a resonating pulse around 10KHz) [47], [48]. The IHCs frequency response may result from different IHCs length inside the cochlea or to their stereocilia and cellular mechanical properties. Furthermore, gradient of IHC ionic channels along the cochlea length exist and increase the frequency hearing sensitivity of the cochlea [49]
- Spiral ganglions density increases slowly and linearly with the cochlea position with respect of the cochlea location hence spiral ganglions repartition is related to the frequency of the sound wave but fails to explain the 4KHz frequency peak (cf spiral ganglions frequency map, presented in Figure 13) [36], [46]

To the authors personal interpretation the frequency selectivity of the cochlea is greatly linked to biophysics of the cochlea, to IHCs potential change and repartition and ear/middle ear resonance rather than nerve fiber topography (as it failed to explain the amplification peak in the 3-4KHz range [46]).

VII. AFFERENT NERVE FIBERS REPARTITION INSIDE THE COCHLEA

As indicated in [29], the number of afferent nerve fibers in the cochlea is around 40000 and their effective stimulation is depending on the sound wave frequency. We hence decided to create an afferent nerve repartition map already including all the physical or anatomical mechanisms presented in Section V (that we called Afferent Nerve Fibers Repartition Map Including Ear Frequency Selection Mechanisms or MEFFRINAM map), in order to roughly define the number of afferent nerve fibers affected by a sound wave. This map presents great interest for cochlear implants application as the electrodes array are directly stimulating these nerve fibers and the outer/middle ear resonance, the BM variations depending on wave frequencies, the Organ of Corti selective mechanisms, etc. are bypassed in cochlear implants, making the use of this map fundamental to recreate a realistic hearing.

To develop this topographic map we took first the reverse function of the human hearing threshold over frequencies [16] to get the human ear sensitivity toward the frequencies.

By making this function linear (R(f)) and then reversing it ($I_R(f)$), it allowed us to estimate the cochlea sensitivity toward frequency. Transforming the $I_R(f)$ function into a probability density function ($P_{IR}(f)$) and multiplying it with the total number of afferent nerves in the cochlea ($Nb_{afferentnerves}$) resulted in the Afferent Nerve Fibers Repartition Map Including Ear Frequency Selection Mechanisms (MEFFRINAM map) of the cochlea as expressed in (4):

$$Threshold\ of\ hearing = 10\log|R(f)| \rightarrow 10\log|I_R(f)| = -10\log|R(f)|$$

$$P_{IRT}(f) = \frac{I_R(f)}{\int_{f_{min}}^{f_{max}} I_R(f)} Nb_{afferentnerves} \quad (4)$$

Where P_{IRT} (f) is the equivalent afferent nerve stimulated repartition map over the frequencies (f).

The Greenwood function [50] was used to pass from the resonant frequency into a position in the cochlea (between the base and the apex) [50]. Therefore $P_{IRT}(f)$ can be transformed into $P_{IRT}(d_A)$ where d_A is the distance from the apex as described in (5):

$$f = 165.4\,(10^{2.1\,d_A} - 1)$$
$$P_{IRT}(f) = P_{IRT}\left(165.4\,(10^{2.1\,d_A} - 1)\right) \quad (5)$$

According to Greenwood parameters for human ear fitting [50].

Figure 12 displays the afferent nerve fibers stimulated map including ear amplification mechanisms (MEFFRINAM map) compared to cochlea position. The comparison between the spiral ganglions topographic map (extracted from [36]) and the created topographic map is presented in Figure 13. Based on the assumptions presented in Section V, both maps have the same number of cells but these are differently affected over frequencies.

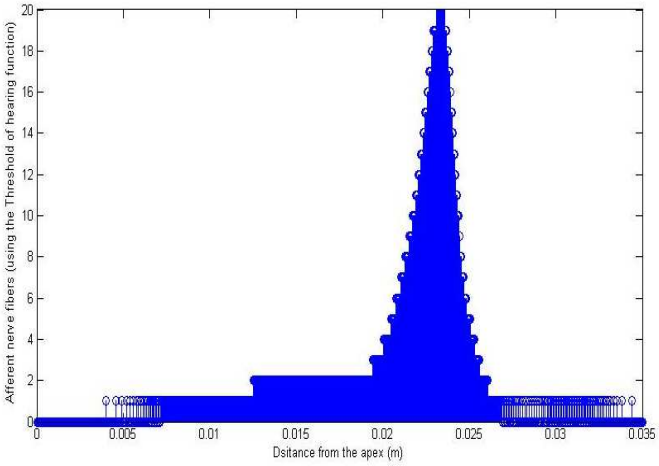

Figure 12. Afferent Nerve Fibers Repartition Map Including Ear Frequency Selection Mechanisms (MEFFRINAM map) in relation to the distance from the apex

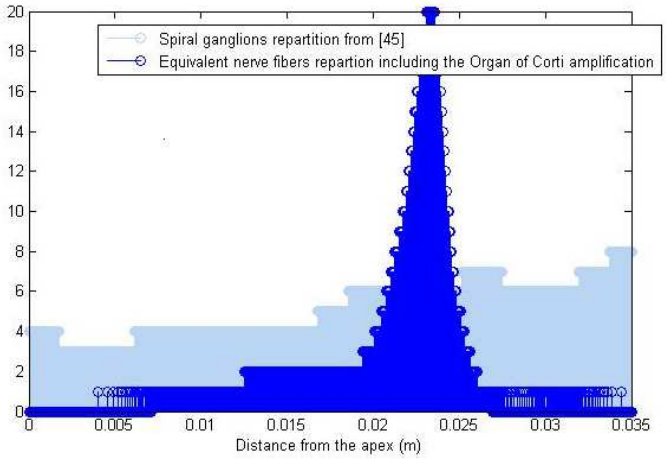

Figure 13. Comparison of spiral ganglions activation [36] and equivalent afferent nerve fibers stimulated map depending on the cochlea and ear biophysics (MEFFRINAM map in dark blue)

VIII. BENEFITS OF THE CREATED TOPOGRAPHIC MAP FOR COCHLEAR IMPLANTS

In severely deaf people the use of cochlear implants helps to partially recover the hearing function. In implanted patients the afferent nerve fibers stimulation is directly done through electrodes and does not require the Organ of Corti as explained in Section I. By remembering that we made the approximation that the afferent nerve fibers were equivalent to the SGC, the afferent nerve fibers selected by the electrodes is given by the spiral ganglions repartition map.

We use CI422 device characteristics with an insertion depth of 20-25mm, a mean diameter of the electrodes around 0.35mm and a spacing between the electrodes around 0.45mm. As explained in [23] the number of nerve fibers stimulated by an electrode is a function of the power magnitude as well as the proximity of the electrodes with the SGC.

We supposed that the electrodes are very close to the SGC, resulting in a window type selection (very accurate) of the afferent nerve fibers. In practice, this may be inexact as the insertion of the electrode array inside the scala tympani is difficult and usually result in spacing between the electrodes array and the Spiral ganglions [51] .In consequence, in practice, the nerve fibers selection mathematical description is closer to a Gaussian function.

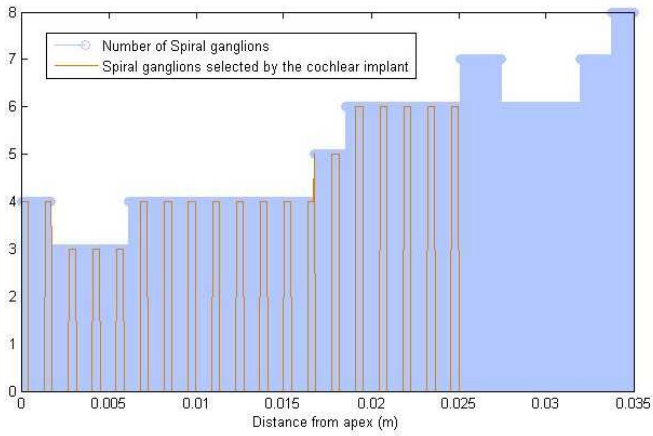

Figure 14. Packet of afferent nerve fibers selected by the electrodes of the cochlear implants

From Figures 13 and 14, it can be easily deduced that the cochlear implant electrodes do not provide the required amplification in the 2KHz – 6KHz frequency range as Cochlear amplification is not done. Algorithmic correction by modifying the energy sent to the electrodes may be used to correct this defective amplification. This algorithmic correction should be based on the human hearing threshold or similarly on the equivalent afferent nerve fibers stimulated map, which takes into consideration the amplification mechanisms of an healthy cochlea.

Using the mathematical logarithmic spiral representation presented in [52], the spatial representation of the cochlea can be performed. The mathematical equation in the cited document describes a flat spiral disagreeing with a real cochlea, however we may use the z direction to plot information such as the nerve fiber topographic map or those nerve fibers selected by the electrodes array, as indicated in Figures 15 and 16.

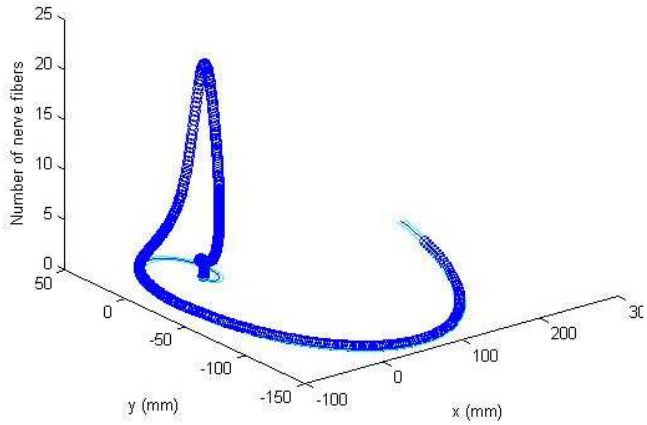

Figure 15. Afferent Nerve Fibers Repartition Map Including Ear Frequency Selection Mechanisms inside the cochlea depending on the cochlea spatial position

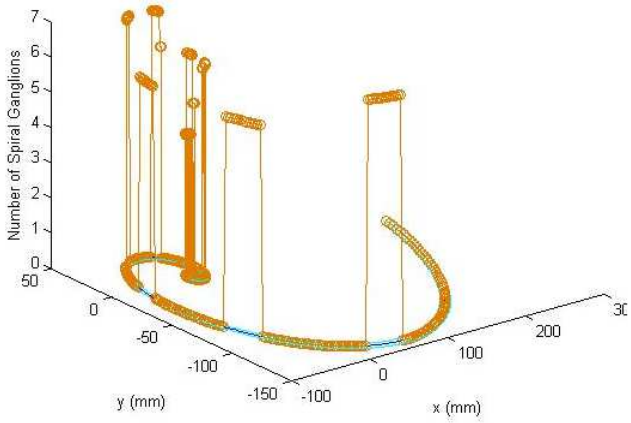

Figure 16. Portion afferent nerve fibers inside the cochlea stimulated by the cochlear implant electrodes

IX. AMPLIFICATION COEFFICIENTS ASSOCIATED WITH THE TOPOGRAPHIC MAPS COMPARISON

Cochlear implant electrodes should hence be multiplied by a scalar coefficient to correctly model the frequency sensitivity of the ear. This correction is compulsory as the Central Nervous System interprets neuronal signals already amplified in some particular frequencies. If the frequency amplitude dependence is not reproduced in cochlear implants it may result in inability to correctly hear certain frequencies (especially in the 3-4KHz band), ultimately resulting in sound distortion. Comparison between the MEFFRIMAM map and the Spiral Ganglions topographic map selected by the cochlear implants is exposed in Figure 17.

To correctly model the frequency response of an healthy ear, each electrode should be multiplied with the coefficient indicated in Figure 18. We further supposed that the number of nerve fibers stimulated is linearly increasing with the amplitude of the electrode. This may be inaccurate for high voltage stimulus or very low voltage stimulus due to saturation mechanisms [53], [54], [55].

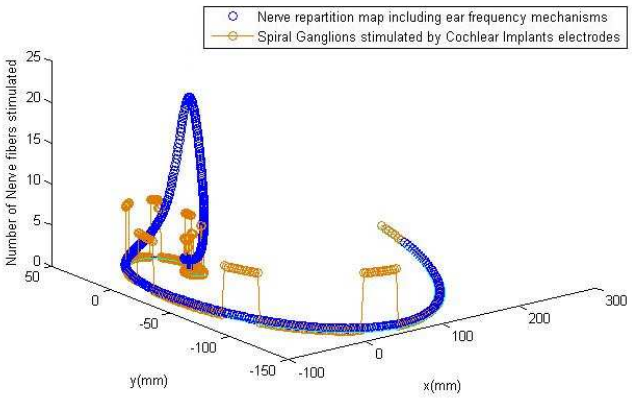

Figure 17. Comparison between the Spiral Ganglions stimulated by the electrodes and the created MEFFRIMAM map

To compute this average coefficient a simple division was performed between the afferent nerve fibers number in the MEFFRIMAM map and the afferent nerve fibers number defined by the spiral ganglions map for the same position inside the cochlea. The average value of this coefficient was retained for each electrode.

The multiplication of these coefficients with the voltage value that must be sent at an electrode to stimulate an afferent nerve fiber response (defined in Section III) could be done in the processing unit of the cochlear implant. Furthermore, coefficients amplitude tuning tests performed in deaf people using cochlear implants for each electrode may add precision in the hearing response of these patients.

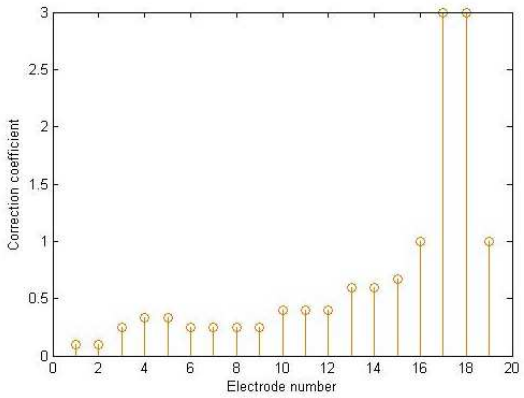

Figure 18. Electrodes amplification coefficients to ensure similar frequency response with an healthy cochlea

X. CONCLUSION

The theoretical electrical description presented in this paper was used to carry out simulations allowing the detection of the minimum voltage needed to ensure nerve fibers stimulation. This voltage was found around 0.9 V. Furthermore, the current peaks during each input signal transitions could reach 1A (peak value), and the mean power consumed per period was around 50mW. These results may be used as requirements for the electrode array design and corresponding control electronics.

It has also been suggested that two consecutive electrodes were not disturbing one another and that the duration of the stimulation did not depend on the input electrode voltage. A more complex model, including the spike trains frequency (which is

the number of spikes generated per second) related to the electrode input voltage is being currently developed.

Furthermore, using the threshold of hearing function, we created a topographic map of afferent nerve fibers repartition inside the cochlea weighted by the frequency selectivity of an healthy ear. This map may be of great value to decrease sound distortion in cochlear implants. Corrective coefficients were defined for each electrodes in order to allow electrode potential fine tuning based on the biophysical properties of the ear.

Besides physical tests are ongoing to ensure that the theoretical results obtained match the measurements. Deaf people using cochlear implants were asked to kindly submit themselves to cochlear implant reprogramming in order to test if the threshold of 0.9 V was sufficient; if not, it would greatly affect the perturbation between electrodes. We are also currently implementing the electrode potential correction algorithm in a portative platform in order to estimate its power consumption and facilitate its integration in cochlear implant device.

XI. REFERENCES

[1] U. Cerasani and W. Tatinian, "Modeling of the Organ of Corti Stimulated by Cochlear Implant Electrodes", CENTRIC 2013, The Sixth International Conference on Advances in Human oriented and Personalized Mechanisms, Technologies, and Services, pp. 80-85, 2013

[2] J. K. Niparko, Cochlear Implants: Principles and Practices (chapter 7). Lippincott Williams & Wilkins, 2009.

[3] G. Clark, Cochlear Implants: Fundamentals and Applications (ch. 4-8): Springer-Verlag, 2003.

[4] G. V. Békésy, Experiments in Hearing, part 3. Chap 12-14, 1989.

[5] F. N. F. Mammano, "Biophysics of the cochlea: linear approximation", J. Acoustic. Soc. Am. 93, vol. 6, June 1993.

[6] C. Kubisch *et al.*, "KCNQ4, a Novel Potassium Channel Expressed in Sensory Outer Hair Cells, Is Mutated in Dominant Deafness", Cell, vol. 96, issue 3, pp.437-446 February 1999.

[7] L. Trussel, "Mutant ion channel in cochlear hair cells", PNAS, vol. 97, issue 8, pp. 3786 –3788, April 2000.

[8] S. K. Griffiths. *INNER EAR.ppt*. [Online]. Available from: http://web.clas.ufl.edu/users/sgriff/A&P.html

[9] S. K. Juhn, B. A. Hunter and R. M. Odland, "Blood-Labyrinth Barrier and Fluid Dynamics of the Inner Ear", The internationnal tinnitus journal, vol. 7, issue 2, pp. 78-83, December 2001.

[10] R. Yehoash and R. A. Altschuler, "Structure and innervation of the cochlea", Elsevier, Brain Research Bulletin, vol. 60, pp. 397 - 422, January 2003.

[11] M. F. Bear, Neuroscience, Chapter 4, The Action Potential, ed. Baltimore: Lippincott Williams & Wilkins, 2007.

[12] A. Siegel and H. N. Sapru, Essential Neuroscience, Section II The Neuron, ed. Lippincott Williams & Wilkins, April 2010.

[13] K. X. Charand. *Action Potentials*. [Online]. Available from: http://hyperphysics.phy-astr.gsu.edu/hbase/biology /actpot.html

[14] A. Kral, D. Mortazavi and R. Klinke, "Spatial resolution of cochlear implants: the electrical field and excitation of auditory afferents", Hearing Research, vol. 121, pp. 11-28, 1998.

[15] L. Sileo *et al.*, "Electrical coupling of mammalian neurons to microelectrodes with 3D nanoprotrusions", Elsevier, Microelectronic Engineering, vol. 111, pp. 384–390, November 2013

[16] C. Fielding. *Lecture 007 in Hearing II*. [Online]. Available from: http://www.feilding.net/sfuad/musi3012-01/html/lectures/007_hearing_II.htm

[17] M. Hubin. *Propriétés des milieux biologiques*. [Online]. Available from: http://michel.hubin.pagesperso-orange.fr/capteurs/biomed/chap_b6.htm

[18] R. Nave. *Parallel Plate Capacitor*. [Online]. Available from: http://hyperphysics.phy-astr.gsu.edu/hbase/electric/pplate.html,

[19] P. Glover, *Resistivity theory*. [Online]. Available from: http://www2.ggl.ulaval.ca/personnel/paglover/CD%20Contents/GGL-66565%20Petrophysics%20English/Chapter%2017.PDF

[20] J. D. Bronzin, "The Electrical Conductivity of Tissues", in The Biomedical Engineering Handbook: Second Edition, ed. Myer Kutz, 2000.

[21] N. Ida, "9.2 electromagnetic properties of materials", in Engineering Electromagnetics, ed. Springer, 2003.

[22] Scitable by Nature. *Microtubules and Filaments*. [Online]. Available from: http://www.nature.com/scitable/topicpage/microtubules-and-filaments-14052932

[23] Cochlear®. *Delivering choice, cochlear's electrodes portofolio-as unique as our customers*. [Online]. Available from: www.cochlear.com

[24] J. Yang and J. B. Wang, "Morphological observation and electrophysiological properties of isolated Deiters' cells from guinea pig cochlea", NCBI Pubmed, vol. 14, issue 1, pp. 29-31, January 2000.

[25] A. L. Hodgkin and A. F. Huxley, "A quantitative description of membrane current and its application to conduction and excitation in nerve", The Journal of Physiology, vol. 117, issue 4, pp. 500-544, 1952.

[26] X. Wang. *Neural representation of Sensory stimuli: Properties of Spike trains*. [Online]. Available from: http://www.shadmehrlab.org/

[27] R. F. Lyon and C. A. Mead. *Cochlear Hydrodynamics demystified*. [Online]. Available from: Department of Computer Sciences, California Institute of Technology

[28] L. Watts. *Cochlear mechanics: Analysis and analog VLSI*. [Online]. Available from: California Institute of Technology

[29] E. L. Mancall and D. G. Brock, Gray's clinical neuroanatomy, ed. Elsevier Health Sciences, 2011.

[30] University of Rochester. *Auditory Nerve I, Innervation of the Cochlea Frequency & Level Coding*. [Online]. Available from: http://www.bcs.rochester.edu/courses/crsinf/221/ARCHIVES/S11/Auditory_Nerve1.pdf

[31] L. A. Werner. *The auditory nerve response*. [Online]. Available from: http://depts.washington.edu/

[32] R. Jonsson, "Field interactions in the peripheral auditory neural system with reference to cochlear implants",

Electrical, Electronic and Computer Engineering, University of Pretoria, 2011.

[33] A. F. Jahn and J. Santos-Sacchi, Physiology of the Ear, ed. Cengage Learning, 2001.

[34] M. Deol and S. Gluecksohn-Waelsch, "The role of inner hair cells in hearing", Nature, vol. 278, pp.250 - 252, 1979

[35] J. Zheng, W. Shen, D. Z. He, K. B. Long, L. D. Madison and P. Dallos, "Prestin is the motor protein of cochlear outer hair cells", Nature, vol. 405, pp. 149-155, 2000

[36] I. Chen, C. J. Limb, and D. K. Ryugo, "The effect of cochlear-implant-mediated electrical stimulation on spiral ganglion cells in congenitally deaf white cats", Journal of the Association for Research in Otolaryngology, vol. 11, pp. 587-603, 2010.

[37] Luisanna State University. *Hearig Range Animals*. [Online]. Available from: http://www.lsu.edu/deafness /HearingRange.html

[38] R. R. Fay, "Structure and function in sound discrimination among vertebrates", The evolutionary biology of hearing, ed. Springer, pp. 229-263, 1992

[39] Steven Errede. *The Human Ear Hearing, Sound Intensity and Loudness Levels*. [Online]. Available from: http://courses.physics.illinois.edu

[40] University of Illinois. *The Human Ear: Hearing, Sound Intensity and Loudness Levels*. [Online]. Available from: http://courses.physics.illinois.edu/phys406/Lecture_Notes/P406POM_Lecture_Notes/P406POM_Lect5.pdf

[41] P. W. Alberti. *The anatomy and physiology of the ear and hearing*. [Online]. Available from: http://www.who.int/occupational_health/publications/noise2.pdf

[42] D. Purves, G. J. Augustine, D. Fitzpatrick, L. C. Katz, A. S. LaMantia, J. O. McNamara, et al., The External Ear, Neuroscience Second Edition, ed. Sinauer Associates, 2001.

[43] S. S. Stevens and H. Davis, Hearing: Its psychology and physiology, ed.Wiley New York, 1938.

[44] University of Utah. *All about ears*. [Online]. Available from: Physics of the Human Body - Physics 3110

[45] University of Wisconsin. *IV. Functions And Pathphysiology Of The Middle Ear*. [Online]. Available from: Departement of Neurophysiology

[46] University of Vermont. *Coclia Anatomy and physiology of hearing*. [Online]. Available from: University of Vermont, College of Medicine

[47] University of Rochester. *Auditory Nerve I, Innervation of the Cochlea Frequency & Level Coding*. [Online]. Available from: http://www.bcs.rochester.edu/courses /crsinf/221/ARCHIVES/S11/Auditory_Nerve1.pdf

[48] P. Dallos, "Response characteristics of mammalian cochlear hair cells", The Journal of neuroscience, vol. 5, pp. 1591-1608, 1985.

[49] J. Ashmore, "Biophysics of the cochlea–biomechanics and ion channelopathies", British medical bulletin, vol. 63, pp. 59-72, 2002.

[50] D. D. Greenwood, "A cochlear frequency-position function for several species—29 years later", The Journal of the Acoustical Society of America, vol. 87, p. 2592, 1990.

[51] R. Shepherd, S. Hatsushika, G. M. Clark, "Electrical stimulation of the auditory nerve: the effect of electrode position on neural excitation", Hearing research, vol. 66, pp. 108-120, 1993.

[52] K. Cheng, V. Cheng, and C. H. Zou, "A logarithmic spiral function to plot a Cochleaogram", Trends in Medical Research, vol. 3, pp. 36-40, 2008.

[53] S. J. Elliott and C. A. Shera, "The cochlea as a smart structure", Smart Materials and Structures, vol. 21, pp. 064001, 2012.

[54] R. Zelick. *Vertebrate Hair Cells*. [Online]. Available from: http://web.pdx.edu/~zelickr/sensory-physiology /lecture-notes/OLDER/L12b-hair-cells.pdf

[55] A. W. Peng, F. T. Salles, B. Pan, and A. J. Ricci, "Integrating the biophysical and molecular mechanisms of auditory hair cell mechanotransduction", Nature communications, vol. 2, pp. 523, 2011.

Real-Time Teacher Assistance in Technologically-Augmented Smart Classrooms

Georgios Mathioudakis*, Asterios Leonidis*, Maria Korozi*,
George Margetis*, Stavroula Ntoa*, Margherita Antona*, and Constantine Stephanidis*†
*Institute of Computer Science, Foundation of Research and Technology – Hellas (FORTH),
Heraklion, GR-70013, Greece
Email: {gmathiou}{leonidis}{korozi}{margetis}{stant}{antona}{cs}@ics.forth.gr
† Department of Computer Science, University of Crete

***Abstract*—The role of the teacher in the classroom environment is of crucial importance for the effectiveness of the learning process. However, recent studies on the technological enhancement of education have shown that teacher's activities are not adequately supported, as the focus remains rather on the student's side. This article discusses a learner-centric approach towards supporting instructors in improving the teaching and learning processes in ambient educational environments. The proposed solution introduces an intelligent multi-agent infrastructure that monitors unobtrusively the students' activities and identifies potential learning weaknesses and pitfalls that need to be addressed at an individual or classroom level. Such real-time insights enable the instructor to intervene providing help and adapt the teaching process according to the needs of the class. For that to be achieved, several applications have been developed: (i) a real-time classroom activity visualizer, (ii) a behavioral reasoner that aims to identify common behaviors by analyzing classroom activities, (iii) a statistics records manager targeting to showcase students' progress and performance at both an individual and classroom level, and finally (iv) a series of mini-tools that enhance typical procedures that can be found in conventional classrooms, such as the classroom attendance record, the schedule manager, etc. Following the system's description, findings of a preliminary expert-based evaluation are presented and some concluding remarks regarding the deployment of the system in real-life environments are formulated. Finally, potential future extensions of the system are proposed.**

Keywords–ambient intelligence, education, smart classroom, teacher assistance, student monitoring.

I. INTRODUCTION

This article provides an extended version of the work [1] reported in The Fifth International Conference on Mobile, Hybrid, and On-line Learning (eLmL 2013) in Nice, France. In this article, the specification and implementation of an embedded system targeted to support instructors during the educational process are further elaborated and discussed.

Ambient intelligence (AmI) is an emerging technological paradigm that defines sensitive digital environments that monitor their surroundings through pervasive sensorial networks and automatically adapt to facilitate daily activities [2], [3]. According to the Ambient Intelligence vision, digital systems provide user-interfaces embedded in the actual living space, enabling intuitive and natural interaction. AmI initially benefited mainstream areas such as home and office automation [4]. During the past few years though, remarkable efforts have been made towards applying AmI in a variety of domains such as education[1], health[2], entertainment[3] and many more.

The potential of AmI in education led to the introduction of the notion of "Smart Classroom". According to this, typical classroom activities are enhanced with the use of pervasive and mobile computing, artificial intelligence, multimedia content and agent-based software [5]. As a result, traditional artifacts such as desks and whiteboards are replaced by technologically enhanced equivalents aiming to support the learning process. The current realizations of the Smart Classroom vary, covering a wide range of topics. The most prevalent of them include applications for automatic adaptation of the classroom environment according to the context of use [6], [7], automatic capturing of lectures and teacher's notes [8], [9], enhancement of the learner's access to information and personalization of the classroom's material [10] and finally, supporting collaboration among classroom participants [11]. However, the majority of current research approaches focus on the learner's activities, without paying much attention to the role of the teacher.

During the learning sessions in a classroom the teacher duties, among others, include: (i) implementation of a designated curriculum, (ii) maintenance of lesson plans, (iii) assignment of tasks and homework, (iv) performance monitoring, and most importantly, (v) assistance provision when necessary. In general, curriculum activities outweigh monitoring and assistance tasks, especially in crowded classrooms (e.g., more than 20 students). Therefore, to enable effective and personalized tutoring, an automated method that observes students' behavior and identifies common problems is needed [12].

Towards this end, a tool named AmI-RIA (Real-time Instructor Assistant) is introduced in this article, aiming to support the teacher in the context of a learner-centric, ambient intelligence classroom. AmI-RIA monitors and analyzes students' activities in real-time so as to identify potential difficulties, either at an individual or at a classroom level, and notify the teacher accordingly (through the teacher's front-end application). The teacher can therefore concentrate on the lecture and rely on the system to monitor the classroom and prompt for intervention only when necessary (e.g., a student is out of task or performed poorly in a quiz). In addition to real-time monitoring, AmI-RIA offers a performance analysis

[1] AmI Playfield: http://bit.ly/1eM8EWL (Online: 5/2014)
[2] Ambient Intelligence for e-Health: http://bit.ly/1d7jDh6 (Online: 5/2014)
[3] Be There Now!: http://bit.ly/NGPxYb (Online: 5/2014)

tool that provides extensive metrics of students' progress and performance (based on previously collected data) that the teacher can use to either identify topics that require further elaboration or adapt the teaching methodology. Finally, AmI-RIA integrates tools that automate common classroom procedures, like attendance record keeping, quiz assessment and preparation of lesson's curriculum.

The rest of the paper is structured as follows. Section II presents related work on student monitoring in real classrooms and e-learning environments. Section III provides a description of the AmI-RIA system design along with the surrounding Smart Classroom environment. Sections IV and V present the system's implementation details. Section VI reports the evaluation results. Section VII discusses the challenges of a real-world deployment and finally, Section VIII and IX summarize the described work and highlight potential future enhancements.

II. Related Work

The widespread use of ICT (Information and Communication Technology) in learning environments has urged researchers to take advantage of the presence of technological equipment inside classrooms in order to enhance the learning and teaching process. Towards this objective, various intelligent systems that monitor students' activities and report valuable insights to the teacher have been developed, aiming to enhance both real and virtual (i.e., e-learning environments) classrooms.

A. Student Monitoring in Real Classrooms

In [13], the authors introduce Retina, a tool targeted to assist instructors that offer computer science courses to improve their curriculum by reporting the difficulties that students are facing during programming. Retina collects information about students' programming activities, such as attempts to compile their project, compilation and run-time errors, time spent for each assignment, etc. Retina logs past information about students' activities and generates informative reports both for them (i.e., self-evaluation) and the instructors. A live monitoring mechanism enables instructors to get insights for the programming session at run-time, so as to either address issues immediately during a lecture or adjust forthcoming assignments. An additional tool is also included that provides suggestions to the students, based on the collected data, via instant messages.

In [14] it is argued that teachers working in robotic classes have problems in keeping track of students' activities. As the authors claim, the real challenge for the instructors is to know when and how to intervene. Thus, they propose a system that collects data from the robotic environment and inform the teacher about the activities with which students are engaging and how they are progressing. The design of the system relies on the LeJOS programming platform for Lego Mindstorms, where two agent modules are used for data collection, one embodied into the robot and the other deployed in the programming environment.

Another monitoring system targeting programming courses is presented in [15]. The authors envision a system capable of detecting students' frustration, at a coarse-grained level, using measures distilled from student behavior within a learning environment for introductory programming. The monitored data include compilation errors, error messages, source code and other relevant information. As they argue, frustration is potentially a mediator for student disengagement. Thus, detecting it will assist instructors to intervene in ways that will help students remain motivated. Following the same pattern, past [16], [17] and recent studies [18], [19], focus on monitoring student behavior during programming courses in order to generate insights that will assist instructors improve the learning experience.

MiGen [20] is a related intelligent environment designed to support 11-14 year-old students in learning algebraic generalizations. The system aims to assist the teaching process by informing teachers of students' progress, the appearance of potential misconceptions and disengaged students. As the authors claim, this will allow teachers to provide learning in a personalized way. To fulfill this task, MiGen visualizes the students' progress based on their attainment of specific landmarks as they are working on mathematics generalization tasks. MiGen was one of the first to introduce a classroom overview panel to serve the teacher's needs, however remained at a very basic level in terms of the amount of information displayed and the user-interface quality.

A relevant, extended study is presented in [11], [21], [22]. The proposed system, named I-MINDS, consists of a group of intelligent agents that are able to track the activities and progress of students. This tracking mechanism targets to identify any problematic situations that may occur to students and then inform the instructor or assist the student to overcome the problem. The I-MINDS system offers rich insights of students' behavior to the teacher, however, it is mainly focused on the social aspect of the educational process and intended mostly to assist the formation of collaborative groups inside the classroom environment.

The aforementioned systems can partially provide real-time information to the instructor, however, they share some major drawbacks: (i) they are usually targeted to specific contexts of use (e.g., programming courses), (ii) they offer rather poor user interfaces, in terms of usability, that hinder information extraction, and, (iii) they bind the students on using actual computer machines during the educational process.

B. Student Monitoring in E-learning Environments

The Smart Classroom notion usually refers to real classrooms. However, a fair number of studies exist that aim to support instructors within e-learning environments through student monitoring. Some of them also introduce innovative methods of visualizing the students' activities during the educational process.

In [23] and [24] a web-based environment is proposed, capable of collecting students' traces produced by their interactions in order to visualize the virtual classroom. Due to the web-based nature of the system, the provided visualization helps the teacher control and interact with the classroom. Participants are represented by Chernoff faces [25], whose facial characteristics evolve over time according to their activities. Additionally, the system represents the pedagogical activities

as bubbles, which grow or shrink proportionally to the number of the participants.

In [26] and [27] a relevant system is presented, named CourseVis, which is capable of generating graphical representations of what is happening in the classroom by analyzing students' activities data collected in the context of a CMS (Course Management System). CourseVis creates a number of plots in order to visualize social, cognitive and behavioral aspects of the learners. Furthermore, it includes a mechanism for viewing statistical data from students' interactions, such as the number of accesses to each resource, the history of pages visited, etc.

Likewise, [28] presents an intelligent agent system that supports teachers in supervising learners in LAMS (Learning Activity Management System). The system is capable of notifying the instructor for common problems about participation and contribution of students during educational activities. However, for that to be achieved, the instructor is required to determine expectations for the attendance and contribution of the learners for each activity. These expectation parameters include the typical execution time, the contribution level on collaborative activities, the expected score, etc. Finally, a notification agent is used to deliver messages and information to the supervisor of the lesson and to the learners as well.

The systems discussed above constitute representative state-of-the-art approaches in the domain of student monitoring in e-learning environments that aim to assist instructors. However, several drawbacks can be identified in these solutions. On the one hand, the user-interfaces at the teacher's endpoint although they are more expressive and informative than the ones of the real-classroom systems, cannot be considered intuitive and the information extraction still remains a tough task. For instance, Chernoff faces are a useful tool for indicating student inactivity, but in more complex situations (e.g., progress and performance tracking) their expressiveness is limited. On the other hand, the e-learning environments studied do not offer an effective real-time assessment method, which is required in intelligent learning environments [29].

Thus, there is a clear need for a system that can: (i) be deployed and operate in real classrooms, (ii) monitor unobtrusively the students through their interactions taking place during the educational process, (iii) produce valuable insights about their behavior in real-time, and finally, (iv) deliver those insights to the teacher through an intuitive, yet rich, user interface.

III. System Design

The AmI-RIA system proposed in this paper aims to bridge the gap between students and teachers by providing valuable insights to the latter. For that to be achieved, several smart systems are precisely coordinated and tightly collaborate to shape the Smart Classroom (depicted in Figure 1), as it is envisioned and implemented in the context of the FORTH-ICS (Foundation for Research and Techonology Hellas - Institute of Computer Science) AmI Programme[4] (an interdisciplinary RTD Programme aiming to develop and apply pioneering human-centric AmI technologies and Smart Environments).

Figure 1: The Smart Classroom simulation space at FORTH-ICS AmI Facility. Teacher Assistant is installed in the teacher's PC visible on the left.

As depicted in Figure 2, the ClassMATE system [30] forms the backbone infrastructure that supports the intelligent classroom. ClassMATE monitors the Ambient environment and is capable of making context-aware decisions in order to assist the student in conducting learning activities. Furthermore, it is responsible for orchestrating the various artifacts that can be found in the classroom, for example, the augmented desk (Figure 3(a)) and the SMART Board[5] (i.e., the commercial interactive whiteboard depicted in Figure 3(b)). In more details, the augmented desk [31] is an enhanced school desk that uses computer vision technology to recognize books and book pages in order to provide physical and unobtrusive interaction without requiring any special device [32]. The SMART Board supports the educational tasks by offering a shared interactive area that extends the augmented student desks as applications can seamlessly migrate among them. For instance, if the teacher asks a student to start answering the questions of an exercise in front of the class, the achieved progress will be automatically transferred back to the desk when done.

A. Overall Architecture of AmI-RIA

The primary goal of AmI-RIA is to inform the teacher about the students' activities and identify potential weaknesses by monitoring their interactions and generate classroom-wide progress and performance metrics. Towards this objective, a distributed architecture (Figure 4) is introduced that consists of two major components. The first component is an intelligent

[4]http://www.ics.forth.gr/ami (Online: 5/2014)

[5]SMART Board: http://bit.ly/1n5RGKz (Online: 5/2014)

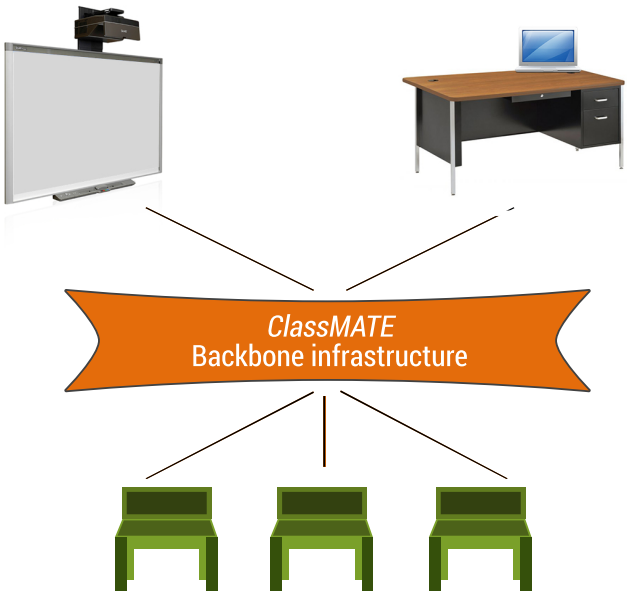

Figure 2: The Smart Classroom prototype as implemented at FORTH-ICS

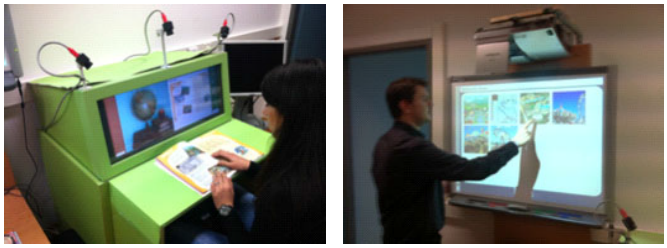

(a) Augmented Desk Prototype v1.0 (b) SMART board

Figure 3: Artifacts of the Smart Classroom environment

agent deployed on the students' desks, named Desk Monitor, which monitors each individual student's interaction. The second major component, the Teacher Assistant, is an intuitive frontend application deployed at the teacher's desk to facilitate the visual representation of the monitoring data (i.e., classroom overview) and simplify classroom control, such as assignment submission, exam distribution, etc.

Desk Monitor agents collect the monitoring traces that students generate when working on their desks and through a reasoning process draw conclusions about their behavior. Both the collected and the inferred knowledge is transmitted in real-time to the Teacher Assistant application, which is responsible to present them appropriately (e.g., highlight inactive students, prompt teacher action, etc.). Data exchange is performed through a generic services interoperability platform, named FAmINE (FORTH's AMI Network Environment), presented in [33]. FAmINE provides the necessary functionality for the intercommunication and interoperability of heterogeneous services hosted in AmI environments. It encapsulates mechanisms for service discovery, event driven communication and remote procedure calls.

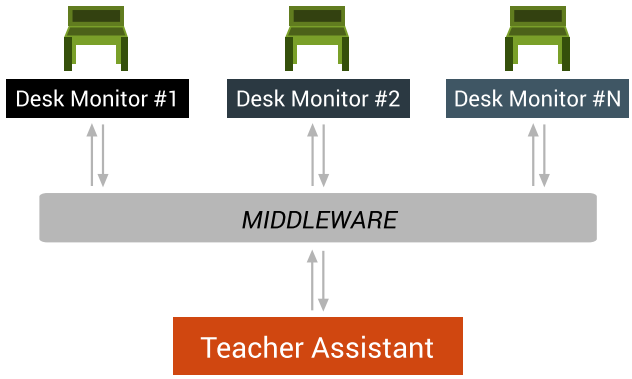

Figure 4: Distributed architecture of AmI-RIA

B. Data Collection

The collection of the monitoring data originating from the students is achieved through the classroom's backbone infrastructure and the aforementioned "smart" artifacts (i.e., smart desks and boards) that appear in the classroom environment. The augmented desk, the most important artifact of the classroom and the main source of monitoring data, is equipped with an interactive learning environment named PUPIL [34]. In short, the PUPIL framework facilitates the design, development and deployment of pervasive educational applications. Using this framework, several applications were developed and deployed in the Smart Classroom environment as already presented:

- ClassBook application: Digitally augments physical books by introducing interactive alternatives to printed elements like images, exercises, etc.
- Multimedia application: Multimedia content exploration and display (e.g., images, videos)
- Dictionary application: Displays textual and/or multimedia information about a topic or word
- Multiple-Choice exercise application: Digital alternative to the classic multiple-choice quiz. Questions are further enhanced with help buttons offering hints to learners
- Hint application: Gradually assists students towards finding the right answer by offering personalized hints. Supports the development of critical thinking skills

The aforementioned applications provide the required data source by exposing any detected interaction of students to the backbone infrastructure of the Smart Classroom. Some of the activities of interest for the AmI-RIA system include:

- login when a student sits on a desk
- course book page fanning
- launch of an exercise session
- answer submission
- use of contextual help provided by the learning system
- browsing and sharing of multimedia galleries

These activities along with the related data become available to the Desk Monitor agents by ClassMATE through a FAmINE-enabled bridge interface. For creating such interfaces FAmINE supports IDL (Interface Description Language), a specification language used to describe a software component's interface. IDL addresses interoperability issues as it

```
{
?student        a                                   student:Student.
?student        student:Current_Exercise            ?exercise.
?exercise       student:HasQuestion                 ?question.
?question       student:Hints_Used_For_Question     ?hints.
?hints          math:greaterThan                    "2"^^xsd:int.
}
=>
{
?question       student:Hints_Overuse               "true"^^xsd:boolean.
}.
```

Figure 5: Example of a N3 rule

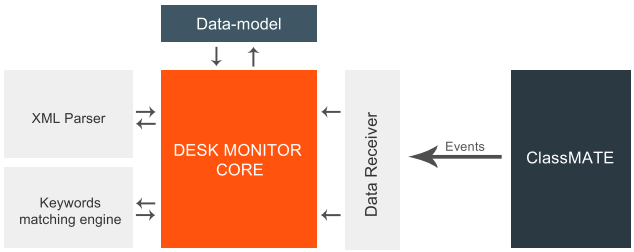

Figure 6: Anatomy of a Desk Monitor agent

is language-independent enabling this way communication between components developed in different languages (e.g., Java, C#). The defined interface includes structures, events and remote procedure calls, used for the regular messages exchange between the classroom's backbone infrastructure and the Desk Monitor agents.

C. Data Management and Reasoning

Ontologies are widely accepted as a tool for modeling contextual information about pervasive applications [35], as they address the problem of data heterogeneity between applications and support data interconnection using external popular vocabularies, such as FOAF [36] and Dublin Core metadata [37]. Furthermore, they also enable knowledge inference using semantic reasoners whose rules are implemented by means of ontologies.

AmI-RIA makes extensive use of ontologies. An RDFS schema [38] has been implemented that defines classes for the relevant entities (e.g., Teacher, Student, Book) and the activities (e.g., Open book, Start exercise) that can potentially take place in a classroom environment. Additionally, a set of taxonomies has been defined, based on RDFS properties, to associate classes and create activity hierarchies (e.g., Submit_Exercise isA Student_Act). Collected data are stored internally in the form of RDF triplet statements following the defined schema.

The required RDFS hierarchies for the entities were implemented using Protege, an open source ontology editor and knowledge base framework described in [39]. Protege offers a suitable environment for modeling the entities and shaping SPARQL [40] queries.

The reasoning process of the AmI-RIA system is supported by the SemWeb library for .NET [41]. SemWeb supports SPARQL queries for information retrieval over the data and incorporates the Euler engine [42], a popular backward chaining inference engine. The rules used by the Euler engine are written in external files using the Notation3 syntax [43] (Figure 5), an RDF syntax designed to be human friendly. Rule decoupling facilitates system maintenance and scalability, as the insertion of new rules or the modification of existing ones can be done without affecting the core of the AmI-RIA system.

IV. Desk Monitor Agents

The Desk Monitor agents constitute the core components of the AmI-RIA system, as they execute the inference rules over the collected interaction data to identify potential troublesome situations (e.g., inactive or off-task behavior, problems in understanding of concepts, etc). To that end, the agents apply a goal-driven reasoning process on contextual knowledge through a backward chaining inference engine (i.e., Euler), to identify such alarming situations, semantically defined using taxonomies, inside the classroom environment.

A. Architecture

As depicted in Figure 6, a desk monitor agent consists of five major components, namely, Data Receiver, Data-model, XML Parser, Keywords-matching engine and the Core.

The backbone infrastructure of the Smart Classroom packs the data collected by the student desks and the SMART Board artifact into events and transmits them through the middleware to a Desk Monitor module. The *Data Receiver* component provides the handlers for listening to such events and is responsible for forwarding the data included in the events to the core of the agent. The latter follows a procedure of forming a *Data Model* of the student based on the monitored interactions, which are then stored internally using RDF triplets. Since the students may switch desks occasionally, no permanent storage exists for the RDF data-model constructed by the Desk Monitor; data are erased at the end of each session. A set of predefined rules is evaluated upon the data-model to infer new knowledge.

An exercise or test in the electronic form of the book presented on the augmented desk is implemented following a custom XML schema. Each exercise file contains, among other data, the type of activity (e.g., multiple-choice), the questions, the available answers for each question, etc. For this to be parsed, Desk Monitor uses a *XML Parser* component that is capable of reading the exercise files and instantiate internal data structures.

For each learning session, a set of relevant material, books and pages is defined and checked against the material that a student has opened on the desk. Thus, it is possible to identify whether a student has opened some non-relevant material (i.e., off-task) just by comparing book titles and page numbers. Although this method is safe and effective, it has the drawback of requiring all the educational material to be analyzed and categorized accordingly at any time. To address this issue, the *Keywords Matching* component is implemented to enhance the aforementioned process by matching semantically the content appearing on a page to that of the learning session. To do so, the component exploits the metadata and text appearing on the materials used in the classroom. The procedure of the keyword matching consists of two phases, one for indexing the keywords and text from the listed relevant pages and one

for matching the current's page keywords against the indexed ones.

B. Behavioral monitoring

The Desk Monitor uses the defined taxonomies and the semantic rules and produces insights about the behavior of a student in the classroom, as soon as student activity is detected. The list of situations that can be currently detected includes: (i) off-task students, (ii) inactive students, (iii) students that face difficulties during exercise solving, (iv) students that face difficulties during exercise submission and, (v) students that misuse the contextual-help of the learning system. A detailed description for each situation, along with its importance within the educational context, is provided in the following sections:

1) Off-task: According to Caroll's Time-On-Task hypothesis [44], the longer students engage with the learning material, the more opportunities they have to learn. Therefore, if students spend a greater fraction of their time engaged in behaviors where learning is not the primary goal, they will spend less time on-task and as a result learn less. In [45], the authors argue that off-task behavior indeed has a negative impact on students' performance and investigate different types of off-task behavior. The evaluation results of the aforementioned study indicate that the frequency of off-task behavior is a good predictor of the students' performance, though, different types of off-task behavior result in different negative correlation to learning. Furthermore, in [46] authors also state that off task behavior appears to be associated with poorer learning performance at an aggregate level. To identify off-task students, the AmI-RIA system checks the material displayed on a student's desk to determine if it is relevant to the topic discussed in the classroom based on the activity in hand. Thus, it examines whether (i) the currently opened book, (ii) the opened page and (iii) the content of the currently opened page semantically belong to the current activity.

2) Inactivity: During classroom activities, especially exercise solving, it is common for students to start working on a task and after a while give up because they get bored or distracted. Inactivity is defined as a type of off-task behavior where the student does not interact with the learning object at hand at the appropriate time. According to [45] and [47], inactivity indicates that a student is disengaged with a certain task and can be used as a quite accurate performance predictor. AmI-RIA exploits the typical learning time describing the amount of time that a student is expected to work with or through a learning object [48], to specify if and when a student's interaction is taking too long to be executed. For that to be achieved, AmI-RIA gets notified by ClassMATE about the actions that a student performs when interacting with a learning object (e.g., an exercise, a text passage, etc.). However, since not all the students interact with the exercise at the same pace, individual factors should be taken into account. Towards this, the learning level of a student is estimated, based on the average score in related activities, and then used as a bias parameter in the formula calculating the total interaction time.

3) Weaknesses during problem solving: The PUPIL framework offers personalized tutoring in the form of contextual help (i.e., hints) for each question of an exercise in order to help students find the right answer. Hints gradually increase the amount of help provided, thus a student using the last hint takes advantage of all the available help. AmI-RIA monitors the amount of help asked and the selection made afterwards to calculate the student's performance. In case a student uses the maximum amount all available hints, but still does not answer correctly, then the system marks that the student has difficulties regarding this question and the concept it refers to.

4) Problems on exercise completion: Identifying whether a student faces difficulties during exercise solving is quite challenging, since a single pass/fail indicator does not always reveal the actual progress of a learner on a specific topic. To this end, instead of generalizing conclusions based merely on the score of the exercise in hand, the student's performance record on relevant topics/similar exercises is taken into consideration. Thus, even if the score is not a failing one, a potential weakness can be identified if there is a large decline on the score based on the student's record.

5) Misusing the Learning System: Sometimes students interact with exercises according to a set of non-learning-oriented strategies described in [45] and further studied in [49], known as gaming the system. Such strategies involve behaviors aimed at systematically misuse the help provided by the system in order to advance in exercise instead of actually making use of the material of the intermediate hints. A set of rules has been created to track students who repeatedly ask for help within a small time frame until they get the maximum one.

C. Extensibility of the Reasoning Mechanism

Deploying the AmI-RIA system in a real classroom may raise the need of adjusting the currently defined semantic rules or the creation of new ones to infer new knowledge. To address this issue, the semantic inference rules are defined in external files, completely separated from the system's logic. Furthermore, to enable even non-programmers (e.g., teachers) to edit or create new rules, the Notation3 RDF format is used, which is designed to be human friendly.

V. Teacher Assistant

AmI-RIA offers an intuitive front-end application deployed at the teacher's computer (or portable tablet device) named Teacher Assistant, through which the instructor can monitor at real-time via live feed the activities that take place in the classroom and identify potential weaknesses. For that to be achieved, every Desk Monitor Agent propagates the collected data and produced inferences through the classroom's middleware to the Teacher Assistant application, which is responsible for presenting them accordingly. By the time a student logs to a desk via an RFID (Radio-frequency identification) sticker appearing on books, the system pairs his/her unique id with that particular desk. Thus, every active desk in the classroom is bound to a specific student and can be uniquely identified.

In terms of data management, the Teacher Assistant makes use of RDF triplets and RDFS taxonomies, which extend the ones defined for the Desk Monitor agents. The implemented Classroom ontology defines entities appearing in the classroom such as courses, books, students, teachers, etc., as well as activities that represent the actions taking place. Indicatively, Figure 7 presents the defined hierarchy for activities involving

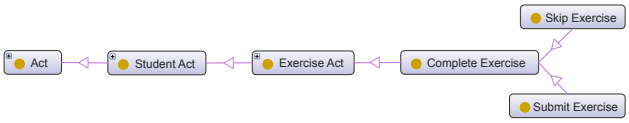

Figure 7: RDFS taxonomy for exercise activities

Figure 8: Classroom overview panel of Teacher Assistant

exercise solving. As the semantic web notion prompts for more structured and connected data, two external popular vocabularies were used in the Classroom ontology, namely, the FOAF specification and the Dublin Core metadata. Using semantic web vocabularies allows intelligent agents make sense of the entities appearing in ontologies and the connections between them.

A. Classroom Overview

In terms of GUI, the Teacher Assistant (Figure 8) adheres to the natural mapping rule [50] that leads to immediate understanding because it takes advantage of physical analogies. As such, each student in the classroom is represented by a Student Card. Non-occupied desks are presented as semi-transparent empty cards, whereas the layout resembles the one of the physical desks. As a result, the teacher can easily locate a student in the classroom through the virtual class map or access the attendance record to see the absent students. The Teacher Assistant, following a responsive philosophy, adapts its layout accordingly to support devices with smaller screen resolution like tablets and portable computers.

B. The Student Card

The Student Card contains both personal information, such as the name and the profile picture, and also information regarding the current activities and status of the student. During the course, the student might be engaged with various activities such as reading a passage from a book, solving an exercise, browsing a multimedia gallery, etc. Providing specific details on such classroom tasks allows the teacher to be constantly informed about the students' attention levels and potential learning difficulties. To this end, each Student Card adjusts to represent the current learner's status at any given moment. For instance, when a student is reading, the card displays

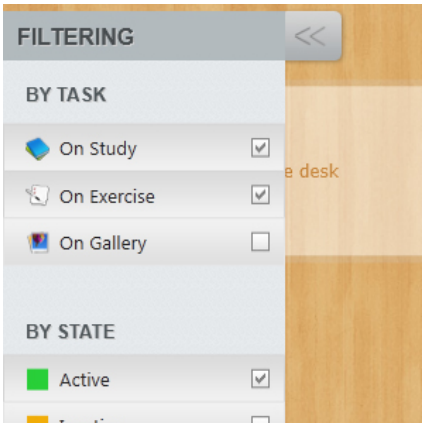

Figure 9: The filtering mechanism of the Teacher Assistant

the book title and the respective page numbers; during an exercise, additional information is displayed regarding the topic, difficulty and the student's progress, finally when a student launches a multimedia gallery, a small set of relevant keywords is displayed on the card.

However, during a lecture the students might lose interest and deviate from the teacher's suggestions. This kind of information could ideally prompt the teacher to investigate the reasons of such attention lapses and try to maintain the student's interest. For that purpose, the Student Cards are enriched with visual cues (e.g., different border colors, self-explanatory icons) to mark on-task, off-task and inactive behaviors. Finally, since the implemented system targets large and crowded classrooms, the visual information may become too large to be handled easily. To overcome this difficulty, a filtering mechanism (Figure 9) that allows the teacher to focus on specific student groups is incorporated. For instance, during exercise time, the teacher can choose to only view inactive students.

C. Assessment

Exercises are considered to be a key aspect of the learning process in a classroom as through performance monitoring potential learning gaps can be revealed and the domains where the teacher should focus are highlighted. AmI-RIA ensures that the teacher will be able to watch students' progress during exercise sessions by adjusting the Student Card appropriately to display the exercise's name, the related topic and the student's current score. More detailed information about student's performance is available through two special-purposed windows.

The first one presents a detailed view of the aspects of the exercise at hand; in particular:

- type (e.g., multiple choice quiz, fill-in the gap, etc.)
- difficulty level (e.g., easy, medium, hard)
- typical learning time as defined in the LOM metadata

The second window (Figure 10) presents a complete log of student's actions regarding that exercise:

- number of answers given
- number of hints used per question

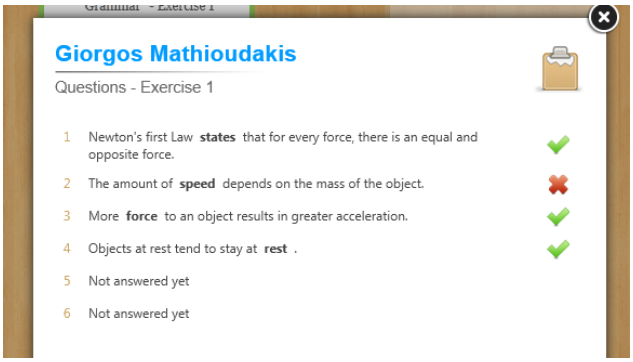

Figure 10: Exercise related interactions window

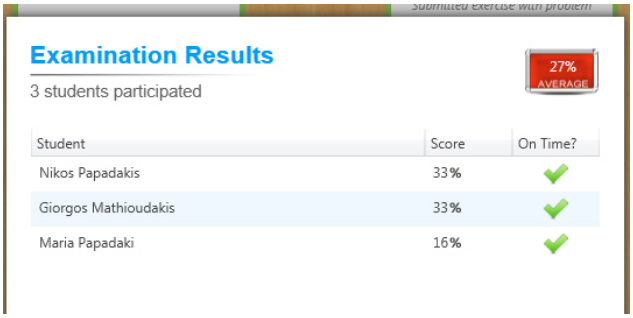

Figure 11: Test results window

- current score
- ratio of correct/wrong answers
- optionally, a problem indicator (if such decision was made by the respective Desk Monitor)

In addition to exercises, tests are also integral part of the educational process. Tests are a type of exercise where every student is obliged to answer and no help is provided. As soon as a test is initiated from the Teacher Assistant application, it automatically launches on every desk and deactivates the various assistive facilities (e.g., Thesaurus, Multimedia, etc.). During tests, the teacher can monitor students' progress as with common exercises and is able to request its immediate submission at any time. At that point, any tests that have not been submitted yet are automatically collected and a summarizing report (Figure 11) is presented with an average score for the entire classroom and a precise score for each student.

D. The Short Term Monitor

A teacher in the envisioned smart classroom is notified in real-time about the activities carried out by the students. However, eventually some notifications for a student will not catch the teacher's attention. Additionally, it is not practical to recall all the past notifications generated for one student. To address this issue, a mechanism is implemented for discovering trends in the student's activities and notify the teacher accordingly. For example, the action of a student to skip one exercise is not considered to be an important issue, however, if this student skips the fifth exercise in a row for the past few hours this means that there is a potential issue that the teacher should look after and intervene providing assistance. Each instructor can adjust the mechanism according to his needs (e.g., to be notified just for continuously inactive students); personal settings are stored on the teacher's profile in the system.

E. The Classroom Monitor

Individual statistics are automatically generated for each student by the respective Desk Monitor agent; however, accumulated metrics for the entire classroom are invaluable tools for teachers as through them behavioral patterns can be identified; an activity is considered to be a pattern if it is observed in a certain number of students in the classroom. For instance, if 85% of the students faced difficulties and performed poorly in an exercise, that may indicate that the exercise is too difficult and the teacher has to adapt the class' schedule to further elaborate on the related concepts. Similarly, if more that 80% of the students are off-task at the same time, then either a break might be helpful or the teacher should attract their attention and enhance their motivation. In any case, when AmI-RIA identifies a pattern, a special alert is generated to notify the teacher. The notifications appear on the top-right corner of the interface and can be dismissed with ease by the instructor.

F. Statistics

The data collected about the students' activities is used to build a rich history record, which is a vast source of semantic information based on the defined RDFS schema. This knowledge is exploited to generate statistics for the progress and performance of the students during short or long periods of time. Based on these statistics the teacher can identify the topics that need to be revisited or adapted and the thematic areas that seemed to have troubled each student in the past days, weeks, months, etc. Additionally, the generated statistics can be printed and handed-out to parents as an unofficial progress report for students.

The statistics component offers two alternative views, one at the classroom level and another for individuals (Figure 12). Both provide information about the overall performance, highlight topics in which the students achieved the highest and the lowest scores, and finally accumulate performance statistics per student and per lesson. More specifically, the individual statistics include: (i) average score per day, (ii) average out-of-context time per day, (iii) higher & lower score topics, and (iv) a lesson ranking based on student's score. The classroom-wide statistics include: (i) average score per day, (ii) out of context time per day, (iii) higher & lower score activities categorized by topic, and (iv) students' score ranking.

Usually in schools lessons for a classroom are taught by several teachers of different teaching professions (Mathematics, Physics, etc.). Therefore, a potential issue arise that the statistics view will also provide information that is not relevant or interesting to some specific instructor. For example, the Math teacher may not be interested in viewing statistics for the History lesson. A filtering mechanism has been incorporated in order to provide personalized views to the teacher values. Therefore, each teacher can choose to display statistics regarding only the lessons he is teaching or interested about.

Figure 12: The individual statistics component

as the insufficient color contrast between the main visual components (e.g., the main menu buttons and the footer's information). The released prototype of AmI-RIA effectively addresses all the identified errors.

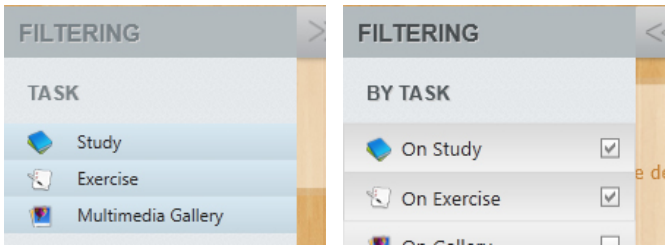

(a) Initial design (b) Adjusted design based on feedback

Figure 13: GUI adjustment based on the feedback of the experts

G. User authentication

The Teacher Assistant application displays sensitive information about the students' activities. Thereby, only authorized users must have access to the system. Additionally, each teacher has a set of preferences that should be loaded when his lessons start. To that end, an authorization mechanism was developed using a magnetic card reader and smart cards assigned to the teachers. A teacher who enters the classroom swipes the magnetic card against the reader; the system reads the id, logs the teacher and loads his preferences (e.g., the short-term reasoner settings).

VI. Evaluation

As a first step towards the evaluation of the system, an expert-based heuristic evaluation was conducted in order to identify usability problems regarding the Teacher Assistant application. Heuristic evaluation is the most popular usability inspection method and is carried out as a systematic inspection of a user interface design for usability. It is targeted to find usability problems in the design so that they can be attended to as part of an iterative design process. Heuristic evaluation requires a small set of evaluators to examine the interface and judge its compliance with a set of recognized usability principles. The optimal approach, according to Nielsen [51], is to involve three to five evaluators, since larger numbers do not provide much additional information. An observer notes down the issues and creates an aggregated list, which is delivered at the end to the evaluators in order to provide severity ratings on each issue.

Four usability experts took part in the evaluation of AmI-RIA and identified 22 issues, out of which 11 were marked as severe (rated above 2.5 on a 0-4 scale) and the other 11 as minor ones (rated bellow 2.5). The identified usability errors were related mostly to the flexibility in access to the several components (e.g., the attendance access button) and the perceived user friendliness when operated on touch-enabled devices (e.g., the sidebar option buttons were difficult to press due to their size and were not identified as toggle buttons, Figure 13). Additionally, some issues were identified regarding the aesthetic design and accessibility of the user-interface such

VII. Deployment Challenges & Limitations

The AmI-RIA system builds upon a Smart Classroom environment that provides the infrastructure required to assist the educational process from the students' perspective, and at the same time provides the monitoring facilities that enable the teacher's assistance. The prototype deployment of AmI-RIA[6] in the envisioned Smart Classroom at FORTH-ICS achieved the coordination of the several components (backbone infrastructure, augmented desk, interactive learning environment, smart board, etc.) and proved the feasibility of a real-world installation.

However, due to the monitoring nature of the system a few behavioral, legal and technological challenges arise that need to be addressed prior to deployment in real classrooms. The most interesting and challenging of them is about the willingness of the students to be constantly monitored, even though monitoring is limited to educational activities and does not involve personal ones. Students may grow the feeling of being continuously evaluated by their supervisor, a situation that may cause alterations in their behavior. Towards this, a further study is under work in order to add feedback from the monitoring process to the student's desk so that the students would demystify the procedure. In addition to this, providing some real-time feedback to students will assist them improve their progress by filling in-time any learning gaps that may occur [52], thus motivating students to support the data collection from their desks.

In addition to the students' willingness to participate in such data collecting environments, legal issues need to be considered as well. As the legislation does not cover such scenarios yet, it must be made clear who (if any) will have to give the permission for the participation of each student. Schools should work on a common policy towards student monitoring and decide whether parental permission will be mandatory.

AmI-RIA is aiming to support the average-size classroom, that is around 22 students per each according to Eurostat

[6] AmI-RIA prototype: http://bit.ly/1iuJIFd (Online: 5/2014)

TABLE I: MAXIMUM NUMBER OF SIMULTANEOUSLY VISIBLE VIRTUAL DESKS IN A SINGLE PAGE PER SCREEN RESOLUTION

Screen resolution	Maximum supported desks
1024 X 768 (XGA)	25
1280 X 1024 (SXGA)	49
1400 X 1050 (SXGA+)	56
1600 X 1200 (UXGA)	72

statistics [53], and even larger ones, up to 72 students (or more). The number of students supported is limited by the number of student cards that can be displayed in the classroom view of the Teacher Assistant and is analogous to the screen resolution of the teacher's computer (Table I). However, the system can be used best at a reasonable amount of students (20 - 30) due to the visual load on the Teacher Assistant frontend. Ways of overcoming this limitation are still under study (e.g., paging of student cards).

VIII. CONCLUSIONS

This article has presented AmI-RIA, a real-time system that assists teachers in the context of an intelligent classroom by exploiting the available ambient technology from their perspective. The proposed system monitors the students' activities in an unobtrusive way and generates valuable insights in order to assist teachers keep track of the classroom's progress and performance. Thereby, the teacher is supplied with the needed information to decide when and how to intervene providing help or adapt the teaching strategy.

For that to be achieved, the Desk Monitor agents of AmI-RIA collects all data generated by students' interactions during the educational process and store them in a semantic way, along with their semantic taxonomies. A knowledge extraction mechanism is then used to produce inferences over the data in order to identify potential weaknesses and pitfalls that need to be addressed.

On the teacher's side, the Teacher Assistant application has been implemented to provide a real-time classroom visualizer. Its rich, yet intuitive user-interface, delivers to the teacher all the information required to control the classroom effectively. Furthermore, a Statistics component is introduced, achieving to replace standard reporting of students' progress. Through that component the teacher is able to review and provide grading to students and their parents, but also compare performance across lessons or topics of a lesson, in order to oversee and address learning gaps. Finally, a set of tools have been developed to enhance typical procedures that can be found in conventional classrooms, such as the classroom attendance record, tasks assignment, etc.

IX. FUTURE WORK

The next step of this work will be to conduct a full-scale user-based evaluation in a real classroom. The evaluation is planned to include 20 different teachers and their students [54], where typical classroom activities will be observed to: (i) assess whether AmI-RIA recognizes problems successfully, and (ii) determine how instructors use the system to identify problems and provide assistance. The evaluation's findings are foreseen to extend the currently implemented rule set and improve the user interface of the teacher's frontend application in terms of usability.

Additionally, some relevant topics are being investigated for future upgrades. A significant addition to the system would be to make the students' desks aware about the knowledge generated from the collected data during the reasoning process. This way, the students will get real-time insights about their progress during the various learning activities and this will help them familiarize with the data collection procedure. The feedback provided could be used by the students to adjust their activities accordingly, while communication between the teacher and the students could be also enhanced. For instance, a valuable feature would be to enable the teacher reward some students for achieving high scores on a task or provide extra material to those who had problems in a topic.

Another important extension of the system would be the development of a graphical tool that will facilitate the fast and simple modification of the reasoning rules used to identify students' problematic states. This tool will offer a friendly frontend enabling teachers to manage rules by combining condition facts and defining the desired knowledge extraction. Ideally, entities, properties and values from the data-model will be presented as graphical elements that can be dragged and dropped, building this way the new rules.

Finally, another promising extension of the system would be to develop the infrastructure that will enable the aggregation of the information originating from multiple classrooms. This tool could be used by the school administration in order to keep track of all the students and classrooms. Relevant changes in the schools policies about grading reports may also enable the replacement of conventional reports by more detailed graphical ones, as generated by AmI-RIA.

X. ACKNOWLEDGMENTS

This work is supported by the FORTH-ICS internal RTD Programme 'Ambient Intelligence and Smart Environments'.

REFERENCES

[1] G. Mathioudakis, A. Leonidis, M. Korozi, G. Margetis, S. Ntoa, M. Antona, and C. Stephanidis, "Ami-ria: Real-time teacher assistance tool for an ambient intelligence classroom," in *eLmL 2013, The Fifth International Conference on Mobile, Hybrid, and On-line Learning*, pp. 37–42, 2013.

[2] J. C. Augusto and P. McCullagh, "Ambient intelligence: Concepts and applications," *Computer Science and Information Systems/ComSIS*, vol. 4, no. 1, pp. 1–26, 2007.

[3] D. J. Cook, J. C. Augusto, and V. R. Jakkula, "Ambient intelligence: Technologies, applications, and opportunities," *Pervasive and Mobile Computing*, vol. 5, no. 4, pp. 277–298, 2009.

[4] J. C. Augusto and C. D. Nugent, *Designing smart homes: the role of artificial intelligence*, vol. 4008. Springer, 2006.

[5] M. Antona, A. Leonidis, G. Margetis, M. Korozi, S. Ntoa, and C. Stephanidis, "A student-centric intelligent classroom," in *Ambient Intelligence*, pp. 248–252, Springer, 2011.

[6] R. A. Ramadan, H. Hagras, M. Nawito, A. E. Faham, and B. Eldesouky, "The intelligent classroom: towards an educational ambient intelligence testbed," in *Intelligent Environments (IE), 2010 Sixth International Conference on*, pp. 344–349, IEEE, 2010.

[7] M. Koutraki, V. Efthymiou, and G. Antoniou, "S-creta: Smart classroom real-time assistance," in *Ambient Intelligence-Software and Applications*, pp. 67–74, Springer, 2012.

[8] G. D. Abowd, C. G. Atkeson, A. Feinstein, C. Hmelo, R. Kooper, S. Long, N. Sawhney, and M. Tani, "Teaching and learning as multimedia authoring: the classroom 2000 project," in *Proceedings of the fourth ACM international conference on Multimedia*, pp. 187–198, ACM, 1997.

[9] Y. Shi, W. Xie, G. Xu, R. Shi, E. Chen, Y. Mao, and F. Liu, "The smart classroom: merging technologies for seamless tele-education," *IEEE Pervasive Computing*, vol. 2, no. 2, pp. 47–55, 2003.

[10] G. Margetis, A. Leonidis, M. Antona, and C. Stephanidis, "Towards ambient intelligence in the classroom," in *Universal Access in Human-Computer Interaction. Applications and Services*, pp. 577–586, Springer, 2011.

[11] L.-K. Soh, N. Khandaker, and H. Jiang, "I-minds: a multiagent system for intelligent computer-supported collaborative learning and classroom management," *International Journal of Artificial Intelligence in Education*, vol. 18, no. 2, pp. 119–151, 2008.

[12] H. McLellan, *Situated learnng perspectives*. Educational Technology, 1996.

[13] C. Murphy, G. Kaiser, K. Loveland, and S. Hasan, "Retina: helping students and instructors based on observed programming activities," in *ACM SIGCSE Bulletin*, vol. 41, pp. 178–182, ACM, 2009.

[14] I. Jormanainen, Y. Zhang, E. Sutinen, *et al.*, "Agency architecture for teacher intervention in robotics classes," in *Advanced Learning Technologies, 2006. Sixth International Conference on*, pp. 142–143, IEEE, 2006.

[15] M. M. T. Rodrigo and R. S. Baker, "Coarse-grained detection of student frustration in an introductory programming course," in *Proceedings of the fifth international workshop on Computing education research workshop*, pp. 75–80, ACM, 2009.

[16] M. Ahmadzadeh, D. Elliman, and C. Higgins, "An analysis of patterns of debugging among novice computer science students," in *ACM SIGCSE Bulletin*, vol. 37, pp. 84–88, ACM, 2005.

[17] M. C. Jadud, "Methods and tools for exploring novice compilation behaviour," in *Proceedings of the second international workshop on Computing education research*, pp. 73–84, ACM, 2006.

[18] E. S. Tabanao, M. M. T. Rodrigo, and M. C. Jadud, "Predicting at-risk novice java programmers through the analysis of online protocols," in *Proceedings of the seventh international workshop on Computing education research*, pp. 85–92, ACM, 2011.

[19] J. Helminen, P. Ihantola, and V. Karavirta, "Recording and analyzing in-browser programming sessions," in *Proceedings of the 13th Koli Calling International Conference on Computing Education Research*, pp. 13–22, ACM, 2013.

[20] D. Pearce-Lazard, A. Poulovassilis, and E. Geraniou, "The design of teacher assistance tools in an exploratory learning environment for mathematics generalisation," in *Sustaining TEL: From innovation to learning and practice*, pp. 260–275, Springer, 2010.

[21] L.-K. Soh, N. Khandaker, X. Liu, and H. Jiang, "A computer-supported cooperative learning system with multiagent intelligence," in *Proceedings of the fifth international joint conference on Autonomous agents and multiagent systems*, pp. 1556–1563, ACM, 2006.

[22] L.-K. Soh, X. Liu, X. Zhang, J. Al-Jaroodi, H. Jiang, and P. Vemuri, "I-minds: an agent-oriented information system for applications in education," in *Agent-Oriented Information Systems*, pp. 16–31, Springer, 2004.

[23] L. France, J.-M. Heraud, J.-C. Marty, T. Carron, and J. Heili, "Monitoring virtual classroom: Visualization techniques to observe student activities in an e-learning system," in *Advanced Learning Technologies, 2006. Sixth International Conference on*, pp. 716–720, IEEE, 2006.

[24] L. Kepka, J.-M. Heraud, L. France, J.-C. Marty, and T. Carron, "Activity visualization and regulation in a virtual classroom," in *Proceedings of the 10th IASTED International Conference on Computers and Advanced Technology in Education*, pp. 507–510, ACTA Press, 2007.

[25] H. Chernoff, "The use of faces to represent points in k-dimensional space graphically," *Journal of the American Statistical Association*, vol. 68, no. 342, pp. 361–368, 1973.

[26] R. Mazza and V. Dimitrova, "Generation of graphical representations of student tracking data in course management systems," in *Information Visualisation, 2005. Proceedings. Ninth International Conference on*, pp. 253–258, IEEE, 2005.

[27] R. Mazza and V. Dimitrova, "Coursevis: A graphical student monitoring tool for supporting instructors in web-based distance courses," *International Journal of Human-Computer Studies*, vol. 65, no. 2, pp. 125–139, 2007.

[28] T. Chronopoulos and I. Hatzilygeroudis, "An intelligent system for monitoring and supervising lessons in lams," in *Intelligent Networking and Collaborative Systems (INCOS), 2010 2nd International Conference on*, pp. 46–53, IEEE, 2010.

[29] S. Kalyuga, "Rapid cognitive assessment of learners' knowledge structures," *Learning and Instruction*, vol. 16, no. 1, pp. 1–11, 2006.

[30] A. Leonidis, G. Margetis, M. Antona, and C. Stephanidis, "Classmate: Enabling ambient intelligence in the classroom," *World Academy of Science, Engineering and Technology*, vol. 66, pp. 594–598, 2010.

[31] M. Antona, G. Margetis, S. Ntoa, A. Leonidis, M. Korozi, G. Paparoulis, and C. Stephanidis, "Ambient intelligence in the classroom: an augmented school desk," in *Proceedings of the 2010 AHFE International Conference (3rd International Conference on Applied Human Factors and Ergonomics), Miami, Florida, USA*, pp. 17–20, 2010.

[32] G. Margetis, X. Zabulis, P. Koutlemanis, M. Antona, and C. Stephanidis, "Augmented interaction with physical books in an ambient intelligence learning environment," *Multimedia Tools and Applications*, pp. 1–23, 2012.

[33] Y. Georgalis, D. Grammenos, and C. Stephanidis, "Middleware for ambient intelligence environments: Reviewing requirements and communication technologies," in *Universal Access in Human-Computer Interaction. Intelligent and Ubiquitous Interaction Environments*, pp. 168–177, Springer, 2009.

[34] M. Korozi, S. Ntoa, M. Antona, A. Leonidis, and C. Stephanidis, "Towards building pervasive uis for the intelligent classroom: the pupil approach," in *Proceedings of the International Working Conference on Advanced Visual Interfaces*, pp. 279–286, ACM, 2012.

[35] R. Krummenacher and T. Strang, "Ontology-based context modeling," in *Proceedings Third Workshop on Context-Aware Proactive Systems (CAPS 2007)(June 2007)*, 2007.

[36] D. Brickley and L. Miller, "Foaf vocabulary specification 0.99," tech. rep., 2014. http://xmlns.com/foaf/spec/.

[37] Dublin Core Metadata Initiative (DCMI), "Dublin core metadata element set, version 1.1," tech. rep., Dublin Core Metadata Initiative (DCMI), 2012. http://dublincore.org/documents/dces/.

[38] D. Brickley and R. Guha, "Rdf schema 1.1," recommendation, W3C, February 2014. http://www.w3.org/TR/rdf-schema/.

[39] T. Tudorache, J. Vendetti, and N. F. Noy, "Web-protege: A lightweight owl ontology editor for the web.," in *OWLED*, vol. 432, 2008.

[40] W3C SPARQL Working Group, "Sparql 1.1 overview," recommendation, W3C, March 2013. http://www.w3.org/TR/sparql11-overview/.

[41] J. Tauberer, "Semweb: A .net library for rdf and the semantic web." http://razor.occams.info/code/semweb/semweb-current/doc/, 2010. [Online; accessed May-2014].

[42] J. D. Roo, "Euler yet another proof engine." http://eulersharp.sourceforge.net/, 2014. [Online; accessed May-2014].

[43] T. Berners-Lee and D. Connolly, "Notation3 (n3): A readable rdf syntax," tech. rep., W3C, March 2011. http://www.w3.org/TeamSubmission/n3/.

[44] J. Carroll, "A model of school learning," *The Teachers College Record*, vol. 64, no. 8, pp. 723–723, 1963.

[45] R. S. Baker, A. T. Corbett, K. R. Koedinger, and A. Z. Wagner, "Off-task behavior in the cognitive tutor classroom: when students game the system," in *Proceedings of the SIGCHI conference on Human factors in computing systems*, pp. 383–390, ACM, 2004.

[46] M. Cocea, A. Hershkovitz, and R. Baker, "The impact of off-task and gaming behaviors on learning: immediate or aggregate?," 2009.

[47] J. E. Beck, "Using response times to model student disengagement," in *Proceedings of the ITS2004 Workshop on Social and Emotional Intelligence in Learning Environments*, pp. 13–20, 2004.

[48] Learning Technology Standards Committee of the IEEE, "Draft standard for learning technology - learning object metadata," tech. rep., IEEE Standards Department, New York, July 2002.

[49] O. Medvedeva, A. M. de Carvalho, R. S. Baker, and R. S. Crowley, "A classifier to detect student gamingof a medical education system,"

[50] D. A. Norman, *The design of everyday things*. [New York]: Basic Books, 2002.

[51] J. Nielsen and R. Molich, "Heuristic evaluation of user interfaces," in *Proceedings of the SIGCHI conference on Human factors in computing systems*, pp. 249–256, ACM, 1990.

[52] D. Curtis and M. Lawson, "Collaborative online learning: An exploratory case study," in *International Conference of Merdsa, Melbourne*, vol. 44, 1999.

[53] Eurostat, "Pupil/student - teacher ratio and average class size (isced 1-3)." http://bit.ly/1aR4jqn, 2014. [Online; accessed May-2014].

[54] J. Nielsen, "Quantitative studies: How many users to test?." http://www.nngroup.com/articles/quantitative-studies-how-many-users/, 2006.

Bioimpedance Parameters as Indicators of the Physiological States of Plants *in situ*

A novel usage of the Electrical Impedance Spectroscopy technique

Elisabeth Borges, Mariana Sequeira, André F. V. Cortez, Helena Catarina Pereira, Tânia Pereira, Vânia Almeida, João Cardoso and Carlos Correia
Physics Department of the University of Coimbra
Instrumentation Center
Coimbra, Portugal
e-mail: eborgesf@gmail.com
e-mail: mariana.rodriguesequeira@gmail.com
e-mail: andre.f.cortez@gmail.com
e-mail: catawina.p@gmail.com
e-mail: taniapereira10@gmail.com
e-mail: vaniagalmeida@gmail.com
e-mail: joao.mr.cardoso@gmail.com
e-mail: correia@fis.uc.pt

Teresa M. Vasconcelos, Isabel M. Duarte and Neusa Nazaré
Escola Superior Agrária de Coimbra of the Instituto Politécnico de Coimbra
Centro de Estudos de Recursos Naturais Ambiente e Sociedade
Coimbra, Portugal
e-mail: tvasconcelos@esac.pt
e-mail: iduarte@mail.esac.pt
e-mail: neunazare@gmail.com

Abstract **— Diseases promoted by biotic or abiotic agents, characterized by a fast spreading rate and absence of symptomatology, are affecting plant species and crops of huge economic and/or forestall impact worldwide. The standard technique to diagnose diseases is the symptoms visualization by skilled personal, which is only accessible in the last stages of these diseases. As a restriction action, the plant, which is considered affected by a disease, is cut and burn along with neighbouring trees, even if these do not show evidence of the disease. Equipment and techniques able of assessing and characterizing the physiological state of plants *in vivo* and *in situ*, both in the diagnosis of diseases and also as a mean for supporting physiological studies, is clearly lacking. Herein is proposed the usage of impedance techniques to assess the physiological state of plants. Emphasis is given to the assessment of the hydric stress level of plants and its relation with the disease condition. To accomplish the study, a portable electrical impedance spectroscopy system was designed attending the biological application purpose. The procedure and the results obtained for three different species (*Pinus pinaster* Aiton, *Castanea sativa* Mill, and *Jatropha Curcas* L) of relevant economical and/or forestall interest is also presented in order to show the potential of this technique and system.**

Keywords **– plant disease; physiological state; hydric stress; biodiesel; impedance techniques**

I. INTRODUCTION

Living trees, bushes, or other types of plants, are affected by several diseases, which are caused by biological agents (for example: fungus, virus, bacteria, nematodes, insects) and/or adverse environmental conditions (promoted, for example, by: droughts, fires, extreme heat, contamination of soil, and air) [1], [2]. It may be important to assess the health state (or, in other words, the physiological state) of plants, especially when plant crops affected by such diseases and/or environmental conditions have economical and/or forestall impact [1]. Currently, there are several known diseases affecting specific crops of economic importance in certain regions of the planet [1]. For the scope of this paper and the corresponding study, it may be referred, for instance: 1) the pinewood nematode disease (PWD), affecting mostly the *Pinus pinaster* Aiton specie, which has spread worldwide with special relevance in Portugal, Japan and USA; 2) the ink disease in the chestnuts, caused by a fungus, which is affecting crops in Europe; and 3) the esca disease in the grapevines, caused by an association of fungus, which also has spread throughout the planet [1]. The major problem inherent to the referred diseases, whether they are caused by fungus, nematodes or other biotic agent (or, even not being the case, eventually by abiotic agents), is their asymptomatic behavior and fast spread [1], [2], [3]. Additionally, these diseases have no cure properly developed and commercialized to date [1], [2], [3]. The main reason is the arising of new problems due to the application of the studied solutions, mainly based on phytopharmaceutical technology, such as: soil contamination, animal and vegetal species new and unpredictable problems (such as toxicity, diseases, and extinction), among others [2], [3].

Although some instrumental prototypes were studied and patented, there is no defined methodology and accepted techniques to help to assist crops management in what concerns to the assessment of the physiological (or health) states of plants *in situ* [2], [3]. Actually, the golden standard method is the symptomatology visualization by skilled personnel [1], [2], [3]. The problem with this method is its

reduced effectiveness, since the external symptoms are only able of being visually accessible during the terminal stages of the referred diseases [1], [2]. At this point, it is no longer possible to control the disease and, usually, it has already spread all over the crop, even if the symptoms are not visible in all the specimens [2]. In order to avoid the fast spreading, the plant that is considered affected, is cut and destroyed along with the neighbouring plants [2]. This preventive act poses another problem: the deforestation and the resulting economic losses arising due to the massif felling.

The characterization of physiological states of plants is also important in the perspective of marketing, consumption, and in researches for new plants' applications such as the emergent production of biodiesels [1], [4], [5]. In every case it is lacking detailed, fast enough, and robust techniques [1], [5], since the available require expensive laboratory equipment and materials, are time consuming, and hard to implement [1], [2], [6].

Hereupon, it can be said that, in general, there is a lack of equipment and systems able of evaluate and characterize the physiological state of plants, as well as a reliable and expeditious technology to allow an assessment *in situ* [1].

This overall described panorama was the main motivation for the present work [1]. Herein, the authors propose an Electrical Impedance Spectroscopy (EIS) system, developed by the team, and the usage of impedance techniques to assess the physiological states of plants *in situ* [1].

EIS has been proving efficacy and utility in a wide range of areas, from the characterization of biological tissues to living organisms [1], [7]. This passive electrical property, known as electrical impedance, is a measure of the opposition to the flow of an alternating current, which occurs when an external electric field is applied [1]. A current I crossing a section of material of impedance Z, drops the voltage V established between two given points of that section [1]. This yields the well-known generalized Ohm's law: V=IZ, where V and I are, respectively, the voltage and current complex scalars and Z the complex impedance [1]. Therefore, the result of the EIS measurements is a set of complex values (magnitude and phase), of impedance versus frequency [1].

Any biological material has its own electrical signature, whereby the physiological changes, due to diseases and nutritional or hydration levels, have direct influence in the impedance spectrum [1].

The major contributors for the biological tissues impedance are the cell membranes and the intra- and extracellular fluids [1], [7]. To electrically represent a biological tissue it is generally used a circuit that consists of a parallel arrangement between a resistor, representing the extracellular fluid, and a second arrangement connecting a resistor, simulating the intracellular fluid, and a capacitor as the membrane [1], [8], [9]. The determination of the ohmic values of the intra- and extracellular fluids, and also the capacitive value of the membrane, can be achieved by means of the theoretical Cole model [1], [10]. In this model, the achieved impedance spectrum (resistance versus reactance) is named by Cole-Cole plot [10].

The phase angle and other interrelated indexes, such as the ratio between impedance at the lowest and at the highest frequencies the system can output, Z_0/Z_∞, [7], and the ratio between impedance at the lowest frequency the system can output and 50 kHz, Z_0/Z_{50} [11], have been used to extract information about the physiological condition of biological materials. Work such the one being presented, where a deep study was carried out, the amount of data to be analyzed may hamper the use of the Cole model. The usage of the referred impedance indexes, and also the study of new ones, may be a lighter and equally valid approach.

Currently, there are instruments commercially available with high precision and resolution that can operate within a frequency range from some Hz to tens of MHz [1], [7]. However, the degradation of the excitation signal, occurring at low and high frequencies (already above 100 kHz), affects the accuracy of the measurements [1], [7]. Besides, the existing equipment is unfeasible for *in vivo* [1], [7] and in field applications, since it consists in desktop instruments, such as impedance analyzers and LCR meters [1].

It is possible to excite the sample with a current and measure a voltage or do the exact opposite [1]. The choice of the most suitable source, current or voltage, is a topic that still remains in discussion [1]. Current sources (CS) provide more controlled means of signal injection [12] and present reduced noise due to spatial variation when compared with voltage sources (VS) [1], [13]. However, due to their output impedance degradation [13], CS accuracy decreases for high frequencies [1], [14]. For this reason and since the impedance measurements are only possible when current is linear with respect to the voltage applied [9], or vice-versa, CS need expensive high-precision components [15] and a limited bandwidth operation range [1], [14], [15]. On the other hand, although EIS systems based on VS are less accurate [15], they can be built with less expensive components [15] and operate over a larger frequency range [1], [14], [15].

The developed EIS system, presented also in this paper, is able to perform AC scans within a selectable frequency range [1] and it can drive either a current or a voltage signal to excite a biological sample *in situ* or *in vivo*. It also implements the phase sensitive detection (PSD) method, although the one used has a novel implication, which is presented in further section. The instrumentation was designed to be cost-effective and usable in several applications [1]. The Table I resumes the main characteristics of the developed EIS system.

This paper will present the most relevant studies obtained for three different plant species: pine *(Pinus pinaster* Aiton), cheastnut (*Castanea sativa* Mill) and *Jatropha Curcas* L. The choice of the plant species under study was substantiated by the economic and/or forestalls relevance they have. Chestnuts and pines have a crucial economic impact in our

country and are currently affected by uncontrolled diseases: the nematode disease, in the case of pine trees, and the ink disease, in the case of chestnut trees. *Jatropha curcas*, by other hand, is a tropical species, which seeds are being studied and used for biodiesel production. The available equipment to assess seeds quality is mainly constituted by heavy and expensive laboratorial instruments, which required methodology is time consuming and usually implies the usage of expensive materials/reagents. Accordingly, a true physiological assessment, based on a reliable technique, may help to assist the ongoing studies and contribute for the advance of its state of the art.

The assessment of the hydric stress (HS) level and its relation with the disease condition was the main physiological state being focused on this work [1].

The HS refers the internal hydration condition of a plant and it is one of the most relevant parameters to assess physiological states [5]. This parameter takes special significance in the assessment of diseases, since water absorption by the plant is one of the physiological processes firstly and strongly affected during a biotic or abiotic disease condition [5].

The following sections of this paper are: 1) *System Design*, where the developed EIS system is presented in detail; 2) *Assessment of the HS Level*, which presents the method and the results obtained for the HS assessment for the three studied species; 3) *Study of Disease Condition*, which presents the method and the results obtained for the study of the nematode disease in *Pinus pinaster* specie; 4) *Discussion*, where results are explained with more detail; and 5) *Conclusions*, where the main obtained results is resumed.

TABLE I. SUMMARY OF SPECIfiCATIONS OF THE EIS SYSTEM

	Range	
Parameter	***Current Mode***	***Voltage Mode***
Measuring method	2 electrodes	
Frequency	1 kHz to 1 MHz	
Signal amplitude	25 uA	4.6 V
Impedance magnitude	2.5 kΩ to 100 kΩ	1.5 kΩ to 2.2 MΩ
Impedance phase	-π rad to π rad	-π rad to π rad
Mean absolute magnitude error	1675.45 Ω	709.37 Ω
Mean absolute phase error	2.45 %	2.06 %
Mean distortion	0.29 %	0.48 %
Mean SNR	117.0 dB	118.8 dB
Calibration	Automatically calibrated by software	

II. SYSTEM DESIGN

In order to study the plants' bioimpedance behaviour and extract conclusions from their physiological states, an EIS system was designed and built attending the requirements of portability, reliability, fast data assessment, and accessible methodology.

A. General Description

The developed EIS system employs three main modules: signal conditioning unit, acquisition system (PicoScope® 3205A) and a laptop for data processing (Matlab® based software) [1] (see Figure 1).

The digital oscilloscope PicoScope® 3205A synthesizes and provides the excitation AC signal to the conditioning unit (ADC function) [1]. It also digitizes both excitation and induction signals at high sampling rates (12.5 MSps) and transfers data to the computer via USB where it is stored [1].

The signal conditioning unit receives the excitation AC signal, coming from the PicoScope®, and amplifies it to be applied, through an electrode, to the sample under study [1]. The induced AC signal is collected by a second electrode, which redirects it to the conditioning unit, where it is amplified. Both excitation and induced signals are conduced to the PicoScope® to be digitized [1].

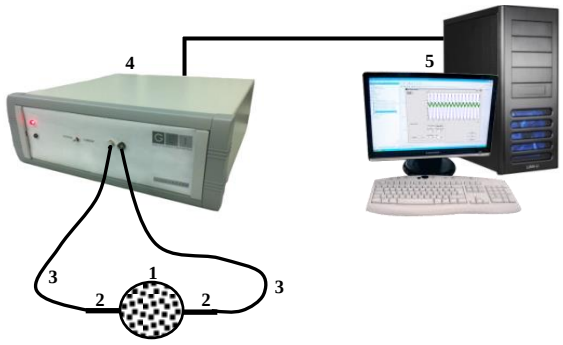

Figure 1. Schematics of the EIS system (OEM version) – 1) Biologic sample; 2) electrodes; 3) short coaxial cables; 4) EIS system conditioning unit and acquisition system, with the Picoscope®3205A incorporated; 5) laptop/PC.

The EIS system is able to generate both voltage and current signals. An external switch allows the user to select one of these two sources of excitation leads to optimal data. The specifications of both excitation modes are described below.

B. Design Specifications

Already studied by Seoane, Bragós and Lindecrantz, 2006 [16], the current mode circuit employs the current-feedback amplifier AD844 in a non-inverting ac-coupled CS configuration (see Figure 2) [1].

During the impedance measurements, the dc-blocking capacitor, between the source and the electrode, tends to charge due to residual DC currents [1], [15]. For this reason, the transimpedance output of the AD844 easily reaches the saturation [1]. To overcome this problem, it was implemented a DC feedback configuration, which maintains

the dc voltage at the output close to 0V, without compromising the output impedance of the source [1]. Therefore, the output current is maintained almost constant over a wide range of frequencies [1].

The high speed voltage-feedback amplifier LM7171 is employed in the voltage mode circuit (see Figure 2) [1]. Although it behaves like a current-feedback amplifier due to its high slew rate, wide unit-gain bandwidth and low current consumption, it can be applied in all traditional voltage-feedback amplifier configurations, as the one used [1]. These characteristics allow maintaining an almost constant voltage output over a wide range of frequencies [1].

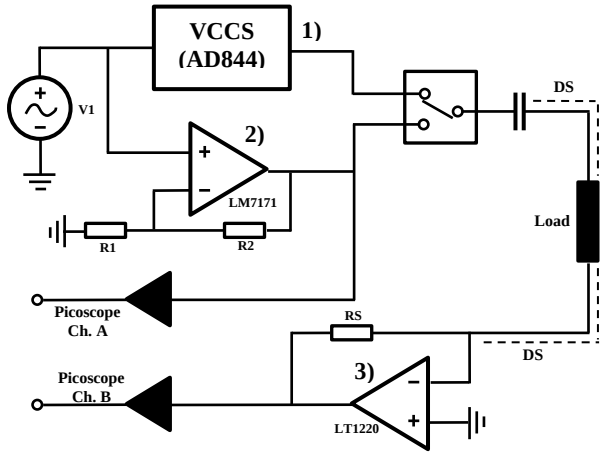

Figure 2. Schematic of the EIS system conditioning unit - 1) AC current source; 2) AC voltage source; 3) current/voltage sense.

The high speed operational amplifier, LT1220 (see Figure 2), senses the current or voltage signals from voltage or current excitation modes, respectively [1]. It performs input with reduced offset voltage and it is able of driving large capacitive loads [1].

The value of the gain, for both current and voltage excitation sources, can be changed in order to extend the range of impedance magnitude [1]. The transductance gain of the LT1220 is currently set to 5.1 kΩ [1]. This value actually defines the gain of the system, which is taken into account for the impedance data algorithmic calculation. This means that, since the gain values are known and also the amplitude of the AC excitation signal, V_1, from the PicoScope® (see Figure 2), the EIS system is calibrated automatically by software [1].

C. PSD Method

To assess the impedance phase shift it is implemented a digital Phase Sensitive Detection (PSD) method with a novel implication. As stated in the literature, the PSD method is a quadrature demodulation technique that implements a coherent phase demodulation of two reference (matched in phase and quadrature) signals [17]. It is also known that this method is preferable over others especially when signals are affected by noise [17].

The signal from the Picoscope® that corresponds to the current, VI=Bsin(ωt+φ2), is set as the reference signal. Since the phase of the signal VI is not controlled, it is easily understandable that it does not necessarily contain a null phase. This statement remains valid whether VI is used to excite the sample, in the current mode, or whether it corresponds to the current passing through the sample, in the voltage mode. The signal from the Picoscope® that corresponds to the voltage, VV=A sin(ωt+φ1), also contains a non-null phase. Both amplitudes, A and B, are also different from each other and none equals to 1.

The following block diagram, shown in Figure 3, supports the mathematics implicit in this novel PSD method.

Along with the mathematical demonstration (not presented in this paper due to its extension), the developed PSD algorithm was tested with Matlab® for several phases and amplitudes, without the theoretical requirements (i.e., ensure that the reference signal has null phase at the origin and that its amplitude equals to 1 [17]). For all the tests it was showed an always corrected phase shift assessment, when compared to the results obtained for a reference signal with the theoretical characteristics (see Figure 4).

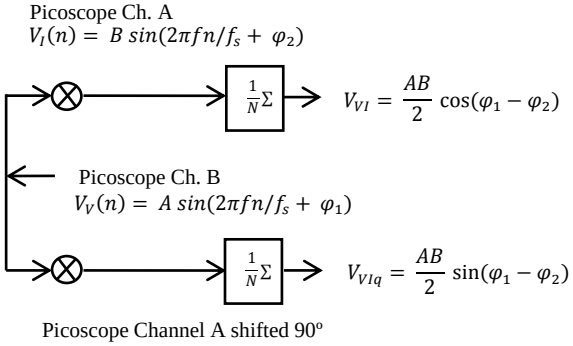

Figure 3. Schematic of Phase-Sensitive Demodulator implemented in the developed EIS system.

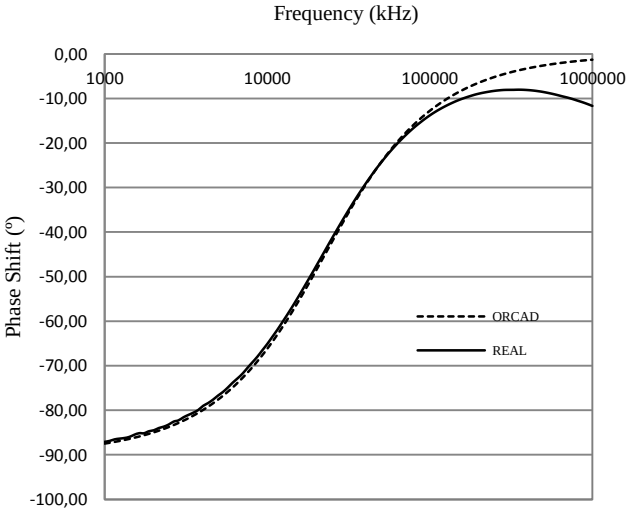

Figure 4. Comparison between impedance phase of a real data and Cadence® simulated data for a RC circuit. The deviation that occurs between the graphics, at high frequencies, is due to the influence of stray capacitances (see section below).

D. Electrodes and Cables

The developed EIS system employs two beryllium cooper gold platted needles as electrodes, each with around 1.02 mm in diameter [1]. In order to reduce the dispersion of the surface current density flow [1], [10] and also to reduce damage on the biologic sample [1], the electrodes are inserted so lightly as possible (1 to 5 mm deep depending on the thickness of the cork).

The electrodes are connected to the acquisition unit through coaxial cables. The employment of this type of cables is justified by the necessity to obtain an optimized signal-to-noise ratio [1]. However, coaxial cables introduce high equivalent parasitic capacitances, which promote phase shift errors, especially at high frequencies, during the bioimpedance measurements [1]. For this reason, the employed RG174 RF coaxial cables (capacitance of 100 pF.m-1) are as short as possible (around 15 cm). It was also implemented the driven shield technique to the coaxial cables, which permits to partially cancel the capacitive effect, that otherwise is generated between the internal and the external conductors, by putting both at the same voltage [18]. Reductions in the capacitive effect of 20.4%, in the current mode, and around 35.8%, in the voltage mode, at the highest frequencies are verified. Figure 5 depicts the capacitive effect reduction by the usage of the driven shield technique.

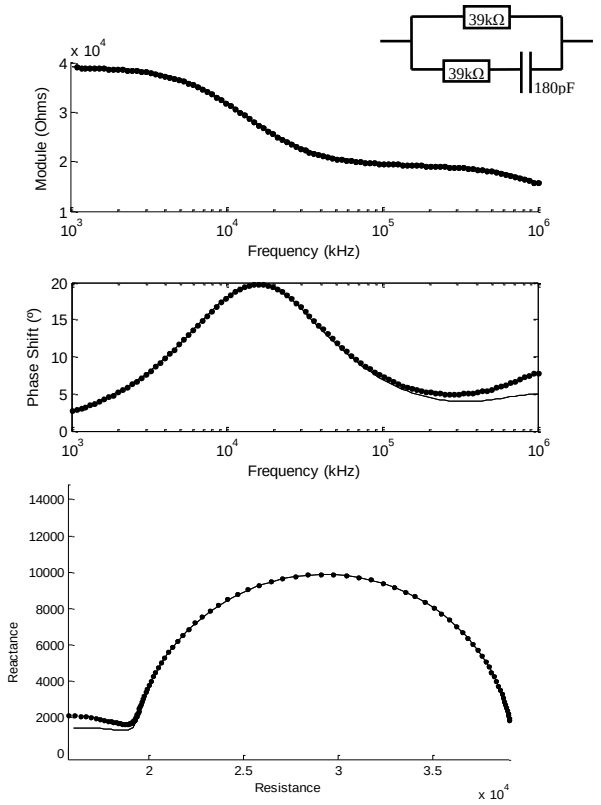

Figure 5. Bode and Cole-Cole diagram showing the reduction of cables capacitive effect by the application of the driven shield technique. The voltage mode excitation was used to analyze the circuit at the right top. The reduction is more noticeable at high frequencies where the capacitive effects have more influence.

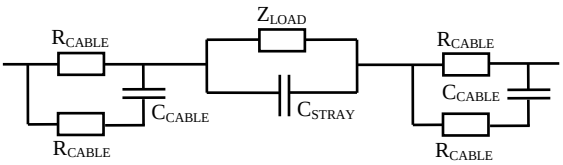

Figure 6. Equivalent electric circuit of all parasitic elements affecting impedance measurements of a load, Z_{LOAD}. The effect of the stray capacitances from cables, C_{CABLE}, is minimized by the driven shield. Other stray capacitance effect, C_{STRAY}, due primarily to the phase shift of amplifiers, can be minimized by software.

The phase shift occurred due to capacitive effects is not only promoted by cables, but also by the amplifiers [1]. The cumulative effect of the phase shift errors outcomes in an inflexion point in the impedance spectra that occurs at high frequencies (see Figure 5) [1].

This type of error affects not only the phase at high frequencies, but also the impedance magnitude, which presents a typical decline shown at the Bode diagrams (see Figure 5) [1]. In the developed EIS system, the slight decline of the impedance magnitude is due to the loss of the product gain-bandwidth of the LT1220 for high frequencies [1].

The equivalent electric circuit of such a system foresees this capacitive effect behavior, which is represented through an extra capacitor, called stray capacitance, placed in parallel with the load in analysis [1]. It is considered that stray capacitances induce systematic errors since their effect is present in all measurements. Although the results are not greatly affected by the influence of stray capacitances, it is opportune to be aware of the real equivalent circuit (see Figure 6). By this way, it is possible to consider and/or discount the effect of all parasitic elements where justified.

III. Assessment of Hydric Stress Level

The HS level was one of the studied impedance parameters due to its significance, as explained in Section I. Below are presented the used materials and methods, along with the main results.

A. Materials and Methods

For assessing EIS profiles and studying the HS level the following specimens were used: 1) eight young healthy pine trees (*Pinus pinaster* Aiton), with about 0.8 meters tall and 1 to 2 centimeters in diameter; 2) eight young healthy chestnuts trees (*Castanea sativa* Mill), with about 0.5 meters tall and 1 to 2 centimeters in diameter; and 3) eight young healthy *Jatropha Curcas* L. trees, with about 0.2 meters tall and 3 to 4 centimeters in diameter [1].

The populations of different plant species were kept under controlled environment conditions – temperature (27 – 30 ºC), luminosity, soil content and watering – in order to reduce the quantity of variables that may change the EIS profiles [1].

A portable EIS system version was employed to perform the EIS measurements. The electrodes were placed in the

trunk of each tree, in a diametric position, and about 20 cm above the soil, in the case of the pine and chestnut trees, and about 10 cm above de soil, in the case of *Jatropha curcas* (since these specimens were shorter in height) [1]. It was used the voltage mode of excitation [1], since the achieved impedance signals were cleaner for this mode (i.e., optimal signal-to-noise ratio due to better current signals amplitudes). A frequency range between 1 kHz and 1 MHz was selected to accomplish the EIS analysis [1], since this frequency range has been shown to be sufficiently wide for studying these species.

Routine acquisitions took place between 11 a.m. and 1 p.m. since it was already verified in previous studies that at this time period the trees' impedance is lower and presents less variation (see Figure 7, for example) [1].

To study the HS level variation, EIS monitoring was performed over 8 months, for one individual at a time, and for each plant species [1]. After understanding the variation of the EIS profile of regularly watered plants, the specimen being monitored was kept without watering during a period of a time (usually 3 to 4 weeks). When the HS effects were visible through external plant morphology symptoms, the specimen was regularly watered again to avoid the dead of the biologic material. In the case of the studied pines, the visualization of external symptoms was only possible near the time the specimen was about to die (which precluded the recovery of some individuals). For this reason, the variation of the water abstinence time period (WAP) and the plant response to it, measured by the EIS system, was one of the main focuses of this study.

B. Results

Several impedance parameters were determined for each impedance spectrum, however only the main indexes, such as the index $Z_1/Z_{50,}$ will be presented as results, due to paper space limitations and also because this is a parameter already studied in the literature [1]. The index 1 is used instead of the index 0, as stated in the Introduction section, which corresponds to the lowest frequency analyzed by the system (1 kHz) [1].

The time continuous measurements allowed revealing a daily oscillation of the EIS profiles [1]. To verify this behaviour it was assessed the R_1/R_{50} (R representing the magnitude module) for a period of 6 days [1]. A Fast Fourier Transform was determined for this ratio just to confirm that the rhythmic signal had a period of exactly 24 h [1]. A clear frequency value of 11.57 μHz, which corresponds to a frequency of 24 h, was founded [1]. This rhythmic signal was also perceptible for other studied indexes, although they are not presented in the paper.

The higher values of the ratio R_1/R_{50} correspond to the night period, where the luminance and temperature are lower in relation to the day period [1]. Furthermore, these studies and previous ones revealed that the variation of the impedance values is lower during the period where the illumination was higher (between 11 a.m. and 1p.m.).

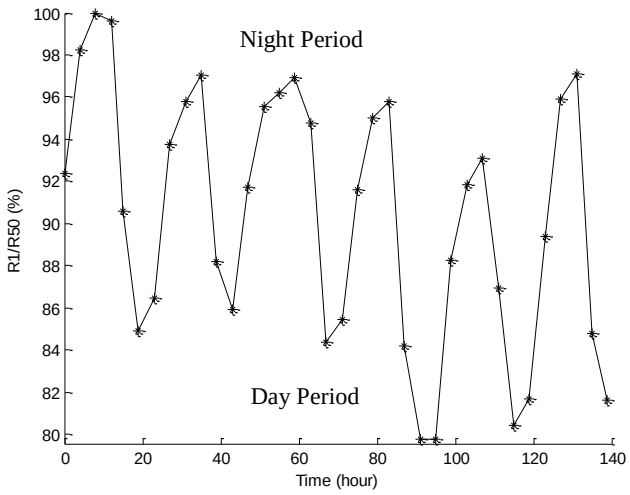

Figure 7. Variation of the R_1/R_{50} ratio during the monitoring of a healthy pine tree with regular watering. The impedance values show a daily oscillation that is characteristic of the studied trees.

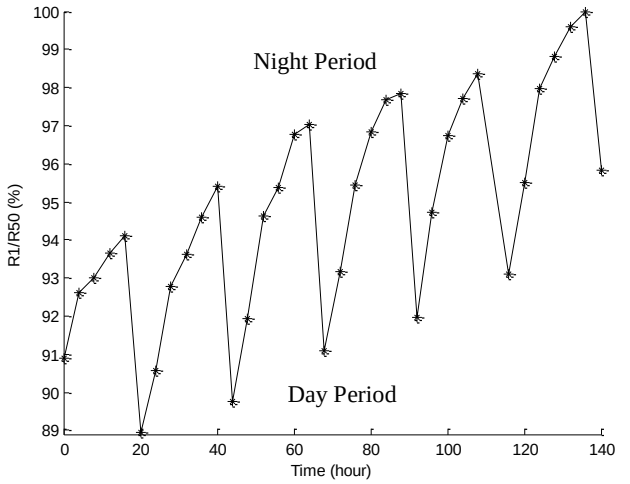

Figure 8. Variation of the R_1/R_{50} ratio during the monitoring of a healthy chestnut without watering. The impedance values show a daily oscillation that is characteristic of the studied trees. The successive higher values of each cycle are due to the incrinsing level of HS.

Data obtained for the EIS monitoring and the study of the HS level, revealed a consistent behavior for all the studied species: the R_1/R_{50} ratio tends to increase with higher values of HS [1]. After introducing regular watering, the same parameter progressively tended to the typical values of hydrated trees [1]. This effect is much more visible in the chestnuts, i.e., the variation of impedance parameters due to HS is higher and faster for the chestnuts, when compared with pines [1].

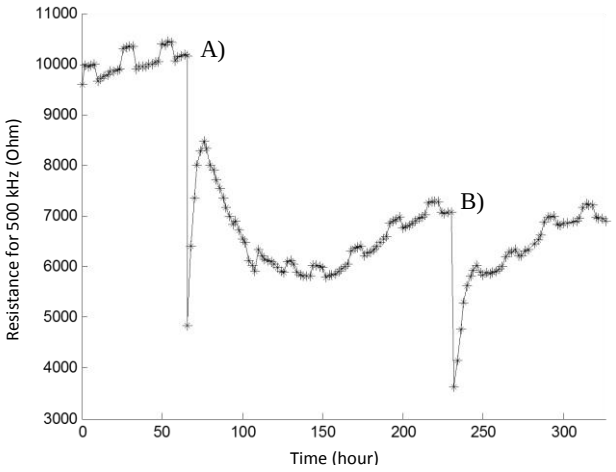

Figure 9. Variation of the R_{500} index during the monitoring of a healthy *Jatropha curcas* (12 days). The initial WAP was 6 months, period after which the EIS measurements started. The plant was watered at the 4th and 9th days of monitoring, points A) and B) respectively. It is visible the immediate response to watering and also an immediate rise of resistance after the normal impedance values restoration.

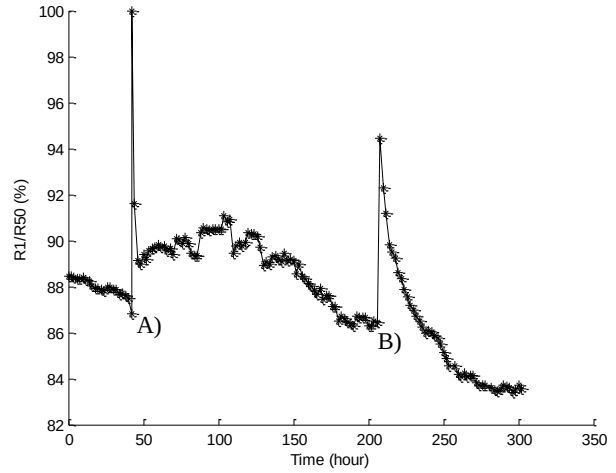

Figure 10. Variation of the R_1/R_{50} index during the monitoring of a healthy *Jatropha curcas* (12 days). The initial WAP was 6 months, period after which the EIS measurements started. The plant was watered at the 4th and 9th days of monitoring, points A) and B) respectively. It is visible the immediate response to watering and also an immediate rise of resistance after the normal impedance values restoration.

In relation to *Jatropha curcas* it was observed a totally different behaviour. To achieve measurable and significant levels of HS it was necessary to leave the plant without watering during months (5 months at least). After watering, the response of the plant was instantaneous, even faster than the chestnut response. However, depending on the HS level, the establishment of the normal hydration values may take 1 to 2 days or, otherwise, it may be practically immediate (see Figure 9). Once the HS levels were established, impedance values start to rise also immediately.

The rate of impedance augmentation is faster for the first weeks (2 to 3 weeks) when the plant is without watering and then tends to stabilize towards a value, which is maintained during months. The achieved different results, in relation to pine and chestnut trees, could be explained due the existence of latex vessels in the *Jatropha curcas* specie [1]. Figure 9 shows the particular behaviour of *Jatropha curcas* for the index R_{500} (resistance at a frequency of 500 kHz).

In relation to the R_1/R_{50} index – just to compare with the previous two cases – it tends to decrease for higher values of HS level and, after introducing regular watering, the ratio abruptly assumes the typical values (see Figure 10) [1].

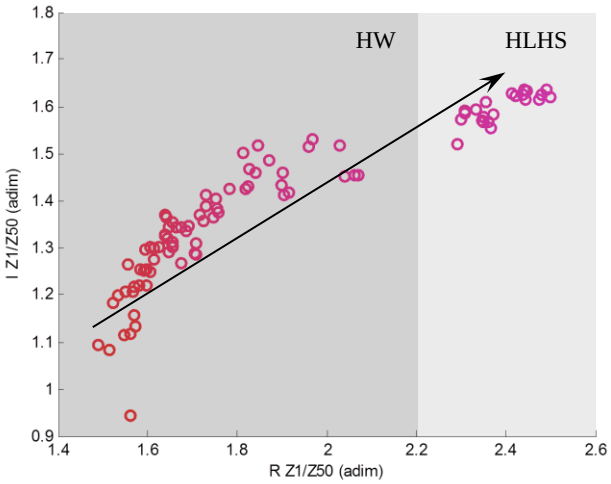

Figure 11. Evolution of the Z_1/Z_{50} ratio, in a real vs imaginary plot, during the monitoring of a healthy chestnut tree while kept without watering. The arrow indicates the direction of the Z_1/Z_{50} ratio evolution. The impedance values of the regions HW (healthy and watered) and HLHS (high level of HS) correspond to the indicated physiological states.

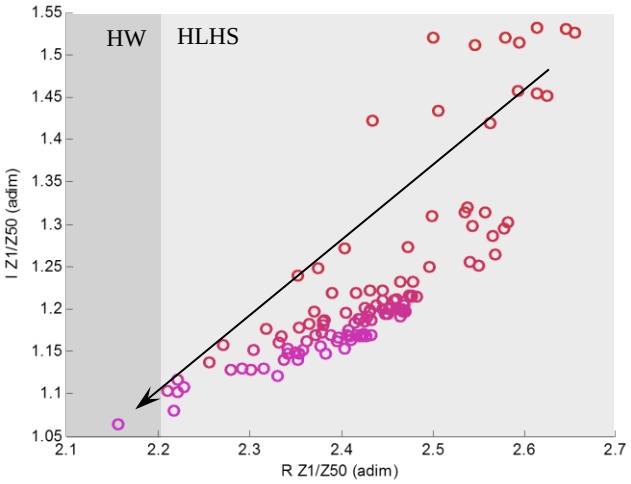

Figure 12. Evolution of the Z_1/Z_{50} ratio, in a real vs imaginary plot, during the monitoring of a healthy chestnut, with high level of HS, after intruducing regular watering. The arrow indicates the direction of the Z_1/Z_{50} ratio evolution. The impedance values of the regions HW (healthy and watered) and HLHS (high level of HS) correspond to the indicated physiological states.

In order to consider the variation of the total impedance, and not only the variation of its real part (resistance), there were studied other impedance indexes, such as the Z_1/Z_{50} index, presented in this paper.

Besides the monitoring of one plant of each group/specie, there were also performed single acquisitions to the seven remaining plants, which were kept under regular conditions (including watering).

The calculation of the mean HS values of these healthy and watered trees, allowed the determination of trees with higher HS levels and also tress with diseases (see Section IV). This information together with the graphical representation of this specific index, Z_1/Z_{50}, allows the easy identification of regions that corresponds to different plant physiological conditions.

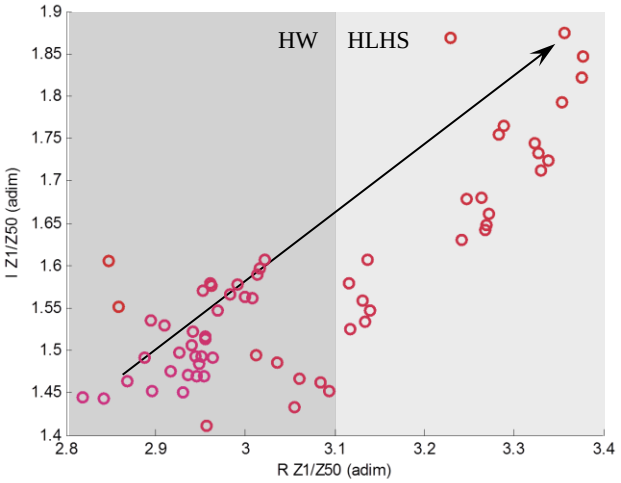

Figure 13. Evolution of the Z_1/Z_{50} ratio, in a real vs imaginary plot, during the monitoring of a healthy *Jatropha curcas* tree, with high level of HS, after intruducing regular watering. The arrow indicates the direction of the Z_1/Z_{50} ratio evolution. The impedance values of the regions HW (healthy and watered) and HLHS (high level of HS) correspond to the indicated physiological states.

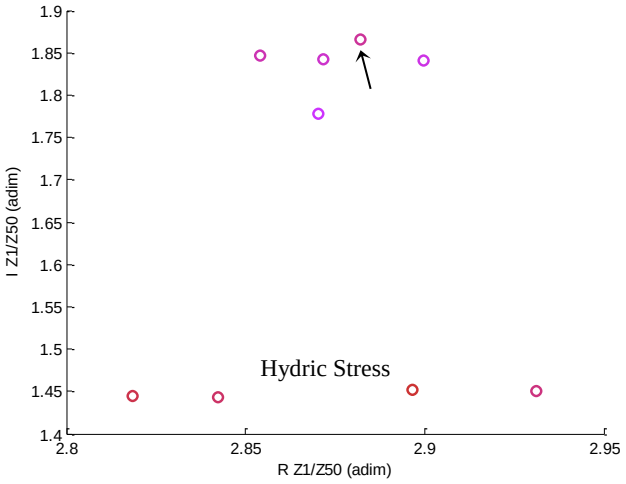

Figure 14. Example of the abrupt evolution of the Z_1/Z_{50} ratio, in a real vs imaginary plot, during the monitoring of a healthy *Jatropha curcas* tree after watering. The arrow indicates the first Z_1/Z_{50} value after watering.

The previous figures do not include the region that corresponds to the disease physiological condition, since this was not the purpose of the *Jatropha curcas* study. As it will be shown in the following section, the impedance values for this condition are much higher (at least for the imaginary part of the impedance) whereby they are out of the range of the presented plots.

IV. Study of Disease Condition

In order to understand the EIS behaviour and the physiological states variations for a plant affected with a disease, it was performed a study with pines where some individuals were inoculated with nematodes. Below, the study undergone is explained, along with the main obtained results.

A. Materials and Methods

To perform this study, there were used twenty four pine trees (*Pinus pinaster* Aiton), with about 2.5 meters tall and 2 to 3 centimetres in diameter [1]. Pine trees were placed at a greenhouse, in vases, and under controlled water environment [1]. Temperature, humidity and luminosity were also controlled. In order to keep a difference of the hydric stress level, half of the tree population was less watered (2 minutes per day, ~ 66.67 mL/day) when compared with the other half (5 minutes per day, ~133.37 mL/day) [1].

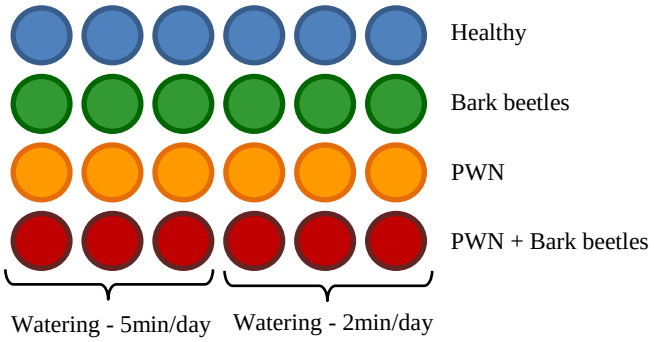

Figure 15. Schematic of the distribution of the sub-population groups of pines at the greenhouse. Each group of three pines has different conditions.

The main purpose of this study was to assess the disease physiological state condition of the pines for the specific case of the PWD. As stated in the Introduction section, this disease is caused by the pinewood nematode (*Bursaphelenchus xylophilus* Nickle), PWN, which is housed in the tracheas of the *T. destruens* Wollaston, a bark beetle. Before the PWN arrival, the bark beetles coexisted with pines without causing tree damage. To prove the harmlessness of this pest, in terms of HS, and also to have a control population group, both PWN and the bark beetles were inoculated in separated groups of pines. Six pines were inoculated with PWN, other 6 pines were inoculated with

bark beetles, other 6 pines were inoculated both with PWN and bark beetles, while the remaining 6 were kept healthy [1]. The pines of each sub-group were positioned at the greenhouse in such a way that half of them, i.e. three pines for each sub-group, were regularly watered (5 min/day) while the other half was less watered (2 min/day) [1] (see Figure 15 for a better understanding).

The pines inoculated with bark beetles were covered with a Lusatril tissue to avoid beetles escape [1]. In each tree there were placed 15 insects, which were collected immediately after the emergence phase [1].

The method used to inoculate the PWN was somehow innovative [1]. Three 2 x 2 cm rectangle of cork were removed at different locations of the trunks and, the exposed phloem, was erased with a scalpel in order to improve the adhesion of the nematodes [1]. In each incision it was placed a 0.05 mL of a PWN suspension, in a total of 6000 nematodes per tree [1]. After the inoculation, each removed rectangle of cork was fixed in the respective place and wrapped with plastic tape [1].

The EIS measurements started seventy days after the inoculations [1]. At this period, pines inoculated with PWN presented a decay rounding the 40% and certain symptoms of the disease were already visually accessible [1]. Two of the healthy pines died (decay of 100%) due to hydric stress, and all the remaining trees appeared healthy [1].

There were taken two EIS measurements per tree between 11 a.m. and 1 p.m. The portable version of the EIS system was used with a frequency range from 1 kHz to 1 MHz was applied in the voltage mode [1]. The electrodes were placed in the trunk of each tree in a diametric position, about 30 cm above the soil [1].

The trunk of each pine tree, inoculated with the PWN, was cut in three different regions in order to relate the EIS data with the stage of the disease and the number of nematodes per section [1]. The cuts were performed: a) immediately below the inoculation incision (180 cm above the soil); b) 30 cm above the soil (where EIS measurements took place); and c) in the middle of the previous two cuts (approximately 80 cm above the soil) [1].

After these measurements, two healthy pines were monitored independently by two EIS portable systems [1]. After a week of monitoring, both pines were inoculated with PWN and the measurement continued during 7 more weeks [1]. The purpose of this last experiment was to study the variation of the EIS profiles during the pine decay due to the PWD [1].

B. Results

Several impedance parameters were assessed in order to study the physiological states of the trees [1]. Z_1/Z_{50} was the impedance parameter that showed the best results [1].

Similar values of Z_1/Z_{50} were obtained for both healthy pines and pines inoculated with bark beetles, suggesting that the beetles' action does not affect the physiological states of pines [1], at least in terms of the HS levels variation. In fact, it was expected a similarity between both EIS profiles since it is known that these insects does not damage the inner structure of the trees.

The pines inoculated with nematodes and those inoculated both with nematodes and bark beetles presented also similar values for the Z_1/Z_{50} index, but different from those obtained for the previous sub-groups [1]. In relation to the previous sub-populations, the values are characterized by a higher dispersion in terms of reactance (see Figure 16) [1]. Besides, it is observed a clear relation between the number of nematodes and the reactance dispersion for the Z_1/Z_{50} parameter: the higher the number of nematodes is, the higher the reactance value of Z_1/Z_{50} becomes (see Figure 17) [1].

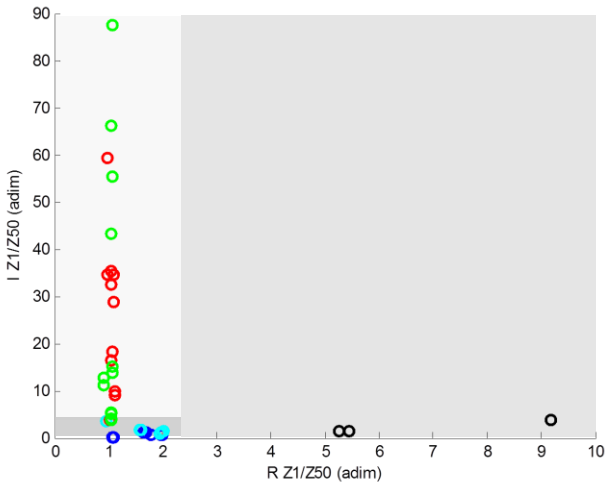

Figure 16. Values of the impedance parameter Z_1/Z_{50} for each of the 24 pine trees. Note that two values are represented for each pine. The impedance values of the regions HW (healthy and watered), HLHS (high level of HS) and D (disease) correspond to the indicated physiological states.

TABLE II. NUMBER OF NEMATODES IN THE TRUNKS OF PINE TREES PER CUT SECTION

Tree	Cut Section	Number of nematodes in 0,05 mL
1	***a***	1
	b	0
	c	133
2	***a***	0
	b	43
	c	1
3	***a***	0
	b	0
	c	112
4	***a***	4
	b	20
	c	0
5	***a***	0
	b	17
	c	0
6	***a***	0
	b	0
	c	14

In fact, the counting of nematodes in the several cut sections revealed that the concentration of nematodes was higher in the cut sections b) and c) for the pines less watered (pines 1, 2 and 3) – see Table II [1]. The concentration of nematodes in the lower parts of the trunks was much higher for the pines with less watering than for those with regular watering (pines 4, 5 and 6), since nematodes tend to move toward watered regions along the trunk [1]. For this reason, the referred relation was more perceptible for the pines with lower watering, than for those receiving more watering (see Figure 18), since the accumulation of nematodes in section c (see Table II) was higher for the first group [1].

The dispersion in terms of resistance is not significant when compared with values from pines in other physiological conditions (see Figure 16).

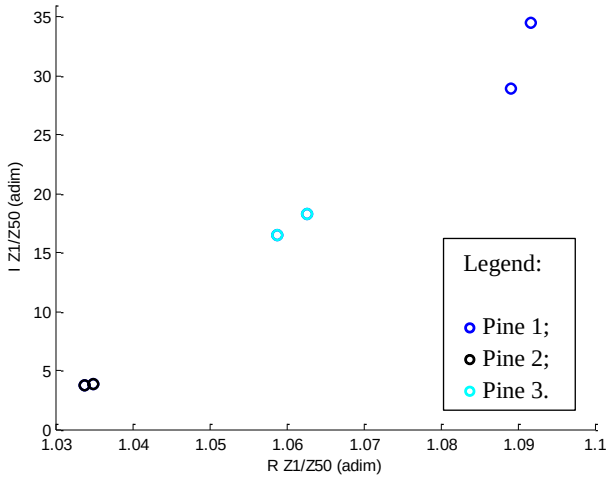

Figure 17. Values of the impedance parameter Z_1/Z_{50} for the pines inoculated with nematodes and with low watering (pines 1, 2 and 3 from the Table II). Note that there are represented two values for each pine.

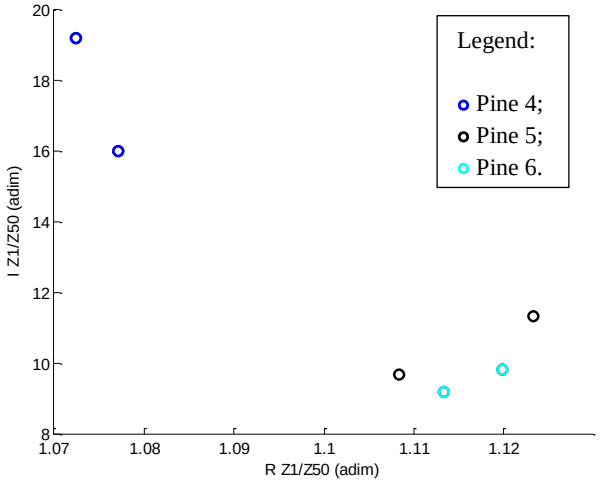

Figure 18. Values of the impedance parameter Z_1/Z_{50} for the pines inoculated with nematodes and with regular watering (pines 4, 5 and 6 from the Table II). Since the number of nematodes is low in these pines, the linear relation between them and the Z_1/Z_{50} values is not perceptible. Note that there are represented two values for each pine.

The pines that died due to HS (decay of 100%) were also studied and the Z_1/Z_{50} parameter presented the highest resistance values, in relation to all the other pines [1].

The monitored healthy pines were watered at different rates: one with low watering (2 min/day) and another with regular watering (5 min/day) [1]. After one week of monitoring both were inoculated with PWN [1]. As Figure 19 a) shows, it was again observed dispersion in reactance for the Z_1/Z_{50} index [1]. The reactance values, and consequently this dispersion, were successively higher as time was passing and the disease was evolving [1]. The higher values of reactance were achieved for the pine with less watering [1].

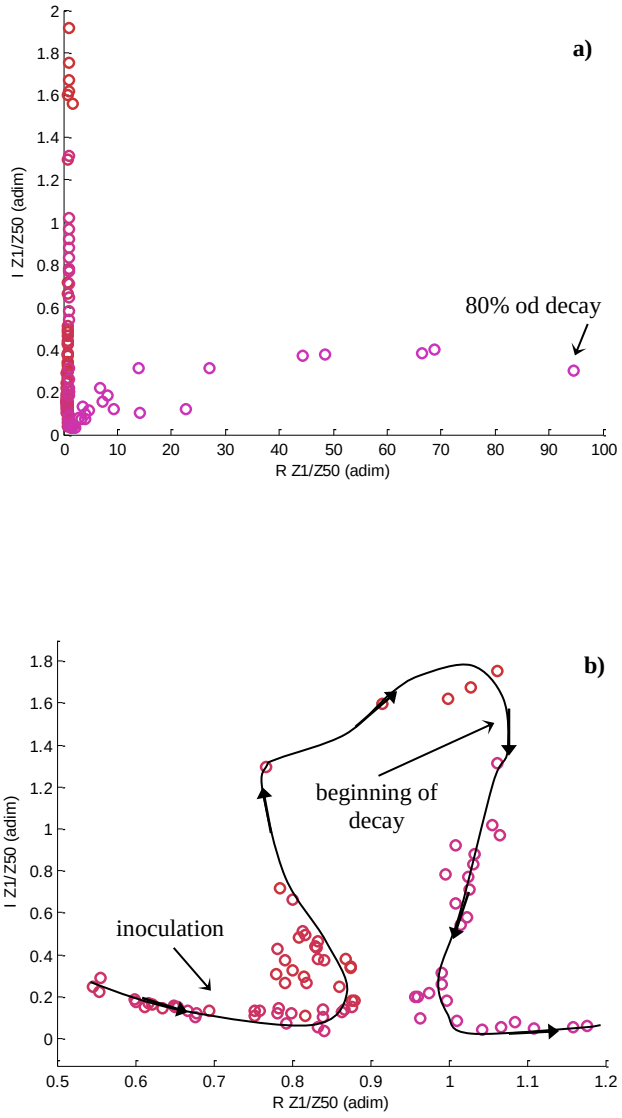

Figure 19. a) Evolution of the Z_1/Z_{50} during the monitoring of a pine, which was inoculated with nematodes during the measurements. b) Closer view from the Z_1/Z_{50} evolution, showing a hysteresis-like behaviour.

These results corroborate the previous ones: it was expected that the number of nematodes increase in the below part of the trunk for the pines with less watering and, consequently, to observe a higher rising of the reactance for the Z_1/Z_{50} parameter [1]. After the 6th week, pines start to decay strongly and it was observed a relevant decrease of the reactance and a significant increase of the resistance for the same parameter – see Figure 19 a). The higher values of resistance were achieved for the pine with less watering, and also in a shorter period of time [1]. At the end of the monitoring, the decay of the pines, evaluated by an expertise, was about 80 % for the pine with regular watering and 100 % for the pine with less watering [1].

From the Figure 19 b), which shows a closer view of the Z_1/Z_{50} index evolution during the monitoring, it is observed that the path that corresponds to the rising of the population of nematodes is different from the path followed during the period of decay [1]. For this reason, it is possible to affirm that PWD evolution has a hysteresis-like behavior [1].

It is worth noting that some impedance parameters may be preferable than others, depending on the physiological condition that is being studied. To evaluate the disease condition, the Z_1/Z_{50} index, allowed showing the great reactance increase that is characteristic of these diseases (since the cellular membranes are affected, which promotes a decrease of membranes capacitor effect) – see Figure 19.

Other parameters, such as R_1/R_{50}, which shown to be useful in the previous study, may not be the most adequate to study this specific case of disease condition (see Figure 20).

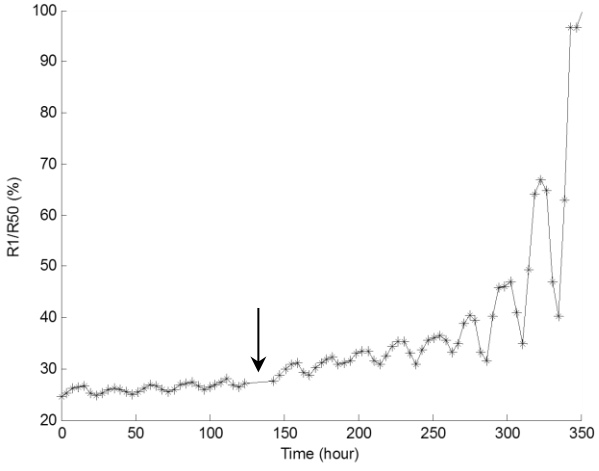

Figure 20. Evolution of the R_1/R_{50} during the monitoring of a pine, which was inoculated with nematodes during the measurements. It is possible to observe the daily oscilation and the increase of reactance for higher levels of HS as time was passing and the disease was evolving. The arrow indicates the graph bellow were some data is missing due to a system crash during the monitoring.

V. DISCUSSION

Assessing physiological states of plants, using impedance techniques, implies the knowledge of the typical EIS profiles of the species under study, i.e., the EIS profiles for healthy individuals under controlled environment conditions [1]. For this reason, the studies presented herein required an exhaustive EIS assessment and monitoring, performed over months, and extensive data analysis [1].

The greatest difficulty inherent in this type of studies is the purchase and maintenance of the plant specimens, which in addition to being time consuming, is extremely expensive. Besides, some of the performed tests required the death of the specimen under study, which worsens the referred problem. For this reason, a true statistical analysis, which may be required to achieve reliable results, was not possible to accomplish. However, the results presented herein constitute an innovative approach to assess physiological conditions of plants, giving plausible and interesting clues to solve the problem of the lack of techniques, and also methods, in this specific area.

The biological application study aimed at discriminating between different physiological states of three plant species, which have economical/forestall relevance: pine *(Pinus pinaster* Aiton), cheastnut (*Castanea sativa* Mill) and *Jatropha Curcas* L. [1] Attention was given to the assessment of the HS level and the disease condition.

To accomplish this task, an EIS system able to perform AC sweeps over a sufficient large frequency range, was developed. The design of the EIS system took into account the robustness, efficiency and celerity of the bioimpedance analysis [1]. The portability, adaptability to different biological applications and the implementation of easily accessible and affordable components were also considered aspects [1]. The system versatility is another advantage [1]. It allows the user to choose the settings of the analysis that best fit a specific application, such as: frequency limits, number of intervals of the scan and type of signal excitation (voltage or current) [1]. Besides, a driven shield technique is applied in order to overcome problems inherent to stray capacitive effects from cables [1]. The maximum phase shift reduction estimated was about 20.4 % for the current excitation mode and about 35.8% for the voltage mode [1]. The system also implements a PSD method with a novel implication to determine the impedance values, which shown to be effective.

The great amount of data, typical in these types of studies, imposes a problem to the use of theoretical models; such is the case of the Cole model. For this reason, the approach followed in this work was the research of bioimpedance indexes that better expressed specific physiological conditions. Although, a specific bioimpidance index does not require a true impedance analysis, i.e., a frequency scan, the method used has proven the necessity of a spectroscopy analysis, since the indexes relations and their

correlation to the physiological conditions may be better expressed for some frequencies than others.

The obtained results suggest that the implemented method may constitute a first innovative approach for the assessment of physiological states of plants and to the early diagnosis of plant diseases [1]. The consistency of the results obtained for the three studied species reveals the transversality of the method [1].

Two of the most interesting bioimpedance indexes are the ratio Z_1/Z_{50} and also the ratio R_1/R_{50}, which were studied and presented in this paper.

EIS profiles showed a consistent behaviour whit the HS level of the three studied species [1]. The Z_1/Z_{50} impedance parameter presents increased values of both reactance and resistance when the hydric stress is high, for the pines and chestnuts [1]. In the case of the *Jatropha curcas*, this parameter presented decreased values of both reactance and resistance when the HS was high [1]. This inverse behaviour may be explained due to the presence of latex vessels in this species, which may function as water reservoirs [1].

The evolution of the Z_1/Z_{50} impedance parameter may be used to predict risky HS levels of a plant.

However, as it was shown, the HS level of a plant exerts much more influence over the real part of the impedance than over its imaginary part. Actually, the phase shift alterations due to progressively higher levels of HS are almost inexistent. For this reason, the R_1/R_{50} or other interrelated resistance (real part of the impedance) indexes may constitute preferable approaches to study the HS level and its use as a risk predictor.

In addition to the study of the HS level and its influence in the plant physiological condition, it was studied the disease physiological condition for the pines, were inoculations with PWN and bark beetles were performed.

The pines inoculated with PWN presented Z_1/Z_{50} ratio with high values of reactance, what suggests that current flows preferably trough the cytosol [1]. In fact, the action of the nematodes inside the tree may destroy cell membranes, which means that membranes capacitor effect becomes less significant in the impedance measurement [1].

It was also shown a relation between the number of nematodes and the Z_1/Z_{50} index: the increasing of nematodes number is proportional to the reactance ratio augmentation [1].

On the other hand, the action of bark beetles seems not to interfere, at least in measurable terms, in the level of HS of pines, since the values obtained were similar to those obtained for healthy pines [1].

The index Z_1/Z_{50} for healthy trees with high levels of HS (decays above 80) presented high values of resistance, due to water loss [1]. High resistance values were also obtained for the trees in advanced stages of the disease [1]. This means, that for this specific case, the method is not able to distinguish between healthy trees and trees with the PWD [1]. However, it is known that the advanced stages of the PWD induce high levels of hydric stress, which allows to infer that, in practical terms, the situation is exactly the same, i.e., the tree presents high probability to die [1]. On the other hand, in the stages where the method is able to distinguish between trees with the PWD and healthy trees, and since the decay was determined to round the 40%, the diagnosis could help to assist pine management [1]. If a cure is available, at these stages, a treatment could be administrated and reverse the disease evolution [1].

The implemented method has allowed identifying three clear regions on the Z_1/Z_{50} graph that corresponds to: healthy and watered trees (HW), tress with high level of HS (HLHS) and trees with disease (D). Although, the high levels of HS, obtained by the R_1/R_{50} analysis, may drive the tree to dead or, in other words, the levels of HS may be used as a risk indicator, the use of several indicators and biompedance indexes is necessary to perform a reliable study (at least these two: R_1/R_{50} and Z_1/Z_{50}). In fact, the studied disease indicated a clear region characterized by higher levels of Z_1/Z_{50} reactance and normal levels of Z_1/Z_0 resistance, where the levels of HS based on the R_1/R_{50} ratio seemed normal. Besides, as stated, the final stages of the disease presented impedance similar values to those obtained for trees with HS levels. What is worth adding is that it may be possible to interfere, with a cure for example, during the evolution of the disease when the Z_1/Z_{50} graph shows a D physiological condition. If the graph shows a HLHS condition the tree is probably about to die either it has a disease promoted by biologic agents, such the PWN, or not.

In order to summarize the discussion, the method studied and presented herein, based on bioimpedance indexes, may constitute a first innovative approach to the assessment of the main physiological conditions (healthy state, HS level and disease), since the referred indexes may be used as risk predictors.

VI. CONCLUSION

The developed EIS system showed to be a robust, reliable and easy to implement equipment in the assessment of the physiological states of living plants. Its main advantages are: portability, since it allows *in vivo* and *in situ* measurements; adaptability to different biological samples; and versatility, since it is possible to adjust the parameters of the acquisition according to the sample under study.

The method studied and presented herein, based on bioimpedance indexes, such as Z_1/Z_{50} and R_1/R_{50}, allowed to determine three distinct physiological states: healthy and watered plants, plants with high level of HS and plants with disease.

Although a real statistical analysis is missing, the method presented in this paper may constitute an interesting solution for the assessment of physiological states of plants, since the bioimpedance indexes may easily be implemented as risk predictors, which may help to assist forest and crops management and also physiological plant studies.

ACKNOWLEDGMENT

We acknowledge support from Fundação para a Ciência e Tecnologia, FCT (scholarship SFRH/BD/61522/2009).

REFERENCES

[1] E. Borges, M. Sequeira, A. F. V. Cortez, H. C. Pereira, T. Pereira, V. Almeida, *et al*, "Assessment of Physiological States of Plants in situ – An Innovative Approach to the use of Electrical Impedance Spectroscopy", BIOTECHNO 2013, pp. 1–8, March 2013.

[2] L. Martins, J. Castro, W. Macedo, C. Marques, and c. Abreu, "Assessment of the spread of chestnut ink disease using remote sensing and geostatistical methods," Eur J Plant Pathol, vol. 119, pp. 159–164, April 2007.

[3] CABI and EPPO, "Data sheets on quarantine pests – *Bursaphelenchus xylophilus*," EPPO quarantine pests, contract 90/399003.

[4] W. Parawira, "Biodiesel production from *Jatropha curcas*: a review," Scientific Research and Essays, vol. 5(14), pp. 1796–1808, July 2010.

[5] T. Repo, G. Zhang, A. Ryyppo, and R. Rikala, "The electrical impedance spectroscopy of scots Pine (*Pinus sylvestris* L.) shoots in relation to cold acclimation," Journal of Experimental Botany, vol. 51 (353), pp. 2095–2107, December 2000.

[6] A. Pirzad, M. K. Shakiba, S. Zehtab-Salmasi, S. A. Mohammadi, R. Darvishzadeh, and A. Samadi, "Effect of water stress on leaf relative water content, chlorophyll, proline and soluble carbohydrates in *Matricaria chamomilla* L.," Journal of Medicinal Plants Research, vol. 5(12), pp. 2483–2488, June 2011.

[7] L. Callegaro, "The metrology of electrical impedance at high frequency: a review," Meas. Sci. Techno, vol. 20, 022002, February 2009.

[8] U. G. Kyle, I. Bosaeus, A. D. De Lorenzo, P. Deurenberg, M. Elia, J. M. Gómez, *et al*, "Bioelectrical impedance analysis – part I: review of principles and methods," Clinical Nutrition, vol. 23(5), pp. 1226–1243, October 2004.

[9] U. Pliquett, "Bioimpedance: a review for food processing," Food Engineering Reviews, vol. 2(2), pp. 74–94, June 2010.

[10] S. Grimnes and O. G. Martinsen, "Bioimpedance and bioelectricity basics," 2nd Edition, Academic Press of Elsevier, 2008.

[11] T. Hayashi, M. Iwamoto, and K. Kawashima, "Identification of irradiated potatoes by impedance measurements," Biosci Biotechnol Biochem, vol. 56(12), pp. 1929–1932, December 1992.

[12] M. Rafiei-Naeini, P. Wright, and H. McCann, "Low-noise measurement for electrical impedance tomography," IFMBE Proceedings, vol. 17(10), pp. 324–327, 2007.

[13] A. S. Ross, G. J. Saulnier, J. C. Newell, and D. Isaacson, "Current source design for electrical impedance tomography," Physiol Meas, vol. 24(2), pp. 509–516, May 2003.

[14] P. J. Yoo, D. H. Lee, T. I. Oh, and E. J.Woo, "Wideband bio-impedance spectroscopy using voltage source and tetra-polar electrode configuration," Journal of Physics, vol. 224(1), pp. 224-228, 2010.

[15] G. J. Saulnier, A. S. Ross, and N. Liu, "A high-precision voltage source for EIT," Physiol Meas, vol. 27(5), pp. 221–236, May 2006.

[16] F. Seoane, R. Bragós, and K. Lindecrantz, "Current source for multifrequency broadband electrical impedance spectroscopy systems – a novel approach," Proceedings IEEE Eng Med Biol Soc, vol. 1, pp. 5121–5125, August 2006.

[17] C. He, L. Zhang, B. Liu, Z. Xu, and Z. Zhang, "A Digital Phase-sensitive Detector for Electrical Impedance Tomography", IEEE proceedings, 2008.

[18] T. Yamamoto, Y. Oomura, H. Nishino, S. Aou, and Y. Nakano, "Driven shield for multi-barrel electrode," Brain Research Bulletin, vol. 14(1), pp. 103-104, January 1985.

www.iariajournals.org

International Journal On Advances in Intelligent Systems

ICAS, ACHI, ICCGI, UBICOMM, ADVCOMP, CENTRIC, GEOProcessing, SEMAPRO, BIOSYSCOM, BIOINFO, BIOTECHNO, FUTURE COMPUTING, SERVICE COMPUTATION, COGNITIVE, ADAPTIVE, CONTENT, PATTERNS, CLOUD COMPUTING, COMPUTATION TOOLS, ENERGY, COLLA, IMMM, INTELLI, SMART, DATA ANALYTICS

issn: 1942-2679

International Journal On Advances in Internet Technology

ICDS, ICIW, CTRQ, UBICOMM, ICSNC, AFIN, INTERNET, AP2PS, EMERGING, MOBILITY, WEB

issn: 1942-2652

International Journal On Advances in Life Sciences

eTELEMED, eKNOW, eL&mL, BIODIV, BIOENVIRONMENT, BIOGREEN, BIOSYSCOM, BIOINFO, BIOTECHNO, SOTICS, GLOBAL HEALTH

issn: 1942-2660

International Journal On Advances in Networks and Services

ICN, ICNS, ICIW, ICWMC, SENSORCOMM, MESH, CENTRIC, MMEDIA, SERVICE COMPUTATION, VEHICULAR, INNOV

issn: 1942-2644

International Journal On Advances in Security

ICQNM, SECURWARE, MESH, DEPEND, INTERNET, CYBERLAWS

issn: 1942-2636

International Journal On Advances in Software

ICSEA, ICCGI, ADVCOMP, GEOProcessing, DBKDA, INTENSIVE, VALID, SIMUL, FUTURE COMPUTING, SERVICE COMPUTATION, COGNITIVE, ADAPTIVE, CONTENT, PATTERNS, CLOUD COMPUTING, COMPUTATION TOOLS, IMMM, MOBILITY, VEHICULAR, DATA ANALYTICS

issn: 1942-2628

International Journal On Advances in Systems and Measurements

ICQNM, ICONS, ICIMP, SENSORCOMM, CENICS, VALID, SIMUL, INFOCOMP

issn: 1942-261x

International Journal On Advances in Telecommunications

AICT, ICDT, ICWMC, ICSNC, CTRQ, SPACOMM, MMEDIA, COCORA, PESARO, INNOV

issn: 1942-2601